SIMULATION LAND USE AND LAND COVER SCENARIO AND WATER YIELD ESTIMATION FOR WATER BALANCE ANALYSIS IN PHUKET ISLAND, THAILAND

NATTAPONG PUANGKAEW

A Thesis Submitted in Partial Fulfillment of the Requirements for the
Degree of Doctor of Philosophy in Geoinformatics
Suranaree University of Technology
Academic Year 2021

การจำลองภาพเหตุการณ์การใช้ประโยชน์ที่ดินและสิ่งปกคลุมดินและการประมาณค่าปริมาณน้ำท่าสำหรับการวิเคราะห์สมดุลน้ำในเกาะภูเก็ต ประเทศไทย

นายนัฐพงษ์ พวงแก้ว

วิทยานิพนธ์นี้เป็นส่วนหนึ่งของการศึกษาตามหลักสูตรปริญญาวิทยาศาสตรดุษฎีบัณฑิต
สาขาวิชาภูมิสารสนเทศ
มหาวิทยาลัยเทคโนโลยีสุรนารี
ปีการศึกษา 2564

SIMULATION LAND USE AND LAND COVER SCENARIO AND WATER YIELD ESTIMATION FOR WATER BALANCE ANALYSIS IN PHUKET ISLAND, THAILAND

Suranaree University of Technology has approved this thesis submitted in partial fulfillment of the requirements for the Degree of Doctor of Philosophy.

Thesis Examining Committee

Y. Trisurat

(Prof. Dr. Yongyut Trisurat)
Chairperson

Suwit Ong.

(Assoc. Prof. Dr. Suwit Ongsomwang)
Member (Thesis Advisor)

S. Dasananda

(Assoc. Prof. Dr. Songkot Dasananda)
Member

(Asst. Prof. Dr. Pantip Piyatadsananon)
Member

Tanakorn Sritarapipat

(Dr. Tanakorn Sritarapipat)
Member

Chatchai Jothity

(Assoc. Prof. Dr. Chatchai Jothityangkoon)
Vice Rector for Academic Affairs
and Quality Assurance

(Prof. Dr. Santi Maensiri)
Dean of Institute of Science

นัฐพงษ์ พวงแก้ว : การจำลองภาพเหตุการณ์การใช้ประโยชน์ที่ดินและสิ่งปกคลุมดินและการประมาณค่าปริมาณน้ำท่าสำหรับการวิเคราะห์สมดุลน้ำ ในเกาะภูเก็ต ประเทศไทย (SIMULATION LAND USE AND LAND COVER SCENARIO AND WATER YIELD ESTIMATION FOR WATER BALANCE ANALYSIS IN PHUKET ISLAND, THAILAND) อาจารย์ที่ปรึกษา : รองศาสตราจารย์ ดร.สุวิทย์ อ๋องสมหวัง, 242 หน้า.

คำสำคัญ: การเปลี่ยนแปลงการใช้ประโยชน์ที่ดินและสิ่งปกคลุมดิน/ น้ำท่า/ อุปทานน้ำ/ อุปสงค์น้ำ/ สมดุลน้ำ/ แบบจำลอง CLUE-S/ แบบจำลอง SWAT/ เกาะภูเก็ต

เกาะภูเก็ตเป็นสถานที่ปรารถนาของนักท่องเที่ยวมากสุด ในช่วงเวลา 30 ปีที่ผ่านมา เกาะภูเก็ตมีนักท่องเที่ยวเพิ่มขึ้นและมีการเจริญเติบโตทางเศรษฐกิจอย่างต่อเนื่อง ปัจจุบันเกาะภูเก็ตกำลังเผชิญกับปัญหาการขาดแคลนน้ำ ดังนั้น การจำลองสถานการณ์การใช้ประโยชน์ที่ดินและสิ่งปกคลุมดินและการประมาณค่าปริมาณน้ำท่า เพื่อศึกษาสมดุลของอุปทานและอุปสงค์น้ำสำหรับการจัดการทรัพยากรน้ำนับว่าเป็นสิ่งจำเป็นและมีความสำคัญมาก โดยเฉพาะอย่างยิ่ง การขาดแคลนน้ำ วัตถุประสงค์สำคัญของการศึกษา คือ (1) เพื่อประเมินสถานภาพและการเปลี่ยนแปลงการใช้ประโยชน์ที่ดินและสิ่งปกคลุมดินในระหว่างปี พ.ศ. 2557 ถึง พ.ศ. 2562 และการจำลองภาพเหตุการณ์ข้อมูลการใช้ประโยชน์ที่ดินและสิ่งปกคลุมดินในระหว่างปี พ.ศ. 2563 และ 2572 (2) เพื่อประมาณค่าปริมาณน้ำท่าจากข้อมูลการใช้ประโยชน์ที่ดินและสิ่งปกคลุมดินที่ได้จากการแปลตีความและจากการจำลองภาพเหตุการณ์ (3) เพื่อประมาณค่าอุปสงค์น้ำโดยอาศัยการประเมินรอยเท้าการใช้น้ำ และ (4) เพื่อประเมินค่าความสมดุลของอุปสงค์และอุปทานน้ำในระหว่างปี พ.ศ. 2563 และ 2572 วิธีการศึกษาแบ่งออกเป็น 6 ส่วน ประกอบด้วย การรวบรวมและเตรียมข้อมูล การประเมินสถานภาพและการเปลี่ยนแปลงการใช้ประโยชน์ที่ดินและสิ่งปกคลุมดิน การจำลองภาพเหตุการณ์การใช้ประโยชน์ที่ดินและสิ่งปกคลุมดิน การประมาณค่าปริมาณน้ำท่า การประมาณค่าอุปสงค์น้ำ และการประเมินสมดุลน้ำ

จากผลการศึกษา พบว่า ประเภทการใช้ประโยชน์ที่ดินและสิ่งปกคลุมดินในปี พ.ศ. 2562 ที่สำคัญสามอันดับแรก ได้แก่ ไม้ยืนต้นและไม้ผล (35.32%) พื้นที่ชุมชนและสิ่งปลูกสร้าง (27.13%) และป่าดิบชื้น (14.20%) จากผลการตรวจสอบการเปลี่ยนแปลงการใช้ประโยชน์ที่ดินและสิ่งปกคลุมดินระหว่างในปี พ.ศ. 2557 ถึง พ.ศ. 2562 พบว่า ประเภทการใช้ประโยชน์ที่ดินและสิ่งปกคลุมดินที่เพิ่มขึ้นอย่างมีนัยสำคัญ ได้แก่ พื้นที่ชุมชนและสิ่งปลูกสร้างและที่รกร้างว่างเปล่า ในขณะเดียวกันประเภทการใช้ประโยชน์ที่ดินและสิ่งปกคลุมดินที่ลดลงอย่างมีนัยสำคัญ ได้แก่ ไม้ยืนต้นและไม้ผลและ

ป่าดิบชื้น ในทำนองเดียวกัน การจำลองภาพเหตุการณ์ข้อมูลการใช้ประโยชน์ที่ดินและสิ่งปกคลุมดินจากจำลองในระหว่างปี พ.ศ. 2563 และ 2572 ได้แสดงให้เห็นถึง การเพิ่มขึ้นของพื้นที่ชุมชนและสิ่งปลูกสร้างและที่รกร้างว่างเปล่า ในเวลาเดียวกัน ไม้ยืนต้นและไม้ผลและป่าดิบชื้นลดลง สำหรับการประมาณค่าอุปทานน้ำในระหว่างปี พ.ศ. 2563 และ 2572 ภายใต้ภาพเหตุการณ์ปีแห้ง ปริมาณน้ำท่ารายปีผันแปรระหว่าง 505.01 ถึง 521.79 ล้านลูกบาศก์เมตร ในทางตรงกันข้าม ภายใต้ภาพเหตุการณ์ปีเปียก ปริมาณน้ำท่ารายปีผันแปรระหว่าง 1,225.48 ถึง 1,242.08 ล้านลูกบาศก์เมตร ในเวลาเดียวกัน อุปสงค์น้ำภายใต้สถานการณ์ปกติผันแปรระหว่าง 442.09 ถึง 475.86 ล้านลูกบาศก์เมตร ในขณะที่อุปสงค์น้ำภายใต้สถานการณ์วิถีใหม่ผันแปรระหว่าง 442.09 ถึง 461.53 ล้านลูกบาศก์เมตร สำหรับการประเมินสมดุลน้ำรายปีที่พิจารณาความต้องการน้ำเพื่อรักษาระบบนิเวศ พบว่า มีการขาดแคลนน้ำทุกปีภายใต้ภาพเหตุการณ์ปีแห้งทั้งสถานการณ์แบบปกติและสถานการณ์แบบวิถีใหม่ แต่อย่างไรก็ตาม หากพิจารณาสมดุลน้ำรายเดือน พบว่า มีการขาดแคลนน้ำในฤดูร้อนของทุกปีแม้ว่าไม่พิจารณาหรือพิจารณาความต้องการน้ำเพื่อรักษาระบบนิเวศ

จากผลการศึกษาที่ได้รับทั้งหมด สามารถสรุปได้ว่า การบูรณาการข้อมูลการรับรู้จากระยะไกลร่วมกับแบบจำลองเชิงพื้นที่ขั้นสูงสามารถให้สารสนเทศที่จำเป็นต่อการบรรเทาปัญหาการขาดแคลนน้ำในอนาคตของเกาะภูเก็ต นอกจากนี้ กรอบแนวคิดและขั้นตอนการวิจัยของการศึกษานี้สามารถนำมาใช้เพื่อเป็นแนวทางให้กับหน่วยงานของรัฐในการตรวจสอบการขาดแคลนน้ำในพื้นที่อื่นได้

สาขาวิชาภูมิสารสนเทศ ลายมือชื่อนักศึกษา นัฐพงษ์

ปีการศึกษา 2564 ลายมือชื่ออาจารย์ที่ปรึกษา

NATTAPONG PUANGKAEW : SIMULATION LAND USE AND LAND COVER SCENARIO AND WATER YIELD ESTIMATION FOR WATER BALANCE ANALYSIS IN PHUKET ISLAND, THAILAND. THESIS ADVISOR : ASSOC. PROF. SUWIT ONGSOMWANG, Dr. rer. Nat. 242 PP.

Keyword: LAND USE AND LAND COVER CHANGE/ WATER YIELD/ WATER SUPPLY/ WATER DEMAND/ WATER BALANCE/ CLUE-S MODEL/ SWAT MODEL/ PHUKET ISLAND

Phuket Island is the most desired place for tourist destinations. Over 30 years, Phuket Island has been continuously increased tourists and economic growth. Currently, Phuket Island is facing water scarcity. Therefore, to simulate the land use and land cover (LULC) trend and water yield estimation for balancing water supply and demand for water resources management, particularly water scarcity, is necessary and very important. The specific research objectives are (1) to assess LULC status and its change between 2014 and 2019 and to simulate LULC data between 2020 and 2029, (2) to estimate water yield based on interpreted and simulated LULC data, (3) to estimate water demand based on the water footprint assessment, and (4) to evaluate water supply and demand balance between 2020 and 2029. The research methodology consisted of six components: data collection and preparation, LULC assessment and change detection, LULC simulation, water yield estimation, water demand estimation, and water balance evaluation.

As the derived results, the top three most dominant LULC types in 2019 were perennial trees and orchards (35.32%), urban and built-up area (27.13%), and evergreen forests (14.20%). According to LULC change detection between 2014 and 2019, the significantly increasing LULC types were urban and built-up areas and idle land, while the significantly decreasing LULC types were perennial trees and orchards, and evergreen forests. Likewise, the simulated LULC data between 2020 and 2029 showed an increase in urban and built-up areas and idle land while decreasing perennial trees and orchards, and evergreen forests. For water supply estimation between 2020 and 2029, under the dry year scenario, the annual water yield varied from 505.01 to 521.79 million m^3. On the contrary, under the wet year scenario, the annual water yield varied from 1,225.48 to 1,242.08 million m^3. At the same time, the water demand under the normal condition varied from 442.09 to 475.86 million m^3, while the water demand under the new normal condition varied from 442.09 to 461.53 million m^3. For annual water balance evaluation with ecological water requirement consideration, it discovered that water deficit every year under dry year scenarios with normal and new normal conditions. However, the monthly water balance was a water deficit in the summer seasons every year, both without and with ecological water requirement consideration.

Consequently, it can be concluded that integrating remote sensing data with advanced geospatial models can provide essential information to mitigate future water scarcity in Phuket Island. Additionally, this study's conceptual framework and research workflows can be used as a guideline for government agencies to examine the water deficit in another area.

School of Geoinformatics — Student's Signature Nattapong

Academic Year 2021 — Advisor's Signature

ACKNOWLEDGEMENTS

Undertaking this Ph. D. has been a truly life-changing experience for me, and it would not have been possible to do without the support and guidance that I received from many people.

I would like to first express profound gratitude to my advisor, Assoc. Prof. Dr. Suwit Ongsomwang, for his help with valuable instructions, guidance, and suggestions to complete this thesis, and for giving me the opportunity to grow in this field of research, as well as being a good role model of lecturer and everyday life.

I would like to thank the chairman and members of this thesis defense committee: Prof. Dr. Yongyut Trisurat, Assoc. Prof. Dr. Songkot Dasananda, Asst. Prof. Dr. Pantip Piyatadsanaon, and Dr. Tanakorn Sritarapipat for all valuable suggestions and critical comments during the proposal and thesis defense.

I would also like to thank the Phuket City municipality, Phuket Irrigation Project, Southern Region Irrigation Hydrology Center, and Thai Meteorological Department for supporting the data needed for the research.

I am especially thankful to Prince of Songkla University for the opportunity to continue my education.

In addition, I am grateful to my colleagues for all their support and all of my friends in the School of Geoinformatics, especially Miss Jiraporn Kulsoontornrat, Mr. Athiwat Phinyoyang, Miss Juthamas Noina, and Miss Warunee Aunphoklang, for all their help and encouragement throughout tough times.

Finally, the completion of this study would have been not possible if not dependent on the steadfast support and encouragement of my parents.

Nattapong Puangkaew

CONTENTS

Page

ABSTRACT IN THAI I
ABSTRACT IN ENGLISH III
ACKNOWLEDGEMENTS V
CONTENTS VI
LIST OF TABLES X
LIST OF FIGURES XVI
LIST OF ABBREVIATIONS XXIV

CHAPTER

I INTRODUCTION 1
- 1.1 Background problems and significance of the study 1
- 1.2 Research objectives 5
- 1.3 Scope and limitations of the study 5
  - 1.3.1 Scope of the study 5
  - 1.3.2 Limitation of the study 6
- 1.4 Study area 8
- 1.5 Benefit of the study 10

II BASIC CONCEPTS AND LITERATURE REVIEWS 11
- 2.1 Elements of image interpretation 11
- 2.2 CLUE-S model and its applications 14
  - 2.2.1 Background and model structure of the CLUE-S model 14
  - 2.2.2 CLUE-S model applications 17
- 2.3 SWAT model and its applications 19
  - 2.3.1 Background of the SWAT model 19
  - 2.3.2 Procedure of water yield estimation 20

CONTENTS (Continued)

Page

2.3.3 Model performance evaluation 24

2.3.4 SWAT model applications 26

2.4 Water demand estimation based on water footprint and its applications 28

2.4.1 Water footprint concepts 28

2.4.2 Water footprint assessment 30

2.4.3 Water demand estimation based on water footprint applications 31

III RESEARCH PROCEDURES 33

3.1 Equipment 33

3.2 Data... 34

3.3 Research methodology 35

3.3.1 Land use and land cover assessment and change detection 35

3.3.2 Land use and land cover simulation 39

3.3.3 Water yield estimation 41

3.3.4 Water demand estimation 51

3.3.5 Water balance evaluation 56

IV LAND USE AND LAND COVER ASSESSMENT AND CHANGE DETECTION 58

4.1 LULC assessment in 2014 and 2019 58

4.2 LULC change detection between 2014 and 2019 69

V LAND USE AND LAND COVER SIMULATION 76

5.1 Driving force on LULC change 76

5.1.1 Driving force for urban and built-up area allocation 81

5.1.2 Driving force for paddy field allocation 82

5.1.3 Driving force for field crop and horticulture allocation 82

5.1.4 Driving force for perennial trees and orchards allocation 83

CONTENTS (Continued)

Page
5.1.5 Driving force for aquaculture allocation 84
5.1.6 Driving force for idle land allocation 84
5.1.7 Driving force for evergreen forest allocation 85
5.1.8 Driving force for mangrove forest allocation 86
5.1.9 Driving force for scrub forest allocation 87
5.1.10 Driving force for waterbody allocation 87
5.1.11 Driving force for miscellaneous land allocation 88
5.2 Local parameter of the CLUE-S model for LULC simulation 89
5.3 Land demand estimation 91
5.4 LULC simulation between 2020 and 2029 93
VI WATER YIELD ESTIMATION 102
6.1 Hydrologic Response Unit 102
6.2 Sensitivity analysis 106
6.3 Model calibration and validation 107
6.3.1 Dry year condition 107
6.3.2 Wet year condition 111
6.4 Baseline information of water yield estimation in 2019 116
6.5 Water yield estimation between 2020 and 2029 117
6.5.1 Water yield estimation of dry year scenario 119
6.5.2 Water yield estimation of wet year scenario 128
6.6 Effect of LULC change on water yield 137
VII WATER DEMAND ESTIMATION 163
7.1 Baseline information of water demand estimation in 2019 163
7.2 Residential water demand between 2020 and 2029 163
7.3 Tourist water demand between 2020 and 2029 175

CONTENTS (Continued)

Page

7.4 Water demand for agriculture and forest uses between 2020 and 2029.......182

VIII WATER BALANCE EVALUATION...191

8.1 Baseline information of water balance in 2019...192

8.2 Annual and monthly water balance without ecological water requirement consideration 192

8.2.1 Annual water balance without ecological water requirement consideration 192

8.2.2 Monthly water balance without ecological water requirement consideration 197

8.3 Annual and monthly water balance with ecological water requirement consideration 207

8.3.1 Annual water balance with ecological water requirement consideration 207

8.3.2 Monthly water balance with ecological water requirement consideration 211

IX CONCLUSION AND RECOMMENDATIONS 222

9.1 Conclusion...222

9.1.1 Land use and land cover assessment and change detection 222

9.1.2 Land use and land cover simulation..223

9.1.3 Water yield estimation 223

9.1.4 Water demand estimation...224

9.1.5 Water balance evaluation..225

9.2 Recommendations..226

REFFERENCES 228

CURRICULUM VITAE...242

LIST OF TABLES

Table Page

2.1 Model performance scale 26

3.1 List of data collection and preparation for analysis and modeling in the study 34

3.2 Description of LULC classification system 38

3.3 LULC code for linkage with the SWAT database 43

3.4 SWAT soil classification table from the ArcSWAT STATSGO database. 44

3.5 Slope classification from the Land Development Department 45

3.6 Model performance scale 50

3.7 Water consumption rates in different community characteristics 54

3.8 The modified water consumption rate for tourists 55

3.9 The evapotranspiration coefficient of each agriculture and forest type 55

3.10 The reference evapotranspiration under the Penman-Monteith method 56

3.11 The criteria of minimum water from the flow duration curve 57

4.1 Photo interpretation key of LULC types in Phuket Island.. 60

4.2 Area and percentage of LULC data in 2014 63

4.3 Area and percentage of LULC data in 2019 65

4.4 Error matrixes and accuracy assessment of LULC in 2019 67

4.5 Comparison of LULC change between 2014 and 2019 69

4.6 LULC change between 2014 and 2019 as a transitional matrix 71

4.7 Comparison of the annual rate of LULC change in two periods (1995-2014 and 2014-2019) 74

5.1 Multicollinearity statistics test of driving factors effect to LULC type 79

5.2 Multiple linear regression equation of each LULC type location preference and AUC value by logistic regression analysis 80

5.3 Conversion matrix of possible LULC change between 2019 and 2029 91

LIST OF TABLES (Continued)

Table Page

5.4 Transition probability matrix of LULC change between 2014 and 2019 by the Markov Chain model 91
5.5 Transition area matrix of LULC change between 2019 and 2029 from the Markov Chain model 92
5.6 Annual land demand of each LULC type for LULC simulation 92
5.7 Area of simulated LULC between 2020 and 2029 95
5.8 Percentage of simulated LULC between 2020 and 2029 96
5.9 Transition LULC change matrix between 2019 (Base year) and 2029. 101
6.1 SWAT parameter sensitivity to monthly streamflow at the X.191 station 106
6.2 Optimum parameter values of SWAT model for hydrologic component estimation under dry year condition 108
6.3 Average annual water balance components in calibration and validation periods of Khlong Bang Yai watershed under dry year condition 109
6.4 Model performance of the SWAT model for water flow estimation under dry year condition 110
6.5 Optimum parameter values of SWAT model for hydrologic component estimation under wet year condition 112
6.6 Average annual water balance components in calibration and validation periods of Khlong Bang Yai watershed under wet year condition 113
6.7 Model performance of the SWAT model for water flow estimation under wet year condition 114
6.8 Annual water balance of Phuket Island between 2020 and 2029 under dry year scenario (mm) 119
6.9 Annual water yield and average in each watershed between 2020 and 2029 under dry year scenario (mm) 123
6.10 Annual water yield and average in each watershed between 2020 and 2029 under dry year scenario (million m^3) 124

LIST OF TABLES (Continued)

Table Page

6.11 Average monthly water yield of Phuket Island between 2020 and 2029 under dry year scenario (mm) 126
6.12 Average monthly water yield of Phuket Island between 2020 and 2029 under dry year scenario (million m^3) 127
6.13 Annual water balance in Phuket Island between 2020 and 2029 under wet year scenario (mm) 128
6.14 Annual water yield and average in each watershed between 2020 and 2029 under wet year scenario (mm) 132
6.15 Annual water yield and average in each watershed between 2020 and 2029 under wet year scenario (million m^3)....133
6.16 Average monthly water yield of Phuket Island between 2020 and 2029 under wet year scenario (mm) 135
6.17 Average monthly water yield of Phuket Island between 2020 and 2029 under wet year scenario (million m^3) 136
6.18 Annual water balance in Phuket Island between 2020 and 2029 under dry and wet year scenarios (million m^3)....137
6.19 Area of primary LULC type in Phuket Island between 2020 and 2029 (km^2)....138
6.20 Data of urban and built-up area and water yield between 2020 and 2029 for six selected watersheds under dry year scenario 141
6.21 Data of urban and built-up area and water yield between 2020 and 2029 for six selected watersheds under wet year scenario 142
6.22 Data of idle land and water yield between 2020 and 2029 for six selected watersheds under dry year scenario. 143
6.23 Data of idle land and water yield between 2020 and 2029 for six selected watersheds under wet year scenario. 144

LIST OF TABLES (Continued)

Table Page

6.24 Data of perennial trees and orchards and water yield between 2020 and 2029 for six selected watersheds under dry year scenario. 145
6.25 Data of perennial trees and orchards and water yield between 2020 and 2029 for six selected watersheds under wet year scenario. 146
6.26 Data of evergreen forest and water yield between 2020 and 2029 for six selected watersheds under dry year scenario 147
6.27 Data of evergreen forest and water yield between 2020 and 2029 for six selected watersheds under wet year scenario 148
6.28 Summary basic information about the relationship between four LULC types and water yield in six watersheds under dry year scenario....158
6.29 Summary basic information about the relationship between four LULC types and water yield in six watersheds under wet year scenario....159
7.1 Register population by different community characteristics in Phuket Island between 2020 and 2029....166
7.2 Non-register population by different community characteristics in Phuket Island between 2020 and 2029....167
7.3 Residential population by different community characteristics in Phuket Island between 2020 and 2029....168
7.4 Residential water demand for the registered population by different community characteristics between 2020 and 2029....170
7.5 Residential water demand for the non-registered population by different community characteristics between 2020 and 2029....171
7.6 Total residential water demand by different community characteristics between 2020 and 2029....172

LIST OF TABLES (Continued)

Table Page
7.7 Tourist water demand between 2020 and 2029 under normal conditions............178
7.8 Tourist water demand between 2020 and 2029 under new normal conditions......180
7.9 Area of each agriculture and forest type between 2020 and 2029.....................183
7.10 Water demand for agriculture use between 2020 and 2029 185
7.11 Water demand for forest use between 2020 and 2029..186
7.12 Total water demand in different conditions between 2020 and 2029...............189
8.1 The annual water supply and demand balance evaluation without considering ecological water requirements between 2020 and 2029 195
8.2 Monthly tourist arrival and proportional rate 199
8.3 The average monthly tourists and excursionists between 2020 and 2029 under normal condition..200
8.4 The average monthly tourists and excursionists between 2020 and 2029 under new normal condition...200
8.5 The average monthly tourist water demand between 2020 and 2029 under normal and new normal conditions 201
8.6 The average monthly water demand estimation for agriculture and forest uses between 2020 and 2029...202
8.7 Average monthly water demand estimation of each category between 2020 and 2029 under normal and new normal conditions.................203
8.8 Monthly water supply and demand balance evaluation without ecological water requirement consideration between 2020 and 2029 204
8.9 The annual water supply and demand balance evaluation with ecological water requirement consideration between 2020 and 2029 209
8.10 Monthly water supply without and with ecological water requirement consideration under dry and wet year scenarios between 2020 and 2029.......212

LIST OF TABLES (Continued)

Table **Page**

8.11 Monthly water supply and demand balance evaluation with ecological water requirement consideration between 2020 and 2029 213

8.12 The annual water supply and demand balance evaluation in 25 watersheds without ecological water requirement consideration..218

8.13 The annual water supply and demand balance evaluation in 25 watersheds with ecological water requirement consideration..219

LIST OF FIGURES

Figure **Page**

1.1 Tourist arrivals to Phuket Island during 1993-2020 2
1.2 Population of Phuket province during 1993-2020 3
1.3 Elevation and topographic characteristics of the study area 9
2.1 Ordering of image elements in image interpretation 12
2.2 Overview of the information flow in the CLUE-S model 15
2.3 Flow chart of the allocation module of the CLUE-S model. 17
2.4 Schematic representation of the hydrologic cycle. 20
2.5 Schematic representation of the components of a water footprint. 29
2.6 Four distinct phases in water footprint assessment 31
3.1 Overview of research methodology framework 36
3.2 Schematic workflow of land use and land cover assessment and change detection 37
3.3 Schematic workflow of land use and land cover simulation 40
3.4 Schematic workflow of water yield estimation 42
3.5 Location of weather stations 46
3.6 Distribution of annual runoff in the dry and wet years at the X.191 station (Satree Phuket School) 48
3.7 Location of the X.191 station (Satree Phuket School) at Khlong Bang Yai watershed 49
3.8 Long-term historical rainfall data from the Thai Meteorological Department at Phuket and Phuket airport stations between 1999 and 2019 51
3.9 Schematic workflow of water demand estimation under normal conditions 52
3.10 Schematic workflow of water demand estimation under new normal conditions 53

LIST OF FIGURES (Continued)

Figure **Page**

3.11 Schematic workflow of water balance evaluation 56

3.12 The flow duration curve of X.191 station (Satree Phuket School) 57

4.1 Pleiades and SPOT imageries 59

4.2 Spatial distribution of LULC classification in 2014 62

4.3 Spatial distribution of LULC classification in 2019 64

4.4 Spatial distribution of sampling points superimposed on Google Earth image (2 Mar 2019) for accuracy assessment of thematic LULC map in 2019 66

4.5 Comparison satellite images with the ground photograph for inducing commission and omission error in visual interpretation among perennial trees and orchards and evergreen forest: (a) and (b) commission error of perennial trees and orchards from the evergreen forest, (c) and (d) omission error of evergreen forest from the mature rubber trees, and (e) and (f) omission error of evergreen forest from orchards 68

4.6 Comparison of the annual change rate of LULC type between 2014 and 2019 69

4.7 Development area of built-up areas found during the field survey in 2020 70

4.8 Distribution of LULC change between 2014 and 2019 72

4.9 Pattern of LULC change in terms of gain and loss of each LULC type of two periods (1995-2014 and 2014-2019) 74

5.1 Driving factors on LULC change: (a) Elevation (m), (b) Slope (%), (c) Distance to settlement (m), (d) Distance to road (m), (e) Distance to water bodies (m), (f) Soil fertility, (g) Population density at sub-district level, and (h) Average income per capita of the sub-district 77

5.2 Spatial distribution of the simulated LULC scenario between 2020 and 2029 93

LIST OF FIGURES (Continued)

Figure **Page**

6.1 Topographic map of Khlong Bang Yai watershed....................103

6.2 LULC in 2014 of Khlong Bang Yai watershed....................104

6.3 Soil texture distribution of Khlong Bang Yai watershed....................104

6.4 Slope distribution of Khlong Bang Yai watershed....................105

6.5 Spatial distribution of HRUs and catchments in Khlong Bang Yai watershed....................105

6.6 Monthly streamflow during calibration period of Khlong Bang Yai watershed under dry year condition....................110

6.7 Monthly streamflow during validation period of Khlong Bang Yai watershed under dry year condition....................110

6.8 Scatter plot between observed and estimated streamflow of Khlong Bang Yai watershed during calibration period under the dry year condition....................111

6.9 Scatter plot between observed and estimated streamflow of Khlong Bang Yai watershed during validation period under the dry year condition....................111

6.10 Monthly streamflow during calibration period of Khlong Bang Yai watershed under wet year condition....................114

6.11 Monthly streamflow during validation period of Khlong Bang Yai watershed under wet year condition....................114

6.12 Scatter plot between observed and estimated streamflow of Khlong Bang Yai watershed during calibration period under wet year condition....................115

6.13 Scatter plot between observed and estimated streamflow of Khlong Bang Yai watershed during validation period under wet year condition....................115

LIST OF FIGURES (Continued)

Figure Page

6.14 Monthly Phuket Island’s water yield in 2019 117

6.15 Twenty-five watershed for water yield estimation in Phuket Island 118

6.16 Temporal estimated water yield of Phuket Island between 2020 and 2029 under dry year scenario 120

6.17 Proportional hydrologic components of Phuket Island between 2020 and 2029 under dry year scenario 121

6.18 Temporal estimated evapotranspiration of Phuket Island between 2020 and 2029 under dry year scenarios...121

6.19 Average water yield between 2020 and 2029 in 25 watersheds under dry year scenario 122

6.20 Monthly average water yield in Phuket Island between 2020 and 2029 under dry year scenario 125

6.21 Temporal estimated water yield of Phuket Island between 2020 and 2029 under wet year scenario 129

6.22 Proportional hydrologic components of Phuket Island between 2020 and 2029 under wet year scenario 130

6.23 Temporal estimated evapotranspiration of Phuket Island between 2020 and 2029 under wet year scenario 130

6.24 Average water yield between 2020 and 2029 in 25 watersheds under wet year scenario 131

6.25 Monthly average water yield in Phuket Island between 2020 and 2029 under wet year scenario 134

6.26 Simple linear regression analysis between LULC type and water yield under dry year scenario 139

6.27 Simple linear regression analysis between LULC type and water yield under wet year scenario 140

LIST OF FIGURES (Continued)

Figure Page

6.28 Simple linear regression analysis between areas of urban and built-up area and water yield data from six watersheds under dry year scenario: (a) Khlong Bang Yai, (b) Khlong Kala, (c) Khlong Tha Rua, (d) Khlong Ban Na Kha, (e) Khlong Chang Phan Lang, and Khlong Ya Yai 150

6.29 Simple linear regression analysis between areas of urban and built-up area and water yield data from six watersheds under wet year scenario: (a) Khlong Bang Yai, (b) Khlong Kala, (c) Khlong Tha Rua, (d) Khlong Ban Na Kha, (e) Khlong Chang Phan Lang, and Khlong Ya Yai 151

6.30 Simple linear regression analysis between areas of idle land and water yield data from six watersheds under dry year scenario: (a) Khlong Bang Yai, (b) Khlong Kala, (c) Khlong Tha Rua, (d) Khlong Ban Na Kha, (e) Khlong Chang Phan Lang, and Khlong Ya Yai 152

6.31 Simple linear regression analysis between areas of idle land and water yield data from six watersheds under wet year scenario: (a) Khlong Bang Yai, (b) Khlong Kala, (c) Khlong Tha Rua, (d) Khlong Ban Na Kha, (e) Khlong Chang Phan Lang, and Khlong Ya Yai 153

6.32 Simple linear regression analysis between areas of perennial trees and orchards and water yield data from six watersheds under dry year scenario: (a) Khlong Bang Yai, (b) Khlong Kala, (c) Khlong Tha Rua, (d) Khlong Ban Na Kha, (e) Khlong Chang Phan Lang, and Khlong Ya Yai 154

6.33 Simple linear regression analysis between areas of perennial trees and orchards and water yield data from six watersheds under wet year scenario: (a) Khlong Bang Yai, (b) Khlong Kala, (c) Khlong Tha Rua, (d) Khlong Ban Na Kha, (e) Khlong Chang Phan Lang, and Khlong Ya Yai 155

LIST OF FIGURES (Continued)

Figure **Page**

6.34 Simple linear regression analysis between areas of evergreen forest and water yield data from six watersheds under dry year scenario: (a) Khlong Bang Yai, (b) Khlong Kala, (c) Khlong Tha Rua, (d) Khlong Ban Na Kha, (e) Khlong Chang Phan Lang, and Khlong Ya Yai 156

6.35 Simple linear regression analysis between areas of evergreen forest and water yield data from six watersheds under wet year scenario: (a) Khlong Bang Yai, (b) Khlong Kala, (c) Khlong Tha Rua, (d) Khlong Ban Na Kha, (e) Khlong Chang Phan Lang, and Khlong Ya Yai 157

6.36 Proportional LULC type area between 2020 and 2029: (a) Phuket Island and (b) Khlong Bang Yai watershed..161

7.1 The total number of registered populations of Phuket Island between 2020 and 2029 165

7.2 The spatial distribution of Phuket Island's average annual residential water demand between 2020 and 2029...173

7.3 Average annual residential water demand between 2020 and 2029 in different community characteristics 175

7.4 Number of tourists between 2020 and 2029 under normal conditions.............177

7.5 Tourist water demand between 2020 and 2029 under normal conditions 177

7.6 Number of tourists between 2020 and 2029 under new normal conditions 179

7.7 Tourist water demand between 2020 and 2029 under new normal conditions 179

7.8 The relationship between tourism growth and urban expansion in Phuket Island between 2020 and 2029 under normal conditions..................181

7.9 The relationship between tourism growth and urban expansion in Phuket Island between 2020 and 2029 under new normal conditions.........181

LIST OF FIGURES (Continued)

Figure **Page**

7.10 Monthly average water demand for agriculture use in Phuket Island between 2020 and 2029. 187

7.11 Monthly average water demand for forest use in Phuket Island between 2020 and 2029 187

8.1 Structure of water balance description with and without ecological water requirement consideration 191

8.2 Annual water supply without consideration for ecological water requirement and water demand between 2020 and 2029 under dry year scenario with normal and new conditions 196

8.3 Annual water supply without consideration for ecological water requirement and water demand between 2020 and 2029 under wet year scenario with normal and new normal conditions 197

8.4 The proportional rate of monthly tourist arrival in Phuket Island 199

8.5 Monthly water balance without ecological water requirement consideration between 2020 and 2029 under dry year scenario with normal and new normal condition 205

8.6 Monthly water balance without ecological water requirement consideration between 2020 and 2029 under wet year scenario with normal and new normal condition 206

8.7 Annual water supply with ecological water requirement consideration and water demand between 2020 and 2029 under dry year scenario with normal and new normal conditions 210

8.8 Annual water supply with ecological water requirement consideration and water demand between 2020 and 2029 under wet year scenario with normal and new normal conditions 211

LIST OF FIGURES (Continued)

Figure **Page**

8.9 Monthly water balance with ecological water requirement consideration between 2020 and 2029 under dry year scenario with normal and new normal condition....214

8.10 Monthly water balance with ecological water requirement consideration between 2020 and 2029 under wet year scenario with normal and new normal condition....215

9.1 The conceptual framework and research workflows 227

LIST OF ABBREVIATIONS

AUC = Area Under Curve
CLUE-S = Conversion of Land Use and Its Effects at Small regional extent
DEM = Digital Elevation Model
DOPA = Department of Provincial Administration
HRU = Hydrologic Response Unit
LDD = Land Development Department
LULC = Land use and Land Cover
NSE = Nash-Sutcliffe efficiency
PBIAS = Percent bias
R2 = Coefficient of determination
RID = Royal Irrigation Department
RSR = RMSE-observations standard deviation ratio
SWAT = The Soil and Water Assessment Tool
TAT = Tourism Authority of Thailand
TMD = Thai Meteorological Department
USGS = The United States Geological Survey

CHAPTER I

INTRODUCTION

1.1 Background problem and significance of the study

Water is a substance that plays a crucial component in the existence of life on Earth. Many water uses include agricultural, industrial, household, recreational, and environmental activities (Jermar, 1987), while water scarcity and droughts pose severe threats to the livelihood of farming communities and the economy (Alam, 2015). Recently, the balancing of water demand and supply has been investigated to mitigate water shortage problems in many countries. Kundu, Khare, and Mondal (2017) applied the SWAT model to assess the impact of the land use change on the water balance of the Narmada river basin in Madhya Pradesh, India. Kifle, Mengistu, Stoffberg, and Tadesse (2017) applied the Water Evaluation and Planning (WEAP) hydrological model and used population growth trends and climate change scenarios to investigate water demand and supply prospects for the City of Addis Ababa, Ethiopia. Reyes Perez (2017) applied Multi-Criteria Decision Analysis, considering environmental, technical, economic, and social aspects and relevant stakeholders' perspectives to assess water supply and demand management in Santa Cruz, Galápagos Island, Ecuador. Li, Yang, and Tan (2019) applied a system dynamics approach to simulate and optimize water supply and demand balance in Shenzhen, China. Liersch et al. (2019) applied the Soil and Water Integrated Model (SWIM) to assess the gaps between water demand and supply for water resources planning in Upper Niger and Bani River Basins (UNBB) in West Africa.

Phuket Island is the largest island in Thailand. It is located in the Andaman Sea, and it is the most desired place for tourist destinations. In the past 30 years, Phuket Island has seen considerable tourist growth (Sakunboonpanich, 2011). The information from TAT Intelligence Center, Tourism Authority of Thailand (2020) and Economics Tourism and Sports Division, Ministry of Tourism and Sports (2020) showed that the total number of domestic (Thai) and international (foreigner) tourists between 1993 and 2019 has dramatically increased from 2,088,179 persons in 1993 to 14,576,466 persons in 2019 (Figure 1.1). It can be observed that the threefold of tourists increased in the last decade while the number of tourists was dropped in some years. For instance, tourists declined to 2,510,276 in 2005 after the Indian Ocean Tsunami on 26 December 2004. Likewise, in the pandemic of H1N1 in 2009, the number of tourists dropped from 5,313,308 in 2008 to 3,375,931 in 2009. Similarly, tourists dropped from 14,576,466 in 2019 to 4,003,290 in 2020 due to the COVID-19 pandemic.

In the meantime, the number of the registered population of Phuket province has been continuously increased from 1993 to 2020 (Figure 1.2). The Phuket province population increased from 194,178 persons in 1993 to 414,471 persons in 2020 (Department of Provincial Administration, Ministry of Interior, 2020).

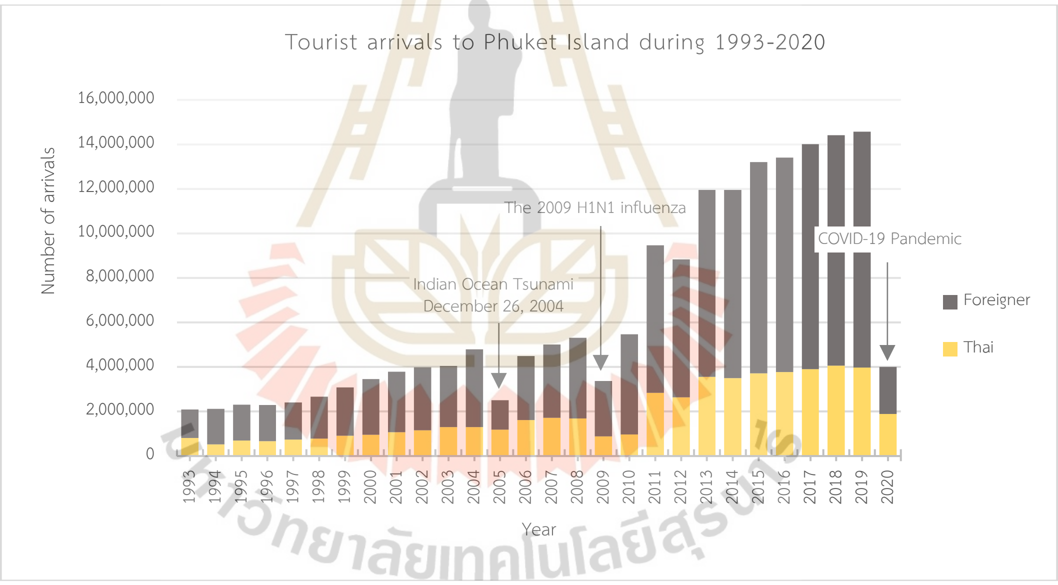

Source: Tourist arrivals to Phuket Island during 1993-2020 from TAT Intelligence Center, Tourism Authority of Thailand (2020) and Economics Tourism and Sports Division, Ministry of Tourism and Sports (2020).

Figure 1.1 Tourist arrivals to Phuket Island during 1993-2020.

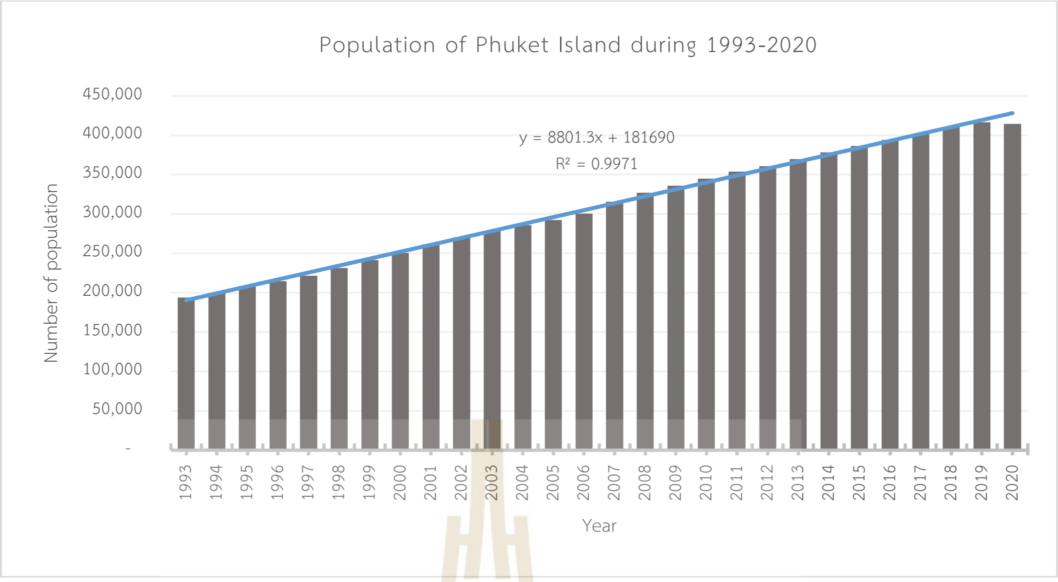

Source: Department of Provincial Administration, Ministry of Interior (2020).

Figure 1.2 Population of Phuket province during 1993-2020.

According to the annual report of Phuket province in 2010, water demand for consumption was approximately 51 million m^3/year, whereas water supply was about 46 million m^3/year. The water supply is categorized into three groups: surface water, groundwater, and seawater. Surface water accounts for about 38 million m^3/year, or 82% of the total water supply. In comparison, groundwater accounts for about 4 million m^3/year or 9% of the total water supply, and seawater was 4 million m^3/year or 9% of the total water supply.

Besides, average water demand in the future increases by about 2% per year according to economic growth and tourists. As a result, the estimation of water demand in 2017, 2027, and 2037 will be approximately 61 million m^3, 78 million m^3, and 101 million m^3, respectively (Information Technology and Communication Division, Phuket Provincial Office, 2010). Accordingly, balancing water supply and demand for consumption is very important for preventing water scarcity in Phuket Island.

During the last three decades, many researchers conducted various studies on Phuket Island’s water supply, demand, and balance. Charupongsopon (1990) applied statistical and field data to explore the location and distribution of water resources for the situation and trend of water demand and set areas to develop as a water storage source. Leelawattanagoon (2003) applied spatial data and stepwise regression to assess the streamflow characteristics of Phuket Island. Thepnuan (2007) applied System Dynamics (SD) to develop a system tool to analyze and explain significant variables that affect tourism development carrying capacity of water resources. Vongtanaboon, Boochabun, Meunpon, and Sriyaporn (2010) applied the runoff coefficient to assess water supply and water demand in terms of quantity and time, evaluate water situation in the future, and propose water resource management. Sma-air (2012) applied remote sensing data and field surveys to analyze surface-water resource amounts for water management. Hanuphab (2013) applied Geographic Information Systems (GIS) and SCS model to assess the water budget in Phuket Island. While, Suwanprasit, Puangkeaw, and Srichai (2013) applied Geographic Information Systems (GIS) and SCS model to assess the water balance of Phuket Island. Recently, Prince of Songkla University, Phuket Campus (2017) applied SCADA (Supervisory Control And Data Acquisition) to explorer surface water and created a database of current water sources. It is reliable for Phuket Island with an online display, can display the water level in real-time, and apply the information for Phuket Island water management.

Currently, water scarcity is a significant challenge to managing water resources in all regions of Thailand. Especially in tourist cities like Phuket Island, the increasing water demand trends depend on the registered population and tourists. However, previous research has not conducted the water balancing trend change in the long-term period (past, present, and future) based on LULC and weather scenarios. Thus, the integration of remote sensing, land use change modeling (CLUES model), and a distributed hydrological model (SWAT model) will be helpful to understand the trend of the water balance for mitigating water scarcity in the future. Over the last decades, the CLUE-S model has been one of the most widely applied models over different regions globally, addressing a wide range of land use change trajectories, including agricultural, urbanization, spatial policy, minimum environmental impact, and hydrological responses (Verburg and Overmars, 2007). Likewise, the SWAT model is recognized as one of the top hydrological models applied for addressing hydrologic and environmental issues (Arnold, Srinivasan, Muttiah, and Williams, 1998; Arnold and Fohrer, 2005). The SWAT model can be applied to assess monthly water yield based on LULC and its scenario and the impact of LULC change on water balance (e.g., Schilling, Jha, Zhang, Gassman, and Wolter, 2008; Zhou et al., 2013; Kundu et al., 2017).

Therefore, this study aims to simulate the LULC by the CLUE-S model, water supply estimation by the SWAT model, water demand using water footprint, and water balance analysis for sustainable water resources in Phuket Island. In addition, tourist water demand was separately estimated under normal and new normal conditions (COVID-19 pandemic) to fit with the actual situation at national and international levels. The results can quantify Phuket Island's water supply, demand, and water balance for sustainable water resources management in the future, mainly to prevent water scarcity.

1.2 Research objectives

The ultimate goal of the research is to simulate the LULC trend and water yield estimation for balancing water consumption supply and demand with a combination of different scenarios and conditions of water requirement considerations for mitigating water scarcity in Phuket Island. Specific research objectives are set as follows:

1. To assess LULC status and its change between 2014 and 2019 and to simulate LULC data between 2020 and 2029 using the CLUE-S model,
2. To estimate water yield (supply side) based on interpreted and simulated LULC data by SWAT model,
3. To estimate water demand (consumption) based on the water footprint, and
4. To evaluate water supply and demand balance between 2020 and 2029 for water resource management recommendations.

1.3 Scope and limitations of the study

1.3.1 Scope of the study

The scope of the study can be summarized as follows:

(1) To assess LULC status and its change between 2014 and 2019, LULC data in 2014 was adopted from Boonchoo (2015), while LULC data in 2019 was visually interpreted from Pleiades and SPOT imageries. In the meantime, LULC data between 2020 and 2029 were simulated using the CLUE-S model. Herein, the LULC classification

system consists of (1) urban and built-up areas (city and commercial, institutional land, industrial land, poultry farms, houses, airport, and seaport), (2) paddy fields, (3) field crops and horticulture, (4) perennial trees and orchards (para rubber and mixed orchards), (5) aquaculture areas, (6) idle land, (7) evergreen forests, (8) mangrove forests, (9) scrub forests, (10) water bodies (natural and artificial), and (11) miscellaneous land (beaches, soil pits, laterite pits, and landfill).

(2) Water supply data between 2020 and 2029 were estimated under two different weather scenarios (dry and wet year scenarios) based on weather data from the Thai Meteorological Department and Southern Region Irrigation Hydrology Center, Royal Irrigation Department in 2019 and 2016 for dry and wet year scenarios, respectively.

(3) Water demand data between 2020 and 2029 were estimated under two different conditions: normal and new normal (COVID-19 pandemic) based on water footprint from four primary consumption components (residential, tourists, agriculture, and forest uses).

This study considers the normal and new normal conditions in the tourist component since both conditions depend on tourist arrivals to Phuket Island. The normal condition denotes the tourist arrivals to Phuket Island in the normal situation; tourist arrivals were calculated according to the historical trend. On the contrary, the new normal condition represents the tourist arrivals to Phuket Island during the COVID-19 pandemic; tourist arrivals were calculated in three scenarios according to historical data and projected data in 2019 and 2020.

(4) Water balance data between 2020 and 2029 under two different scenarios (dry and wet years) and two different conditions (normal and new normal) were evaluated with and without ecological water requirement consideration in terms of surplus and deficit for water resource management.

1.3.2 Limitation of the study

Limitations of the study can be summarized as follows:

(1) For water supply estimation using the SWAT model, weather data between 1996 and 2019 were collected from local and surrounding meteorological stations of the study area include Phuket province, Phuket Airport, Krabi province, Ko

Lanta, and Takua Pa districts (TMD) and Bang wad reservoir (RID).

(2) For water demand estimation using a water footprint, the water consumption rate of people (residential and tourists) was estimated based on literature reviews and reports. Firstly, the water consumption rate for the residential was used from the Royal Irrigation Department (2011b). Secondly, the water consumption rate for the tourists was modified from Pansawad (1997) and Department of Public Works and Town and Country Planning (1993) as cited in Royal Irrigation Department (2011b), and Srichai, Kuayrakan, and Suwanprasit (2016). Thirdly, the water demand of agriculture and forest uses was estimated based on the evapotranspiration coefficient and reference evapotranspiration, as suggested by Allen, Pereira, Raes, and Smith (1998).

(3) To calculate the number of residential (registered and non-registered population) for water demand estimation under normal and new normal (COVID-19 pandemic) conditions. The number of registered populations in 2020 was extracted from a database of the Department of Provincial Administration (DOPA), Ministry of Interior, while the number of non-registered populations in 2020 was calculated by subtraction between censused and registered populations. Meanwhile, the number of residential (registered and non-registered populations) between 2021 and 2029 was estimated based on historical data using the Trend Analysis tool of MS Excel software.

(4) To calculate the number of tourists for water demand estimation under normal conditions, the number of tourists between 2020 and 2029 was estimated based on historical data using Trend Analysis. On the contrary, the number of tourists between 2020 and 2029 under new normal conditions (COVID-19 pandemic) was adopted from the projected tourists in the future by the Economics Tourism and Sports Division, Ministry of Tourism and Sports (2020), according to historical data and projected data, in 2019 and 2020, respectively. In this condition, three future tourist scenarios were presented with 45%, 65%, and 85% of tourists in 2019 for 2021, 2022, and 2023 respectively. In the meantime, the number of tourists between 2024 and 2029 was used the same data as normal conditions.

1.4 Study area

Phuket Island is located in Southern Thailand. It is the largest island of Thailand and sits on the Andaman Sea. Phuket Island is 49 kilometers from north to south and 21 kilometers from east to west. Phuket Island has an area of about 522 km^2 (Figure 1.3). The mountain area represents around 70% of the island. A few peaks are located in the north/east of Phuket, and it's the place to discover some exotic waterfalls in the evergreen forest. The other 30% of the island is a flat area located in the central and eastern parts of Phuket Island. The elevation of the study area varies from 0 to 546 meters above mean sea level. Phuket Island has a tropical monsoon climate, which is influenced by the Southwest monsoon. Phuket Island has two distinct seasons: summer (December to March) and rainy (April to November) (Information Technology and Communication Division, Phuket Provincial Office, 2012). The average annual rainfall from 2002 to 2011 was approximately 2,350 mm (Suwanprasit et al. 2013), while the average annual temperature of approximately 28.1 degrees Celsius (Thai Meteorological Department, 2017). Two primary water resources of the island are surface water and groundwater. There are 111 sources for water consumption for surface water, with a total volume of 38.42 million m^3 (Prince of Songkla University, Phuket Campus, 2017). Meanwhile, the groundwater sources have the highest potential in the Metasediment aquifers area at Thep Kasattri Sub District, Thalang District. It can develop groundwater use at a depth of 20-40 m with 10-30 m^3/hour (Information Technology and Communication Division, Phuket Provincial Office, 2012).

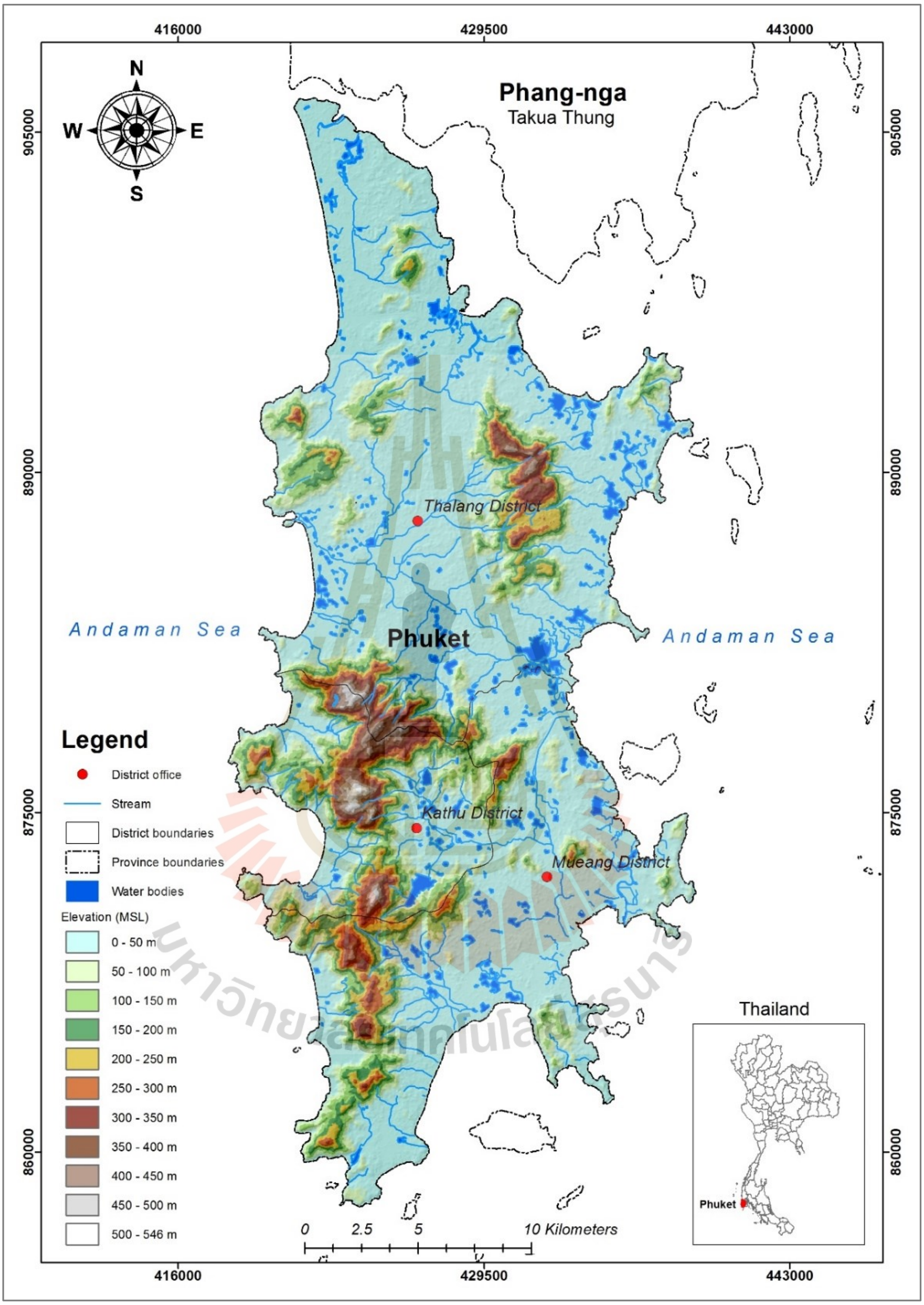
416000
429500
443000
905000
890000
875000
860000
N
W
E
S
Phang-nga
Takua Thung
Thalang District
Andaman Sea
Phuket
Andaman Sea
Kathu District
Mueang District
Legend
District office
Stream
District boundaries
Province boundaries
Water bodies
Elevation (MSL)
0 - 50 m
50 - 100 m
100 - 150 m
150 - 200 m
200 - 250 m
250 - 300 m
300 - 350 m
350 - 400 m
400 - 450 m
450 - 500 m
500 - 546 m
0 2.5 5 10 Kilometers
Thailand
Phuket

Figure 1.3 Elevation and topographic characteristics of the study area.

1.5 Benefits of the study

The benefits of the study are as follows:

(1) Understand the LULC status and its change in the past, present, and future between 2014 and 2029,

(2) Understand the water supply and water demand over the study periods,

(3) Realize the water balance in terms of surplus or deficit from a combination of different scenarios (dry and wet years) and different conditions (normal and new normal), and different water requirement considerations (with and without ecological water requirement consideration), and

(4) The derived information of this study can be used as obligatory information to support decision-makers, policymakers, and land use planners for the sustainable use of natural resources in Phuket Island.

CHAPTER II

BASIC CONCEPTS AND LITERATURE REVIEWS

The basic concepts, theories, and applications that are related to this study include (1) elements of image interpretation, (2) CLUE-S model and its applications, (3) SWAT model and its applications, and (4) water demand estimation based on water footprint and its applications, are summarized in this chapter.

2.1 Elements of image interpretation

Although most individuals have had substantial experience in interpreting "conventional" photographs in their daily lives (e.g., newspaper photographs), the interpretation of aerial and space images often departs from everyday image interpretation in three essential respects: (1) the portrayal of features from an overhead, often unfamiliar, perspective; (2) the frequent use of wavelengths outside of the visible portion of the spectrum; and (3) the depiction of the Earth's surface at unfamiliar scales and resolutions. While these factors may be insignificant to the experienced image interpreter, they can represent a substantial challenge to the novice image analyst! However, even this challenge continues to be mitigated by the extensive use of aerial and space imagery in such day-to-day activities as navigation, GIS applications, and weather forecasting. A systematic study of aerial and space images usually involves several essential features of an image. The extracted characteristics of features are helpful for any specific task and how they are considered to depend on the application. However, most applications consider the essential characteristics or variations, including shape, size, pattern, tone (or hue), texture, shadows, site, and association (Lillesand, Kiefer, and Chipman, 2004; Lillesand, Kiefer, and Chipman, 2015). These elements are shown in the order of their complexity in Figure 2.1.

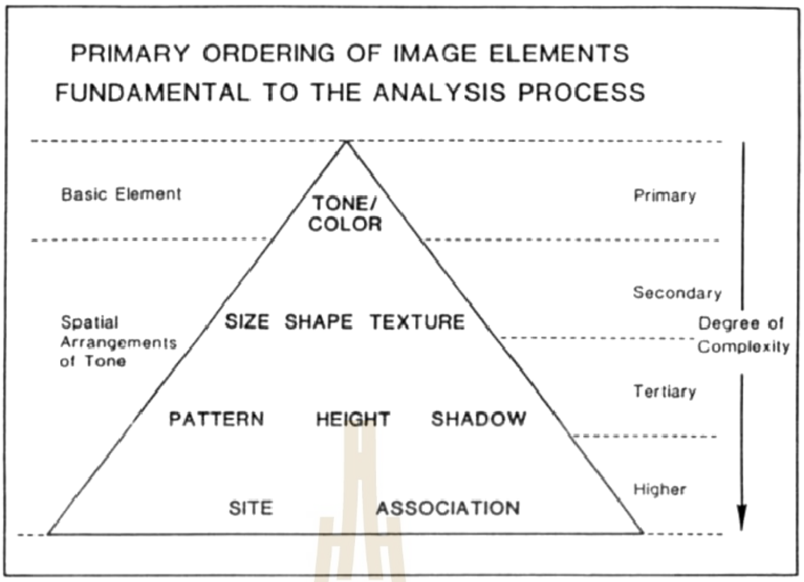
PRIMARY ORDERING OF IMAGE ELEMENTS
FUNDAMENTAL TO THE ANALYSIS PROCESS
Basic Element
TONE/
COLOR
Primary
Secondary
Spatial
Arrangements
of Tone
SIZE SHAPE TEXTURE
Degree of
Complexity
Tertiary
PATTERN HEIGHT SHADOW
Higher
SITE ASSOCIATION

Source: Estes et al. (1983) quoted in Herold, Liu, and Clarke (2003).

Figure 2.1 Ordering of image elements in image interpretation.

Brief information of elements for image interpretation based on Lillesand et al., 2004; Campbell and Wynne, 2011; Lillesand et al., 2015; Dhopte, 2017 can be summarized in the following sections.

Tone (or hue) refers to the relative brightness or color of objects on an image. Image tone is the fundamental element for distinguishing between different objects. It can be defined as the relative brightness or darkness, or color of objects or regions within an image. The variations in image tone also allow the elements of shape, texture, and pattern of objects to be distinguished.

The size of objects on images must be considered in the context of the image scale. For example, small storage might be misinterpreted as a dam if the size was not considered. Relative sizes among objects on images of the same scale must also be considered during image interpretation.

Shape refers to the general form, configuration, or outline of individual objects. In the case of stereoscopic images, the object’s height also defines its shape. The shape of some objects is so distinctive that their images may be identified solely from this criterion. The Pentagon building near Washington, DC, is a classic example. All shapes are not this diagnostic, but every shape is of some significance to the image interpreter.

The texture is the frequency of tonal change in an image. The texture is produced by an aggregation of unit features that may be too small to be discerned individually on the image, such as tree leaves and leaf shadows. It is a product of their shape, size, pattern, shadow, and tone. It determines the overall visual "smoothness" or "coarseness" of image features. As the image scale reduces, the texture of any given object or area becomes progressively finer and ultimately disappears. An interpreter can often distinguish between features with similar reflectances based on their texture differences. An example would be the smooth texture of green grass as contrasted with the rough texture of green tree crowns on medium-scale air photos.

The pattern relates to the spatial arrangement of objects. The repetition of certain general forms or relationships is characteristic of many objects, both natural and constructed, and gives objects a pattern that aids the image interpreter in recognizing them. For example, the ordered spatial arrangement of trees in an orchard contrasts with forest tree stands.

Shadow is also helpful in interpretation as it may provide an idea of the profile and relative height of a target or targets, making identification easier. However, a shadow is vital to interpreters in two opposing aspects: (1) the shape or outline of a shadow affords an impression of the profile view of objects (which aids interpretation), and (2) objects within shadows reflect little light and are difficult to discern on an image (which hinders interpretation). For example, the shadows cast by various tree species or cultural features (bridges, silos, towers, etc.) can help identify air photos.

Site refers to topographic or geographic location and is a precious aid in identifying vegetation types. For example, specific tree species would be expected to occur on well-drained upland sites, whereas other species would occur on poorly drained lowland sites. Also, various tree species occur only in specific geographic regions (e.g., redwoods occur in California, but not in Indiana).

Association refers to the occurrence of specific features to others. For example, a Ferris wheel might be challenging to identify if standing in a field near a barn, but it would be easy to identify if in an area recognized as an amusement park.

Besides, the spatial resolution depends on many factors. Still, it always places a practical limit on interpretation because some objects are too small or have too little contrast with their surroundings to be seen on the image. Other factors, such as image scale, image color balance, and condition of images (e.g., torn or faded photographic prints), also affect the success of image interpretation activities. However, the visual interpretation of satellite images is applied successfully in many fields, including geology, geography, agriculture, forestry, and water resources.

2.2 CLUE-S model and its applications

2.2.1 Background and model structure of the CLUE-S model

The Conversion of Land Use and its Effects (CLUE) modeling framework was developed to simulate land use change using empirically quantified relations between land use and its driving factors in combination with dynamic modeling of competition between land use types (Veldkamp and Fresco, 1996; Verburg, Koning, Kok, Veldkamp, and Bouma, 1999). Initially, the model was developed for the national and continental levels. Then, the modeling approach was modified for study areas with a relatively small spatial extent, called CLUE-S (Conversion of Land Use and its Effects at Small regional extent). The model structure is based on systems theory to allow the integrated analysis of land use change concerning socio-economic and biophysical driving factors (Verburg et al., 2002). Additionally, the CLUE-S model can simulate the future LULC map cartographically to continue the former CLUE model (Verburg and Overmars, 2007).

Verburg et al. (1999) stated that the information needed to run the CLUE-S model is shown in Figure 2.2. The required information of CLUE-S can be categorized into four groups: (1) spatial policies and restrictions, (2) land use types specific conversion settings, (3) land requirements, and (4) location characteristics.

(1) Spatial policies and restrictions

Spatial policies and restrictions mainly indicate areas where land use changes are restricted through policies or tenure status. Some spatial policies restrict a set of specific land use conversions, e.g., residential construction in designated agricultural areas or permanent agriculture in the buffer zone of a nature reserve. The conversions restricted by a specific spatial policy can be indicated in a land use conversion matrix. For all possible land use conversions, it is indicated if the spatial policy applies.

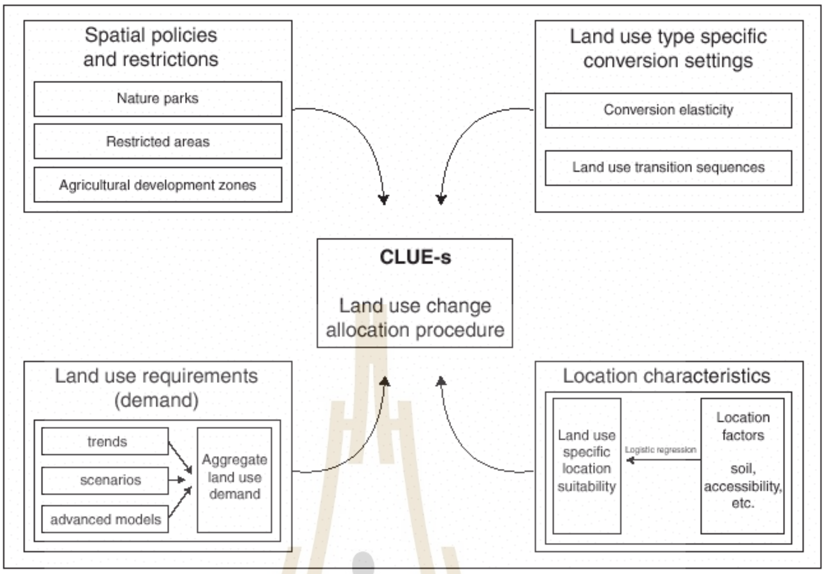
Spatial policies and restrictions
Nature parks
Restricted areas
Agricultural development zones
Land use type specific conversion settings
Conversion elasticity
Land use transition sequences
CLUE-s
Land use change allocation procedure
Land use requirements (demand)
trends
scenarios
advanced models
Aggregate land use demand
Location characteristics
Land use specific location suitability
Logistic regression
Location factors
soil, accessibility, etc.

Source: Verburg et al. (1999).

Figure 2.2 Overview of the information flow in the CLUE-S model.

(2) Specific land use type conversion settings

Specific land use type conversion settings determine the temporal dynamics of the simulations. Two parameters are needed to characterize the individual land use types: conversion elasticities and land use transition sequences. The conversion elasticity is related to the reversibility of land use change. Examples are residential locations but also plantations with permanent crops (fruit trees). Meanwhile, land use type characteristics needed to be specified are land use type, specific conversion settings, and temporal characteristics. The simulation of these interactions combined within the constraints set in the conversion matrix will determine the length of the period before a conversion occurs.

(3) Land use requirements (demand)

Land use requirements (demand) are calculated at the aggregate level (the case study level as a whole) as part of a specific scenario. The land use requirements constrain the simulation by defining the required change in land use.

(4) Location characteristics

Land use conversions are expected to occur at locations with the highest preference for the specific type of land use at that moment in time. The preference of a location is empirically estimated from factors based on the different disciplinary understandings of the determinants of land use change. The preference is calculated using the following equation.

$$R_{ki} = a_k X_{1i} + b_k X_{2i} + \ldots.. \tag{2.1}$$

Where R is the preference to devote location i to land use type k, $X_{1,2,..}$ are biophysical or socio-economical characteristics of location i and a_k and b_k the relative impact of these characteristics on the preference for land use type k.

A statistical model can be developed as a binomial logit model. The function that relates these probabilities to biophysical and socio-economic location characteristics is defined as a logit model using the following equation.

$$Log\left(\frac{P_i}{1-P_i}\right) = \beta_0 + \beta_1 X_{1,i} + \beta_2 X_{2,i} \ldots.. + \beta_n X_{n,i} \tag{2.2}$$

Where P_i is the probability of a grid cell for the considered land use type on location i, and the X's are the location factors. The coefficients (β) are estimated through logistic regression using the actual land use pattern as the dependent variable.

In summary, the allocation procedure is displayed in Figure 2.3. The following steps are taken to allocate the changes in land use:

1. The first step includes the determination of all grid cells that are allowed to change. Grid cells that are either part of a protected area or presently under a land use type that is not allowed to change are excluded from the further calculation.

2. For each grid cell i, the total probability ($TPROP_{i,u}$) is calculated for each land use type u according to Equation (2.3).

$$TPROP_{i,u} = P_{i,u} + ELAS_u + ITER_u \tag{2.3}$$

Where $P_{i,u}$ are the suitability of location i for land use type u (based upon the logit model), $ELAS_u$ is the conversion elasticity for land use u, and $ITER_u$ is an iteration variable that is specific for the land use type and indicative for the relative competitive strength of the land use type. $ELAS_u$, the specific land use type elasticity to change the value, is only added if grid-cell i is already under land use type u in the year considered. $P_{i,u}$ consists of a part based on the biophysical and socio-economic factors and a neighborhood interaction part.

3. A preliminary allocation is made with an equal value of the iteration variable (*ITERu*) for all land use types by allocating the land use type with the highest total probability for the considered grid cell.

4. The total allocated area of each land use is compared with the land use requirements (demand).

5. Steps 2 to 4 are repeated as long as the demands are not correctly allocated. When allocation equals demand, the final map is saved, and the calculations can continue next.

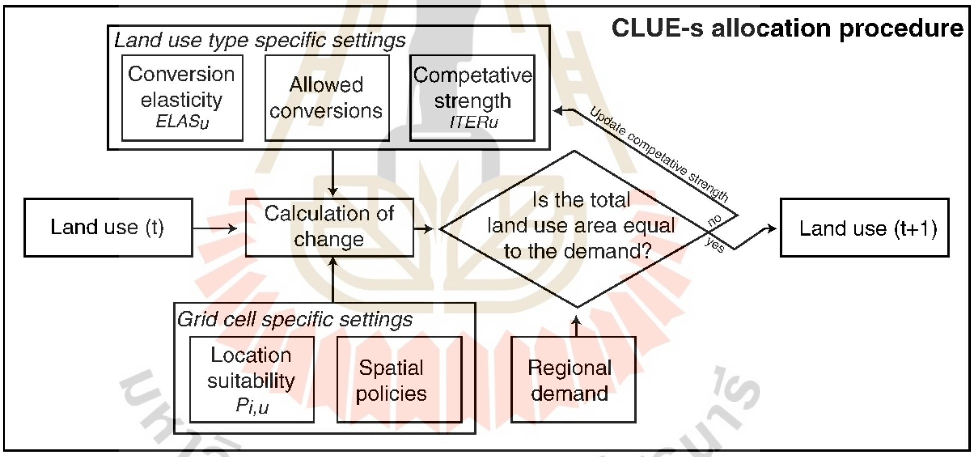
CLUE-s allocation procedure
Land use type specific settings
Conversion elasticity ELASu
Allowed conversions
Competative strength ITERu
Update competative strength
Land use (t)
Calculation of change
Is the total land use area equal to the demand?
no
yes
Land use (t+1)
Grid cell specific settings
Location suitability Pi,u
Spatial policies
Regional demand

Source: Verburg et al. (1999).

Figure 2.3 Flow chart of the allocation module of the CLUE-S model.

2.2.2 CLUE-S model applications

CLUE-S model is one of the most widely applied models over the different regions of the globe, addressing a wide range of land use changes. It can be summarized in the following sections.

Oh, Yoo, Lee, and Choi (2011) applied the CLUE-S model to predict future paddy field area changes under climate change scenarios in Yongin, Icheon, and Anseong, South Korea. Hu, Zheng, and Zheng (2013) applied the CLUE-S model and

Markov model to investigate and simulate land use patterns in Beijing. Zhou et al. (2013) applied the CLUE-S and the SWAT model to understand and quantify the hydrological responses of LULC changes in the Xitiaoxi River basin, China. Han, Yang, and Song (2015) applied LULC models to simulate future land use demand by combining a CLUE-S model with a Markov model to deal with some shortcomings of existing LULC models in Beijing, China. While, Ongsomwang and Iamchuen (2015) applied the CLUE-S model to integrate geospatial models for minimum environmental impact in Upper Lam Phra Phloeng Watershed, Nakhon Ratchasima Province, Thailand. Ongsomwang and Boonchoo (2016) applied the CA-Markov model, Land Change Modeler (LCM), and CLUE-S model to optimum geospatial model identification for the LULC prediction and its integration of geospatial models for the deforestation vulnerability analysis (DVA) for the allocation of deforestation hotspots and forest protection units to prevent deforestation protected forest areas (PFAs) of Phuket Island. While, Trisurat, Eawpanich, and Kalliola (2016) applied the CLUE-S model to predict future LULC changes during 2009-2020, and conceivable changes in rainfall may influence future rainfall levels of water yield and sediment load in the Thadee River. Also, Zhang et al. (2016) applied the CLUE-S model to predict the spatial distribution of green manure in cropland and orchards in 2020 in Pinggu District located in Beijing, China. Liu et al. (2017) applied the CLUE-S model to investigate the relationship between government policy and land use change to develop an understanding applicable to formulating strategies for sustainable land use in Lijiang River Basin, Guangxi Zhuang Autonomous Region, China. Recently, Ongsomwang, Pattanakiat, and Srisuwan (2019) applied object-based image analysis (OBIA) and CLUE-S model to assess the impact of LULC Change on Ecosystem Service Values in Khon Kaen, Thailand. Srichaichana, Ongsomwang, and Trisurat (2019) applied the Integrated Valuation of Ecosystem Services and Trade-offs (InVEST) and CLUE-S model to identify the LULC scenario for optimum water yield and sediment retention ecosystem services in the Klong U-Tapao watershed, Songkhla Province, Thailand.

The literature reviews about CLUE-S model applications can be highlighted as follows:

(1) CLUE-S model is one of the most widely applied models over the different regions globally, addressing a wide range of land use change trajectories, including agricultural, urbanization, spatial policy, minimum environmental impact, and hydrological responses (e.g., Verburg and Overmars, 2007).

(2) The CLUE-S model is an integrated land use change model that can simulate land use change with socio-economic and biophysical driving factors such as the economy, population, and government policy. This advantage is limited by using the CA-Markov model (e.g., Verburg and Overmars, 2007; Han et al., 2015).

(3) CLUE-S model is compelling for LULC prediction under different scenarios (e.g., Ongsomwang and Iamchuen, 2015; Ongsomwang and Boonchoo, 2016; Ongsomwang et al., 2019; Srichaichana et al., 2019).

2.3 SWAT model and its applications

2.3.1 Background of the SWAT model

The SWAT model is a conceptual, continuous-time model that was developed in the early 1990s to assist water resource managers in assessing the impact of management and climate on water supplies and non-point source pollution in watersheds and large river basins (Arnold et al., 1998; Arnold and Fohrer, 2005) and it is the continuation of over 30 years of model development. Dr. Jeff Arnold first developed the US Department of Agriculture's Agricultural Research Service model, and it was developed to "scale-up" past field-scale models to large river basins. The SWAT model is a basin-scale, continuous-time model that operates daily and is designed to predict the impact of management on water, sediment, and agricultural chemical yields in ungauged watersheds. The model is physically based, computationally efficient, and capable of continuous simulation over long periods. Major model components include weather, hydrology, soil temperature and properties, plant growth, nutrients, pesticides, bacteria and pathogens, and land management. (Arnold and Fohrer, 2005; Gassman, Reyes, Green, and Arnold, 2007; Douglas-Mankin, Srinivasan, and Arnold, 2010).

2.3.2 Procedure of water yield estimation

Water balance is the main driving force behind all the processes in SWAT because it impacts plant growth and the movement of sediments, nutrients, pesticides, and pathogens. Simulation of watershed hydrology is separated into the land phase, which controls the amount of water, sediment, nutrient, and pesticide loadings to the main channel in each sub-basin (Figure 2.4), and the in-stream or routing phase, which is the movement of water, sediments, etc., through the channel network of the watershed to the outlet (Arnold, Moriasi, et al., 2012).

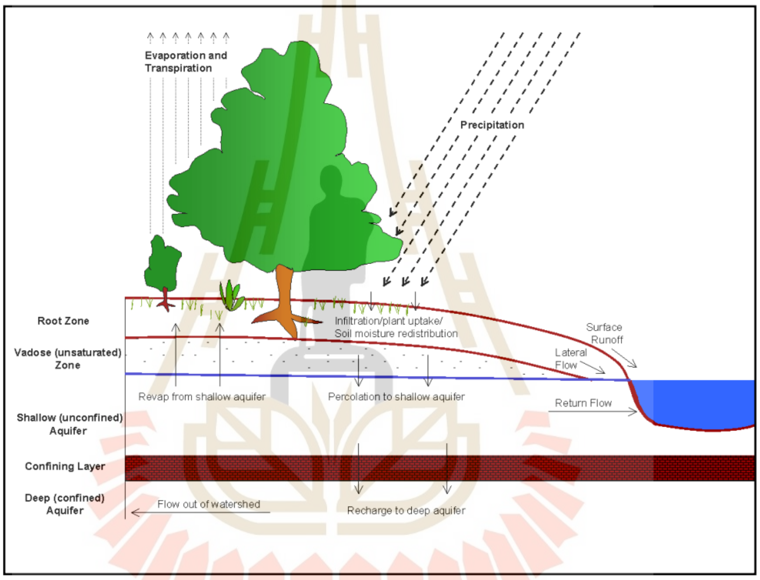
Evaporation and Transpiration
Precipitation
Root Zone
Vadose (unsaturated) Zone
Shallow (unconfined) Aquifer
Confining Layer
Deep (confined) Aquifer
Infiltration/plant uptake/ Soil moisture redistribution
Surface Runoff
Lateral Flow
Revap from shallow aquifer
Percolation to shallow aquifer
Return Flow
Flow out of watershed
Recharge to deep aquifer

Source: Neitsch et al. (2009).

Figure 2.4 Schematic representation of the hydrologic cycle.

According to the hydrological cycle, the SWAT model simulates final soil water content, as shown in Equation (2.4) (Neitsch, Arnold, Kiniry, and Williams, 2005; Neitsch, Arnold, Kiniry, and Williams, 2009).

$$SW_t = SW_o + \sum_{i=1}^{t} (R_{day} - Q_{surf} - E_a - W_{seep} - Q_{gw})_i \qquad (2.4)$$

Where SW_t is the final soil water content (mm water); SW_o is the initial soil water content in day i (mm water); t is the time (days); R_{day} is the amount of precipitation in day i (mm water); Q_{surf} is the amount of surface runoff in day i (mm water); E_a is the amount of evapotranspiration in day i (mm water); W_{seep} is the amount of water entering the vadose zone from the soil profile in day i (mm water); and Q_{gw} is the amount of return flow in the day i (mm water).

One of the critical parameters applied to evaluate sustainable water resource management of the study area is the water yield. Water yield is the aggregate sum of water, leaving the HRU and entering the principle channel during the time step (Arnold, Moriasi, et al., 2012). The water yield of a watershed is evaluated by the model based on Equation (2.5).

$$W_{yld} = Q_{surf} + Q_{gw} + Q_{lat} - T_{loss} \tag{2.5}$$

Where W_{yld} is the measure of water yield (mm), Q_{surf} is the surface runoff (mm), Q_{lat} is the lateral flow contribution to stream (mm), Q_{gw} is the groundwater contribution to streamflow (mm), and T_{loss} is the transmission losses (mm) from tributary in the HRU using transmission through the bed. The estimation of surface runoff can be performed by the model using the SCS curve number system by the USDA Soil Conservation Service in Equation (2.6).

$$Q_{surf} = \frac{(R_{day}-0.2S)^2}{(R_{day}+0.8S)} \tag{2.6}$$

Where Q_{surf} is the accumulated runoff or rainfall excess (mm), R_{day} is the rainfall depth for the day (mm), S is the retention parameter (mm). The retention parameter S and the prediction of lateral flow (Q_{lat}) by the SWAT model are defined in Equations (2.7) and (2.8), respectively.

$$S = 25.4\left(\frac{100}{CN}-10\right) \tag{2.7}$$

$$Q_{lat} = 0.024\,\frac{(2SSC \sin \alpha)}{\theta_d L} \tag{2.8}$$

Where Q_{lat} is lateral flow (mm/day); S is a drainable volume of soil water per unit area of the saturated thickness (mm/day); SC is saturated hydraulic conductivity (mm/h); L is flow length, α is the slope of the land, θ_d is drainable porosity, and CN is the soil curve number. The estimation of the base flow was done using Equation (2.9).

$$Q_{gwj} = Q_{gwj-1.}\ e^{(-\alpha_{gwj}.\Delta t)} + W_{rchrg.}\ (1-e^{(-\alpha_{gwj}.\Delta t)}) \tag{2.9}$$

Where Q_{gwj} is groundwater flow into the main channel on day_j; α_{gw} is base flow recession constant; Δt is the time step, and W_{rchrg} is the amount of recharge entering the aquifers (mm day -1).

A watershed is divided into multiple catchments in the SWAT model; they are then subdivided into hydrologic response units (HRUs) consisting of homogeneous land use, management, topographical, and soil characteristics. The HRUs are represented as a percentage of the catchment area and may not be contiguous or spatially identified within a SWAT simulation. Alternatively, a watershed can be subdivided into catchments characterized by dominant land use, soil type, and management (Arnold, Moriasi, et al., 2012).

Below is a brief description of the processes simulated by SWAT. The hydrologic cycle is climate-driven and provides moisture and energy inputs, such as daily precipitation, maximum/minimum air temperature, solar radiation, wind speed, and relative humidity, that control the water balance. SWAT can read these observed data directly from files or generate simulated data from observed monthly statistics at runtime. Snow is computed when temperatures are below freezing, and soil temperature is computed because it impacts water movement and the decay rate of residue in the soil (Arnold, Moriasi, et al., 2012).

Hydrologic processes simulated by SWAT include canopy storage, surface runoff, infiltration, evapotranspiration, lateral flow, tile drainage, redistribution of water within the soil profile, consumptive use through pumping (if any), return flow, and recharge by seepage from surface water bodies, ponds, and tributary channels. SWAT uses a single plant growth model to simulate all land cover types and differentiates between annual and perennial plants. The plant growth model is used to assess the removal of water and nutrients from the root zone, transpiration, and biomass/yield production. SWAT uses the Modified Universal Soil Loss Equation (MUSLE) to predict sediment yield from the landscape. Besides, SWAT models the movement and transformation of several forms of nitrogen and phosphorus, pesticides, and sediment in the watershed. SWAT allows the user to define management practices taking place in every HRU. Once the loadings of water, sediment, nutrients, and pesticides from the land phase to the main channel have been determined, the loadings are routed through the streams and reservoirs within the watershed. The water balance for reservoirs includes inflow, outflow, rainfall on the surface, evaporation, seepage from the reservoir bottom, and diversions (Arnold, Moriasi, et al., 2012).

SWAT input parameters are process-based and must be held within a realistic uncertainty range. The first step in the calibration and validation process in SWAT is determining the most sensitive parameters for a given watershed or catchment. The user determines which variables to adjust based on expert judgment or sensitivity analysis. Sensitivity analysis determines the rate of change in model output to changes in model inputs (parameters). It is necessary to identify critical parameters and the parameter precision required for calibration.

In a practical sense, this first step helps determine the effective processes for the component of interest. Two types of sensitivity analysis are generally performed: local, by changing values one at a time, and global, by allowing all parameter values to change. The two analyses, however, may yield different results. The sensitivity of one parameter often depends on the value of other related parameters; hence, the problem with the one-at-a-time analysis is that the correct values of fixed parameters are never known. The disadvantage of the global sensitivity analysis is that it needs a large number of simulations. Both procedures, however, provide insight into the sensitivity of the parameters and are necessary steps in model calibration.

The second step is the calibration process. Calibration is an effort to better parameterize a model to a given set of local conditions, reducing the prediction uncertainty. Model calibration is performed by carefully selecting values for model input parameters (within their respective uncertainty ranges) by comparing model predictions (output) for a given set of assumed conditions with observed data for the same conditions.

The final step is validation for the component of interest (streamflow, sediment yields, etc.). Model validation is the process of demonstrating that a given site-specific model can make sufficiently accurate simulations, although “sufficiently accurate” can vary based on project goals. Validation involves running a model using parameters determined during the calibration process and comparing the predictions to observed data not used in the calibration process. In general, proper model calibration and validation should involve: (1) observed data that include wet, average, and dry years, (2) multiple evaluation techniques, (3) calibrating all constituents to be evaluated, and (4) verification that other important model outputs are reasonable (Arnold, Moriasi, et al., 2012).

2.3.3 Model performance evaluation

Generally, graphical and statistical methods with objective statistical criteria determine when the model has been calibrated and validated. Calibration and validation can be accomplished manually or using auto-calibration tools in SWAT-Calibration and Uncertainty Program (SWAT-CUP). SWAT-CUP software provides users with the ability to select specific model parameters for auto-calibration within defined boundaries. It executes hundreds of SWAT runs to find the optimal set of parameter values that minimize the error between model predictions and observed data (Arnold, Moriasi, et al., 2012).

Calibration and validation are typically performed by splitting the available observed data into two datasets: calibration and validation. Data are most frequently split by periods, carefully ensuring that the climate data used for both calibration and validation are not substantially different, i.e., wet, moderate, and dry years occur in both periods. Data may also be split spatially, with all available data at a given monitoring location assigned to the calibration phase and correspondingly performing the validation at one or more other gauges within the watershed. This approach can be necessary when users are faced with data-limited situations that preclude performing a split-time calibration and validation using a single gauge. Although these are the recommended calibration and validation approaches, they are not enforced, and thus there are several ways in which SWAT has been calibrated and validated (Arnold, Moriasi, et al., 2012).

Most published SWAT applications report both graphical and statistical hydrologic calibration results, especially for streamflow, and hydrologic validation results are also reported for a large percentage of the studies. By far, the most widely used statistics reported for calibration and validation are RMSE-observations standard deviation ratio (RSR), Nash-Sutcliffe efficiency (NSE), and Percent bias (PBIAS) based on Equations (2.10) to (2.12), respectively.

RSR is the standardized RMSE using the observed standard deviation. RSR is calculated as the ratio of the RMSE and the standard deviation of measured data. It varies from 0 to large positive values. The lower the RSR, the better the model fit (Legates and McCabe, 1999).

NSE is a normalized statistic that determines the relative magnitude of the residual variance ("noise") compared to the measured data variance ("information"). NSE values can range between −∞ and 1.0 (1 inclusive), with NSE = 1 being the optimal value. Values between 0.0 and 1.0 are generally viewed as acceptable performance levels, whereas values <0.0 indicate that the mean observed value is a better predictor than the simulated value, indicating unacceptable performance (Nash and Sutcliffe, 1970).

PBIAS measures the average tendency of the simulated data to be larger or smaller than their observed counterparts. The optimal value of PBIAS is 0.0, with low-magnitude values indicating accurate model simulation. Positive values indicate underestimation bias, whereas negative values indicate model overestimation bias (Gupta, Sorooshian, and Yapo, 1999).

$$RSR = \frac{RMSE}{STDEV_{Obs}} = \frac{\sqrt{\sum_{i=1}^{n} (O_i - S_i)^2}}{\sqrt{\sum_{i=1}^{n} (O_i - \bar{O})^2}} \tag{2.10}$$

$$NSE = 1 - \frac{\sum_{i=1}^{n} (O_i - S_i)^2}{\sum_{i=1}^{n} (O_i - \bar{O})^2} \tag{2.11}$$

$$PBIAS = \frac{\sum_{i=1}^{n} (O_i - S_i) \times 100}{\sum_{i=1}^{n} (O_i)} \tag{2.12}$$

Where S_i is the simulated value and O_i is the observed value at the time i. $\bar{O}$ is the mean of the individual observations of O_i, and n is the number of observations. The statistics check the model efficiency, and the performance of these statistics is rated according to Moriasi et al. (2007), given in Table 2.1.

Table 2.1 Model performance scale.

Performance rating	RSR	NSE	PBIAS
Very good	0.00 < RSR < 0.50	0.75 < NSE < 1.00	PBIAS < ± 10
Good	0.50 < RSR < 0.60	0.65 < NSE < 0.75	±10 < PBIAS < ± 15
Satisfactory	0.60 < RSR < 0.70	0.50 < NSE < 0.65	±15 < PBIAS < ± 25
Unsatisfactory	RSR >0.70	NSE <0.50	PBIAS > ± 25

Source: Moriasi et al. (2007).

2.3.4 SWAT model applications

The SWAT model is recognized as one of the top hydrological models applied for addressing hydrologic and environmental issues. It can be summarized in the following sections.

Prachayasittikul (2006) applied the SWAT model to simulate managing water resources in the Songkhla Lake Basin, Thailand. Schilling et al. (2008) applied the SWAT model to consider the possible consequences of future LULC change from biofuel expansion on the water balance of the Raccoon River watershed, USA. Baker and Miller (2013) applied the SWAT model to assess land use impact on water resources in an East African watershed. While, Ongsomwang and Kunto (2013) applied the SWAT model to estimate water runoff and the CA Markov model to predict land use changes in the Huay Tung Lung watershed of Mun basin, Ubon Ratchathani province. Wuttichaikitcharoen and Santan (2013) applied the SWAT model to determine the proper parameters for assessing accurate and reliable runoff in Mae Chaem Basin. Wangpimool, Pongput, Sukvibool, Sombatpanit, and Gassman (2013) applied the SWAT model to evaluate the impact of changing conditions in the river basin affected by streamflow due to reforestation in the Upper Nan river basin, Nan Province. At the same time, Zhou et al. (2013) applied the SWAT and CLUE-S model to examine the impacts of land use change on hydrological fluxes in a rapid urbanization region in the lower reach of the Yangtze River, China. Adeniyi, Bolaji, Adebayo, and Michael (2014) applied the SWAT to predict water balance and water yield of Upstream Catchment of Jebba Dam in Nigeria. Leta, El-Kadi, Dulai, and Ghazal (2016) applied the SWAT model to illustrate that a watershed model can be applied for water balance analysis in highly permeable (volcanic soils) Heeia watershed in Hawaii, USA. Kundu et al. (2017) applied the SWAT model and Markov Chain model to assess the land use change and its impact on the water balance of the study area, which is a part of the Narmada river basin in Madhya Pradesh, India. Ayivi and Jha (2018) applied the SWAT model to estimate water balance and water yield in the Reedy Fork-Buffalo Creek Watershed in North Carolina. Raksmey and Chantha (2018) applied the SWAT model to test the applicability of simulating the streamflow through daily and monthly calibration and validation in the Stung Pursat River catchment, an ungauged sub-catchment of Tonle Sap Basin in Cambodia. Sangkatananon, Chotamonsak, and Dhanasin (2018) applied the SWAT model to evaluate the model's efficiency for runoff simulation in the Wang River Basin, Thailand. Tamm, Maasikamäe, Padari, and Tamm (2018) applied the SWAT model to estimate the potential impacts of land use (deforestation and afforestation) and climate change on water resources West-Estonian river basin district, located in the north-eastern Baltic Sea region, Estonian. Recently, Abou Rafee et al. (2019) applied the SWAT model to present large-scale hydrological modeling of the Upper Paraná River Basin central-southern, Brazil. Osei et al. (2019) applied the SWAT model to simulate streamflow and establish the water balance and projected streamflow amounts under different climatic and land use scenarios of Owabi catchment, Ghana.

The SWAT model can be applied for many purposes; the interesting results can be highlighted as follows:

(1) The input data required for the SWAT model includes topography or DEM, LULC, soil, weather, and observation runoff data.

(2) The calibration and validation of the SWAT model applied the concept of sensitivity analysis (e.g., Wuttichaikitcharoen and Santan, 2013).

(3) The SWAT model can provide monthly water yield (e.g., Raksmey and Chantha, 2018).

(4) The SWAT model can apply with small island watersheds with large topographic, precipitation, and land use gradients (e.g., Leta et al., 2016).

(5) The SWAT model can be applied to assess water yield based on LULC and its scenario and the impact of LULC change on water balance (e.g., Schilling et al., 2008; Zhou et al., 2013; Kundu et al., 2017).

(6) The performance of the SWAT model is a promising tool to predict water balance and water yield for sustainable management of water resources. Besides, it can apply to quantify blue and green water availability (e.g., Adeniyi et al., 2014).

2.4 Water demand estimation based on water footprint and its applications

2.4.1 Water footprint concepts

The idea of considering water use along supply chains has gained interest after introducing the "water footprint" concept by Hoekstra in 2002. The water footprint is an indicator of freshwater use that looks at the direct water use of a consumer or producer and indirect water use. The water footprint can be defined as a comprehensive indicator of freshwater resource appropriation, next to the traditional and restricted measure of water withdrawal.

The water footprint is the volume of freshwater used to produce the product, measured over the entire supply chain. It is a multidimensional indicator, showing water consumption volumes by source and polluted volumes by type of pollution; all components of a total water footprint are specified geographically and temporally. The blue water footprint refers to the consumption of blue water resources (surface and groundwater) along the supply chain of a water product. "consumption" refers to water loss from the available ground-surface water body in a catchment area. Losses occur when water evaporates, returns to another catchment area or the sea or is incorporated into a product. The green water footprint refers to the consumption of green water resources (rainwater insofar as it does not become runoff). The grey water footprint refers to pollution, defined as the volume of freshwater required to assimilate pollutants given natural background concentrations and existing ambient water quality standards. As an indicator of "water use," the water footprint differs from the standard measure of "water withdrawal" in three aspects (Figure 2.5):

1. It does not include blue water use insofar as it is returned to where it comes from.

2. It is not restricted to blue water use but also includes green and greywater.

3. It is not restricted to direct water use but also includes indirect water use.

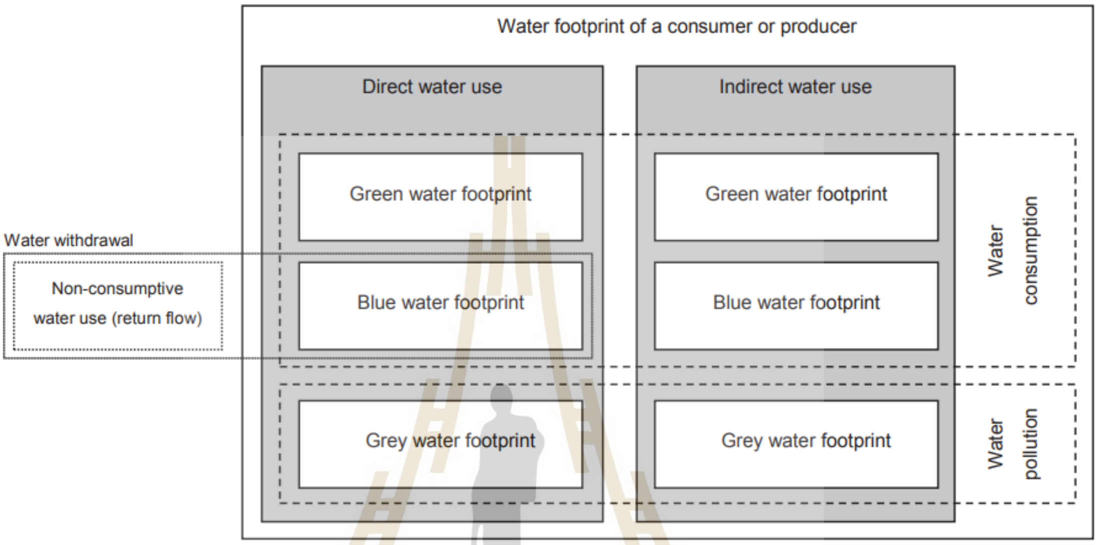
Water footprint of a consumer or producer
Direct water use
Indirect water use
Green water footprint
Green water footprint
Water withdrawal
Non-consumptive water use (return flow)
Blue water footprint
Blue water footprint
Water consumption
Grey water footprint
Grey water footprint
Water pollution

Note: It shows that the non-consumptive part of water withdrawals (the return flow) is not part of the water footprint. It also shows that contrary to the measure of “water withdrawal,” the “water footprint” includes green and grey water and the indirect water-use component.

Source: Hoekstra et al. (2011).

Figure 2.5 Schematic representation of the components of a water footprint.

The water footprint thus offers a better and broader perspective on how a consumer or producer relates to the use of freshwater systems. It is a volumetric measure of water consumption and pollution. It is not a measure of the severity of the local environmental impact of water consumption and pollution. The local environmental impact of a certain amount of water consumption and pollution depends on the vulnerability of the local water system and the number of water consumers and polluters that make use of the same system.

Water footprint accounts give spatiotemporally explicit information regarding how water is appropriated for various human purposes. They can feed the discussion about sustainable and equitable water use and allocation and form a reasonable basis for locally assessing environmental, social, and economic impacts (Hoekstra, Chapagain, Aldaya, and Mekonnen, 2011).

2.4.2 Water footprint assessment

Water footprint assessment studies at the basin level are critical and vital in the sustainable development of freshwater resources (Muratoglu, 2019). Water security assessment based on the water footprint concept becomes widely accepted globally (e.g., Zang and Liu, 2013; Veettil and Mishra, 2016; Giri, Arbab, and Lathrop, 2018; Mosase, Ahiablame, and Srinivasan, 2019; Nouri, Borujeni, and Hoekstra, 2019). By definition, water footprint assessment refers to the full range of activities to (1) quantify and locate the water footprint of a process, product, producer or consumer or to quantify in space and time the water footprint in a specified geographic area; (2) assess the environmental, social and economic sustainability of this water footprint; and (3) formulate a response strategy. In general, assessing water footprints analyzes how human activities or specific products relate to water scarcity and pollution issues and see how activities and products can become more sustainable from a water perspective (Hoekstra et al., 2011). The water footprint assessment is the methodological framework under which a full range of water footprint studies are to be conducted in phases (Figure 2.6), including:

1. Defining goals and scope: determine study objectives, scope, and boundaries,
2. Accounting water footprint: quantify water footprint (of a process or product) and locate where it occurs,
3. Assessing water footprint sustainability: analyze and evaluate the sustainability of the water footprint within a geographical context (e.g., a basin) from environmental, economic, and social perspectives, and
4. Formulating water footprint response strategies: identify response strategies and measures to improve water footprint sustainability.

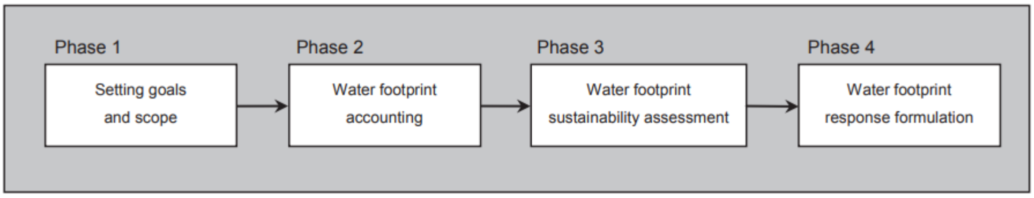
Phase 1
Setting goals and scope
Phase 2
Water footprint accounting
Phase 3
Water footprint sustainability assessment
Phase 4
Water footprint response formulation

Source: Hoekstra et al. (2011).

Figure 2.6 Four distinct phases in water footprint assessment.

2.4.3 Water demand estimation based on water footprint applications

Zang and Liu (2013) assessed the significance of simulation results from the SWAT model for blue and green water flows, the total flow, and the proportion of the total accounted for by green water. They also predicted future trends in the Heihe River, China. Miguel Ayala et al. (2016) applied the water footprint concepts to study the impact of soybean field expansion on water footprint under climate change scenarios in the Amazon, Brazil. Veettil and Mishra (2016) applied the concept of blue and green water footprints and the SWAT model to quantify freshwater (blue water and green water) availability in the Savannah River Basin, USA. Giri et al. (2018) applied blue and green water concepts and the SWAT model to predict the consequences of future land use change on blue versus green water security in The Raritan Basin, Central New Jersey, USA. While, Veettil and Mishra (2018) applied the SWAT model to quantify the Spatio-temporal variability of water security indicators such as blue water scarcity, green water scarcity, Falkenmark index, and freshwater provision indicators in the Savannah River Basin (SRB), USA. At the same time, Luan, Wu, Sun, Wang, and Gao (2018) applied the water footprint and SWAT model to establish a method for calculating the water footprint of crop production based on hydrological processes in the Hetao irrigation district (HID), China. Recently, Mosase et al. (2019) applied the SWAT model to characterize freshwater availability and scarcity in the Limpopo River Basin (LRB) in Southern Africa. Nouri et al. (2019) assessed the blue water footprint (WF) of urban greenery in Adelaide, South Australia.

Application of water demand estimation based on water footprint can be summarized as follows:

(1) The geographical water footprint assessment can be helpful when applied at the regional level since it gives a good insight into the current uses of water and their potential impact in the future (e.g., Miguel Ayala et al., 2016).

(2) The blue and green water scarcity will support watershed managers' and policy-makers efforts to sustainably manage water resources under changing land use and climate (e.g., Giri et al., 2018).

(3) An integrated assessment of water footprint, environmental flow, anthropogenic factors, and climatic variables can provide helpful information on the rising (how and where) of water-related risk to human and ecological health (e.g., Veettil and Mishra, 2016, 2018).

(4) The water footprint is incorporated into the set of indicators that usually are applied in water resources management and hydrological planning (e.g., Zang and Liu, 2013; Veettil and Mishra, 2016, 2018).

CHAPTER III

RESEARCH PROCEDURES

The research procedures, which include equipment, data, and research methodology, are described in this chapter.

3.1 Equipment

Equipment includes hardware and software are summarized below:

- Desktop Computer, Notebook,
- GPS Handheld,
- Camera,
- ESRI ArcMap (visual interpretation),
- ERDAS Imagine (change detection analysis),
- IDRISI (Markov chain model; Land requirement (demand), Elasticity value, and LULC conversion matrix),
- CLUE-S Model (LULC simulation), and
- ArcSWAT Model Version 2012 (water yield estimation)

3.2 Data

Data collected and prepared in advance include remotely sensed data, GIS data, and primary and secondary data, summarized in Table 3.1.

Table 3.1 List of data collection and preparation for analysis and modeling in the study.

Data	Data collection	Data preparation	Source	Component
RS	Pleiades and SPOT imagery in 2019 (spatial resolution of 2.4 meters)		CNES/Airbus, Maxar Technologies (Google satellite maps)	1
GIS	1. Administrative boundary		DEQP	2
	2. LULC data in 2002 (color orthophoto image)	LULC SWAT code to link with the SWAT database	Boonchoo (2015)	3
	3. LULC data in 2014 (Pan-sharpened THEOS image, spatial resolution of 2 meters)	LULC SWAT code to link with the SWAT database	Boonchoo (2015)	1 and 3
	4. Digital elevation model	1. Resampling into 50 meters spatial resolution (only for LULC simulation) 2. Buffering distance from elevation (meter) 3. Slope 3.1 Buffering distance from the slope (meter) 3.2 Slope class for cerate HRU 4. Create a watershed and catchments	USGS	2 and 3
	5. Soil series	1. Recode soil fertility 2. Create a hydrologic soil group 3. Soil code to link with the SWAT database	LDD	2 and 3
	6. Stream	Create a catchments	DEQP	3
	7. Road	Buffering distance from road (meter)	PSO MOT	2
	8. Settlement	Buffering distance from the settlement (meter)	LULC data in 2019	2
	9. Waterbody	Buffering distance from the water body (meter)	LULC data in 2019	2
Primary	Ground verification in 2020	1. Multinomial distribution 2. Stratified random sampling		1
Secondary	1. Daily weather between 1996 and 2019		TMD and SRIHC RID	3
	2. Daily weather between 2000 and 2010		NCEP	3
	3. Daily runoff observed between 1999 and 2019		SRIHC RID	3
	4. Registered population between 1993 and 2020	Calculate population density (people/km^2)	DOPA MOI	2 and 4
	5. Census data between 1960 and 2010		NSO	4
	6. Tourist arrivals data between 1993 and 2020		TATIC TAT and ETSD MOTS	4
	7. The average income of the population	Calculation from personal income by sub-district area	NSO	2

Note: USGS: The United States Geological Survey; LDD: Land Development Department; DEQP: Department of Environmental Quality Promotion; PSO MOT: Permanent Secretary Office, Ministry of Transport; TMD: Thai Meteorological Department; SRIHC RID: Southern Region Irrigation Hydrology Center, Royal Irrigation Department; NCEP: The National Centers for Environmental Prediction; DOPA MOI: Department of Provincial Administration, Ministry of Interior; NSO: National Statistical Office; TATIC TAT: TAT Intelligence Center, Tourism Authority of Thailand; ETSD MOTS: Economics Tourism and Sports Division, Ministry of Tourism and Sports.

3.3 Research methodology

The overview of the research methodology framework, which includes data collection and preparation, land use and land cover assessment and change detection, land use and land cover simulation, water yield estimation, water demand estimation, and water balance evaluation, is displayed in Figure 3.1. Details of each component, excluding data collection and preparation, were separately described in the following sections.

3.3.1 Land use and land cover assessment and change detection

Under this component, the LULC data in 2019 was visually interpreted based on Pleiades and SPOT imagery. Then, the interpreted LULC in 2019 was assessed accuracy using randomly stratified sampling points based on the multinomial distribution theory and a field survey in 2020 with additional high spatial images as reference data. Finally, the collected and interpreted LULC data were used to assess its status and detect LULC change between 2014 and 2019 using a post-classification comparison change detection algorithm. The derived results of this component are further applied to simulate LULC data between 2020 and 2029 using the CLUE-S model in the next component.

The workflow of land use and land cover assessment and change detection is displayed in Figure 3.2. At the same time, details of significant tasks under this component include (1) LULC visual interpretation, (2) accuracy assessment, and (3) LULC change detection are explained in the following sections.

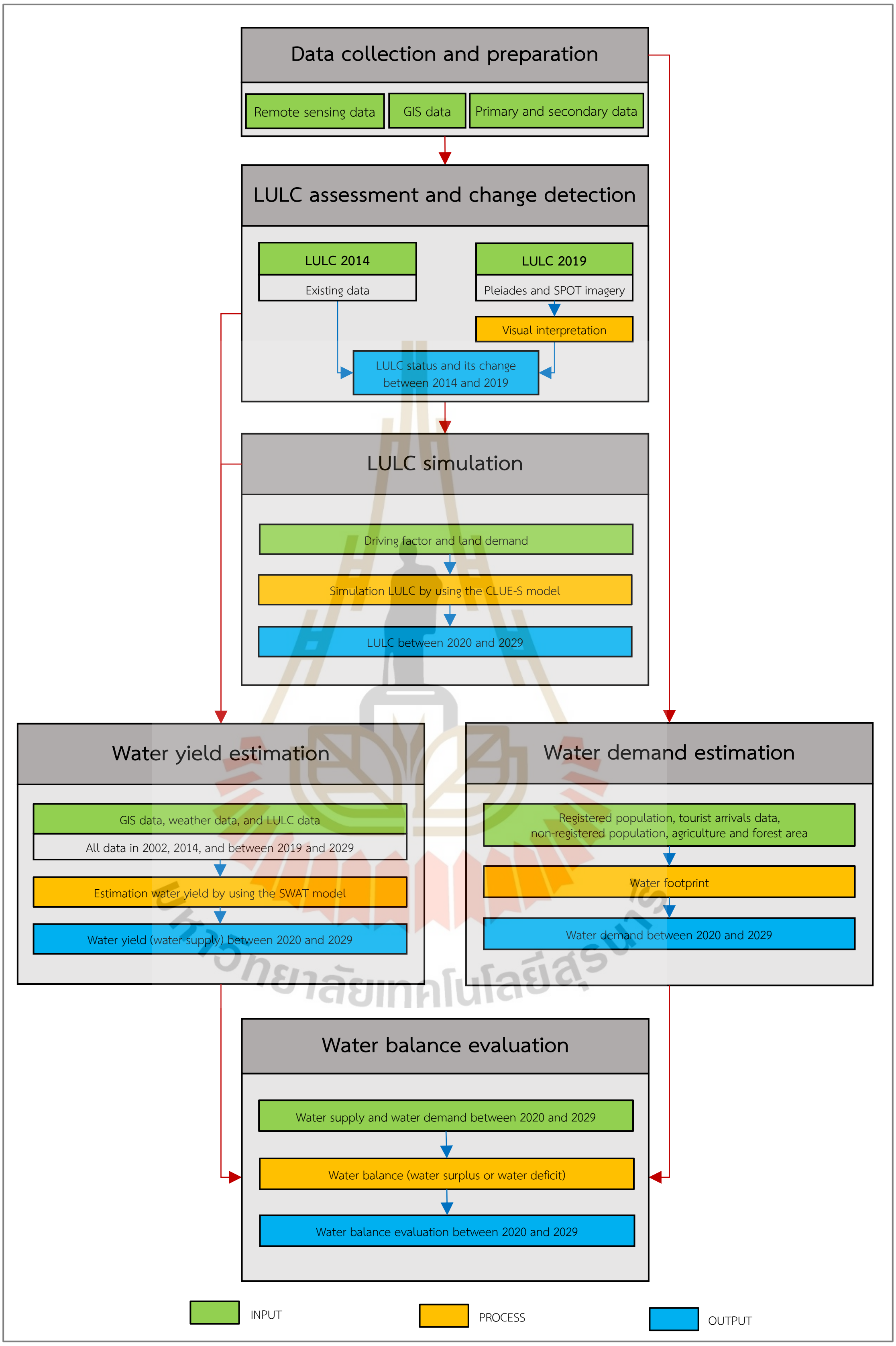
Data collection and preparation
Remote sensing data
GIS data
Primary and secondary data
LULC assessment and change detection
LULC 2014
Existing data
LULC 2019
Pleiades and SPOT imagery
Visual interpretation
LULC status and its change between 2014 and 2019
LULC simulation
Driving factor and land demand
Simulation LULC by using the CLUE-S model
LULC between 2020 and 2029
Water yield estimation
GIS data, weather data, and LULC data
All data in 2002, 2014, and between 2019 and 2029
Estimation water yield by using the SWAT model
Water yield (water supply) between 2020 and 2029
Water demand estimation
Registered population, tourist arrivals data, non-registered population, agriculture and forest area
Water footprint
Water demand between 2020 and 2029
Water balance evaluation
Water supply and water demand between 2020 and 2029
Water balance (water surplus or water deficit)
Water balance evaluation between 2020 and 2029
INPUT
PROCESS
OUTPUT

Figure 3.1 Overview of research methodology framework.

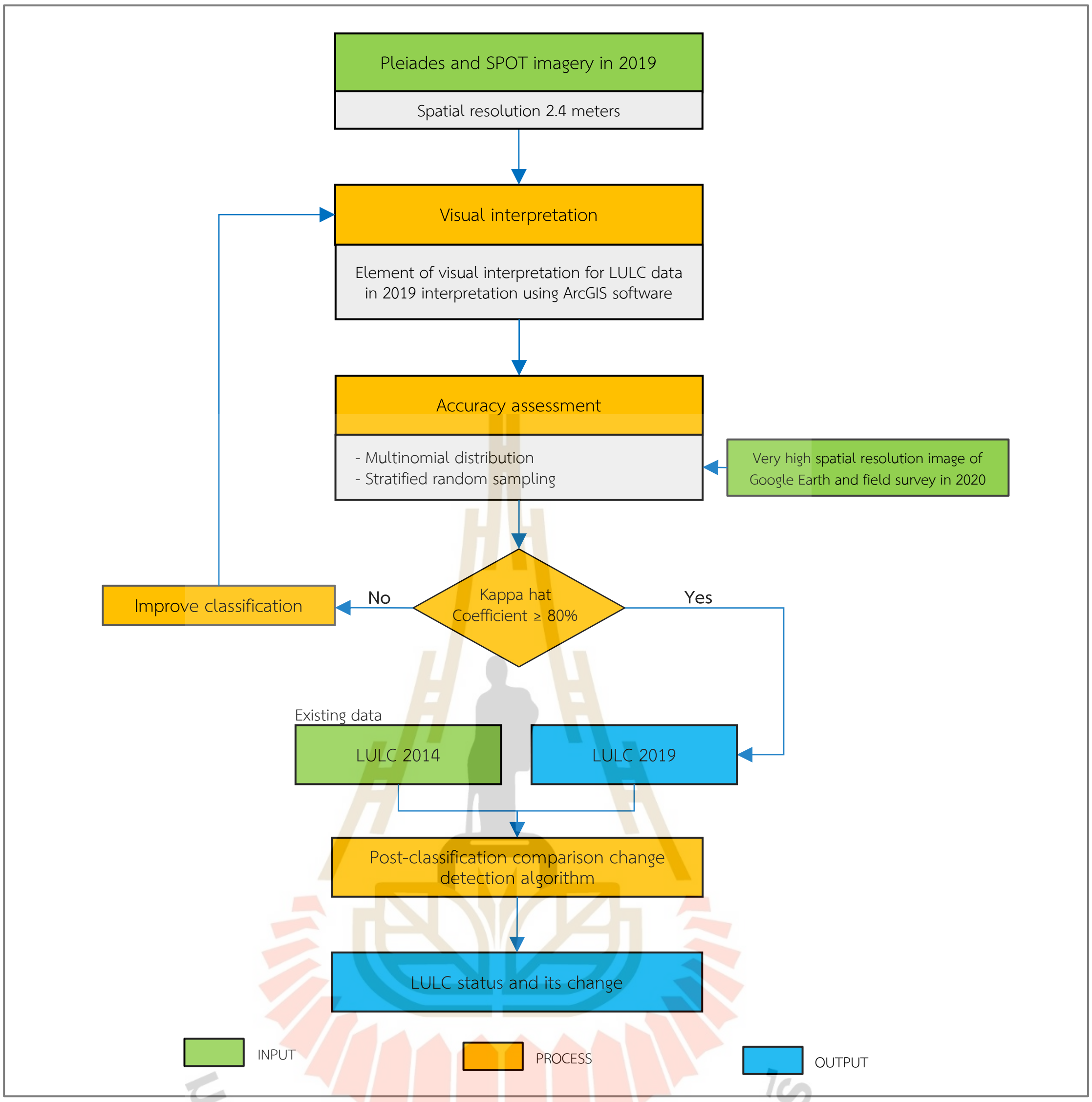
Pleiades and SPOT imagery in 2019
Spatial resolution 2.4 meters
Visual interpretation
Element of visual interpretation for LULC data in 2019 interpretation using ArcGIS software
Accuracy assessment
- Multinomial distribution
- Stratified random sampling
Very high spatial resolution image of Google Earth and field survey in 2020
Kappa hat Coefficient ≥ 80%
No
Yes
Improve classification
Existing data
LULC 2014
LULC 2019
Post-classification comparison change detection algorithm
LULC status and its change
INPUT
PROCESS
OUTPUT

Figure 3.2 Schematic workflow of land use and land cover assessment and change detection.

Table 3.2 Description of LULC classification system.

No.	LULC classes	Description
1	Urban and built-up area	It consists of villages, city and commercial, institutional land, industrial land, airport, golf course, and seaport.
2	Paddy field	It is an active paddy field.
3	Field crop and horticulture	It consists of pineapple, mixed field crop, truck crop, floricultural/ornamental plant, and mixed horticulture.
4	Perennial trees and orchards	It comprises perennial trees and orchards (e.g., rubber tree, palm tree, coconut, durian, mangosteen, rambutan, and longan).
5	Aquaculture	The aquatic culture area includes a shrimp farm and fish pond.
6	Idle land	It is cultivated but is now in a state of disuse, abandoned land, and fallow land.
7	Evergreen forest	It is a natural forest and primarily situates in hilly and mountainous areas.
8	Mangrove forest	It is a natural forest and primarily situates in mud soil along the coastal zone.
9	Scrub forest	It consists of thickets of shrubs and young trees.
10	Waterbody	It includes rivers and streams, ponds, and reservoirs.
11	Miscellaneous land	It consists of a beach, soil pit, laterite pit, and landfill.

(1) LULC visual interpretation

The LULC map in 2019 was visually interpreted from Pleiades and SPOT imagery using the element of visual interpretation (Lillesand et al., 2004, 2015). In this study, the LULC classes consist of (1) urban and built-up areas (city and commercial, institutional land, industrial land, poultry farms, houses, airport, and seaport), (2) paddy fields, (3) field crops and horticulture, (4) perennial trees and orchards (para rubber trees and mixed orchards), (5) aquaculture areas, (6) idle land, (7) evergreen forests, (8) mangrove forests, (9) scrub forests, (10) water bodies (natural and artificial), and (11) miscellaneous land (beaches, soil pits, laterite pits, and landfill). The description of the LULC type is summarized in Table 3.2.

(2) Accuracy assessment

The preliminary LULC map in 2019 was assessed thematic accuracy using 660 randomly stratified sampling points based on the multinomial distribution theory (Tortora (1978) as cited in Congalton and Green (2009) with the desired levels of 95% confidence and 5% precision by field survey in 2020. The desired statistical measurements include producer's accuracy (commission error), user's accuracy (omission error), overall accuracy, and Kappa coefficient of agreement.

(3) LULC change detection

The collected and interpreted LULC data were used to detect LULC change between 2014 and 2019 using a post-classification comparison change detection algorithm, which is widely used to extract "from-to" change class information (Coppin, Jonckheere, Nackaerts, Muys and Lambin (2004); Jensen, 2015).

3.3.2 Land use and land cover simulation

Under this component, land demand in the future (between 2020 and 2029) was first estimated based on the annual rate of each LULC class from the transition area matrix of LULC change between 2014 and 2019 using the Markov Chain model. Then, the driving factors on LULC change were identified LULC type location preference by binomial logistic regression analysis for allocating LULC type between 2020 and 2029. Finally, the future LULC data between 2020 and 2029 were simulated using the CLUE-S model.

The workflow of land use and land cover simulation is shown in Figure 3.3. At the same time, details of significant tasks under this component include (1) land demand estimation, (2) LULC type location preference, and (3) LULC simulation using the CLUE-S model are described in the following sections.

(1) Land demand estimation

Land demand between 2020 and 2029 was estimated based on the annual rate of LULC change between 2014 and 2019 from the transition area matrix using the Markov chain model. In general, the Markov chain is a stochastic process model that describes the probability of change from one state to another, i.e., from one land use type to another, using a transition probability matrix. The transition probability is that a land cover type (pixels) at the time t_0 changes to another land cover type at the time t_1. Therefore, changes in land use between the dates are used to develop a probability transition matrix and then predict land uses later (Cabral and Zamyatin, 2009). The mathematical expression of the transition probability is:

$$\sum_{l=1}^{m} P_{ij}=1,\ i=1,2,\ldots m \tag{3.1}$$

$$P = \left(P_{ij}\right) = \begin{Bmatrix} P_{11} & P_{12}\ldots P_{1m} \\ P_{21} & P_{22}\ldots P_{2m} \\ P_{31} & P_{32}\ldots P_{3m} \end{Bmatrix}$$

Where, P_{ij} is the probability of transition from one land use to another, m is the type within land use of the area studied, P_{ij} values are within the range 0-1.

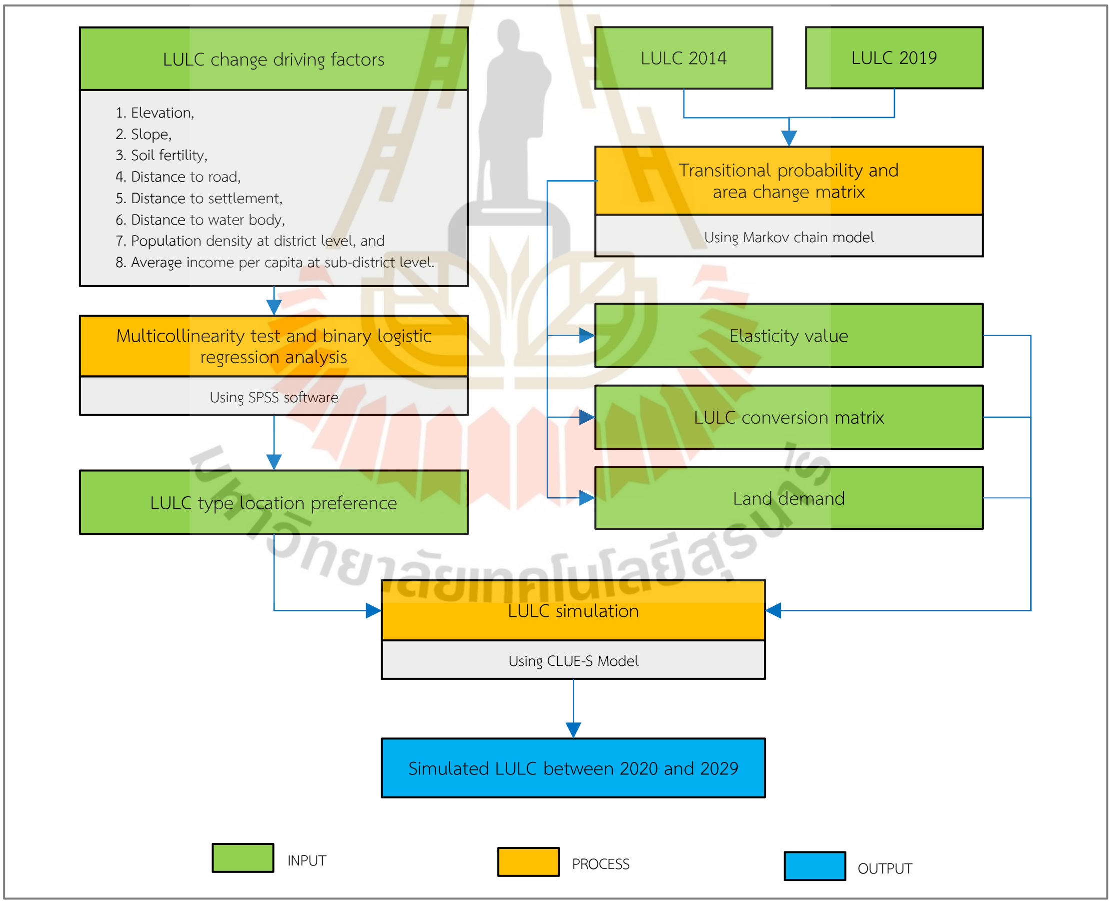
LULC change driving factors
1. Elevation,
2. Slope,
3. Soil fertility,
4. Distance to road,
5. Distance to settlement,
6. Distance to water body,
7. Population density at district level, and
8. Average income per capita at sub-district level.
LULC 2014
LULC 2019
Transitional probability and area change matrix
Using Markov chain model
Multicollinearity test and binary logistic regression analysis
Using SPSS software
Elasticity value
LULC conversion matrix
LULC type location preference
Land demand
LULC simulation
Using CLUE-S Model
Simulated LULC between 2020 and 2029
INPUT
PROCESS
OUTPUT

Figure 3.3 Schematic workflow of land use and land cover simulation.

(2) LULC type location preference

LULC type location preference according to driving force on LULC change was identified by binomial logistic regression analysis. The driving factors on LULC change for specific LULC type location preferences applied in this study were adopted from Ongsomwang and Boonchoo (2016). They include elevation, slope, distance to water bodies, distance to road, distance to settlement, soil fertility, population density at the sub-district level, and average income per capita at the sub-district level.

(3) LULC simulation using the CLUE-S model

For LULC simulation using the CLUE-S model, the conversion matrix and elasticity of LULC change, land use demand was simultaneously combined to allocate LULC data between 2020 and 2029 according to the driving factors on LULC change for specific LULC type location preference (Verburg et al., 1999, 2002; Verburg and Overmars, 2007).

3.3.3 Water yield estimation

Under this component, the Khlong Bang Yai watershed was first chosen to examine an optimum parameter for operating the SWAT model. The hydrologic response unit (HRU) was first generated based on LULC, soil, and slope data in the catchments. Then, the sensitivity analysis was conducted to determine the influence of parameters on predicting total flow to find the most sensitive parameters in the study. After that, these parameters were used for calibration and validation to get the optimum parameters for each condition (dry and wet conditions). Finally, the model's optimum parameters were further applied to estimate water yield in Phuket Island under dry and wet year scenarios between 2020 and 2029.

The workflow of water yield estimation is shown in Figure 3.4. At the same time, details of significant tasks under this component include (1) Hydrologic response unit, (2) sensitivity analysis, (3) model calibration and validation, and (4) water yield estimation between 2020 and 2029 are described in the following sections.

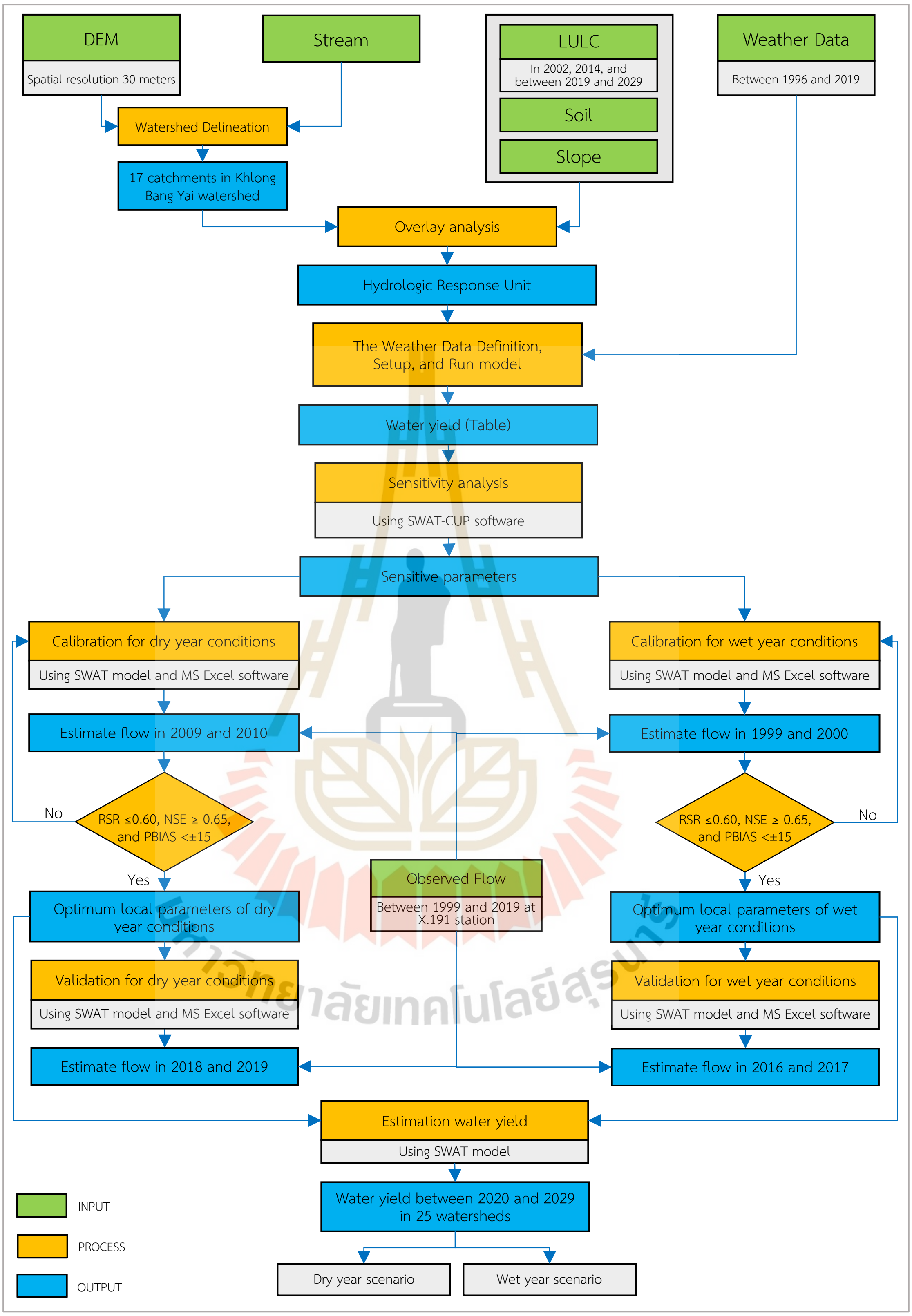
DEM
Spatial resolution 30 meters
Stream
LULC
In 2002, 2014, and between 2019 and 2029
Soil
Slope
Weather Data
Between 1996 and 2019
Watershed Delineation
17 catchments in Khlong Bang Yai watershed
Overlay analysis
Hydrologic Response Unit
The Weather Data Definition, Setup, and Run model
Water yield (Table)
Sensitivity analysis
Using SWAT-CUP software
Sensitive parameters
Calibration for dry year conditions
Using SWAT model and MS Excel software
Calibration for wet year conditions
Using SWAT model and MS Excel software
Estimate flow in 2009 and 2010
Estimate flow in 1999 and 2000
No
RSR ≤0.60, NSE ≥ 0.65, and PBIAS <±15
No
RSR ≤0.60, NSE ≥ 0.65, and PBIAS <±15
Yes
Yes
Observed Flow
Between 1999 and 2019 at X.191 station
Optimum local parameters of dry year conditions
Optimum local parameters of wet year conditions
Validation for dry year conditions
Using SWAT model and MS Excel software
Validation for wet year conditions
Using SWAT model and MS Excel software
Estimate flow in 2018 and 2019
Estimate flow in 2016 and 2017
Estimation water yield
Using SWAT model
Water yield between 2020 and 2029 in 25 watersheds
Dry year scenario
Wet year scenario
INPUT
PROCESS
OUTPUT

Figure 3.4 Schematic workflow of water yield estimation.

(1) Hydrologic response unit

Under this part, the SWAT model divides a watershed of Khlong Bang Yai into catchments based on topographic information. Then, the hydrologic response unit (HRU) was generated based on LULC in 2014, soil, and slope in each catchment. Meanwhile, the required weather data between 1996 and 2008 were extracted from six weather stations for model operation (The model warm-up period was defined in three years (between 1996 and 1998)). Finally, the characteristics of catchments and HRU were calculated and used for water yield estimations.

In practice, LULC data in 2014 was prepared to connect with the SWAT database, as displayed in Table 3.3. In the meantime, soil data were prepared to connect with the SWAT database. The SWAT soils classification table and the corresponding "STMUID" from ArcSWAT STATSGO (State Soil Geographic) database are displayed in Table 3.4. Meanwhile, slope data were used in five classes (see in Table 3.5) from the standard slope classification of the Land Development Department (2000) include the upper limit of "slope class 1" to be 5%. Then, the upper limit of the "slope class 2" to be 12%, the upper limit of the "slope class 3" to be 20%, the upper limit of the "slope class 4" to be 35%, and the upper limit of the "slope class 5" to be >35%. Then, the multiple HRUs were generated using a 20 percent land use, a 10 percent soil, and a 20 percent slope threshold suitable for most applications (Kunto and Ongsomwang, 2013; Sisay, Halefom, Khare, Singh, and Meshesha, 2017).

Table 3.3 LULC code for linkage with the SWAT database.

No	LULC type	SWAT Code
1	Urban and built-up area	URBN (Residential)
2	Paddy field	RICE (Rice)
3	Field crop and horticulture	AGRL (Agricultural Land-Generic)
4	Perennial trees and orchards	RUBR (Rubber Trees)
5	Aquaculture	WATR (Water)
6	Idle land	AGRC (Agricultural Land-Close-grown)
7	Evergreen forest	FRSE (Forest-Evergreen)
8	Mangrove forest	WETF (Wetlands-Forested)
9	Scrub forest	RNGB (Range-Brush)
10	Waterbody	WATR (Water)
11	Miscellaneous land	WETL (Wetlands-Mixed)

Table 3.4 SWAT soil classification table from the ArcSWAT STATSGO database.

No	Series Name	TEXTURE	STMUID Code
1	Alluvial soil poorly drained	Clay loam	48412
2	Ao Luek	Clay	48080
3	Bacho	Loamy sand	48430
4	Ban Thon	Sand	48241
5	Bang Nara	Clay loam	48412
6	Chalong	Loam	48273
7	Estuarine deposit Complex	Clay	48080
8	Hua Hin	Sand	48241
9	Huai Pong	Sandy loam	48430
10	Kantang	Clay	48080
11	Khao Khat	Sandy loam	48430
12	Khlong Chak	Clay loam	48412
13	Khlong Teng	Silty loam	48307
14	Kho Hong	Loamy sand	48430
15	Khok Khain	Sandy loam	48430
16	Khok Kloi	Sandy loam	48430
17	Krabi	Clay loam	48412
18	Lahan	Sandy loam	48430
19	Lamphu La	Loam	48273
20	Mai Khao	Sand	48241
21	Na Tham	Sandy loam	48430
22	Na Thon	Silty loam	48307
23	Pak Chan	Clay loam	48412
24	Phang-nga	Sandy loam	48430
25	Phuket	Sandy clay loam	48596
26	Ranong	Sandy loam	48430
27	Rayong	Sand	48241
28	Recent Beach	Sand	48241
29	Satun	Sandy loam	48430
30	Slope complex	Loam	48273
31	Su-ngai Padi	Sandy loam	48430
32	Thai Muang	Sandy loam	48430
33	Tin Mine Land	VAR	48053
34	Urban Land	VAR	48425

Table 3.5 Slope classification from the Land Development Department.

No	Slope (%)	Landform
1	0-2	Flat or almost flat
2	2-5	Slightly undulating
3	5-12	Undulating
4	12-20	Rolling
5	20-35	Hilly
6	>35	Steep

Source: Standard slope classification of the Land Development Department (2000).

After that, the weather data between 1996 and 2008 (precipitation, temperature, solar radiation, wind speed, and humidity data) were used to input into the model from the Thai Meteorological Department and Southern Region Irrigation Hydrology Center, Royal Irrigation Department in six stations include Phuket, Phuket Airport, Bang wad, Krabi, Ko Lanta, and Takua Pa stations as shown in Figure 3.5. Finally, the characteristics of catchments and HRU were calculated and used for water yield estimations.

(2) Sensitivity analysis

The seven critical parameters, which affect surface runoff and baseflow include Curve number at moisture condition II (CN2), available soil water capacity (SOL_AWC), soil evaporation compensation factor (ESCO), surface runoff lag coefficient (SURLAG), baseflow alpha factor (ALPHA_BF), Groundwater “revap” coefficient (GW_REVAP), and groundwater delay (GW_DELAY), as suggested by Schilling et al. (2008); Arnold, Moriasi et al. (2012); Leta et al. (2016); Veettil and Mishra (2016); Kundu et al. (2017); Ayivi and Jha (2018); Luan et al. (2018); and Osei et al. (2019) were analyzed to identify the most suitable value of each parameter for water yield estimation in the Khlong Bang Yai watershed under two conditions (dry and wet years). These values were further used as optimum parameters for calibration and validation for each watershed in Phuket Island. The watershed’s sensitive parameters were analyzed using t-statistics, and their p-values are significant at a 5% level of significance under SWAT-CUP software.

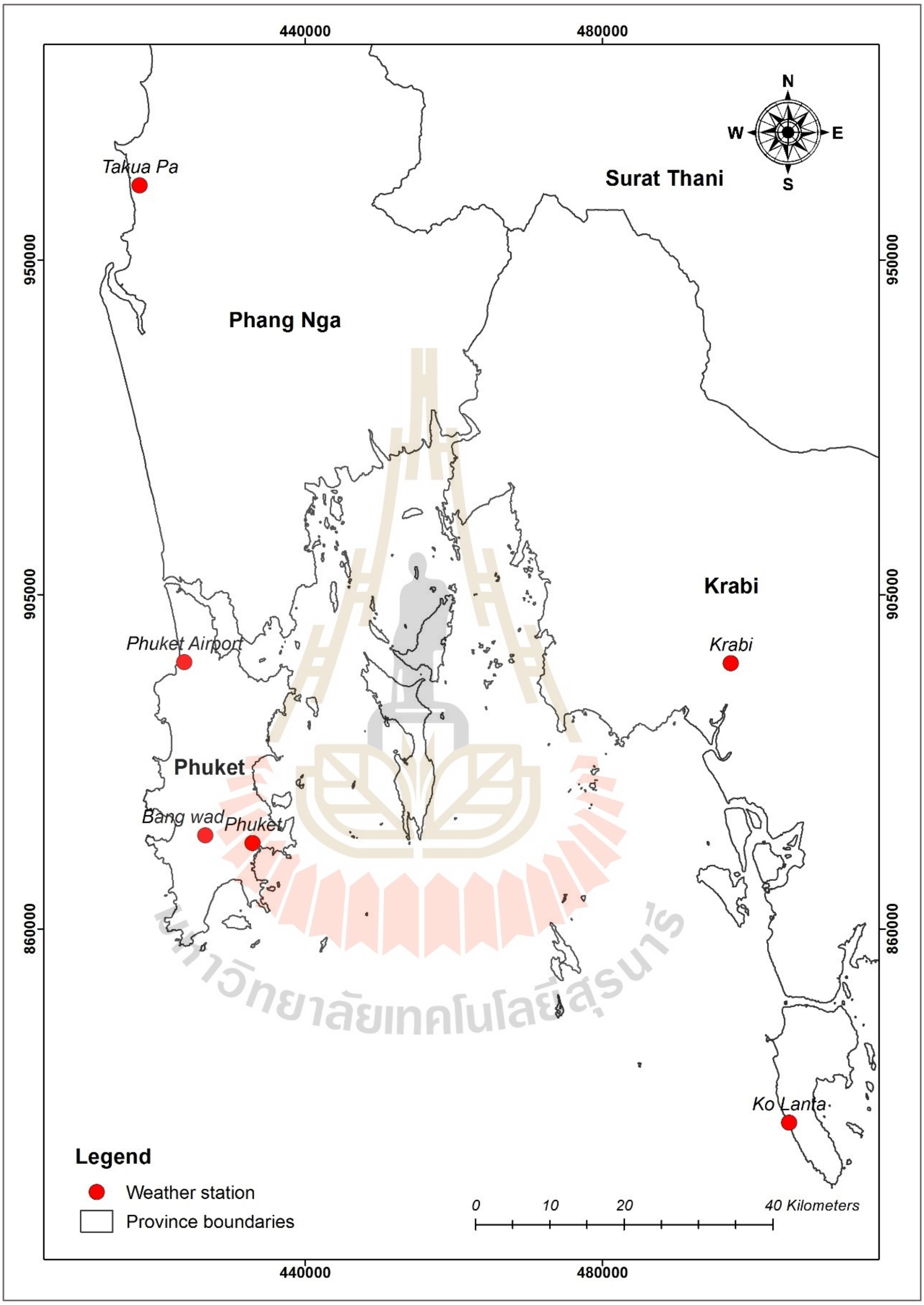
440000
480000
950000
905000
860000
N
W
E
S
Surat Thani
Takua Pa
Phang Nga
Krabi
Phuket Airport
Krabi
Phuket
Bang wad
Phuket
Ko Lanta
Legend
● Weather station
Province boundaries
0
10
20
40 Kilometers

Figure 3.5 Location of weather stations.

(3) Model calibration and validation

According to annual runoff data, the model calibration and validation for water yield estimation in the Khlong Bang Yai watershed as a reference area were separately conducted. This study categorized annual runoff data into two conditions: dry and wet years, with the long-term mean annual runoff (between 1999 and 2019) at the X.191 station (Satree Phuket School) was used as a threshold for this study (Figure 3.6). Any year whose annual runoff is higher than the mean annual runoff is identified as a wet year. Meanwhile, any year with annual runoff less than the mean annual runoff was identified as a dry year.

(3.1) Dry year conditions. The dry year condition represents a dry year of annual runoff characteristics. The annual runoff statistics (an average, standard deviation, and summation) were considered and chosen the period to estimate the water yield for calibration and validation of this condition.

The model calibration was performed under dry year conditions based on the estimated water balance from the SWAT model for 2009 and 2010. Meanwhile, model validation was conducted based on the estimated water balance from the SWAT model for 2018 and 2019. The model calibration and validation were performed manually by adjusting the most sensitive hydrologic-related parameters for the optimum parameter values for the dry year condition. Under this condition, LULC data in 2014 were used for model calibration, and LULC data in 2019 were applied for model validation. Meanwhile, the multiple HRU definition in the watershed was generated using a combination of 20 percent land use, 10 percent soil, and 20 percent slope threshold. The weather data from six weather stations from 2006 to 2010 and 2015 to 2019 were used for model calibration and validation. This study defined the model warm-up period in three years for model calibration and validation, between 2006 and 2008 and between 2015 and 2017, respectively.

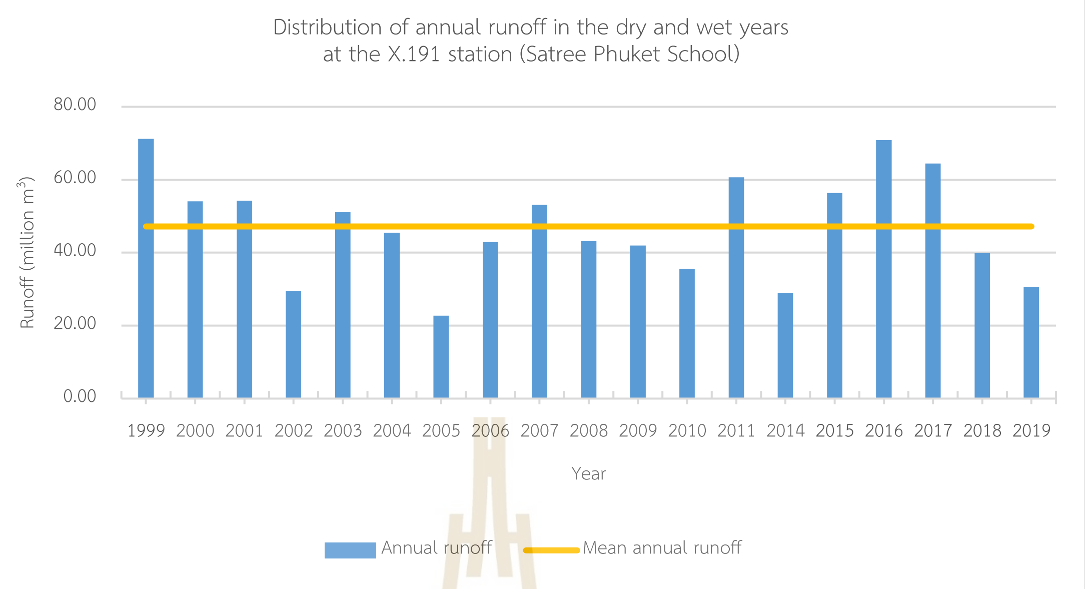

Figure 3.6 Distribution of annual runoff in the dry and wet years at the X.191 station (Satree Phuket School).

(3.2) Wet year conditions. The wet year condition represents a wet year of annual runoff characteristics. The annual runoff statistics (an average, standard deviation, and summation) were considered and chosen the period to estimate the water yield for calibration and validation of this condition.

The model calibration was performed under wet year conditions based on the estimated water balance from the SWAT model for 1999 and 2000. In the meantime, model validation was conducted based on the estimated water balance from the SWAT model for 2016 and 2017. Like dry year conditions, the model calibration and validation were performed manually by adjusting the most sensitive hydrologic-related parameters for optimum parameter value identification for wet year conditions. Under this condition, LULC data in 2002 was applied for model calibration, while LULC data in 2014 were used for model validation. The multiple HRU definition was created using a combination of 20 percent land use, 10 percent soil, and 20 percent slope threshold. The weather data from six weather stations from 1996 to 2000 and 2013 to 2017 were used for model calibration and validation. This study defined the model warm-up period in three years for model calibration and validation, between 1996 and 1998 and between 2013 and 2015, respectively.

This study used monthly streamflow data at the X.191 station (Satree Phuket School) between 1999 and 2019 for model calibration and validation (Figure 3.7).

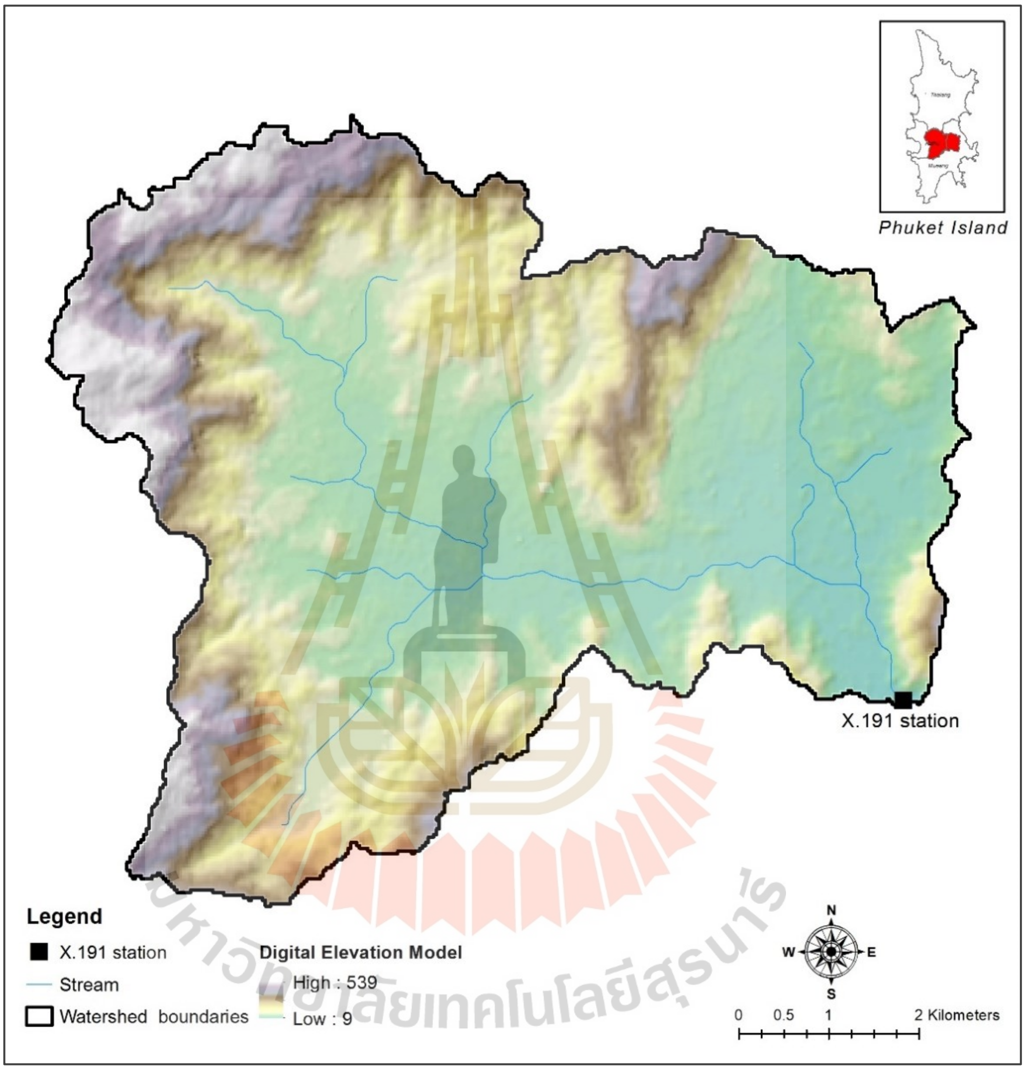
Phuket Island
X.191 station
Legend
X.191 station
Stream
Watershed boundaries
Digital Elevation Model
High : 539
Low : 9
N
W
E
S
0
0.5
1
2 Kilometers

Figure 3.7 Location of the X.191 station (Satree Phuket School) at Khlong Bang Yai watershed.

RMSE-observations standard deviation ratio (RSR) (Legates and McCabe, 1999), Nash-Sutcliffe efficiency (NSE) (Nash and Sutcliffe, 1970), and Percent bias (PBIAS) (Gupta et al., 1999) based on Equations (3.2) to (3.4) were applied to evaluate the performance of the model with a threshold value of ≤0.60, ≥0.65, ≤±15, respectively.

$$\mathrm{RSR} = \frac{\mathrm{RMSE}}{\mathrm{STDEV_{Obs}}} = \frac{\sqrt{\sum_{i=1}^{n} (O_i - E_i)^2}}{\sqrt{\sum_{i=1}^{n} (O_i - \bar{O})^2}} \tag{3.2}$$

$$\mathrm{NSE} = 1 - \frac{\sum_{i=1}^{n} \left(O_i - E_i\right)^2}{\sum_{i=1}^{n} \left(O_i - \bar{O}\right)^2} \tag{3.3}$$

$$\mathrm{PBIAS} = \frac{\sum_{i=1}^{n} \left(O_i - E_i\right) \times 100}{\sum_{i=1}^{n} (O_i)} \tag{3.4}$$

Where E_i is the estimated value and O_i is the observed value at the time i. $\bar{O}$ is the mean of the individual observations of O_i, and n is the number of observations. The model efficiency is checked by the statistics, and the performance of these statistics is rated according to Moriasi et al. (2007), given in Table 3.6.

Table 3.6 Model performance scale.

Performance rating	RSR	NSE	PBIAS
Very good	0.00 < RSR < 0.50	0.75 < NSE < 1.00	PBIAS < ± 10
Good	0.50 < RSR < 0.60	0.65 < NSE < 0.75	±10 < PBIAS < ± 15
Satisfactory	0.60 < RSR < 0.70	0.50 < NSE < 0.65	±15 < PBIAS < ± 25
Unsatisfactory	RSR >0.70	NSE <0.50	PBIAS > ± 25

Source: Moriasi et al. (2007).

(4) Water yield estimation between 2020 and 2029

Under this session, the optimum local dry and wet conditions parameters were used to estimate the time-series water yield in Phuket Island between 2020 and 2029. Herein, the 25 watersheds and stream networks of each watershed were used for watershed delineation using pre-defined streams and watersheds dataset to estimate the water yield of Phuket Island (522.05 km^2) in two different scenarios: dry year and wet year.

Based on long-term historical rainfall data from the Thai Meteorological Department at Phuket and Phuket Airport stations. In this study, the lowest rainfall value for the extremely dry year occurred in 2019. Actually, dry year conditions should be applied annual rainfall data in 2004 or 2005, but these data are unavailable at Krabi and Takua Pa stations. At the same time, the highest rainfall value for the extreme wet year was found in 2016 (Figure 3.8). Thus, time-series water yield data between 2020 and 2029 under dry year scenarios were estimated based on weather data in 2019. On the contrary, time-series water yield data between 2020 and 2029 under wet year scenarios were estimated based on weather data in 2016.

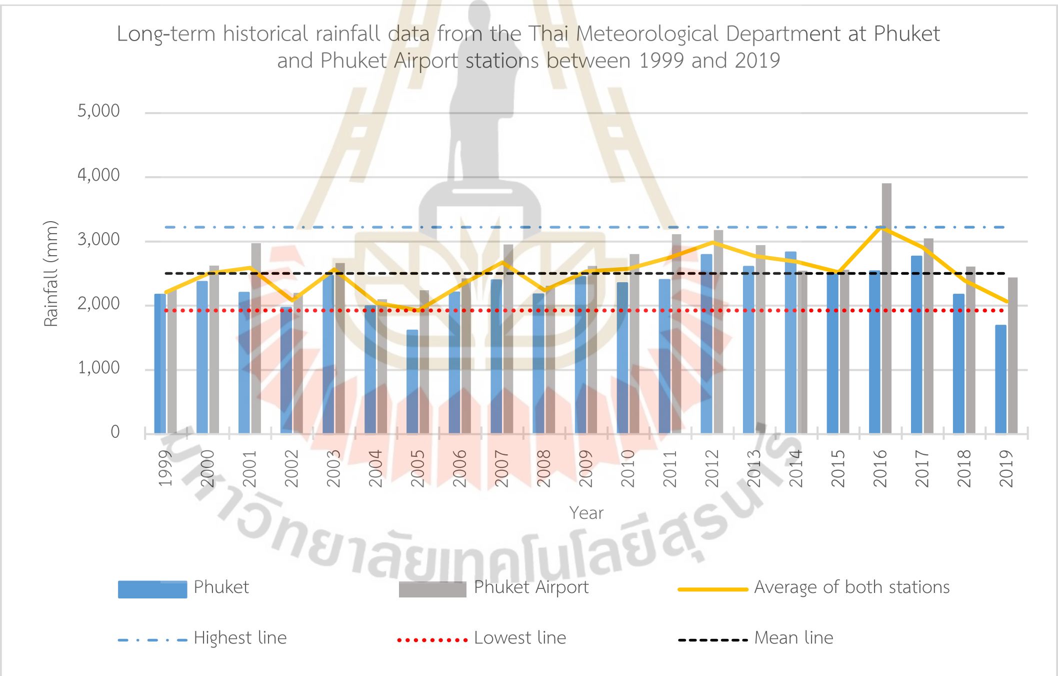

Figure 3.8 Long-term historical rainfall data from the Thai Meteorological Department at Phuket and Phuket Airport stations between 1999 and 2019.

3.3.4 Water demand estimation

Under this component, water demand estimation based on water footprint was separately displayed according to two different conditions: normal and new normal (COVID-19 pandemic). This study estimated Phuket Island’s water demand between 2020 and 2029 under normal and new normal conditions for four primary consumption components: residential, tourist, agriculture, and forest uses.

The workflow of water demand estimation is shown in Figures 3.9 and 3.10. At the same time, details of significant tasks under this component include (1) residential water demand, (2) tourist water demand, and (3) water demand for agriculture and forest uses are described in the following sections.

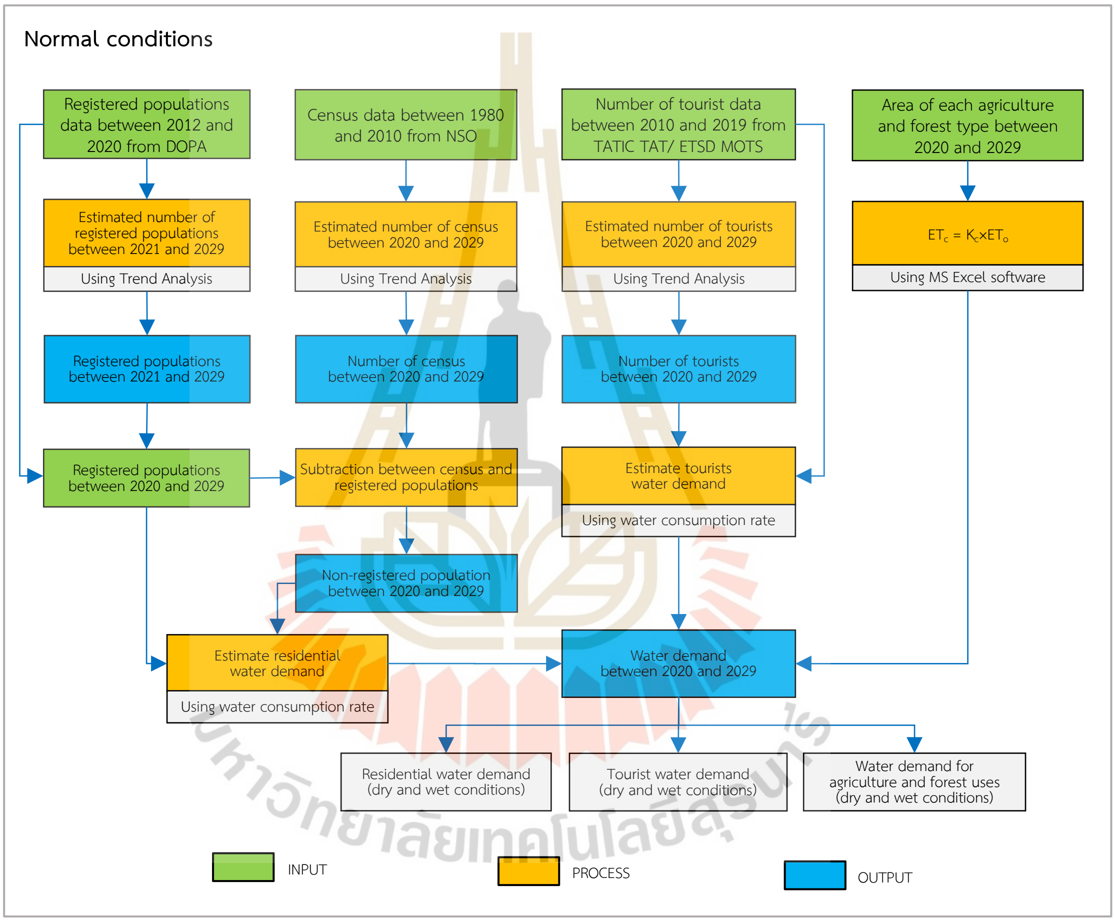
Normal conditions
Registered populations data between 2012 and 2020 from DOPA
Census data between 1980 and 2010 from NSO
Number of tourist data between 2010 and 2019 from TATIC TAT/ ETSD MOTS
Area of each agriculture and forest type between 2020 and 2029
Estimated number of registered populations between 2021 and 2029
Using Trend Analysis
Estimated number of census between 2020 and 2029
Using Trend Analysis
Estimated number of tourists between 2020 and 2029
Using Trend Analysis
$ET_c = K_c \times ET_o$
Using MS Excel software
Registered populations between 2021 and 2029
Number of census between 2020 and 2029
Number of tourists between 2020 and 2029
Registered populations between 2020 and 2029
Subtraction between census and registered populations
Estimate tourists water demand
Using water consumption rate
Non-registered population between 2020 and 2029
Estimate residential water demand
Using water consumption rate
Water demand between 2020 and 2029
Residential water demand (dry and wet conditions)
Tourist water demand (dry and wet conditions)
Water demand for agriculture and forest uses (dry and wet conditions)
INPUT
PROCESS
OUTPUT

Figure 3.9 Schematic workflow of water demand estimation under normal conditions.

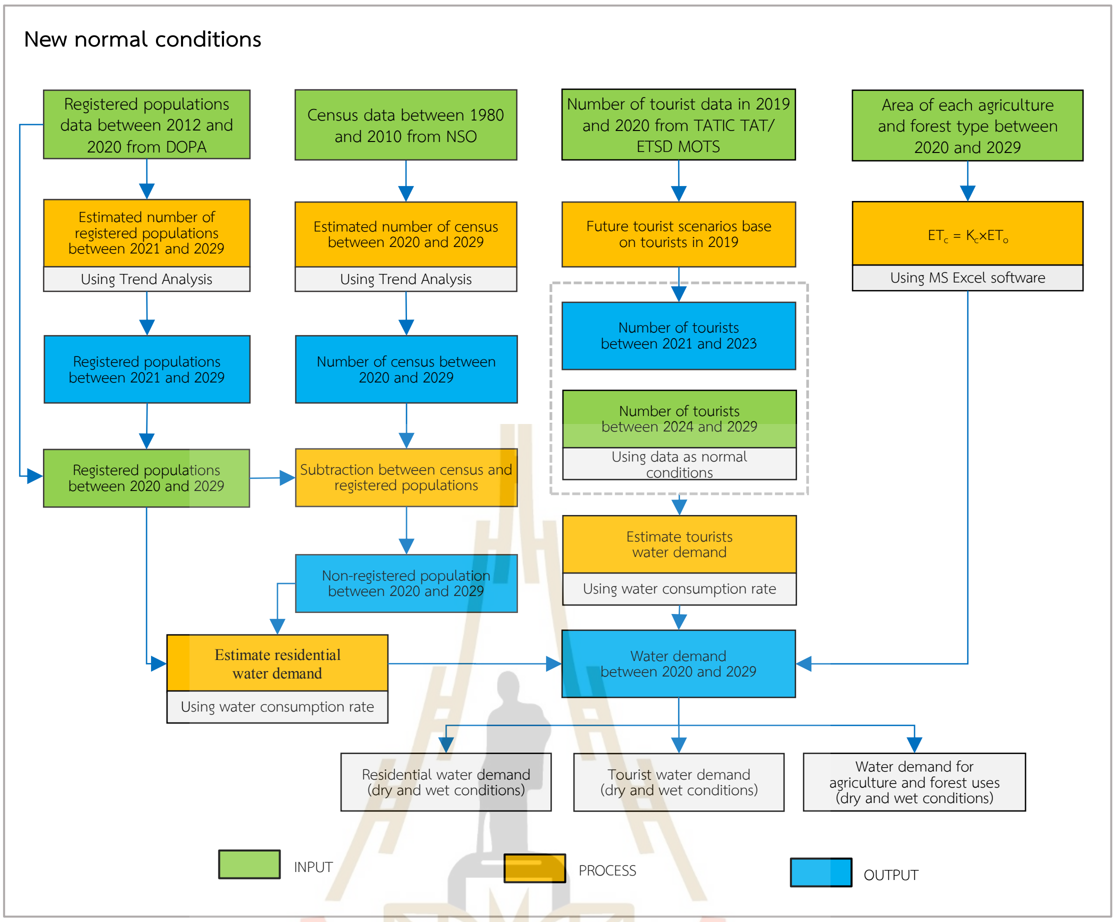
New normal conditions
Registered populations data between 2012 and 2020 from DOPA
Census data between 1980 and 2010 from NSO
Number of tourist data in 2019 and 2020 from TATIC TAT/ ETSD MOTS
Area of each agriculture and forest type between 2020 and 2029
Estimated number of registered populations between 2021 and 2029
Using Trend Analysis
Estimated number of census between 2020 and 2029
Using Trend Analysis
Future tourist scenarios base on tourists in 2019
$ET_c = K_c \times ET_o$
Using MS Excel software
Registered populations between 2021 and 2029
Number of census between 2020 and 2029
Number of tourists between 2021 and 2023
Number of tourists between 2024 and 2029
Using data as normal conditions
Registered populations between 2020 and 2029
Subtraction between census and registered populations
Estimate tourists water demand
Using water consumption rate
Non-registered population between 2020 and 2029
Estimate residential water demand
Using water consumption rate
Water demand between 2020 and 2029
Residential water demand (dry and wet conditions)
Tourist water demand (dry and wet conditions)
Water demand for agriculture and forest uses (dry and wet conditions)
INPUT
PROCESS
OUTPUT

Figure 3.10 Schematic workflow of water demand estimation under new normal conditions.

(1) Residential water demand

Under normal and new normal conditions, the number of registered populations in 2020 was extracted from the DOPA database, Ministry of Interior. Meanwhile, the number of non-registered populations in 2020 was calculated by subtraction between censused and registered populations. In addition, censused data in 2020 was estimated based on historical data between 1980 and 2010 using Trend Analysis with a simple linear regression under MS Excel software.

Meanwhile, the number of people (registered and non-registered populations) between 2021 and 2029 was estimated base on history data using Trend Analysis with a simple linear regression under MS Excel software. The registered population was estimated based on historical data between 2012 and 2020, while censused data were estimated based on historical data between 1980 and 2010.

Finally, residential water demand was estimated using the water consumption rate in different community characteristics of the Royal Irrigation Department (2011b), as a summary in Table 3.7.

Table 3.7 Water consumption rates in different community characteristics.

No	Community characteristics	Water consumption rate (liters/person/day)
1	City Municipality.	250
2	Town Municipality	200
3	Sub-district Municipality	120
4	Outside the municipality	50

Source: Royal Irrigation Department (2011b).

(2) Tourist water demand

Under this session, the number of tourists under normal conditions between 2020 and 2029 was estimated using Trend Analysis with a simple linear regression based on historical data between 2010 and 2019 using MS Excel software. In contrast, the number of tourists under new normal conditions (COVID-19 pandemic) was adopted from the projected tourists in the future by the Economics Tourism and Sports Division, Ministry of Tourism and Sports (2020), according to historical data and projected data, in 2019 and 2020, respectively. In this condition, three future tourist scenarios were presented with 45%, 65%, and 85% of tourists in 2019 for 2021, 2022, and 2023 respectively. In the meantime, the number of tourists between 2024 and 2029 was used the same data as normal conditions.

Finally, tourist water demand between 2020 and 2029 under normal and new normal conditions were estimated based on the modified water consumption rate (see Table 3.8) of Pansawad (1997) and the Department of Public Works and Town and Country Planning (1993), as cited in Royal Irrigation Department (2011b); Srichai et al. (2016) with an average length of stay (day) by four days (The average between 2015 and 2019) (TAT Intelligence Center, Tourism Authority of Thailand, 2019).

Table 3.8 The modified water consumption rate for tourists.

No	Tourists types	Water consumption rate (liters/person/day)
1	Tourists	300
2	Excursionists	30

(3) Water demand for agriculture and forest uses

Under normal and new normal conditions, the water demand for agriculture and forest uses was estimated based on evapotranspiration coefficient and reference evapotranspiration (Allen et al., 1998), as shown in the following equation.

$$ET_c = K_c \times ET_o \tag{3.5}$$

Where ET_c is water requirement (mm/day), K_c is evapotranspiration coefficient, and ET_o is reference evapotranspiration (mm/day). In practice, the water demand for agriculture and forest use between 2020 and 2029 was calculated based on the area of each agriculture and forest type, evapotranspiration coefficient (K_c) (see in Table 3.9), and reference evapotranspiration under the Penman-Monteith method with an average value between Phuket and Phuket Airport stations (see in Table 3.10) from Royal Irrigation Department (2011a).

Table 3.9 The evapotranspiration coefficient of each agriculture and forest type.

No	Agriculture and forest type	Evapotranspiration coefficient (K_c)
1	Field crop	0.6
2	Paddy field	0.6
3	Para rubber trees	1.0
4	Evergreen forest	1.0
5	Mangrove forest	1.0
6	Scrub forest	0.5

Note: The K_c values were obtained from Trisurat, Aekakkararungroj, Johnston, Vanna, and Phan (2017).

Table 3.10 The reference evapotranspiration under the Penman-Monteith method.

Station	ET_o (mm/day)											
	Jan	Feb	Mar	Apr	May	Jun	Jul	Aug	Sep	Oct	Nov	Dec
Phuket	4.29	4.62	4.55	4.34	3.84	3.81	3.78	3.98	3.43	3.53	3.65	3.83
Phuket Airport	4.04	4.37	4.58	4.36	3.93	3.93	3.92	3.78	3.52	3.19	3.32	3.67
Average	**4.17**	**4.50**	**4.57**	**4.35**	**3.89**	**3.87**	**3.85**	**3.88**	**3.48**	**3.36**	**3.49**	**3.75**

Source: Royal Irrigation Department (2011a).

3.3.5 Water balance evaluation

Under this session, the estimated water supply and demand from actual and future under two different scenarios (dry year and wet year) and two different conditions (normal and new normal) were applied to evaluate water balance in terms of surplus and deficit for water resource management recommendation. In practice, water balance evaluation between 2020 and 2029 in two different scenarios (dry year and wet year) under normal and new normal conditions were evaluated with and without ecological water requirement consideration. The schematic workflow of this component is displayed in Figure 3.11.

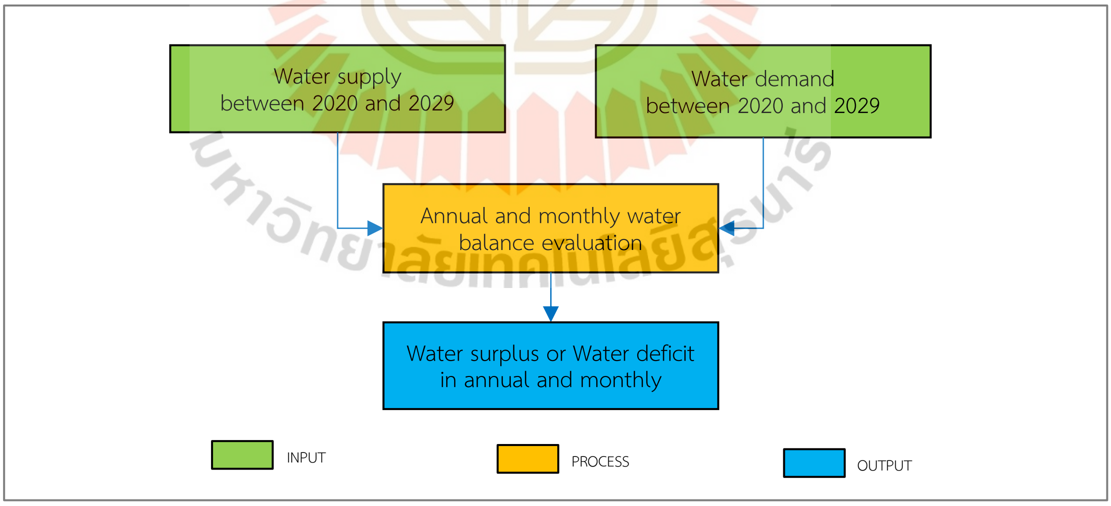
Water supply between 2020 and 2029
Water demand between 2020 and 2029
Annual and monthly water balance evaluation
Water surplus or Water deficit in annual and monthly
INPUT
PROCESS
OUTPUT

Figure 3.11 Schematic workflow of water balance evaluation.

In practice, the annual and monthly water balance without ecological water requirement consideration was evaluated based on the annual and average monthly water supply derived from the SWAT model. Meanwhile, the annual and monthly water balance with ecological water requirement consideration was evaluated based on water supply, which was derived from the SWAT model with consideration 70% of the time and 0.5 m^3 per second of flow (standard criteria) under the criteria of minimum water from the flow duration curve at the outlet of Khlong Bang Yai watershed (X.191 station, Satree Phuket School) as suggested by Southern Region Irrigation Hydrology Center, Royal Irrigation Department (2021) (see Figure 3.12 and Table 3.11). Thus, Phuket Island's ecological water requirement was applied from the ecological water requirement of the Khlong Bang Yai watershed. Finally, the results are summarized to evaluate water balance in terms of surplus and deficit for water resource management recommendations.

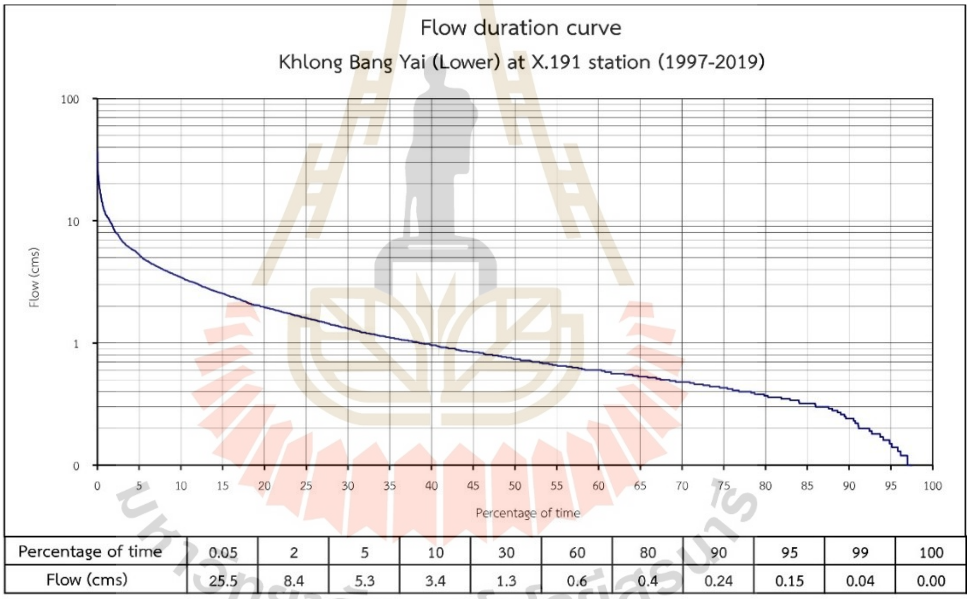

Percentage of time	0.05	2	5	10	30	60	80	90	95	99	100
Flow (cms)	25.5	8.4	5.3	3.4	1.3	0.6	0.4	0.24	0.15	0.04	0.00

Source: Southern Region Irrigation Hydrology Center, Royal Irrigation Department (2021).

Figure 3.12 The flow duration curve of X.191 station (Satree Phuket School).

Table 3.11 The criteria of minimum water from the flow duration curve.

Station code	Flow (cms) in different criteria		
	Normal (70%)	Surveillance (70%-90%)	Critical (90%)
X.191	>0.50	0.50-0.20	0.24

Source: Southern Region Irrigation Hydrology Center, Royal Irrigation Department (2021).

CHAPTER IV

LAND USE AND LAND COVER ASSESSMENT AND CHANGE DETECTION

This chapter presents the results of the first objective focusing on the LULC assessment between 2014 and 2019 and its change using the post-classification comparison algorithm. The main results, which consist of (1) LULC assessment in 2014 and 2019, and (2) LULC change between 2014 and 2019, are described and discussed in detail.

4.1 LULC assessment in 2014 and 2019

LULC data in 2014, which was visually interpreted from a pan-sharpened THEOS image with ground survey verification by Boonchoo (2015), was collected and adopted as a historical record in this study. Meanwhile, the recent LULC data in 2019 was visually interpreted from Pleiades and SPOT imageries (Figure 4.1). In practice, the LULC data were visually interpreted into eleven classes based on the combination of elements of photo interpretation (tone, size, shape, pattern, texture, shadow, site, and association). Table 4.1 displays the photo interpretation keys of eleven LULC types in the study area.

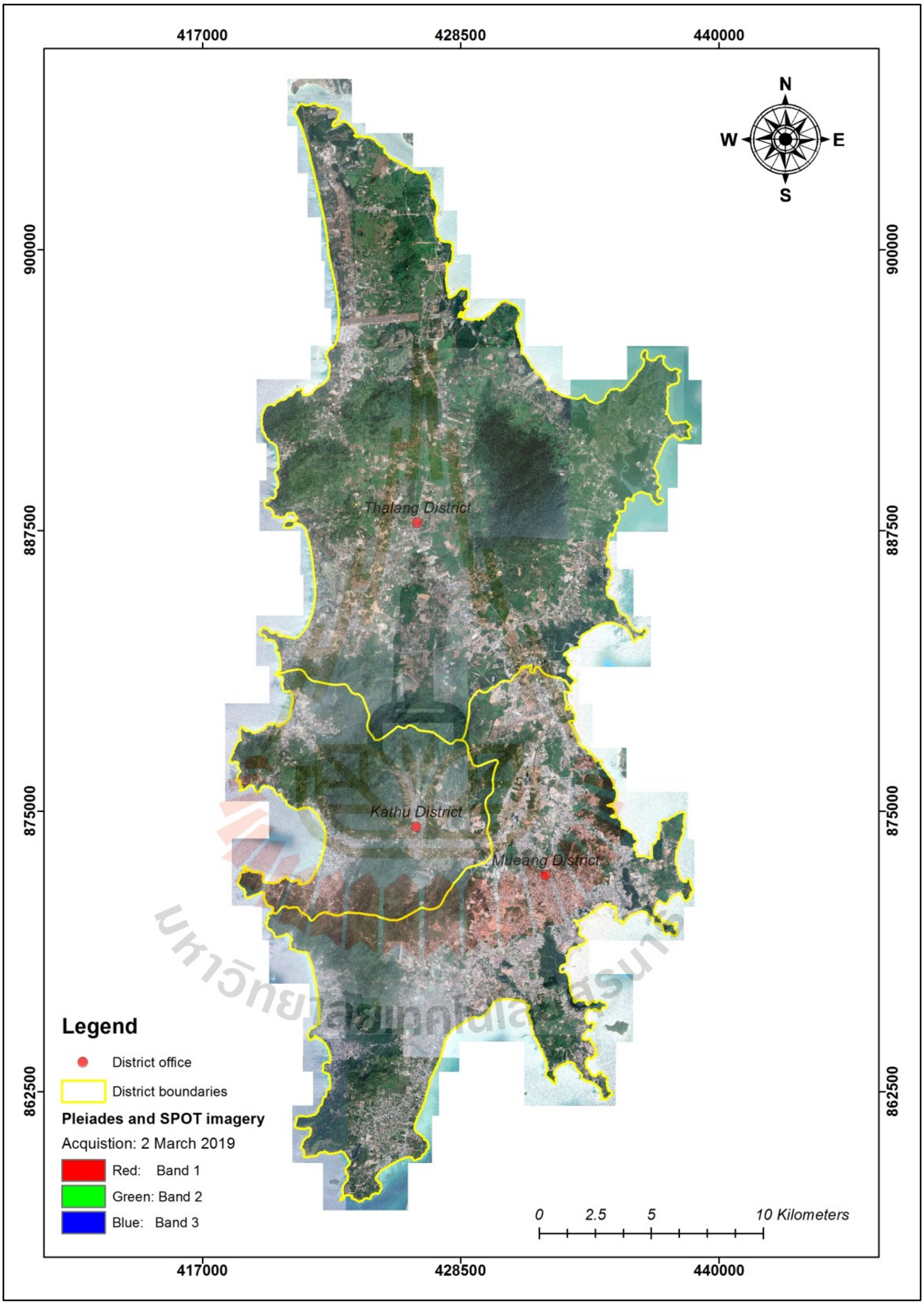
417000
428500
440000
900000
887500
875000
862500
N
W
E
S
Thalang District
Kathu District
Mueang District
Legend
● District office
District boundaries
Pleiades and SPOT imagery
Acquistion: 2 March 2019
🟥 Red: Band 1
🟩 Green: Band 2
🟦 Blue: Band 3
0
2.5
5
10 Kilometers

Figure 4.1 Pleiades and SPOT imageries.

Table 4.1 Photo interpretation key of LULC types in Phuket Island.

No	LULC type	Interpretation key of Pleiades and SPOT imagery		
1	Urban and built-up area	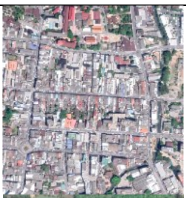	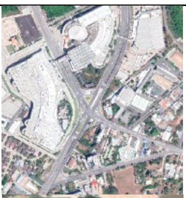	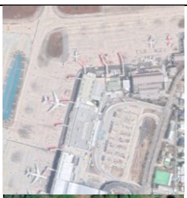
2	Paddy field	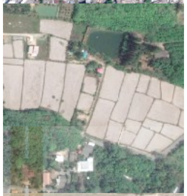	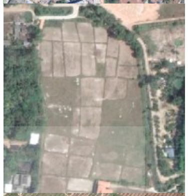	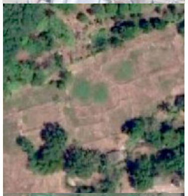
3	Field crop and horticulture	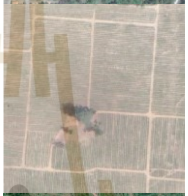	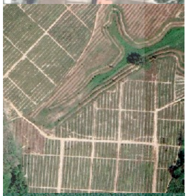	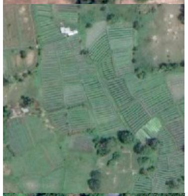
4	Perennial trees and orchards	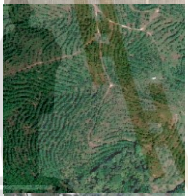	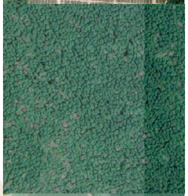	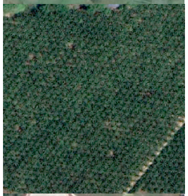
5	Aquaculture	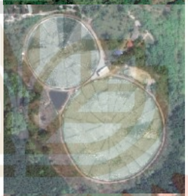	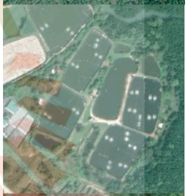	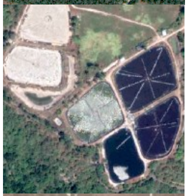
6	Idle land	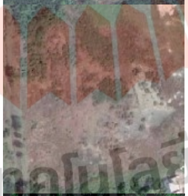	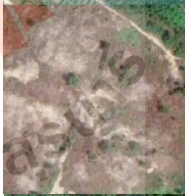	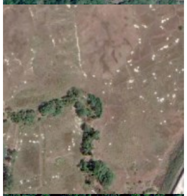
7	Evergreen forest	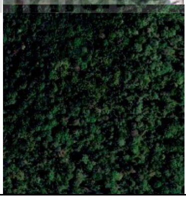	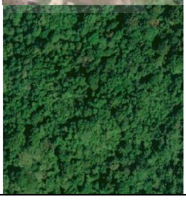	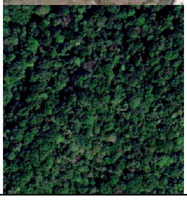

Table 4.1 (Continued).

No	LULC type	Interpretation key in Pleiades and SPOT imagery
8	Mangrove forest	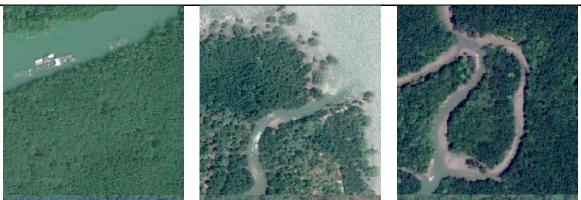
9	Scrub forest	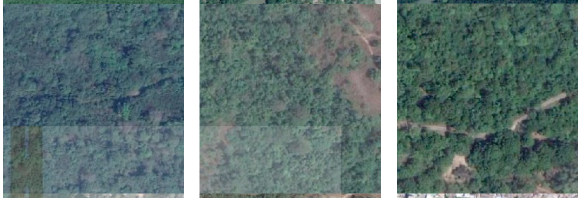
10	Water body	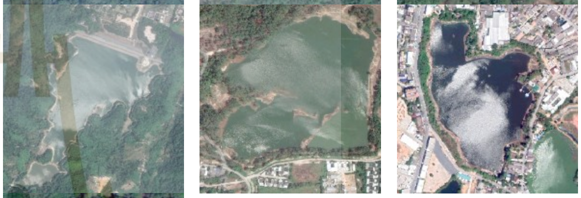
11	Miscellaneous land	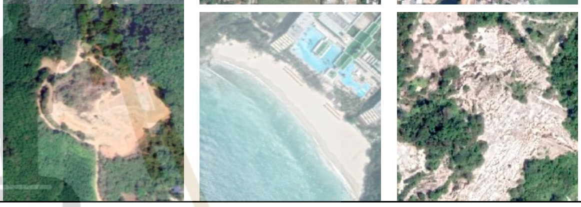

As a result, it was found that the top three most dominant LULC types in 2014 (Figure 4.2 and Table 4.2) are perennial trees and orchards, urban and built-up area, and evergreen forest, which cover the area of 196.63 km^2 or 37.66%, 125.32 km^2 or 24.00% and 80.86 km^2 or 15.49%, respectively. On the contrary, the top three least dominant LULC types in 2014 are field crop and horticulture, paddy field, and miscellaneous land, which cover the area of 1.46 km^2 or 0.28%, 2.15 km^2 or 0.41%, and 5.43 km^2 or 1.04%, respectively.

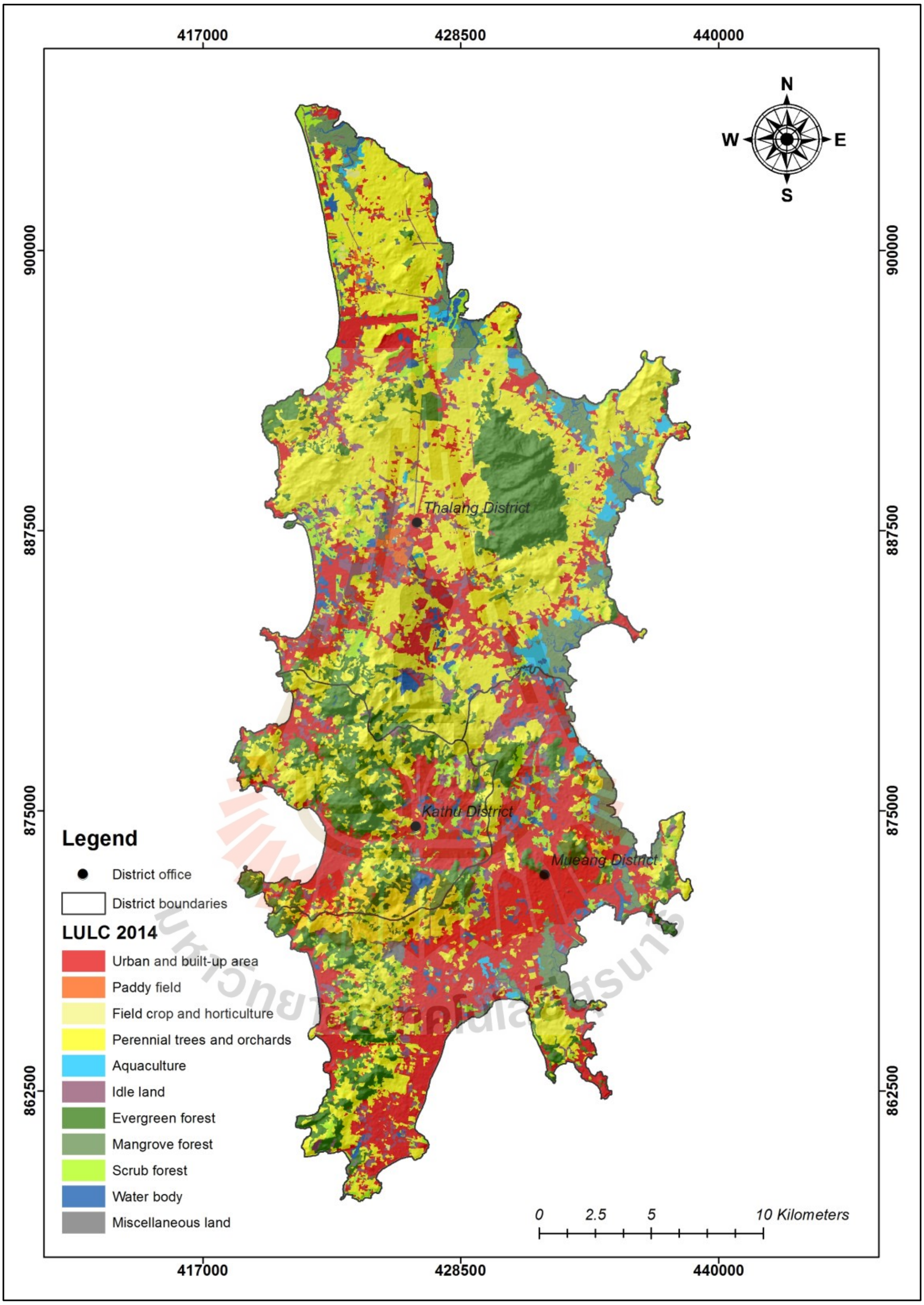
417000
428500
440000
900000
887500
875000
862500
N
W
E
S
Thalang District
Kathu District
Mueang District
Legend
District office
District boundaries
LULC 2014
Urban and built-up area
Paddy field
Field crop and horticulture
Perennial trees and orchards
Aquaculture
Idle land
Evergreen forest
Mangrove forest
Scrub forest
Water body
Miscellaneous land
0
2.5
5
10 Kilometers

Figure 4.2 Spatial distribution of LULC classification in 2014.

Table 4.2 Area and percentage of LULC data in 2014.

No	LULC type	Area in km^2	Percent
1	Urban and built-up area	125.32	24.00
2	Paddy field	2.15	0.41
3	Field crop and horticulture	1.46	0.28
4	Perennial trees and orchards	196.63	37.66
5	Aquaculture	8.74	1.67
6	Idle land	34.67	6.64
7	Evergreen forest	80.86	15.49
8	Mangrove forest	25.15	4.82
9	Scrub forest	27.08	5.19
10	Waterbody	14.56	2.79
11	Miscellaneous land	5.43	1.04
	Total	**522.05**	**100**

Meanwhile, the top three most dominant LULC types in 2019 (Figure 4.3 and Table 4.3) are still perennial trees and orchards, urban and built-up area, and evergreen forest, which cover the area of 184.39 km^2 or 35.32%, 141.64 km^2 or 27.13%, and 74.16 km^2 or 14.20%, respectively. On the contrary, the top three least dominant LULC types in 2019 are paddy field, field crop and horticulture, and miscellaneous land, which cover the area of 0.15 km^2 or 0.03%, 3.43 km^2 or 0.66%, and 3.46 km^2 or 0.66%, respectively.

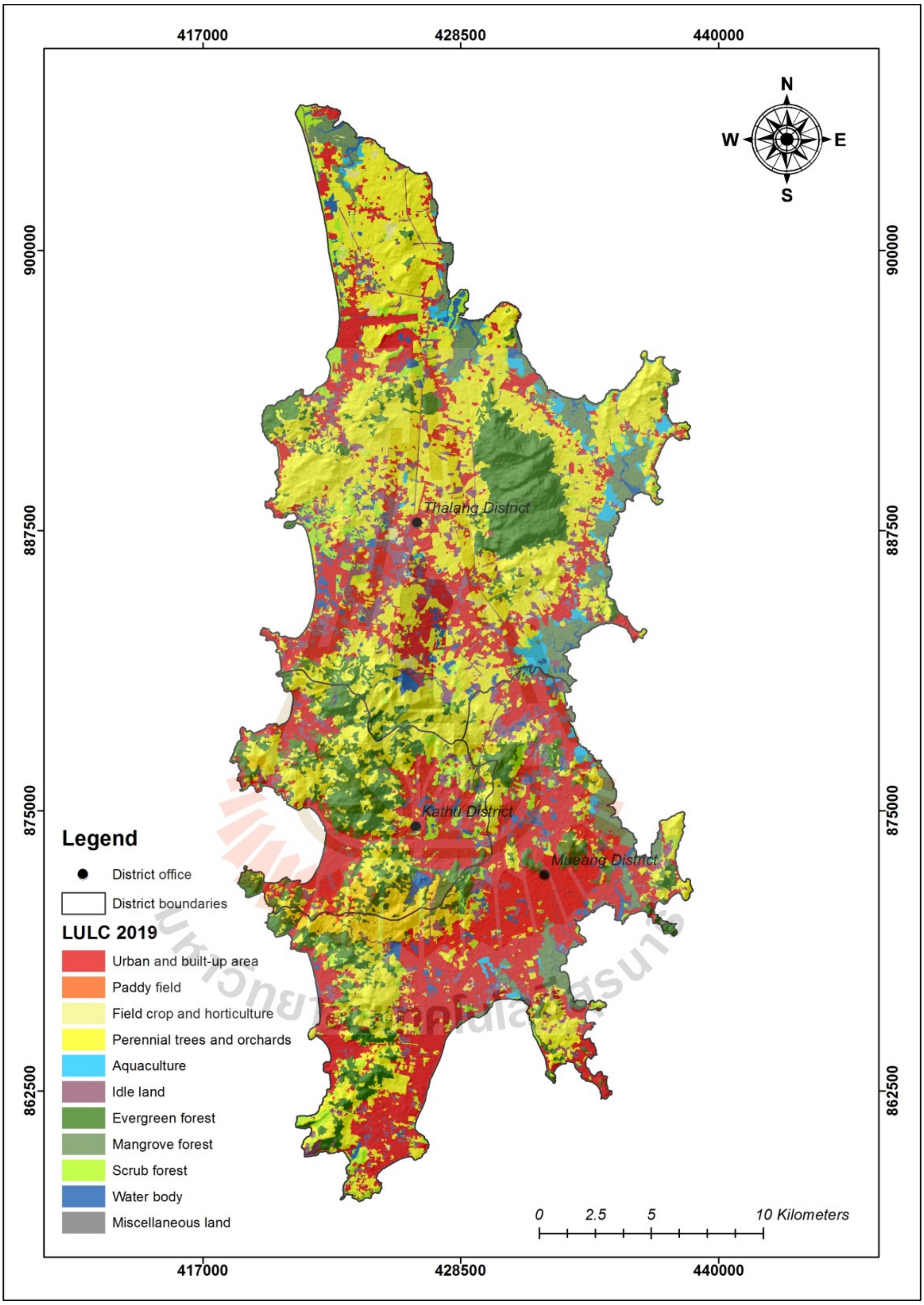
417000
428500
440000
900000
887500
875000
862500
N
W
E
S
Thalang District
Kathu District
Mueang District
Legend
District office
District boundaries
LULC 2019
Urban and built-up area
Paddy field
Field crop and horticulture
Perennial trees and orchards
Aquaculture
Idle land
Evergreen forest
Mangrove forest
Scrub forest
Water body
Miscellaneous land
0
2.5
5
10 Kilometers

Figure 4.3 Spatial distribution of LULC classification in 2019.

Table 4.3 Area and percentage of LULC data in 2019.

No	LULC type	Area in km^2	Percent
1	Urban and built-up area	141.64	27.13
2	Paddy field	0.15	0.03
3	Field crop and horticulture	3.43	0.66
4	Perennial trees and orchards	184.39	35.32
5	Aquaculture	8.56	1.64
6	Idle land	39.74	7.61
7	Evergreen forest	74.16	14.20
8	Mangrove forest	24.72	4.73
9	Scrub forest	27.00	5.17
10	Waterbody	14.81	2.84
11	Miscellaneous land	3.46	0.66
	Total	**522.05**	**100**

Besides, the classified LULC map in 2019 was further assessed its accuracy using 660 stratified random sample points with Google Earth image in 2019 and field survey in 2020 (Figure 4.4), and the error matrix form of thematic LULC accuracy assessment is displayed in Table 4.4.

As a result, it reveals that overall accuracy is 96.06%, and the Kappa hat coefficient is 95.15%. Meanwhile, producer's accuracy (PA), which represents omission error, varies between 87.50% for idle land and 100% for paddy fields, field crop and horticulture, aquaculture, mangrove forest, and miscellaneous land. The user's accuracy (UA), which represents commission error, varies between 87.50% for paddy fields and 100% for the urban and built-up area, evergreen forest, mangrove forest, water body, and miscellaneous land.

Based on Fitzpatrick-Lins (1981), the Kappa hat coefficient of more than 80 percent represents strong agreement or accuracy between the classified map and the reference map. Additionally, the overall accuracy of more than 85% of the LULC map in 2019 can provide an acceptable result (Anderson, Hardy, Roach, and Witmer, 1976). Therefore, the LULC map in 2019 can be accepted in this study.

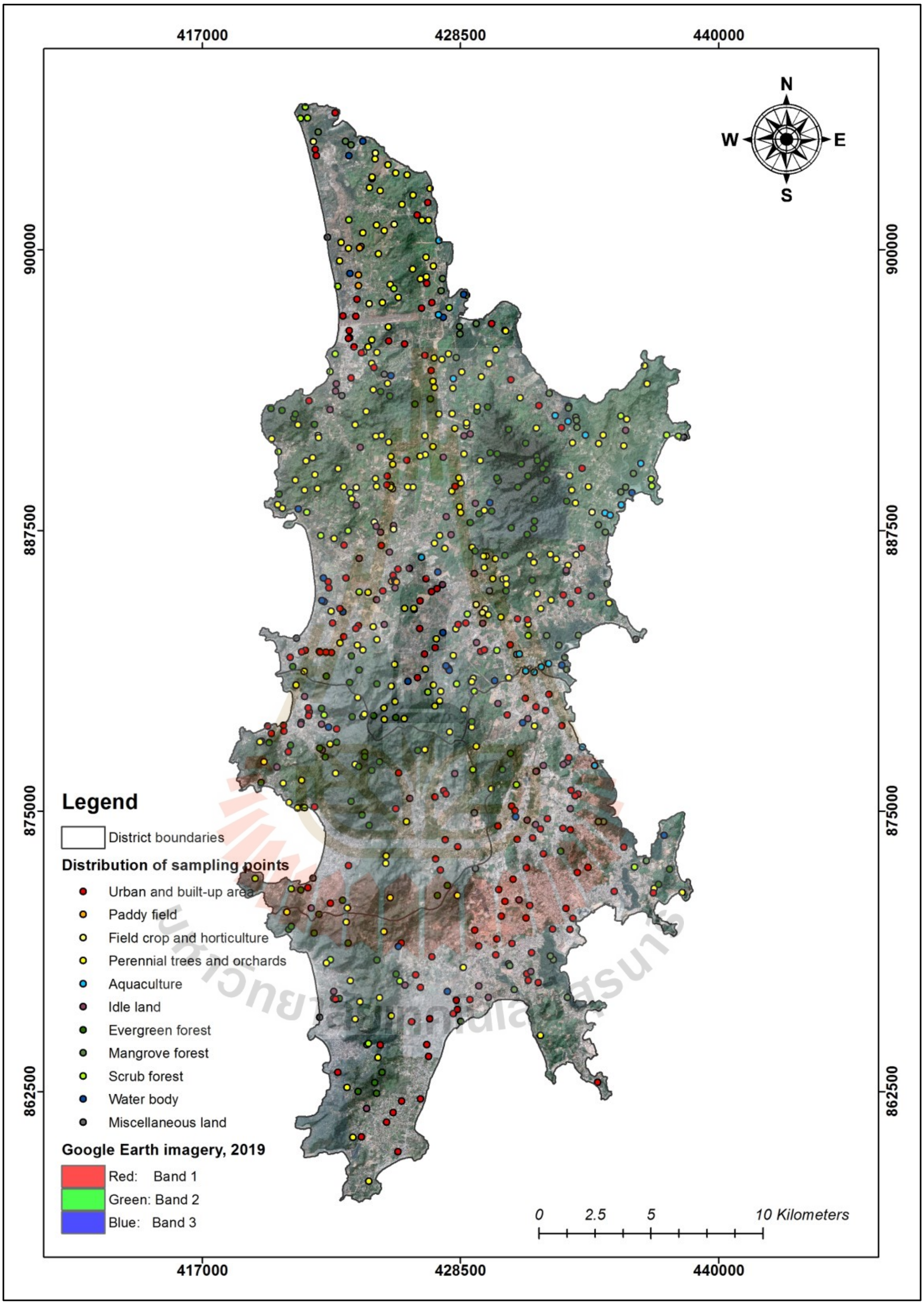
417000
428500
440000
900000
887500
875000
862500
N
W
E
S
Legend
District boundaries
Distribution of sampling points
Urban and built-up area
Paddy field
Field crop and horticulture
Perennial trees and orchards
Aquaculture
Idle land
Evergreen forest
Mangrove forest
Scrub forest
Water body
Miscellaneous land
Google Earth imagery, 2019
Red: Band 1
Green: Band 2
Blue: Band 3
0
2.5
5
10 Kilometers

Figure 4.4 Spatial distribution of sampling points superimposed on Google Earth image (2 Mar 2019) for accuracy assessment of thematic LULC map in 2019.

Table 4.4 Error matrixes and accuracy assessment of LULC in 2019.

	LULC types	Ground reference data from Google Earth in 2019											
		Ur	Pa	Fch	Po	Aq	Id	Ef	Mf	Sf	Wa	Mi	Total
Classified LULC data in 2019	Urban and built-up area (Ur)	161											161
	Paddy field (Pa)		7				1						8
	Field crop and horticulture (Fch)			12	1								13
	Perennial trees and orchards (Po)	1			191		4	7		3			206
	Aquaculture (Aq)					17	1			1			19
	Idle land (Id)				1		49	1		1	1		53
	Evergreen forest (Ef)							88					88
	Mangrove forest (Mf)								36				36
	Scrub forest (Sf)						1	2		36			39
	Waterbody (Wa)										26		26
	Miscellaneous land (Mi)											11	11
	Total	162	7	12	193	17	56	98	36	41	27	11	660
	Producer's accuracy	99.38	100.00	100.00	98.96	100.00	87.50	89.80	100.00	87.80	96.30	100.00	
	User's accuracy	100.00	87.50	92.31	92.72	89.47	92.45	100.00	100.00	92.31	100.00	100.00	
	Overall accuracy	96.06											
	Kappa hat coefficient	95.15											

Moreover, the derived overall accuracy and kappa hat coefficient in the current study are similar to the previous study of Boonchoo (2015), who applied visual interpretation method to classify the series of LULC data and to apply geospatial models and techniques for LULC prediction and deforestation vulnerability analysis in protected forest areas (national parks and national reserved forest areas), Phuket Island, Thailand. The overall accuracy and Kappa hat coefficient for the LULC data in 2014 were 98.38% and 97.89%. Likewise, Ongsomwang and Pimjai (2014) applied visual interpretation method to quantify the characteristics of the LULC change, to identify an optimum LULC change model for a LULC prediction, and to examine the effect of the LULC changes on the surface runoff at in Mueang Maha Sarakham and Kantharawichai districts of Maha Sarakham province. The overall accuracy and Kappa hat coefficient for the LULC data in 2011 were 98.12% and 96.02%, respectively. Similarly, Zhao et al. (2016) applied a visual interpretation method to study the land use transformation rules in the Beijing, Tianjin, and Tangshan Region. The accuracy of the interpretation results is estimated higher than 85%.

Also, it can be observed that the significant commission error of perennial trees and orchards mostly comes from the evergreen forest because the canopy pattern of forest areas is similar to perennial trees and orchards (Figures 4.5(a) and 4.5(b)). Meanwhile, the significant omission error of evergreen forest mostly comes from perennial trees and orchards. The appearance of mature rubber trees on satellite images looks like an evergreen forest (Figures 4.5(c) and 4.5(d)). This phenomenon has also occurred in orchards planted with various species and high density (Figures 4.5(e) and 4.5(f)). Both commission and omission were manually corrected for final LULC map production.

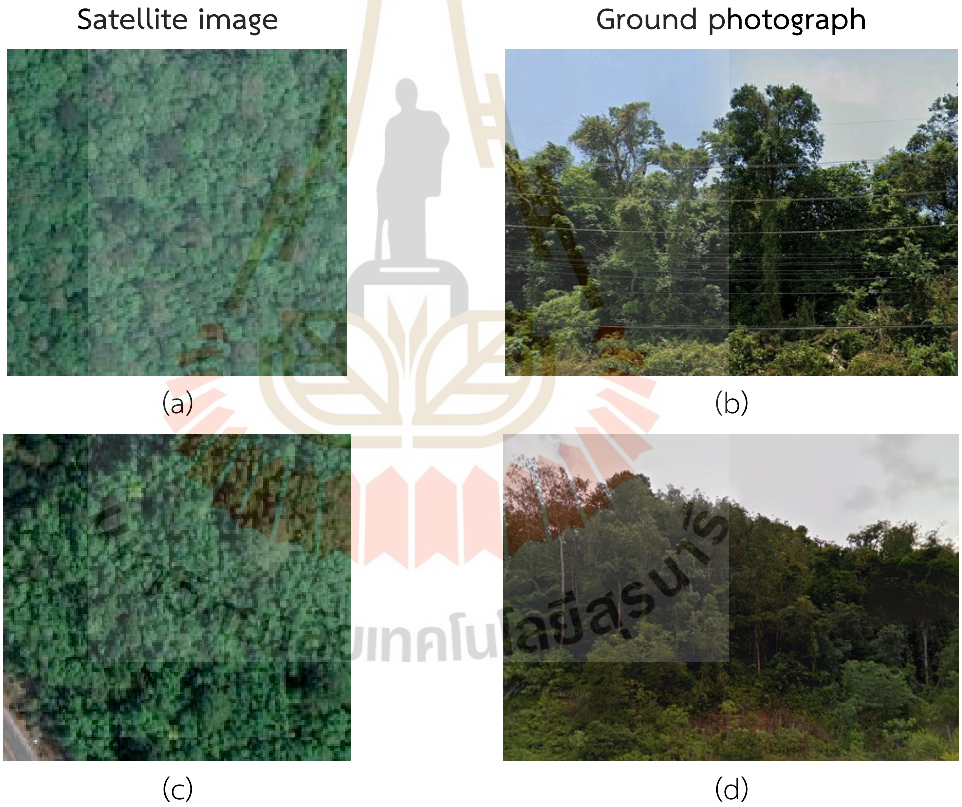

Figure 4.5 Comparison satellite images with the ground photograph for inducing commission and omission error in visual interpretation among perennial trees and orchards and evergreen forest: (a) and (b) commission error of perennial trees and orchards from the evergreen forest, (c) and (d) omission error of evergreen forest from the mature rubber trees, and (e) and (f) omission error of evergreen forest from orchards.

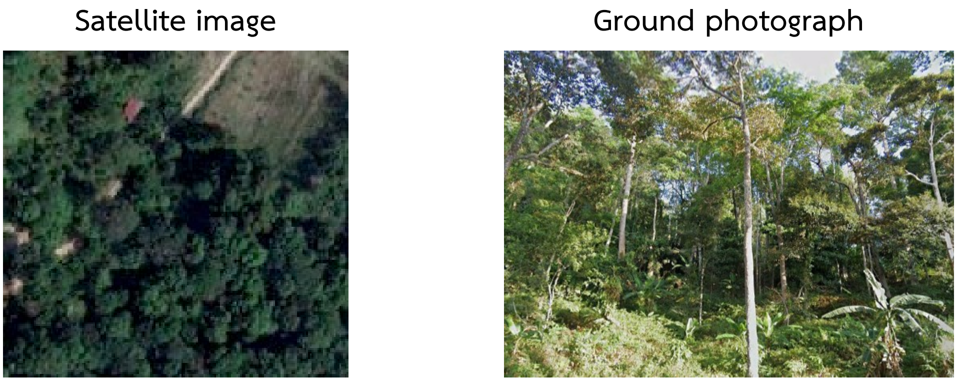

(e) (f)

Figure 4.5 (Continued).

4.2 LULC change detection between 2014 and 2019

A simple comparison of the LULC change area with its annual change rate between 2014 and 2019 is presented in Table 4.5 and Figure 4.6.

Table 4.5 Comparison of LULC change between 2014 and 2019.

LULC	LULC type (Area in km^2)										
	Ur	Pa	Fch	Po	Aq	Id	Ef	Mf	Sf	Wa	Mi
In 2014	125.32	2.15	1.46	196.63	8.74	34.67	80.86	25.15	27.08	14.56	5.43
In 2019	141.64	0.15	3.43	184.39	8.56	39.74	74.16	24.72	27.00	14.81	3.46
Change area	16.33	-2.00	1.96	-12.24	-0.18	5.07	-6.70	-0.43	-0.07	0.24	-1.97
Annual change rate	3.27	-0.40	0.39	-2.45	-0.04	1.01	-1.34	-0.09	-0.01	0.05	-0.39
Percentage of change	3.13	-0.38	0.38	-2.34	-0.03	0.97	-1.28	-0.08	-0.01	0.05	-0.38

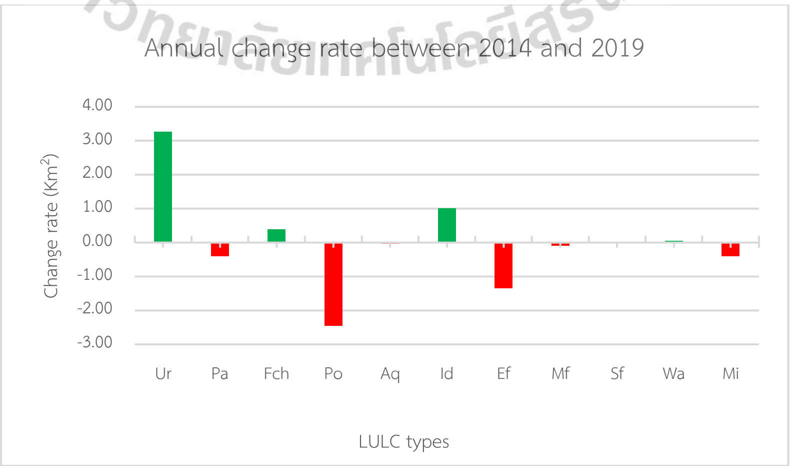

Figure 4.6 Comparison of the annual change rate of LULC type between 2014 and 2019.

As a result, major increasing LULC types between 2014 and 2019 are urban and built-up areas and idle land with an annual change rate of 3.27 and 1.01 km^2/year (Figure 4.7).

Figure 4.7 Development area of built-up areas found during the field survey in 2020.

Meanwhile, minor increasing LULC types in this period are field crop and horticulture, and water body with an annual change rate of 0.39 and 0.05 km^2/year, respectively. In contrast, the major decreasing LULC types between 2014 and 2019 are perennial trees and orchards and evergreen forests with an annual change rate of 2.45 and 1.34 km^2/year, respectively. Minor decreasing LULC types in this period are paddy fields, miscellaneous land, mangrove forest, aquaculture, and scrub forest with an annual change rate of 0.40, 0.39, 0.04, and 0.01 km^2/year, respectively. A transitional change matrix of LULC between 2014 and 2019 using a post-classification comparison change detection algorithm, which provides “from-to” change class information, is summarized in Table 4.6. The LULC change map is displayed in Figure 4.8.

Table 4.6 LULC change between 2014 and 2019 as a transitional matrix.

	LULC types	LULC 2019 (km^2)											
		Ur	Pa	Fch	Po	Aq	Id	Ef	Mf	Sf	Wa	Mi	Total
LULC2 014 (km^2)	Urban and built-up area (Ur)	125.21	-	-	0.02	-	0.09	-	-	-	-	-	**125.32**
	Paddy field (Pa)	0.18	0.15	0.39	0.06	0.02	1.32	-	-	0.03	-	-	**2.15**
	Field crop and horticulture (Fch)	0.28	-	0.91	0.04	-	0.13	-	-	0.10	-	-	**1.46**
	Perennial trees and orchards (Po)	7.29	-	1.80	176.44	-	8.86	0.63	-	1.50	0.05	0.06	**196.63**
	Aquaculture (Aq)	0.11	-	-	0.02	8.52	0.08	-	-	-	0.01	-	**8.74**
	Idle land (Id)	5.19	-	0.29	1.85	-	25.33	0.10	0.01	1.69	0.19	0.01	**34.67**
	Evergreen forest (Ef)	0.58	-	-	3.69	-	0.87	73.28	-	2.43	-	-	**80.86**
	Mangrove forest (Mf)	0.08	-	-	0.02	-	0.14	-	24.70	0.20	-	0.02	**25.15**
	Scrub forest (Sf)	1.53	-	0.03	2.16	-	2.22	0.15	-	20.94	0.02	0.02	**27.08**
	Water body (Wa)	0.14	-	-	0.04	0.01	0.14	-	-	0.02	14.22	-	**14.56**
	Miscellaneous land (Mi)	1.07	-	-	0.05	-	0.56	-	-	0.09	0.32	3.35	**5.43**
	Total	**141.64**	**0.15**	**3.43**	**184.39**	**8.56**	**39.74**	**74.16**	**24.72**	**27.00**	**14.81**	**3.46**	**522.05**

As a result, the highlight of LULC change between 2014 and 2019 can be summarized as follows:

The increasing urban and built-up areas in 2019 are mostly converted from perennial trees and orchards (7.29 km^2) and idle land (5.19 km^2) in 2014. In the meantime, the increase of perennial tree and orchard areas in 2019 are mostly converted from the evergreen forest (3.69 km^2) and scrub forest (2.16 km^2) in 2014. Similarly, the increase of idle land areas in 2019 is mainly converted from perennial trees and orchards (8.86 km^2) in 2014. This finding indicates the increasing land development for real estate, housing, hotels, and resorts in Phuket Island according to the increasing registered population and tourists (Information Technology and Communication Division, Phuket Provincial Office, 2012, 2016; Terra Media and Consulting, 2015; Wongsai, Keson, and Wongsai, 2018).

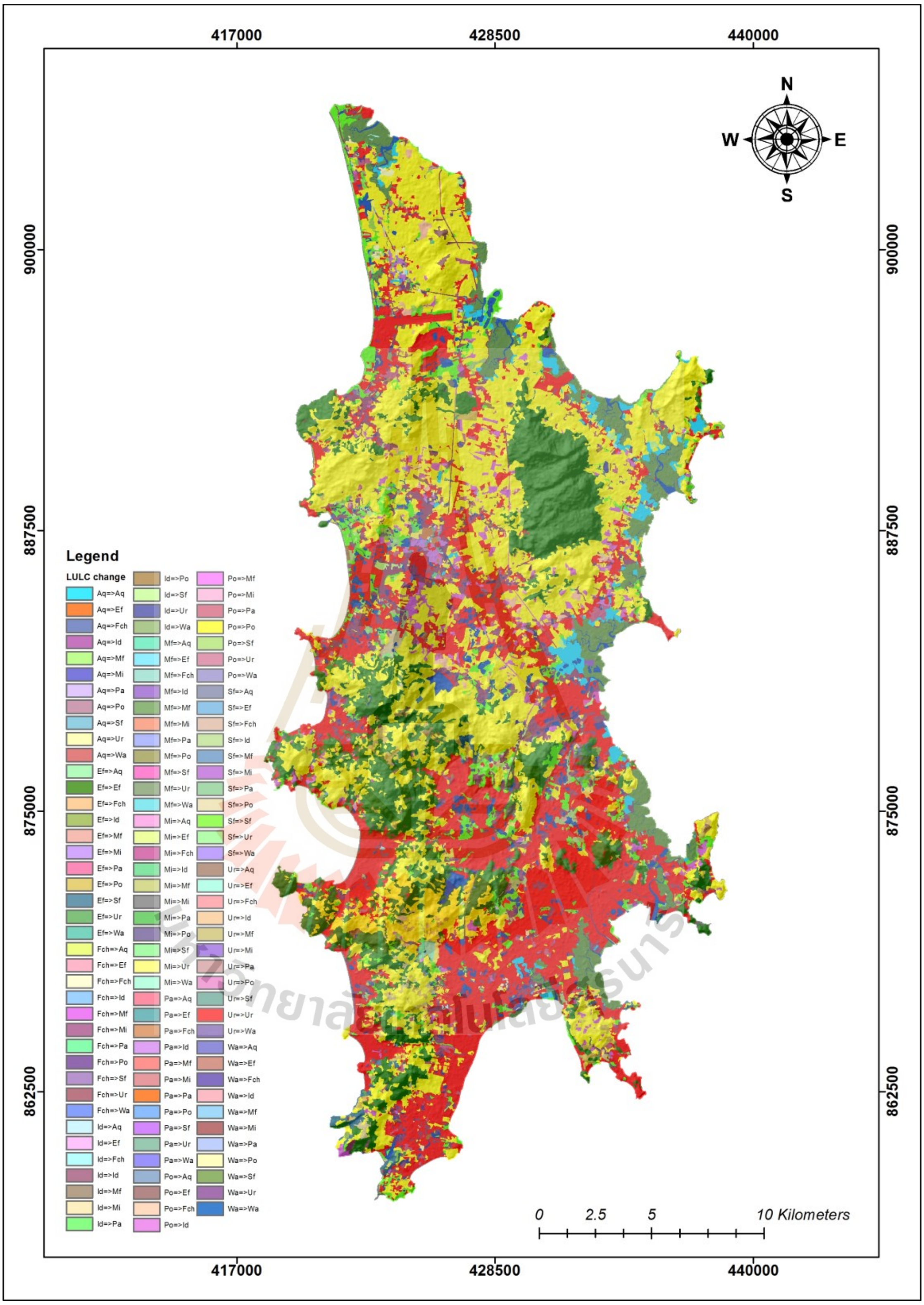
417000
428500
440000
900000
887500
875000
862500
N
W
E
S
Legend
LULC change
Aq=>Aq
Aq=>Ef
Aq=>Fch
Aq=>Id
Aq=>Mf
Aq=>Mi
Aq=>Pa
Aq=>Po
Aq=>Sf
Aq=>Ur
Aq=>Wa
Ef=>Aq
Ef=>Ef
Ef=>Fch
Ef=>Id
Ef=>Mf
Ef=>Mi
Ef=>Pa
Ef=>Po
Ef=>Sf
Ef=>Ur
Ef=>Wa
Fch=>Aq
Fch=>Ef
Fch=>Fch
Fch=>Id
Fch=>Mf
Fch=>Mi
Fch=>Pa
Fch=>Po
Fch=>Sf
Fch=>Ur
Fch=>Wa
Id=>Aq
Id=>Ef
Id=>Fch
Id=>Id
Id=>Mf
Id=>Mi
Id=>Pa
Id=>Po
Id=>Sf
Id=>Ur
Id=>Wa
Mf=>Aq
Mf=>Ef
Mf=>Fch
Mf=>Id
Mf=>Mf
Mf=>Mi
Mf=>Pa
Mf=>Po
Mf=>Sf
Mf=>Ur
Mf=>Wa
Mi=>Aq
Mi=>Ef
Mi=>Fch
Mi=>Id
Mi=>Mf
Mi=>Mi
Mi=>Pa
Mi=>Po
Mi=>Sf
Mi=>Ur
Mi=>Wa
Pa=>Aq
Pa=>Ef
Pa=>Fch
Pa=>Id
Pa=>Mf
Pa=>Mi
Pa=>Pa
Pa=>Po
Pa=>Sf
Pa=>Ur
Pa=>Wa
Po=>Aq
Po=>Ef
Po=>Fch
Po=>Id
Po=>Mf
Po=>Mi
Po=>Pa
Po=>Po
Po=>Sf
Po=>Ur
Po=>Wa
Sf=>Aq
Sf=>Ef
Sf=>Fch
Sf=>Id
Sf=>Mf
Sf=>Mi
Sf=>Pa
Sf=>Po
Sf=>Sf
Sf=>Ur
Sf=>Wa
Ur=>Aq
Ur=>Ef
Ur=>Fch
Ur=>Id
Ur=>Mf
Ur=>Mi
Ur=>Pa
Ur=>Po
Ur=>Sf
Ur=>Ur
Ur=>Wa
Wa=>Aq
Wa=>Ef
Wa=>Fch
Wa=>Id
Wa=>Mf
Wa=>Mi
Wa=>Pa
Wa=>Po
Wa=>Sf
Wa=>Ur
Wa=>Wa
0
2.5
5
10 Kilometers

Figure 4.8 Distribution of LULC change between 2014 and 2019.

In contrast, areas of perennial trees and orchards in 2014 are mostly converted into idle land (8.86 km^2), field crop and horticulture (1.80 km^2), and scrub forest (1.50 km^2) in 2019. Likewise, idle land in 2014 mostly are converted into urban and built-up areas (5.19 km^2), perennial trees and orchards (1.85 km^2), and scrub forests (1.69 km^2) in 2019. Similarly, areas of evergreen forest in 2014 are mostly converted into perennial trees and orchards (3.69 km^2) and scrub forests (2.43 km^2) in 2019.

Besides, LULC change between 2014 and 2019 from the current study is primarily similar in terms of gain and loss of each LULC type with the previous study of Boonchoo (2015) between 1995 and 2014, except field crop and horticulture, idle land, scrub forest and miscellaneous land (Table 4.7 and Figure 4.9).

As a result, the growing LULC areas of both periods are urban and built-up areas and waterbody. In contrast, the decreasing LULC areas are paddy fields, perennial trees and orchards, aquaculture, evergreen forest, and mangrove forest. On the contrary, field crop and horticulture areas were decreased with an annual rate of 0.01 km^2 between 1995 and 2014, but this area was increased with an annual rate of 0.40 km^2 between 2014 and 2019. Likewise, idle land and scrub forest areas were decreased between 1995 and 2014, but these areas were increased between 2014 and 2019. Conversely, areas of miscellaneous land were increased between 1995 and 2014, but these areas were decreased between 2014 and 2019.

Table 4.7 Comparison of the annual rate of LULC change in two periods (1995-2014 and 2014-2019).

No	LULC type	LULC change between 1995 and 2014		LULC change between 2014 and 2019	
		Annual rate (Km^2)	Gain or Loss	Annual rate (Km^2)	Gain or Loss
1	Urban and built-up area	3.12	Gain	3.27	Gain
2	Paddy field	-0.19	Loss	-0.40	Loss
3	Field crop and horticulture	-0.01	Loss	0.40	Gain
4	Perennial trees and orchards	-1.11	Loss	-2.45	Loss
5	Aquaculture	-0.01	Loss	-0.04	Loss
6	Idle land	-1.07	Loss	1.01	Gain
7	Evergreen forest	-0.70	Loss	-1.34	Loss
8	Mangrove forest	-0.08	Loss	-0.09	Loss
9	Scrub forest	-0.10	Loss	0.07	Gain
10	Waterbody	0.03	Gain	0.05	Gain
11	Miscellaneous land	0.10	Gain	-0.39	Loss

Note: LULC change between 1995 and 2014 was adopted from Boonchoo (2015).

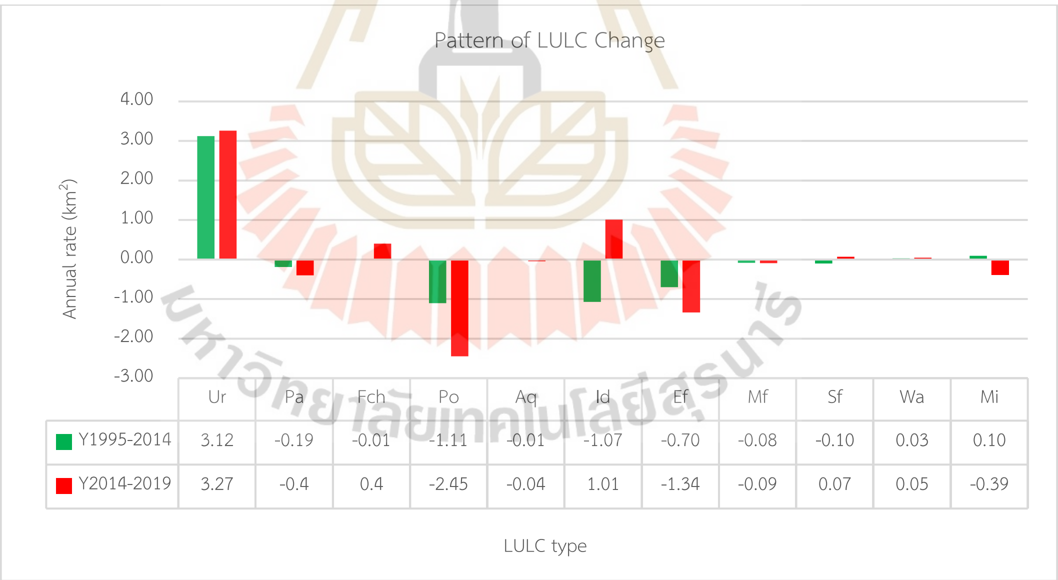

	Ur	Pa	Fch	Po	Aq	Id	Ef	Mf	Sf	Wa	Mi
🟩 Y1995-2014	3.12	-0.19	-0.01	-1.11	-0.01	-1.07	-0.70	-0.08	-0.10	0.03	0.10
🟥 Y2014-2019	3.27	-0.4	0.4	-2.45	-0.04	1.01	-1.34	-0.09	0.07	0.05	-0.39

Figure 4.9 Pattern of LULC change in terms of gain and loss of each LULC type of two periods (1995-2014 and 2014-2019).

In addition, according to the pattern of LULC change from the previous study of Boonchoo (2015) and the current study, it can be concluded that the urban and built-up areas were dramatically increased between 1995 and 2019. Several potential causes of LULC changes have been identified, such as rapid economic development, population growth, and tourist growth, continuously transforming the land use pattern. As a result, tourism development is the primary driver of LULC change in Phuket Island since tourism development led to support for tourist facilities such as the construction of large hotels, huge recreational and commercial areas.

LULC change and urban relevant studies state that urbanization, most of the agricultural land and vegetation areas have been transformed into urban and built-up areas worldwide to meet people’s demands lead to the LULC change, as mentioned by many researchers (e.g., Naikoo, Rihan, Ishtiaque, and Shahfahad, 2020; Imran et al., 2021).

The urban and built-up areas increasing in Phuket Island are primarily expanded in agricultural areas (perennial trees and orchards are the main agricultural area in Phuket Island) and idle land. In contrast, the new agricultural areas like perennial trees and orchards are expanded into the evergreen forest. The probability of urban and built-up areas trend in the future will be increased depending on tourism and economic growth in Phuket Island.

Therefore, LULC studies are helpful to understand the LULC characteristics and their change for land resource management and strategic plan development in the future.

CHAPTER V

LAND USE AND LAND COVER SIMULATION

This chapter presents the results of the first objective focusing on the simulation of the LULC scenario between 2020 and 2029 using the CLUE-S model. The main results, which consist of (1) driving force on LULC change, (2) local parameter of the CLUE-S model for LULC simulation, (3) land demand estimation, and (4) LULC simulation between 2020 and 2029, are here described and discussed in details.

5.1 Driving force on LULC change

Under the CLUE-S model, logistic regression analysis was firstly performed to identify LULC type location preference according to the driving force on LULC change. In this study, eight driving factors on LULC change include elevation, slope, soil fertility, distance to road, distance to settlement, distance to water bodies, population density at the sub-district level, and the average income per capita at the sub-district level (Figure 5.1) were examined as same as Ongsomwang and Boonchoo (2016). Brief information on driving factors on LULC is summarized below.

(1) Elevation. Elevation was collected from the United States Geological Survey, in which spatial resolution is 30 meters. In this study, it was resampled into 50 meters spatial resolution using the nearest method. The domain value of elevation varies from 0 to 545 meters above mean sea level.

(2) Slope. The slope percentage was calculated from the digital elevation model of the United States Geological Survey, and its domain value varies from 0 to 123.37 percent.

(3) Distance to settlement. Distance to an existing urban area is the distance between each cell and the nearest set of urban cells. The settlement was extracted from LULC in 2019, and it was calculated distance to settlement using the Euclidean distance method. The domain value of distance to existing urban areas varies between 0 and 2,102.97 meters.

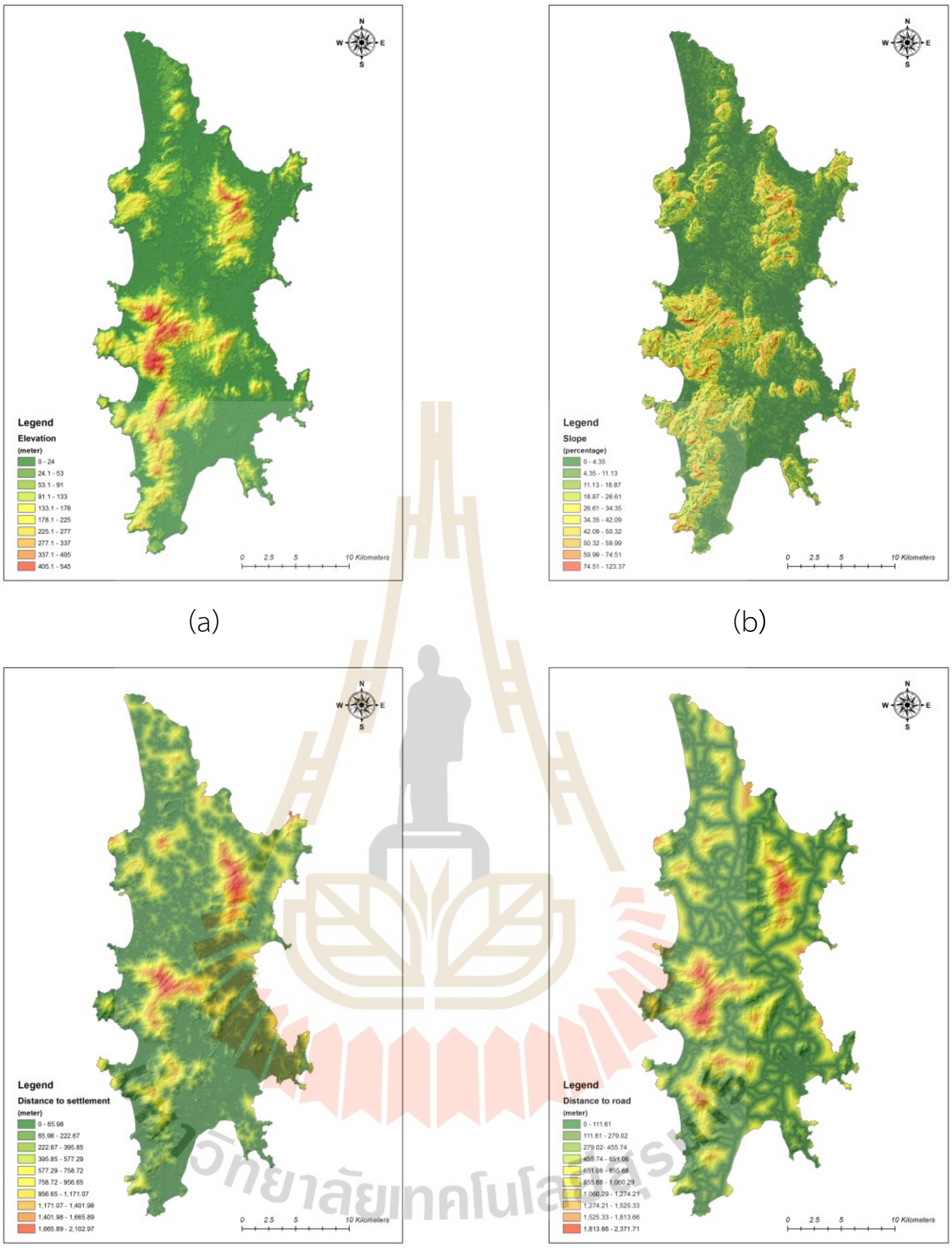
N
W
E
S
Legend
Elevation
(meter)
🟩 0 - 24
🟩 24.1 - 53
🟩 53.1 - 91
🟩 91.1 - 133
🟨 133.1 - 178
🟨 178.1 - 225
🟨 225.1 - 277
🟧 277.1 - 337
🟧 337.1 - 405
🟥 405.1 - 545
0 2.5 5 10 Kilometers
Legend
Slope
(percentage)
🟩 0 - 4.35
🟩 4.35 - 11.13
🟩 11.13 - 18.87
🟩 18.87 - 26.61
🟨 26.61 - 34.35
🟨 34.35 - 42.09
🟨 42.09 - 50.32
🟧 50.32 - 59.99
🟧 59.99 - 74.51
🟥 74.51 - 123.37
0 2.5 5 10 Kilometers
Legend
Distance to settlement
(meter)
🟩 0 - 65.98
🟩 65.98 - 222.67
🟩 222.67 - 395.85
🟩 395.85 - 577.29
🟨 577.29 - 758.72
🟨 758.72 - 956.65
🟨 956.65 - 1,171.07
🟧 1,171.07 - 1,401.98
🟧 1,401.98 - 1,665.89
🟥 1,665.89 - 2,102.97
0 2.5 5 10 Kilometers
Legend
Distance to road
(meter)
🟩 0 - 111.61
🟩 111.61 - 279.02
🟩 279.02- 455.74
🟩 455.74 - 651.06
🟨 651.06 - 855.68
🟨 855.68 - 1,060.29
🟨 1,060.29 - 1,274.21
🟧 1,274.21 - 1,525.33
🟧 1,525.33 - 1,813.66
🟥 1,813.66 - 2,371.71
0 2.5 5 10 Kilometers

(a) (b)

(c) (d)

Figure 5.1 Driving factors on LULC change: (a) Elevation (m), (b) Slope (%), (c) Distance to settlement (m), (d) Distance to road (m), (e) Distance to water bodies (m), (f) Soil fertility, (g) Population density at sub-district level, and (h) Average income per capita of the sub-district.

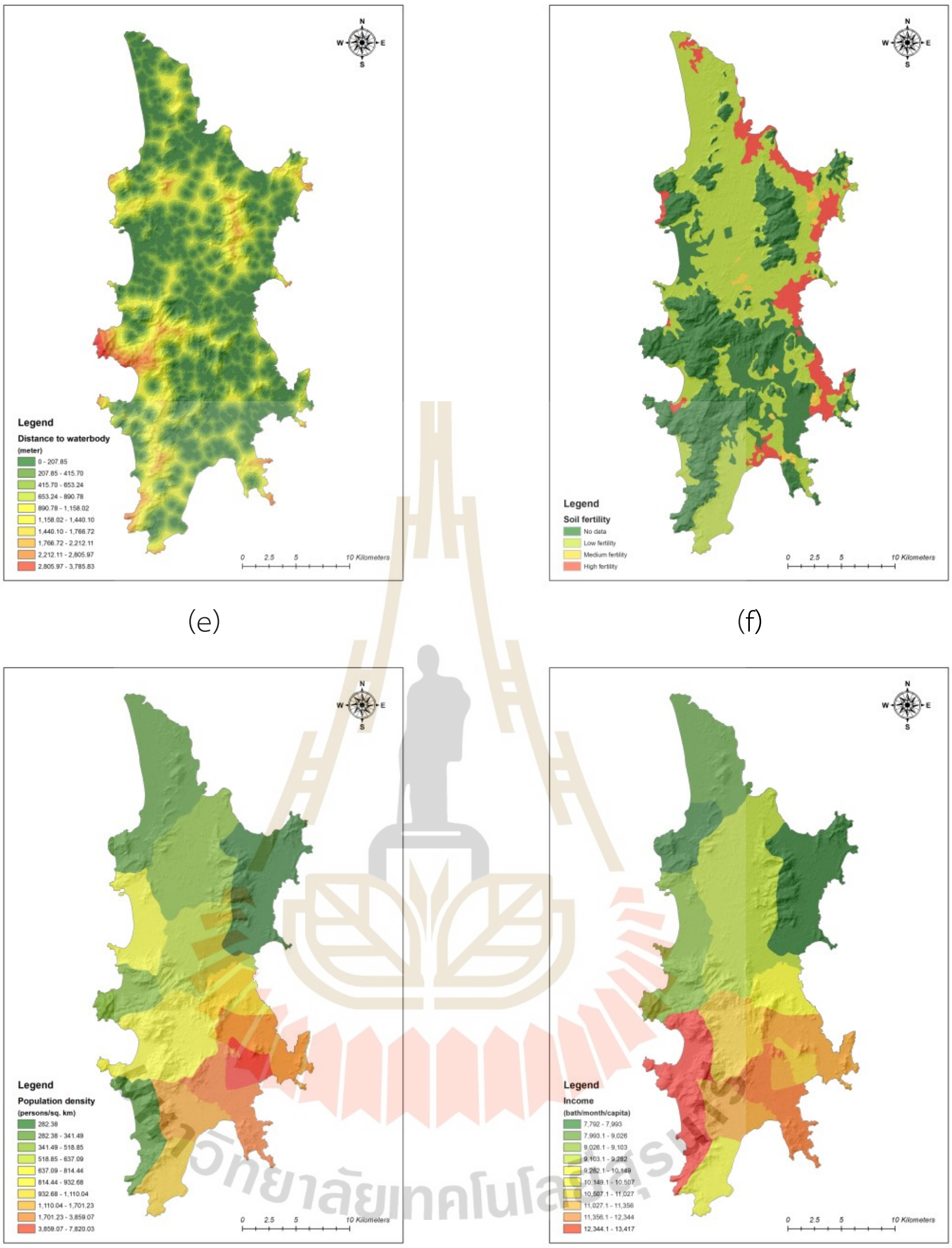
N
W
E
S
Legend
Distance to waterbody
(meter)
0 - 207.85
207.85 - 415.70
415.70 - 653.24
653.24 - 890.78
890.78 - 1,158.02
1,158.02 - 1,440.10
1,440.10 - 1,766.72
1,766.72 - 2,212.11
2,212.11 - 2,805.97
2,805.97 - 3,785.83
0
2.5
5
10 Kilometers
N
W
E
S
Legend
Soil fertility
No data
Low fertility
Medium fertility
High fertility
0
2.5
5
10 Kilometers
N
W
E
S
Legend
Population density
(persons/sq. km)
282.38
282.38 - 341.49
341.49 - 518.85
518.85 - 637.09
637.09 - 814.44
814.44 - 932.68
932.68 - 1,110.04
1,110.04 - 1,701.23
1,701.23 - 3,859.07
3,859.07 - 7,820.03
0
2.5
5
10 Kilometers
N
W
E
S
Legend
Income
(bath/month/capita)
7,792 - 7,993
7,993.1 - 9,026
9,026.1 - 9,103
9,103.1 - 9,282
9,282.1 - 10,149
10,149.1 - 10,507
10,507.1 - 11,027
11,027.1 - 11,356
11,356.1 - 12,344
12,344.1 - 13,417
0
2.5
5
10 Kilometers

(e)

(f)

(g)

(h)

Figure 5.1 (Continued).

(4) Distance to road. Distance to road was computed from the existing road network using the Euclidean distance method. The road network was collected from the Permanent Secretary Office, Ministry of Transport. The domain value of distance to road network varies between 0 and 2,371.71 meters.

(5) Distance to water bodies. Distance to water bodies was computed from the water bodies of LULC in 2019, and it was calculated using the Euclidean distance method. Its domain value varies between 0 and 3,785.83 meters.

(6) Soil fertility. Soil fertility was created from the information of LDD. It was categorized into three groups, including low fertility, medium fertility, and high fertility.

(7) Population density at sub-district level. The population density of each sub-district was calculated based on population data from the Department of Provincial Administration in 2019. The population density of each district diverges between 282.38 and 7,820.03 persons/km^2.

(8) The average income per capita at sub-district level. An average income per capita at the sub-district was calculated based on average income per capita in 2009 from the National Statistical Office. The average income per capita of each district diverges between 7,792 and 13,417 baths/month/capita.

The multicollinearity test results among independent variables with VIF values before binary logistics regression analysis is summarized in Table 5.1. In this study, if the VIF value of each independent variable under the multicollinearity test is less than 10, it is accepted. Meanwhile, the multiple linear regression equation of each LULC type location preference with AUC value by logistic regression analysis is summarized in Table 5.2.

Table 5.1 Multicollinearity statistics test of driving factors effect to LULC type.

Driving factor	Unstandardized Coefficients		Standardized Coefficient	t-test	Sig.	VIF
	Beta	Std. error				
Elevation (X_1)	-.002	.000	-.083	-7.772	.000	3.196
Slope (X_2)	.000	.000	-.049	-8.101	.000	1.025
Distance to settlement (X_3)	.002	.000	.324	31.399	.000	2.987
Distance to road (X_4)	.001	.000	.122	12.906	.000	2.517
Distance to water bodies (X_5)	-.001	.000	-.133	-18.702	.000	1.415
Soil fertility (X_6)	.000	.000	-.100	-12.788	.000	1.708
Population density at sub-district level (X_7)	.000	.000	-.120	-18.065	.000	1.240
The average income per capita at sub-district level (X_8)	.000	.000	.015	2.002	.045	1.485

Table 5.2 Multiple linear regression equation of each LULC type location preference and AUC value by logistic regression analysis.

Driving forces	UR	PA	FCH	PO	AQ	ID	EF	MF	SF	WA	MI
Constance	**-3.33699**	**-6.69685**	**-3.73240**	**-0.44283**	**-2.14060**	**-1.63215**	**-3.43759**	**-1.92855**	**-2.46648**	**-3.21996**	**-5.21909**
Elevation (X_1)	-0.03065	n. s.	n. s.	n. s.	-0.09829	-0.00804	0.00549	-0.12154	n. s.	-0.02983	-0.02009
Slope (X_2)	0.03082	n. s.	n. s.	n. s.	0.09841	0.00829	n. s.	0.12170	n. s.	0.03006	0.01965
Distance to settlement (X_3)	n. s.	n. s.	n. s.	0.00117	0.00154	n. s.	0.00072	0.00270	n. s.	n. s.	n. s.
Distance to road (X_4)	-0.00274	n. s.	n. s.	-0.00068	n. s.	-0.00070	0.00075	0.00213	n. s.	0.00138	0.00099
Distance to water bodies (X_5)	n. s.	-0.00362	n. s.	0.00050	-0.00101	-0.00056	0.00065	-0.00192	-0.00082	n. s.	0.00055
Soil fertility (X_6)	n. s.	n. s.	0.00026	n. s.	n. s.	n. s.	n. s.	0.00007	-0.00002	n. s.	n. s.
Population density at sub-district level (X_7)	0.00025	n. s.	-0.00165	-0.00075	-0.00075	-0.00014	n. s.	n. s.	-0.00015	n. s.	n. s.
The average income per capita at sub-district level (X_8)	0.00037	n. s.	n. s.	n. s.	n. s.	n. s.	n. s.	n. s.	n. s.	n. s.	n. s.
AUC	**0.883058**	**0.668109**	**0.717422**	**0.799695**	**0.879755**	**0.689687**	**0.888607**	**0.935244**	**0.651999**	**0.731248**	**0.695395**

Remark: All explanatory variables are significant at $p < 0.05$ error level; n. s. is not significant at 0.05 level; AUC, area under the curve.

The driving force details on each LULC type allocation with its equation are separately explained and discussed in the following section.

5.1.1 Driving force for urban and built-up area allocation

The multiple linear equation of the binomial logit regression model for urban and built-up area allocation after multicollinearity test is as follows:

$$Log\left(\frac{P_i}{1\text{-}P_i}\right) = -3.33699 - 0.03065X_1 + 0.03082X_2 - 0.00274X_4 + 0.00025X_7 + 0.00037X_8 \quad (5.1)$$

Where

X_1 is Elevation (m);

X_2 is Slope (%);

X_4 is Distance to road (m);

X_7 is Population density at sub-district level (persons per km^2); and

X_8 is Average income per capita at sub-district level (bath/month/capita)

According to Equation (5.1), two driving factors, including elevation and distance to road, show a negative relationship with the urban and built-up area allocation probability. Still, three driving factors, including slope, population density at sub-district levels, and the average income per capita at the sub-district level, show a positive relationship with the probability of urban and built-up area allocation.

All significant driving factors genuinely play a significant role in urban and built-up area allocation. These results imply that when the elevation and distance to road decreases, the probability of the urban and built-up area’s occurrence increases. Meanwhile, when slope, population density at sub-district levels, and the average income per capita at sub-district level increase, the probability of occurrence of the urban and built-up area increases.

Besides, the AUC value for urban and built-up area allocation is 0.88, and it suggests an excellent discrimination fit between the simulated and real LULC transition (Hosmer, Lemeshow, and Sturdivant, 2013).

5.1.2 Driving force for paddy field allocation

The multiple linear equation of the binomial logit regression model for paddy field allocation after multicollinearity test is as follows:

$$Log\left(\frac{P_i}{1\text{-}P_i}\right) = -\ 6.69685 - 0.00362X_5 \qquad (5.2)$$

Where

X_5 is Distance to water bodies (m)

According to Equation (5.2), only one of the driving factors, namely, distance to waterbody, shows a negative relationship with the probability of the paddy field allocation. The possible reason to describe this finding is that the area of the existing paddy field in the study is small compared to other LULC types (see Table 4.3 in Chapter IV). This significant driving factor plays a vital role in paddy field allocation. This finding implies that when the distance to water bodies decreases, the paddy field area's probability increases. However, the AUC value for paddy field allocation with a value of 0.67 suggests a poor discrimination fit between the simulated and real LULC transition (Hosmer et al., 2013).

5.1.3 Driving force for field crop and horticulture allocation

The equation of the binomial logit regression model for field crop and horticulture allocation after multicollinearity test is as follows:

$$Log\left(\frac{P_i}{1\text{-}P_i}\right) = -\ 3.73240 + 0.00026X_6 - 0.00165X_7 \qquad (5.3)$$

Where

X_6 is Soil fertility; and

X_7 is Population density at sub-district level (person per km^2)

Referring to Equation (5.3), only one driving factor, population density at the sub-district level, shows a negative relationship with the field crop and horticulture allocation probability. In contrast, only one driving factor, namely soil fertility, shows a positive relationship with the field crop and horticulture allocation probability.

Both significant driving factors play a vital role in field crop and horticulture allocation. This result implies that when population density at the sub-district level decreases, the probability of field crop and horticulture area occurrence increases. Meanwhile, when soil fertility increases, the probability of field crop and horticulture area occurrence increases. Besides, the AUC value for field crop and horticulture allocation is 0.72, and it suggests an acceptable discrimination fit between the simulated and real LULC transition (Hosmer et al., 2013).

5.1.4 Driving force for perennial trees and orchards allocation

The equation of the binomial logit regression model for perennial trees and orchards allocation after multicollinearity test is as follows:

$$Log\left(\frac{P_i}{1\text{-}P_i}\right) = -\,0.44283 + 0.00117X_3 - 0.00068X_4 + 0.00050X_5 - 0.00075X_7 \quad (5.4)$$

Where

X_3 is Distance to settlement (m);

X_4 is Distance to road (m);

X_5 is Distance to water bodies (m); and

X_7 is Population density at sub-district level (person per km^2)

According to Equation (5.4), two driving factors, distance to road and population density at sub-district level, show a negative relationship with the perennial trees and orchards allocation probability. Still, two driving factors, distance to settlement and distance to a water body, show a positive relationship with the probability of perennial trees and orchards allocation.

All significant driving factors play an essential role in perennial trees and orchards allocation. These results imply that when the distance to road and population density at sub-district level decreases, the occurrence' probability of the perennial trees and orchards area increases. Meanwhile, when the distance to settlement and distance to water bodies increase, the perennial trees and orchards area's probability increases.

Besides, the AUC value for perennial trees and orchards allocation is 0.80, and it suggests an excellent discrimination fit between the simulated and real LULC transition (Hosmer et al., 2013).

5.1.5 Driving force for aquaculture allocation

The equation of the binomial logit regression model for aquaculture allocation after multicollinearity test is as follows:

$$Log\left(\frac{P_i}{1\text{-}P_i}\right) = -\ 2.14060 - 0.09829X_1 + 0.0.09841X_2 + 0.00154X_3$$
$$- 0.000101X_5 - 0.00075X_7 \qquad (5.5)$$

Where

X_1	is	Elevation (m);
X_2	is	Slope (%);
X_3	is	Distance to settlement (m);
X_5	is	Distance to water bodies (m); and
X_7	is	Population density at sub-district level (person per km^2).

According to Equation (5.5), three driving factors: elevation, distance to water bodies, and population density at sub-district level, show a negative relationship with the probability of the aquaculture allocation. Still, two driving factors, slope and distance to settlement, show a positive relationship with the probability of the aquaculture allocation.

All significant driving factors play an essential role in aquaculture allocation. These results imply that when elevation, distance to water bodies, and population density at sub-district level decreases, the aquaculture area's occurrence probability increases. Meanwhile, when the slope and distance to settlement increase, the probability of the aquaculture area's occurrence increases.

Besides, the AUC value for aquaculture allocation is 0.88, and it suggests an excellent discrimination fit between the simulated and real LULC transition (Hosmer et al., 2013).

5.1.6 Driving force for idle land allocation

The equation of the binomial logit regression model for idle land allocation after multicollinearity test is as follows:

$$Log\left(\frac{P_i}{1\text{-}P_i}\right) = -1.63215 - 0.00804X_1 + 0.00829X_2 - 0.00070X_4$$
$$- 0.00056X_5 - 0.00014X_7 \qquad (5.6)$$

Where

X_1 is Elevation (m);

X_2 is Slope (%);

X_4 is Distance to road (m);

X_5 is Distance to water bodies (m); and

X_7 is Population density at sub-district level (person per km^2)

According to Equation (5.6), four driving factors: elevation, distance to road, distance to water bodies, and population density at sub-district level, show a negative relationship with the probability of idle land allocation. Still, only one driving factor, namely, slope, has a positive relationship with the probability of idle land allocation.

All significant driving factors play an essential role in idle land allocation. These results imply that when the elevation, distance to road, distance to water bodies, and population density at sub-district level decreases, the probability of the idle land area's occurrence increases. Meanwhile, when the slope increase, the probability of the idle area's occurrence increases. However, the AUC value for idle land allocation with a value of 0.69 suggests a poor discrimination fit between the simulated and real LULC transition (Hosmer et al., 2013).

5.1.7 Driving force for evergreen forest allocation

The equation of the binomial logit regression model for evergreen forest allocation after multicollinearity test is as follows:

$$Log\left(\frac{P_i}{1\text{-}P_i}\right) = -\ 3.43759 + 0.00549X_1 + 0.00072X_3 + 0.00075X_4 + 0.00065X_5 \qquad (5.7)$$

Where

X_1 is Elevation (m);

X_3 is Distance to settlement (m);

X_4 is Distance to road (m); and

X_5 is Distance to water bodies (m)

According to Equation (5.7), all driving factors elevation, distance to settlement, distance to road, and distance to water bodies show a positive relationship with the probability of the evergreen forest allocation.

All significant driving factors play an important role in evergreen forest allocation. These results imply that when the elevation, distance to settlement, distance to road, and distance to water bodies increase, the probability of the evergreen forest area's occurrence increases. In addition, the AUC value for evergreen forest allocation is 0.89, and it suggests an excellent discrimination fit between the simulated and real LULC transition (Hosmer et al., 2013).

5.1.8 Driving force for mangrove forest allocation

The equation of the binomial logit regression model for mangrove forest allocation after multicollinearity test is as follows:

$$Log\left(\frac{P_i}{1-P_i}\right) = -\ 1.92855 - 0.12154X_1 + 0.12170X_2 + 0.00270X_3 + 0.00213X_4 - 0.00192X_5 + 0.00007X_6 \tag{5.8}$$

Where

X_1 is Elevation (m);
X_2 is Slope (%);
X_3 is Distance to settlement (m);
X_4 is Distance to road (m);
X_5 is Distance to water bodies (m); and
X_6 is Soil fertility

According to Equation (5.8), two driving factors, include elevation and distance to water bodies, show a negative relationship with the probability of mangrove forest allocation. Still, four driving factors include slope, distance to settlement, distance to road, and soil fertility, show a positive relationship with the probability of the mangrove forest allocation.

All significant driving factors play an important role in mangrove forest allocation. These results imply that when the elevation and distance to water bodies decreases, the probability of the mangrove forest area's occurrence increases. Meanwhile, when slope, distance to settlement, distance to road, and soil fertility increase, the mangrove forest area's occurrence increases.

In addition, the AUC value for mangrove forest allocation is 0.94, and it suggests an outstanding discrimination fit between the simulated and real LULC transition (Hosmer et al., 2013).

5.1.9 Driving force for scrub forest allocation

The equation of the binomial logit regression model for scrub forest allocation after multicollinearity test is as follows:

$$Log\left(\frac{P_i}{1\text{-}P_i}\right) = -\ 2.46648 - 0.00082X_5 - 0.00002X_6 - 0.00015X_7 \qquad (5.9)$$

Where

X_5 is Distance to water bodies (m);

X_6 is Soil fertility; and

X_7 is Population density at sub-district level (person per km^2)

According to Equation (5.9), all of the driving factors include distance to water bodies, soil fertility, and population density at the sub-district level, show a negative relationship with the probability of the scrub forest allocation.

All significant driving factors play an important role in scrub forest allocation. These results imply that when the distance to water bodies, soil fertility, and population density at the sub-district level decreases, the probability of scrub forest occurrence increases.

In addition, the AUC value for mangrove forest allocation is 0.65; it suggests a poor discrimination fit between the simulated and real LULC transition (Hosmer et al., 2013).

5.1.10 Driving force for waterbody allocation

The equation of the binomial logit regression model for waterbody allocation after multicollinearity test is as follows:

$$Log\left(\frac{P_i}{1\text{-}P_i}\right) = -\ 3.21996 - 0.02983X_1 + 0.03006X_2 + 0.00138X_4 \qquad (5.10)$$

Where

X_1 is Elevation (m);

X_2 is Slope (%); and

X_4 is Distance to road (m)

According to Equation (5.10), the driving factor, namely elevation, shows a negative relationship with the probability of waterbody allocation. Still, two driving factors, slope and distance to road, show a positive relationship with the probability of the waterbody allocation.

All significant driving factors play an important role in waterbody allocation. These results imply that when the elevation decreases, the probability of the waterbody area's occurrence increases. Meanwhile, when slope and distance to road increase, the probability of the waterbody area's occurrence increases.

In addition, the AUC value for waterbody allocation is 0.73, and it suggests an acceptable discrimination fit between the simulated and real LULC transition (Hosmer et al., 2013).

5.1.11 Driving force for miscellaneous land allocation

The equation of the binomial logit regression model for miscellaneous land allocation after multicollinearity test is as follows:

$$Log\left(\frac{P_i}{1\text{-}P_i}\right) = -\ 5.21909 - 0.02009X_1 + 0.01965X_2 + 0.0099X_4 + 0.00055X_5 \quad (5.11)$$

Where

X_1 is Elevation (m);

X_2 is Slope (%);

X_4 is Distance to road (m); and

X_5 is Distance to water bodies (m);

According to Equation (5.11), the driving factor, elevation, negatively correlates with the probability of miscellaneous land allocation. Still, three driving factors, slope, distance to road, and distance to water bodies, show a positive relationship with the probability of miscellaneous land allocation.

All significant driving factors play an important role in miscellaneous land allocation. These results imply that when the elevation decreases, the probability of the miscellaneous land area's occurrence increases. Meanwhile, when slope, distance to road, and distance to water bodies increase, the probability of the miscellaneous land area's occurrence increases.

In addition, the AUC value for miscellaneous land allocation is 0.70, and it suggests an acceptable discrimination fit between the simulated and real LULC transition (Hosmer et al., 2013).

In summary, it can be here concluded that the most significant driving factor for all LULC type allocation in the study area is the distance to water bodies, which was identified as a significant factor for most LULC type location preference, except urban and built-up land, field crop and horticulture, water bodies. Additionally, this factor is only one significant factor in allocating paddy fields based on its probability during the CLUE-S model simulation process. Meanwhile, the second essential driving factors for LULC type allocation are elevation and distance to road. In the meantime, the third essential driving factors for the LULC type allocation area are slope and population density at the sub-district level. Besides, soil fertility shows a vital role in the land allocation of the field crop and horticulture, mangrove forest, and scrub forest. In the meantime, the distance to settlement shows a vital role for land allocation of the perennial trees and orchards, aquaculture, evergreen forest, and mangrove forest. Likewise, the average income per capita at the sub-district level shows a vital role in urban and built-up area allocation (see Table 5.2). The derived driving factors of each LULC type are further used by the CLUE-S model for LULC allocation during the simulation process.

Furthermore, it can be noted that the derived area under curve (AUC) values for each LULC type allocation using binary logistics regression analysis provides values between 0.65 and 0.94, which means the simulated and real LULC transition is acceptable with fair to outstanding discrimination (Hosmer et al., 2013).

5.2 Local parameter of the CLUE-S model for LULC simulation

Under this section, two required parameters of the CLUE-S model for LULC simulation consist of conversion matrix and elasticity of LULC change, are here considered and assigned based on transitional change matrix between LULC data in 2019 and 2029.

In principle, the conversion matrix, which shows the possibility for LULC change among LULC types, is assigned as 1 when it is allowed or as 0 when it is not allowed. In the meantime, elasticity, which represents a cost for change among LULC types, is set up according to the transitional probability change matrix in the past period.

In this study, the conversion matrix for each LULC type possibly change between 2019 and 2029 is set up based on transitional LULC change between 2014 and 2019 as a summary in Table 5.3. For example, scrub forest allows converting into an urban and built-up area, field crop and horticulture, perennial trees and orchards, idle land, and miscellaneous land. Meanwhile, the transition probability matrix of LULC change between 2014 and 2019 from the Markov Chain model is here applied to assign elasticity value as suggested by Ongsomwang and Iamchuen (2015). Herewith, the elasticity value of the urban and built-up area, paddy field, field crop and horticulture, perennial trees and orchards, aquaculture, idle land, evergreen forest, mangrove forest, scrub forest, water bodies, and miscellaneous land are 1.00, 0.44, 0.40, 0.81, 0.95, 0.54, 0.82, 0.96, 0.60, 1.00, and 0.40 respectively. These elasticity values imply the probability of land use change. For example, urban and built-up areas and water bodies in 2019 do not change to other LULC types in 2029. On the contrary, field crop and horticulture in 2019 can be converted into many LULC types with different probabilities (see Table 5.4).

Table 5.3 Conversion matrix of possible LULC change between 2019 and 2029.

	LULC Types	Possible change in 2029										
		Ur	Pa	Fch	Po	Aq	Id	Ef	Mf	Sf	Wa	Mi
LULC in 2019	Urban and built-up area (Ur)	1	0	0	0	0	0	0	0	0	0	0
	Paddy field (Pa)	1	1	1	1	0	1	0	0	1	0	0
	Field crop and horticulture (Fch)	1	0	1	1	0	1	0	0	1	0	0
	Perennial trees and orchards (Po)	1	0	1	1	0	1	0	0	1	0	0
	Aquaculture (Aq)	1	0	0	0	1	1	0	0	0	1	0
	Idle land (Id)	1	0	1	1	0	1	0	0	1	0	0
	Evergreen forest (Ef)	1	0	1	1	0	1	1	0	1	0	0
	Mangrove forest (Mf)	1	0	0	1	1	1	0	1	1	0	1
	Scrub forest (Sf)	1	0	1	1	0	1	0	0	1	0	1
	Waterbody (Wa)	0	0	0	0	0	0	0	0	0	1	0
	Miscellaneous land (Mi)	1	0	0	0	0	1	0	0	1	1	1

Note: 0 is not allowed and 1 is allowed.

Table 5.4 Transition probability matrix of LULC change between 2014 and 2019 by the Markov Chain model.

	LULC Types	LULC in 2019										
		Ur	Pa	Fch	Po	Aq	Id	Ef	Mf	Sf	Wa	Mi
LULC in 2014	Urban and built-up area (Ur)	**1.000**	-	-	-	-	-	-	-	-	-	-
	Paddy field (Pa)	0.127	**0.440**	0.076	0.034	0.005	0.283	0.001	-	0.031	0.003	-
	Field crop and horticulture (Fch)	0.316	-	**0.400**	0.049	-	0.128	0.001	-	0.106	0.001	-
	Perennial trees and orchards (Po)	0.080	-	0.014	**0.808**	-	0.075	0.006	-	0.016	0.001	-
	Aquaculture (Aq)	0.027	-	-	0.005	**0.948**	0.015	-	0.001	0.001	0.003	-
	Idle land (Id)	0.268	-	0.013	0.089	-	**0.541**	0.005	0.001	0.074	0.010	-
	Evergreen forest (Ef)	0.019	-	0.001	0.085	-	0.023	**0.822**	-	0.051	-	-
	Mangrove forest (Mf)	0.008	-	-	0.003	-	0.010	-	**0.964**	0.014	-	0.001
	Scrub forest (Sf)	0.114	-	0.003	0.138	-	0.130	0.010	-	**0.602**	0.002	0.001
	Water bodies (Wa)	-	-	-	-	-	-	-	-	-	**1.000**	-
	Miscellaneous land (Mi)	0.328	-	0.001	0.022	-	0.138	0.001	-	0.029	0.094	**0.387**

5.3 Land demand estimation

The land demand was estimated based on the annual rate of LULC change from the transition area matrix between LULC in 2014 and 2019 using the Markov Chain model as shown in Table 5.5. Herewith, annual land use demand between 2019 and 2029 was calculated and presented in Table 5.6.

Table 5.5 Transition area matrix of LULC change between 2019 and 2029 from the Markov Chain model.

	LULC Types	LULC in 2029 (km^2)											
		Ur	Pa	Fch	Po	Aq	Id	Ef	Mf	Sf	Wa	Mi	Total
LULC in 2019 in (km^2)	Urban and built-up area (Ur)	141.52	0.00	0.01	0.04	0.00	0.19	0.00	0.00	0.01	0.00	0.00	141.77
	Paddy field (Pa)	0.04	0.00	0.02	0.01	0.00	0.08	0.00	0.00	0.01	0.00	0.00	0.15
	Field crop and horticulture (Fch)	1.10	0.00	1.39	0.17	0.00	0.45	0.00	0.00	0.37	0.00	0.00	3.47
	Perennial trees and orchards (Po)	14.75	0.00	2.64	148.88	0.00	13.83	1.11	0.00	2.88	0.13	0.08	184.29
	Aquaculture (Aq)	0.23	0.00	0.00	0.05	8.03	0.13	0.00	0.01	0.01	0.03	0.00	8.47
	Idle land (Id)	10.65	0.00	0.50	3.53	0.01	21.52	0.20	0.02	2.95	0.39	0.02	39.78
	Evergreen forest (Ef)	1.38	0.00	0.04	6.29	0.00	1.68	60.90	0.00	3.81	0.01	0.01	74.11
	Mangrove forest (Mf)	0.20	0.00	0.00	0.07	0.00	0.25	0.00	23.80	0.35	0.00	0.02	24.68
	Scrub forest (Sf)	3.07	0.00	0.07	3.71	0.01	3.48	0.27	0.00	16.18	0.05	0.03	26.87
	Waterbody (Wa)	0.28	0.00	0.00	0.08	0.01	0.26	0.01	0.00	0.04	14.30	0.00	14.98
	Miscellaneous land (Mi)	1.14	0.00	0.00	0.08	0.00	0.48	0.01	0.00	0.10	0.33	1.35	3.49
	Total	**174.34**	**0.00**	**4.67**	**162.90**	**8.07**	**42.35**	**62.49**	**23.83**	**26.69**	**15.23**	**1.50**	**522.05**

Table 5.6 Annual land demand of each LULC type for LULC simulation.

Year	LULC type (Area of in km^2)										
	Ur	Pa	Fch	Po	Aq	Id	Ef	Mf	Sf	Wa	Mi
2019	141.77	0.15	3.47	184.29	8.47	39.78	74.11	24.68	26.87	14.98	3.49
2020	145.02	0.14	3.59	182.15	8.43	40.03	72.94	24.60	26.85	15.00	3.29
2021	148.28	0.12	3.71	180.01	8.39	40.29	71.78	24.51	26.83	15.03	3.09
2022	151.54	0.11	3.83	177.87	8.35	40.55	70.62	24.43	26.82	15.05	2.89
2023	154.80	0.09	3.95	175.73	8.31	40.80	69.46	24.34	26.80	15.08	2.69
2024	158.05	0.08	4.07	173.60	8.27	41.06	68.30	24.25	26.78	15.10	2.50
2025	161.31	0.06	4.19	171.46	8.23	41.32	67.14	24.17	26.76	15.13	2.30
2026	164.57	0.05	4.31	169.32	8.19	41.57	65.98	24.08	26.75	15.15	2.10
2027	167.82	0.03	4.43	167.18	8.15	41.83	64.82	24.00	26.73	15.18	1.90
2028	171.08	0.02	4.55	165.04	8.11	42.09	63.65	23.91	26.71	15.20	1.70
2029	174.34	0.00	4.67	162.90	8.07	42.35	62.49	23.83	26.69	15.23	1.50
Annual rate	**3.26**	**-0.02**	**0.12**	**-2.14**	**-0.04**	**0.26**	**-1.16**	**-0.09**	**-0.02**	**0.02**	**-0.20**

The increasing LULC classes are urban and built-up areas, field crop and horticulture, idle land, and waterbody with an increasing annual rate of 3.26, 0.12, 0.26, and 0.02 km^2/year. In contrast, the decreasing LULC classes are paddy field, perennial trees and orchards, aquaculture, evergreen forest, mangrove forest, scrub forest, and miscellaneous land with a decreasing annual rate of 0.02, 2.14, 0.04, 1.16, 0.09, 0.02 and 0.20 km^2/year, respectively.

5.4 LULC simulation between 2020 and 2029

For LULC simulation as trend scenario, conversion matrix and elasticity of LULC change and estimated land demand were simultaneously combined with driving force on LULC change to simulate LULC data between 2020 and 2029. The distribution of the simulated LULC scenario between 2020 and 2029 is presented in Figure 5.2, while the area and the percentage of LULC scenarios between 2020 and 2029 are summarized in Tables 5.7 and 5.8, respectively.

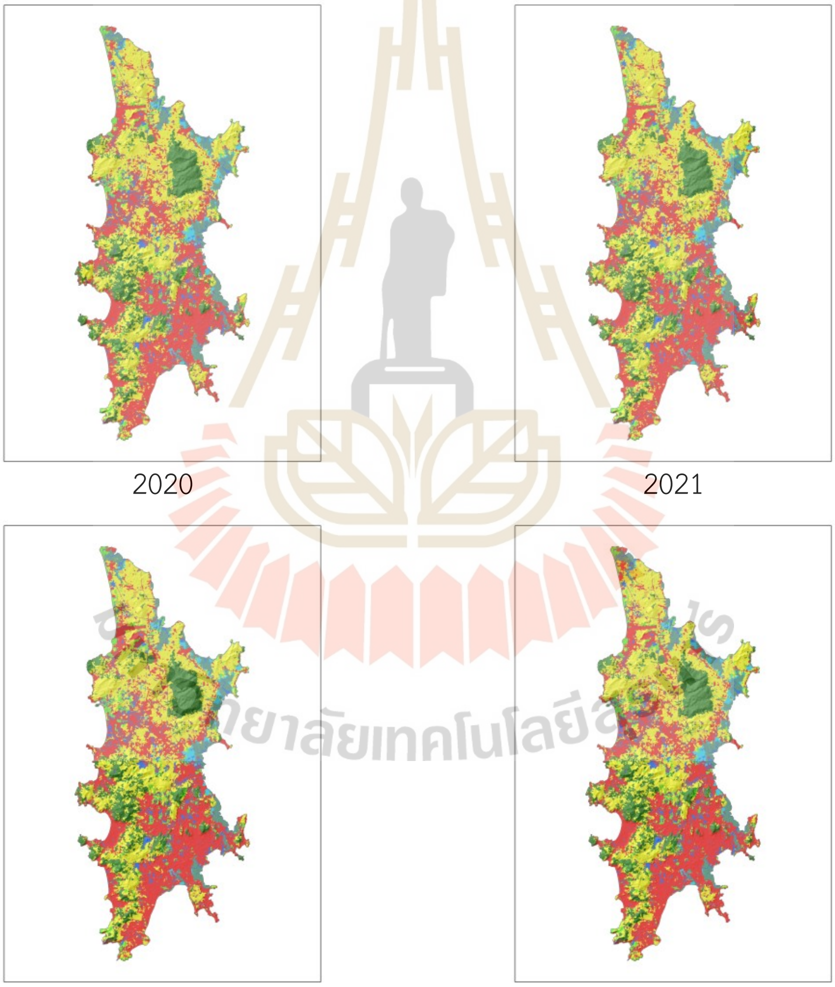

2020 2021

2022 2023

Figure 5.2 Spatial distribution of the simulated LULC scenario between 2020 and 2029.

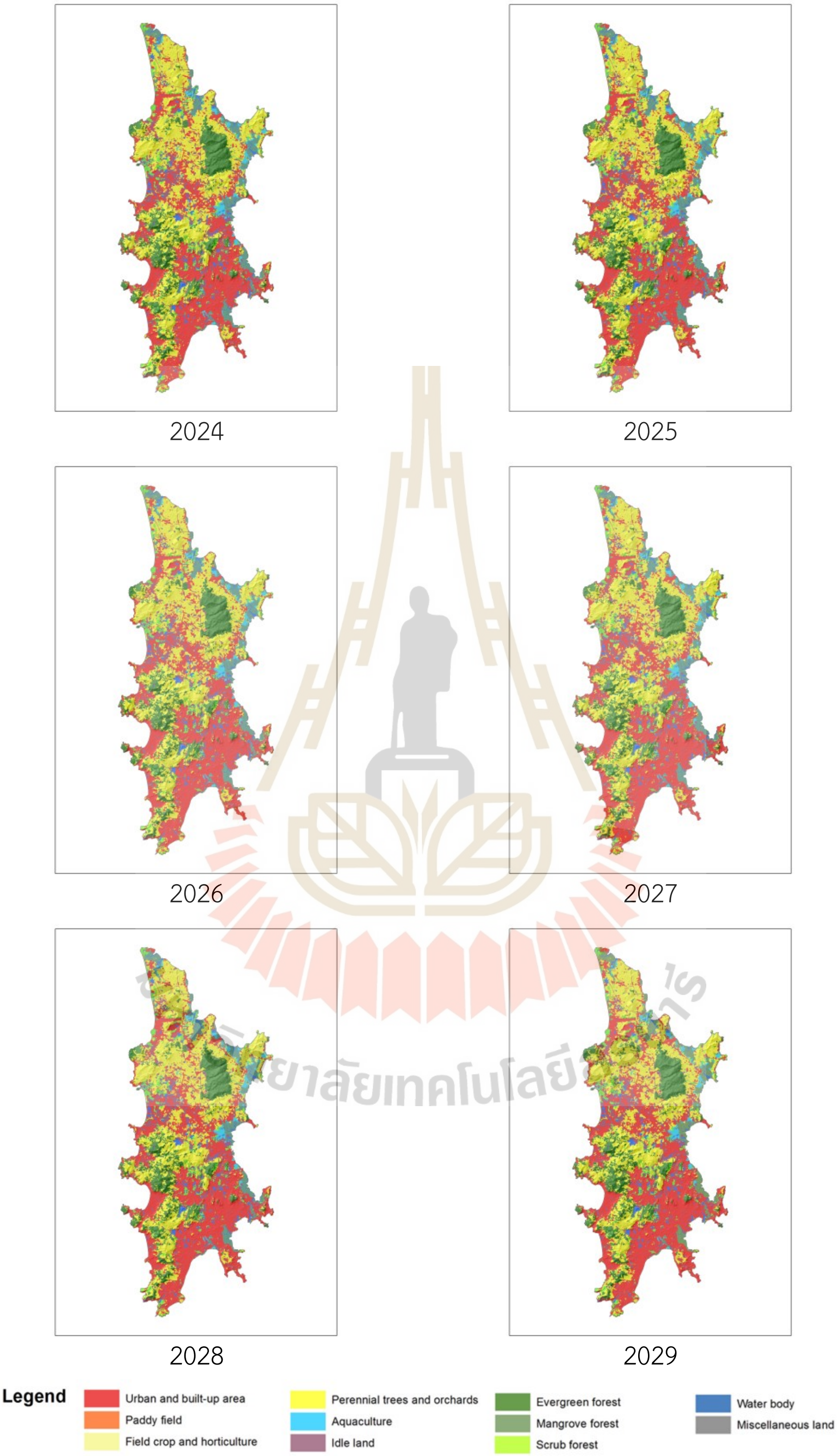
2024
2025
2026
2027
2028
2029

Legend
Urban and built-up area
Paddy field
Field crop and horticulture
Perennial trees and orchards
Aquaculture
Idle land
Evergreen forest
Mangrove forest
Scrub forest
Water body
Miscellaneous land

Figure 5.2 (Continued).

Table 5.7 Area of simulated LULC between 2020 and 2029.

LULC types	Area of simulated LULC in km^2									
	2020	2021	2022	2023	2024	2025	2026	2027	2028	2029
Urban and built-up area (Ur)	145.03	148.29	151.54	154.81	158.07	161.32	164.55	167.83	170.92	174.34
Paddy field (Pa)	0.13	0.13	0.10	0.09	0.07	0.06	0.05	0.03	0.02	0.00
Field crop and horticulture (Fch)	3.47	3.52	3.82	3.76	3.99	4.19	4.30	4.44	4.39	4.67
Perennial trees and orchards (Po)	182.16	180.01	177.87	175.74	173.55	171.46	169.35	167.20	165.21	162.90
Aquaculture (Aq)	8.47	8.47	8.45	8.45	8.45	8.30	8.25	8.17	8.17	8.07
Idle land (Id)	40.03	40.29	40.54	40.82	41.01	41.32	41.59	41.85	42.09	42.35
Evergreen forest (Ef)	72.96	71.79	70.62	69.47	68.27	67.15	65.98	64.83	63.71	62.49
Mangrove forest (Mf)	24.68	24.66	24.44	24.44	24.44	24.19	24.10	24.01	24.01	23.82
Scrub forest (Sf)	26.85	26.84	26.81	26.79	26.74	26.76	26.75	26.74	26.77	26.69
Waterbody (Wa)	14.98	14.98	14.98	14.98	14.98	14.98	15.04	15.04	15.04	15.22
Miscellaneous land (Mi)	3.30	3.08	2.88	2.70	2.48	2.32	2.08	1.91	1.72	1.50
Total	**522.05**	**522.05**	**522.05**	**522.05**	**522.05**	**522.05**	**522.05**	**522.05**	**522.05**	**522.05**

Table 5.8 Percentage of simulated LULC between 2020 and 2029.

LULC types	Percent of simulated LULC									
	2020	**2021**	**2022**	**2023**	**2024**	**2025**	**2026**	**2027**	**2028**	**2029**
Urban and built-up area (Ur)	27.78	28.41	29.03	29.65	30.28	30.90	31.52	32.15	32.74	33.40
Paddy field (Pa)	0.02	0.02	0.02	0.02	0.01	0.01	0.01	0.01	0.00	0.00
Field crop and horticulture (Fch)	0.66	0.67	0.73	0.72	0.76	0.80	0.82	0.85	0.84	0.89
Perennial trees and orchards (Po)	34.89	34.48	34.07	33.66	33.25	32.84	32.44	32.03	31.65	31.20
Aquaculture (Aq)	1.62	1.62	1.62	1.62	1.62	1.59	1.58	1.56	1.56	1.55
Idle land (Id)	7.67	7.72	7.77	7.82	7.86	7.92	7.97	8.02	8.06	8.11
Evergreen forest (Ef)	13.98	13.75	13.53	13.31	13.08	12.86	12.64	12.42	12.20	11.97
Mangrove forest (Mf)	4.73	4.72	4.68	4.68	4.68	4.63	4.62	4.60	4.60	4.56
Scrub forest (Sf)	5.14	5.14	5.13	5.13	5.12	5.13	5.12	5.12	5.13	5.11
Waterbody (Wa)	2.87	2.87	2.87	2.87	2.87	2.87	2.88	2.88	2.88	2.92
Miscellaneous land (Mi)	0.63	0.59	0.55	0.52	0.47	0.44	0.40	0.37	0.33	0.29
Total	**100.00**	**100.00**	**100.00**	**100.00**	**100.00**	**100.00**	**100.00**	**100.00**	**100.00**	**100.00**

As a result, LULC types will increase in 2029 according to a rate of LULC change from transition area matrix between LULC in 2019 and 2029 consisting of urban and built-up area, field crop, and horticulture, idle land, scrub forest, and water bodies. They cover area of 174.34 km^2 or 33.40 %, 4.67 km^2 or 0.89%, 42.35 km^2 or 8.11%, 26.69 km^2 or 5.11%, and 15.22 km^2 or 2.92%, respectively. On the contrary, LULC types that will decrease in 2029 are paddy field, perennial trees and orchards, aquaculture, evergreen forest, mangrove forest, and miscellaneous land. They cover of 0.00 km^2 or 0.00%, 162.90 km^2 or 31.20%, 8.07 km^2 or 1.55%, 62.49 km^2 or 11.97%, 23.82 km^2 or 4.56% and 1.50 km^2 or 0.29%, respectively.

Moreover, the transition LULC change matrix between 2019 and 2029 is displayed in Table 5.9. As a result, the urban and built-up area in 2019 is not converted in other LULC types in 2029, and its area will increase from 141.77 km^2 in 2019 to 174.34 km^2 in 2029. The increasing urban and built area in 2029 mostly comes from perennial trees and orchards (19.68 km^2) and evergreen forest (8.21 km^2) in 2019. Similarly, the water body in 2019 is not converted into other LULC classes in 2029. Its area will increase from 14.98 km^2 in 2019 to 15.22 km^2 in 2029; the increasing water bodies in 2029 come from miscellaneous land (0.24 km^2) in 2019.

On the contrary, the paddy field in 2019 is converted into the urban and built area (0.08 km^2) and idle land (0.07 km^2) in 2029, and its area will decrease from 0.15 km^2 in 2019 to 0.00 km^2 in 2029. Likewise, field crop and horticulture in 2019 is converted into the urban and built-up area (0.16 km^2) in 2029, but its area will increase from 3.47 km^2 in 2019 to 4.67 km^2 in 2029, the increasing areas of field crop and horticulture come from perennial trees and orchards (0.86 km^2) and evergreen forest (0.50 km^2) in 2019. Similarly, perennial trees and orchards in 2019 are mostly converted into the urban and built-up area (19.68 km^2), field crop and horticulture (0.86 km^2), idle land (0.60 km^2) in 2029 and its area will decrease from 184.29 km^2 in 2019 to 162.90 km^2 in 2029. Likewise, aquaculture in 2019 is converted into the urban and built-up area (0.40 km^2), and its area will decrease from 8.47 km^2 in 2019 to 8.07 km^2 in 2029. Similarly, idle land in 2019 is converted into the urban and built-up area (0.70 km^2), but its area will increase from 39.78 km^2 in 2019 to 42.35 km^2 in 2029, the increasing areas of idle land in 2029 most come from the evergreen forest (2.60 km^2) in 2019. In the same way, evergreen forests in 2019 are mostly converted into urban and built-up (8.21 km^2) and idle land (2.60 km^2) in 2029, and its area will decrease from 74.10 km^2 in 2019 to 62.49 km^2 in 2029. Equally, the mangrove forest in 2019 is mainly converted into the urban and built-up area (0.85 km^2), and its area will decrease from 24.68 km^2 in 2019 to 23.82 km^2 in 2029. Likewise, scrub forest in 2019 is mainly converted into the urban and built-up area (0.73 km^2), and its area will increase from 26.87 km^2 in 2019 to 26.69 km^2 in 2029; the increasing areas of the scrub forest come from perennial trees and orchards (0.26 km^2) and evergreen forest (0.32 km^2) in 2019. Similarly, miscellaneous land in 2019 is mainly converted into the urban and built-up area (1.77 km^2), and its area will decrease from 3.49 km^2 in 2019 to 1.50 km^2 in 2029, the decreasing areas of miscellaneous land in 2029 come mangrove forest (0.01 km^2) and from the scrub forest (0.02 km^2) in 2019.

Furthermore, the significant increase of urban and built-up areas in 2029 are mainly converted from the top three dominant LULC types, including perennial trees and orchards (19.68 km^2), evergreen forest (8.21 km^2), and miscellaneous land (1.77 km^2) in 2019.

The increasing of the urban and built-up areas from perennial trees and orchards areas mainly allocated in the Mueang district (about 63%), Thalang district (about 31% and Kathu district (about 6%) of total areas change in perennial trees and orchards (19.68 km^2). In the meantime, the urban and built-up area's occurrence increases occurred in evergreen forest areas mainly allocated in the Mueang district of about 64%, followed by Kathu and Thalang district are about 26% and 10% of total areas change in the evergreen forest (8.21 km^2). Likewise, the urban and built-up area's occurrence increases occurred in miscellaneous land areas mainly allocated in the Mueang district of about 50%, followed by Kathu and Thalang district are about 14% and 36% of total areas change in miscellaneous land (1.77 km^2).

The possible reason to explain this finding is that most agricultural land and vegetation areas have been transformed into urban and built-up areas worldwide to meet people’s demands, leading to the LULC change, as mentioned earlier by many researchers in the previous chapter.

This study found that the urban and built-up area allocation in 2029 occurs expansion from the existing urban and built-up area, which led to decreasing the other LULC (e.g., perennial trees and orchards, evergreen forest, and miscellaneous land). Even though generally urban and built-up areas are primarily expanded in agricultural areas. However, some areas will occur in evergreen forests since the LULC simulation according to the transition probability matrix of LULC change between 2014 and 2019. Therefore, the evergreen forest areas have been transformed into urban and built-up areas, particularly in tourist attractions near existing urban and built-up areas such as the Karon sub-district, Patong sub-district, and the nearby Phuket town area to support tourist facilities and the population and tourist increase. In addition, the relationship between tourism growth and urban expansion in Phuket Island is described and discussed in more detail in part 7.3 in Chapter VII.

In summary, the characteristics of “from-to” change among LULC types between 2019 and 2029 are regulated by driving factors on LULC change, conversion matrix, and elasticity of LULC change and their land requirements, which are applied for LULC simulation between 2020 and 2029. The derived simulated LULC data between 2019 and 2029 is based on historical LULC development during 2014 and 2019 regarding allowed or not allowed change into other classes.

In addition, it was found that there is a slight difference between the land demand (required land area) and the simulated area of each LULC type in 2029. For instance, the land demand area of mangrove forest in 2029 is 23.83 km^2, but it is allocated only 23.82 km^2. Likewise, the land demand area of the waterbody in 2029 is 15.23 km^2, but it is allocated only 15.22 km^2. The deviation values between the land demand and the simulated area in 2029 are -0.01 km^2. Because the deviation value depends on iteration driving factors of each LULC type, which indicates the different maximum allowance between the required and allocated areas of LULC type under the CLUE-S model (Van Asselen and Verburg, 2013; Liu, Wang, Li, and Xia, 2013; Xu, Li, Song, and Yin, 2013). Therefore, the LULC simulation using the CLUE-S model can be accepted as essential information for Phuket Island city planners, land managers, and resource managers. The interpreted and simulated LULC data between 2019 and 2029 will be significant input for water supply and demand estimation in the following components.

Table 5.9 Transition LULC change matrix between 2019 (Base year) and 2029.

	LULC types	LULC 2029 (km^2)											
		Ur	Pa	Fch	Po	Aq	Id	Ef	Mf	Sf	Wa	Mi	Total
LULC2 019 (km^2)	Urban and built-up area (Ur)	141.77	0.00	0.00	0.00	0.00	0.00	0.00	0.00	0.00	0.00	0.00	**141.77**
	Paddy field (Pa)	0.08	0.00	0.00	0.00	0.00	0.07	0.00	0.00	0.00	0.00	0.00	**0.15**
	Field crop and horticulture (Fch)	0.16	0.00	3.31	0.00	0.00	0.00	0.00	0.00	0.00	0.00	0.00	**3.47**
	Perennial trees and orchards (Po)	19.68	0.00	0.86	162.90	0.00	0.60	0.00	0.00	0.26	0.00	0.00	**184.29**
	Aquaculture (Aq)	0.40	0.00	0.00	0.00	8.07	0.00	0.00	0.00	0.00	0.00	0.00	**8.47**
	Idle land (Id)	0.70	0.00	0.00	0.00	0.00	39.08	0.00	0.00	0.00	0.00	0.00	**39.78**
	Evergreen forest (Ef)	8.21	0.00	0.50	0.00	0.00	2.60	62.49	0.00	0.32	0.00	0.00	**74.10**
	Mangrove forest (Mf)	0.85	0.00	0.00	0.00	0.00	0.00	0.00	23.82	0.00	0.00	0.01	**24.68**
	Scrub forest (Sf)	0.73	0.00	0.00	0.00	0.00	0.00	0.00	0.00	26.12	0.00	0.02	**26.87**
	Waterbody (Wa)	0.00	0.00	0.00	0.00	0.00	0.00	0.00	0.00	0.00	14.98	0.00	**14.98**
	Miscellaneous land (Mi)	1.77	0.00	0.00	0.00	0.00	0.00	0.00	0.00	0.00	0.24	1.48	**3.49**
	Total	174.34	0.00	4.67	162.90	8.07	42.35	62.49	23.82	26.69	15.22	1.50	522.05
	Land demand	174.34	0.00	4.67	162.90	8.07	42.35	62.49	23.83	26.69	15.23	1.50	
	Area deviation (km^2)	0.00	0.00	0.00	0.00	0.00	0.00	0.00	-0.01	0.00	-0.01	0.00	
	Area change (km^2)	32.57	-0.15	1.20	-21.39	-0.40	2.57	-11.62	-0.86	-0.17	0.24	-1.99	
	Annual change (km^2)	3.26	-0.02	0.12	-2.14	-0.04	0.26	-1.16	-0.09	-0.02	0.02	-0.20	

CHAPTER VI

WATER YIELD ESTIMATION

This chapter presents the second objective results focusing on the water yield estimation using the SWAT model. The main results, which consist of (1) hydrologic response unit, (2) sensitivity analysis, (3) model calibration and validation, (4) baseline information of water yield estimation in 2019, (5) water yield estimation between 2020 and 2029, and (6) effect of LULC change on water yield, are here described and discussed in detail.

6.1 Hydrologic Response Unit

The Khlong Bang Yai watershed was first chosen to examine an optimum parameter for operating the SWAT model. The model's optimum parameters were then further applied to estimate water yield in the other watersheds in Phuket Island.

Initially, the SWAT model divides a watershed into catchments based on topographic information (Figure 6.1). Then, the hydrologic response unit (HRU) was generated based on LULC in 2014, soil and slope data in each catchment. In this study, the multiple HRUs were generated using a 20 percent land use, a 10 percent soil, and a 20 percent slope threshold, which is suitable for most applications (Kunto and Ongsomwang, 2013; Sisay et al., 2017). Meanwhile, the required weather data between 1996 and 2008 were exacted from six weather stations for model operation (see Figure 3.5 in Chapter III). Characteristics of the Khlong Bang Yai watershed are described below.

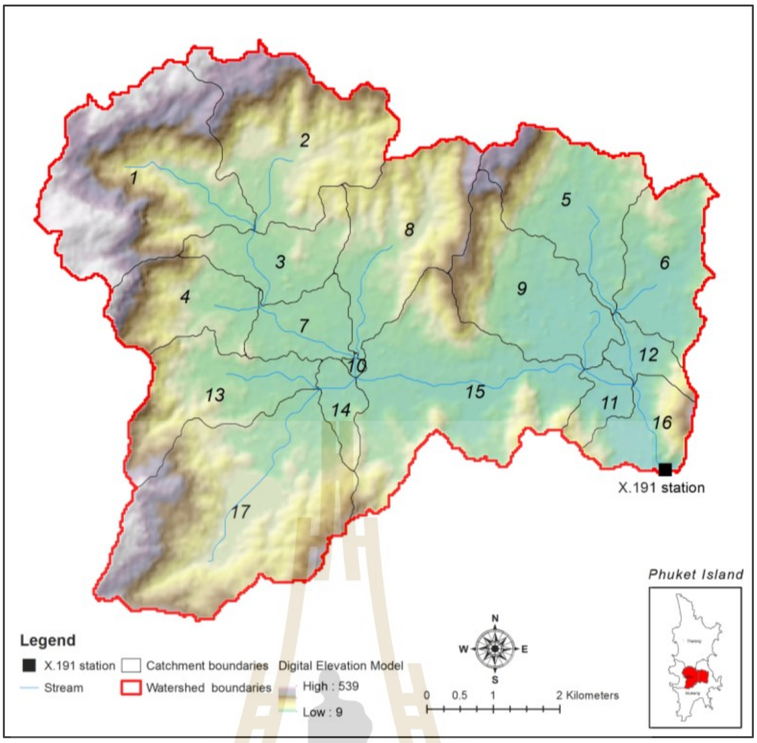
1
2
3
4
5
6
7
8
9
10
11
12
13
14
15
16
17
X.191 station
Phuket Island
Legend
X.191 station
Catchment boundaries
Digital Elevation Model
Stream
Watershed boundaries
High : 539
Low : 9
N
W
E
S
0
0.5
1
2 Kilometers

Figure 6.1 Topographic map of Khlong Bang Yai watershed.

The top three dominant LULC types in 2014 of the Khlong Bang Yai watershed are the residential area (URBN), the evergreen forest area (FRSE), and the rubber trees area (RUBR), and they cover an area of 19.10 km^2 (34.73%), 12.53 km^2 (22.79%), and 12.42 km^2 (22.59%), respectively (Figure 6.2). Meanwhile, the dominant soil texture data in the watershed are loam, variable (Tin Mine Land), and sandy clay loam, and they cover an area of 26.69 km^2 (48.54%), 15.23 km^2 (27.71%), and 7.70 km^2 (14.02%), respectively (Figure 6.3). In the meantime, the three dominant slope classes in the Khlong Bang Yai watershed are slightly undulating (2-5%), steep (>35%), and hilly (20-35%), and they cover an area of 16 km^2 (29.10%), 12.17 km^2 (22.13), and 10.70 km^2 (19.46%), respectively (Figure 6.4).

In the meantime, a total of 17 catchments and 886 HRUs in the Khlong Bang Yai watershed are generated for water yield estimation under the SWAT model (Figure 6.5).

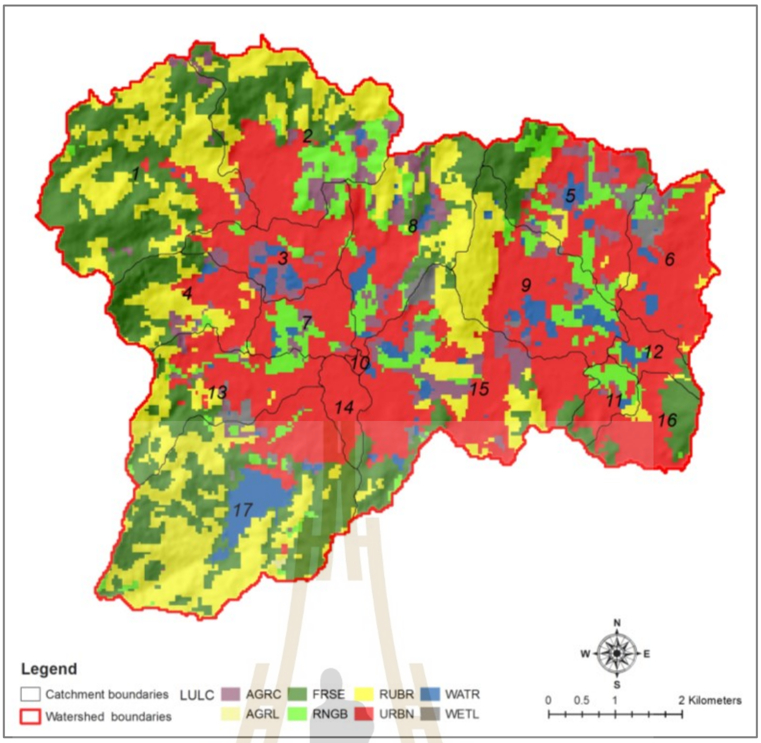
1
2
3
4
5
6
7
8
9
10
11
12
13
14
15
16
17
N
W
E
S
Legend
Catchment boundaries
Watershed boundaries
LULC
AGRC
AGRL
FRSE
RNGB
RUBR
URBN
WATR
WETL
0
0.5
1
2 Kilometers

Figure 6.2 LULC in 2014 of Khlong Bang Yai watershed.

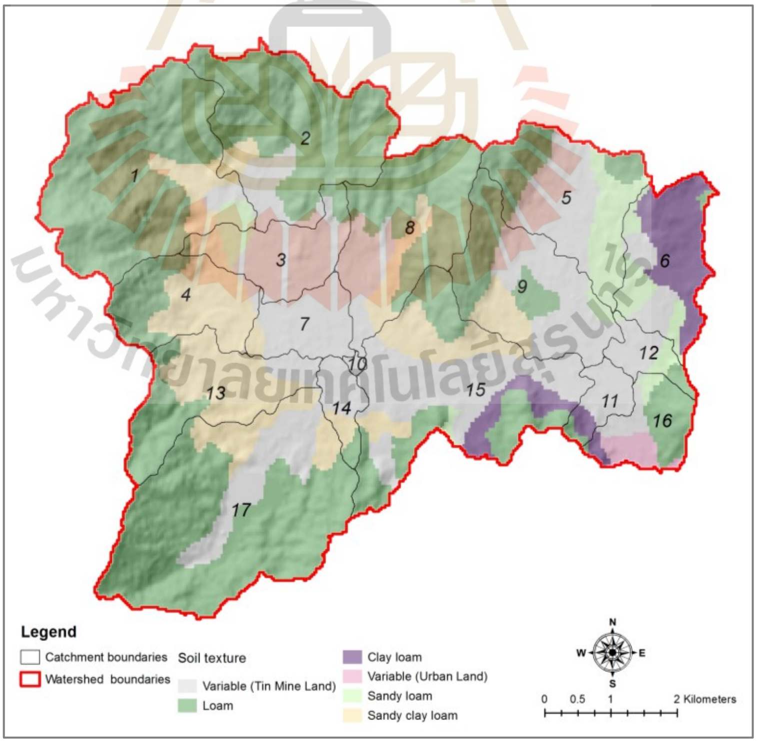
1
2
3
4
5
6
7
8
9
10
11
12
13
14
15
16
17
N
W
E
S
Legend
Catchment boundaries
Watershed boundaries
Soil texture
Variable (Tin Mine Land)
Loam
Clay loam
Variable (Urban Land)
Sandy loam
Sandy clay loam
0
0.5
1
2 Kilometers

Figure 6.3 Soil texture distribution of Khlong Bang Yai watershed.

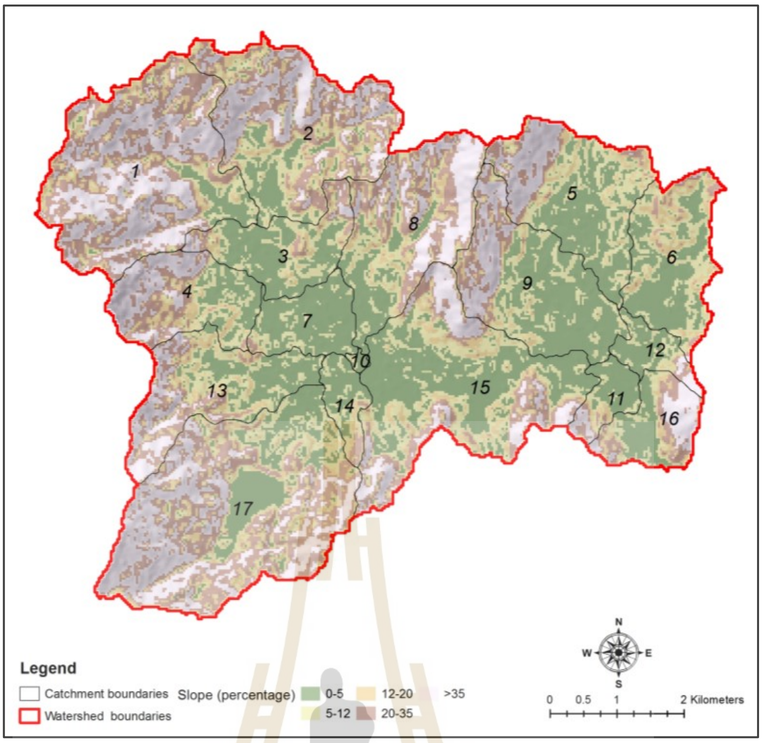
1
2
3
4
5
6
7
8
9
10
11
12
13
14
15
16
17
Legend
Catchment boundaries
Watershed boundaries
Slope (percentage)
0-5
5-12
12-20
20-35
>35
N
W
E
S
0 0.5 1 2 Kilometers

Figure 6.4 Slope distribution of Khlong Bang Yai watershed.

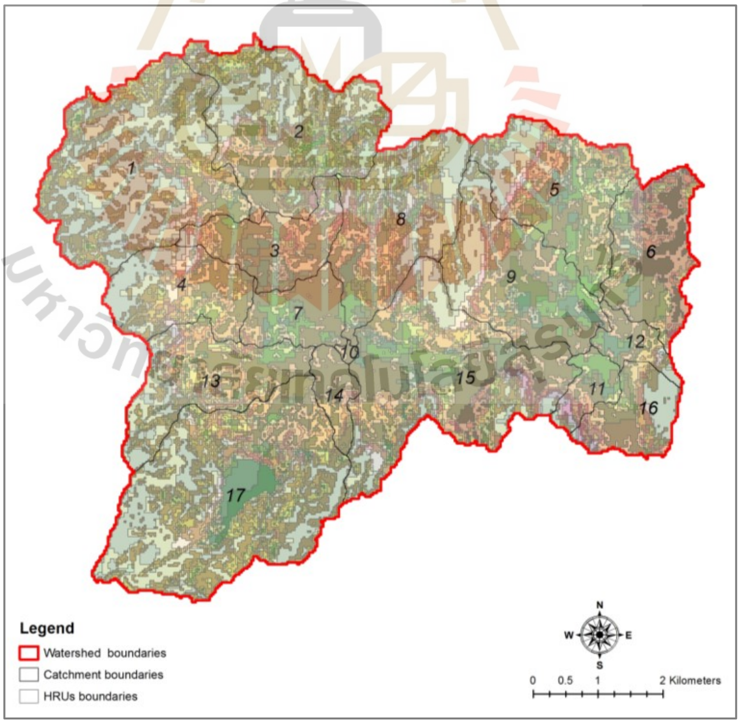
1
2
3
4
5
6
7
8
9
10
11
12
13
14
15
16
17
Legend
Watershed boundaries
Catchment boundaries
HRUs boundaries
N
W
E
S
0 0.5 1 2 Kilometers

Figure 6.5 Spatial distribution of HRUs and catchments in Khlong Bang Yai watershed.

6.2 Sensitivity analysis

In principle, the sensitivity analysis is conducted to determine the influence of streamflow prediction parameters and find the most sensitive parameters in the watershed (Gassman et al., 2007). In this study, the seven literature reviewed parameters, including curve number at moisture condition II (CN2), available soil water capacity (SOL_AWC), soil evaporation compensation factor (ESCO), surface runoff lag coefficient (SURLAG), baseflow alpha factor (ALPHA_BF), groundwater “revap” coefficient (GW_REVAP), and groundwater delay (GW_DELAY) were analyzed to identify the most suitable value of each parameter for water yield estimation in the Khlong Bang Yai watershed under two different conditions. The significant sensitive parameters to monthly streamflow at the X.191 station in this watershed were analyzed using the t-statistics test and their p-values at 95% of confident level under SWAT-CUP software, as summarized in Table 6.1.

As a result in Table 6.1, available soil water capacity (SOL_AWC) is the most sensitive parameter in the Khlong Bang Yai watershed (see Table 6.1), followed by the surface runoff lag coefficient (SURLAG), groundwater delay (GW_DELAY), soil evaporation compensation factor (ESCO), curve number at moisture condition II (CN2), Groundwater “revap” coefficient (GW_REVAP), and baseflow alpha factor (ALPHA_BF).

Therefore, the available soil water capacity (SOL_AWC) is mainly adjusted new value to model calibration. Soil water availability is the soil’s capacity to hold water available for plant use and reflects the soil’s capacity for water storage. The soil’s ability to hold water depends on the soil characteristics that vary within the soil profile and the basin (Tolk, 2003; Opere and Okello, 2011).

Table 6.1 SWAT parameter sensitivity to monthly streamflow at the X.191 station.

Parameter	Description	t-stat	p-value
SOL_AWC	Available soil water capacity	5.7839	0.0286
SURLAG	Surface runoff lag coefficient	2.6590	0.1171
GW_DELAY	Groundwater delay	-2.2600	0.1523
ESCO	Soil evaporation compensation factor	-2.2570	0.1526
CN2	Curve number at moisture condition II	-1.0655	0.3983
GW_REVAP	Groundwater “revap” coefficient	1.0291	0.4116
ALPHA_BF	Baseflow alpha factor	-0.4692	0.6851

Besides, the additional sensitive parameters, including the CN2, ESCO, and GW_REVAP, relate to surface runoff and baseflow are slightly modified in this study. The curve number at moisture condition II (CN2) is a function of soil permeability, LULC, and the antecedent soil moisture; it affects the surface runoff generation rate. Meanwhile, the soil evaporation compensation factor (ESCO) coefficient generally use to modify the depth distribution to meet evaporative soil demands. ESCO affects both base flow and surface flow at the same rate. Likewise, the groundwater "revap" coefficient (GW_REVAP) affects the amount of water that recharges the capillary fringe after evaporation during the dry periods. Change in GW_REVAP is critical as it affects water movement from the shallow aquifer to the root zone (Opere and Okello, 2011).

These identified sensitive parameters are further applied to calibrate and validate the SWAT model for water yield estimation in the reference watershed (Khlong Bang Yai watershed).

6.3 Model calibration and validation

The model calibration and validation for water yield estimation in the Khlong Bang Yai watershed as a reference area were separately conducted according to annual runoff data. In this study, annual runoff data were categorized into two conditions: dry and wet years. In practice, monthly streamflow data at the X.191 station (Satree Phuket School) between 1999 and 2019 were used for model calibration and validation. RMSE-observations, standard deviation ratio (RSR), Nash-Sutcliffe efficiency (NSE), and Percent bias (PBIAS) were applied to evaluate the performance of the model with a threshold value of ≤ 0.60, ≥ 0.65., ≤±15, respectively. The model calibration and validation result with optimum parameters in the Khlong Bang Yai watershed from two different conditions were separately described according to annual runoff data in the following sections.

6.3.1 Dry year condition

The model calibration was performed under dry year conditions based on the SWAT model's estimated water balance for 2009 and 2010. Model validation was conducted based on the estimated water balance from the SWAT model for 2018 and 2019. In practice, the model calibration and validation were performed manually by adjusting the most sensitive hydrologic-related parameters for the optimum parameter values for the dry year condition. Under this condition, LULC data in 2014 were used for model calibration, and LULC data in 2019 were applied for model validation. Meanwhile, the multiple HRU definition in the watershed was generated using a combination of 20 percent land use, 10 percent soil, and 20 percent slope threshold. The weather data from six weather stations from 2006 to 2010 and 2015 to 2019 were used for model calibration and validation.

The optimum parameter values of SOL_AWC, ESCO, CN2, and GW_REVAP under dry year condition were 0.19-0.30, 0.80, 30-68, and 0.050, respectively. Meanwhile, the default values of other parameters, including SURLAG, GW_DELAY, and ALPHA_BF, were applied for model calibration and validation. The summary of optimum parameter values for the dry year condition is displayed in Table 6.2.

Table 6.2 Optimum parameter values of SWAT model for hydrologic component estimation under dry year condition.

Parameter	Unit	Range	Final Calibrated
SOL_AWC [a]		0-1	0.19-0.30
SURLAG	day	0-10	4
GW_DELAY	day	0-100	31
ESCO		0-1	0.80
CN2 [b]		30-100	30-68
GW_REVAP		0-1	0.050
ALPHA_BF	day^{-1}	0-1	0.048

Note: [a] Varies with soil type, [b] Varies with land use, soil and slope.

As a result, it can be noted that the optimum value of available soil water capacity (SOL_AWC) varies according to soil type. Likewise, the curve number at moisture condition II (CN2) depends on land use, soil and slope. The average annual water balance components in the Khlong Bang Yai watershed during the calibration and the validation periods under dry year condition were reported in Table 6.3.

Table 6.3 Average annual water balance components in calibration and validation periods of Khlong Bang Yai watershed under dry year condition.

Water Balance Component (in mm)	Calibration	Validation
Rainfall	2,597.90	2,415.70
Evapotranspiration	1,582.90	1,672.70
Surface runoff	562.97	446.79
Lateral flow	69.61	67.60
Groundwater (shallow aquifer)	163.00	92.02
Groundwater (deep aquifer)	12.24	10.13
Total water yield	**807.82**	**616.54**

As a result, water yield was 807.82 mm under the calibration period, while surface runoff, lateral flow, and groundwater (shallow and deep aquifers) were about 562.97 mm, 69.61 mm 175.24 mm, respectively. In the meantime, under the validation period, water yield was 616.54 mm and surface runoff, lateral flow, and groundwater (shallow and deep aquifers) were about 446.79 mm, 67.60 mm, and 102.15 mm, respectively.

The SWAT model's performance for the dry year condition from calibration and validation was measured using the RSR, NSE, and PBIAS based on the estimated and observed hydrologic data at the X.191 station. The result of model performance under calibration and validation periods are summarized in Table 6.4 and Figures 6.6 and 6.7. The RSR, NSE, and PBIAS values for model calibration were 0.56, 0.69, and -13.60, respectively. These values show good performance of the SWAT model for estimated hydrologic data under dry year condition. Meanwhile, the RSR, NSE, and PBIAS values for model validation were 0.43, 0.82, and 5.25, respectively. They indicate very good performance of the SWAT model, according to Moriasi et al. (2007).

Furthermore, the R^2 value of model calibration and validation under dry year condition (Figures 6.8 and 6.9) were approximately 0.88 and 0.89, respectively.

Table 6.4 Model performance of the SWAT model for water flow estimation under dry year condition.

Parameter	Calibration (year)		Validation (year)	
	In 2009-2010	Performance rating	In 2018-2019	Performance rating
RSR	0.56	Good	0.43	Very good
NSE	0.69	Good	0.82	Very good
PBIAS	-13.60	Good	5.25	Very good

Note: Model performance rating scale by Moriasi et al. (2007).

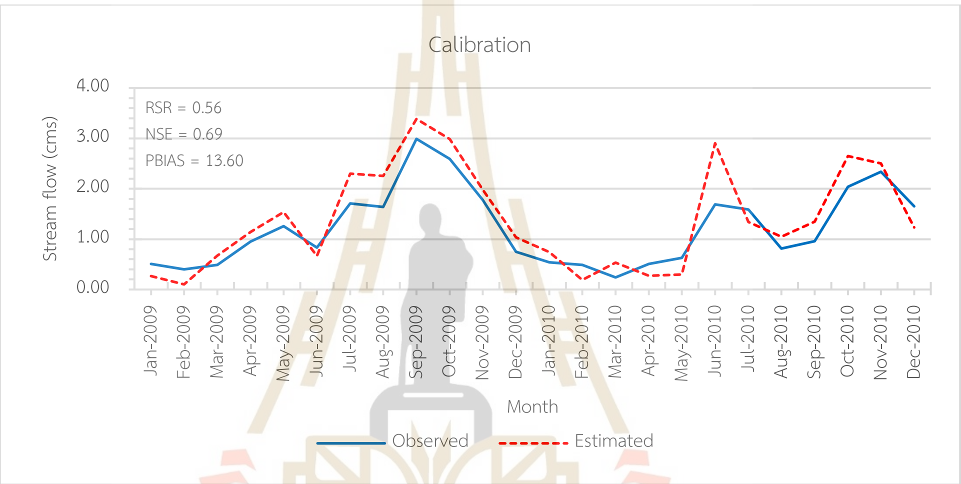

Figure 6.6 Monthly streamflow during calibration period of Khlong Bang Yai watershed under dry year condition.

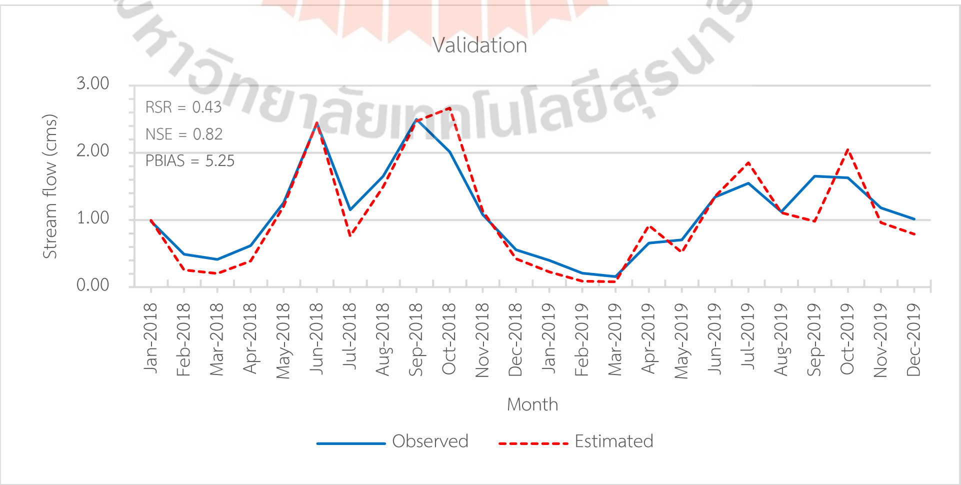

Figure 6.7 Monthly streamflow during validation period of Khlong Bang Yai watershed under dry year condition.

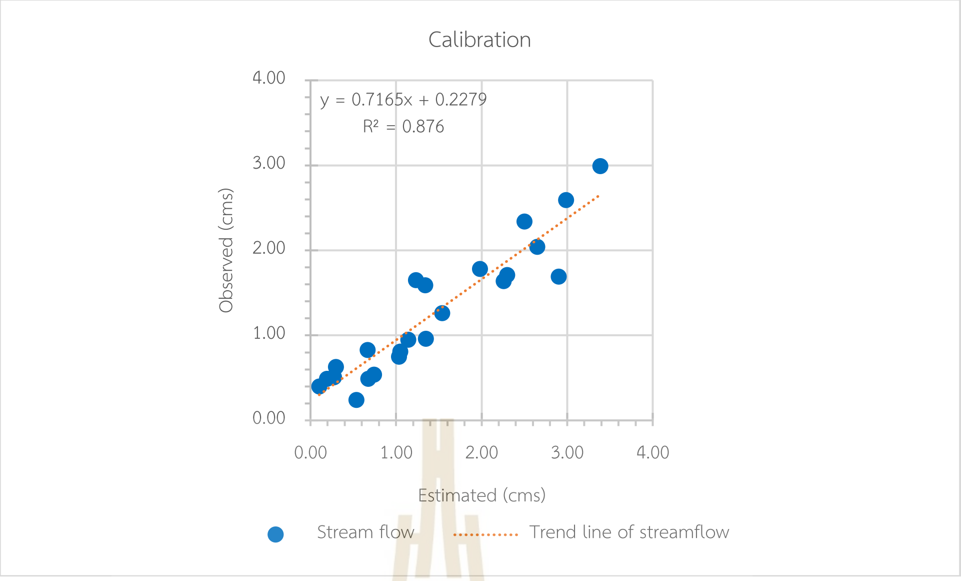

Figure 6.8 Scatter plot between observed and estimated streamflow of Khlong Bang Yai watershed during calibration period under the dry year condition.

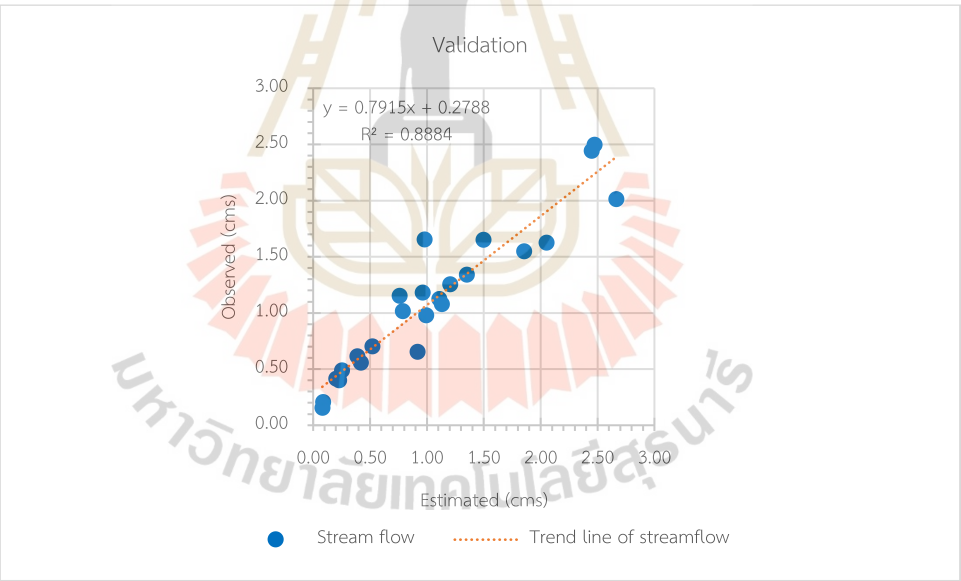

Figure 6.9 Scatter plot between observed and estimated streamflow of Khlong Bang Yai watershed during validation period under the dry year condition.

6.3.2 Wet year condition

The model calibration was performed under wet year conditions based on the SWAT model's estimated water balance for 1999 and 2000. Model validation was conducted based on the estimated water balance from the SWAT model for 2016 and 2017. Like dry year condition, the model calibration and validation were performed manually by adjusting the most sensitive hydrologic-related parameters for optimum parameter value identification for wet year condition. Under this condition, LULC data in 2002 was applied for model calibration, while LULC data in 2014 were used for model validation. The multiple HRU definition was created using a combination of 20 percent land use, 10 percent soil, and 20 percent slope threshold. The weather data from six weather stations from 1996 to 2000 and 2013 to 2017 were used for model calibration and validation.

The optimum parameter values of SOL_AWC, ESCO, CN2, and GW_REVAP under wet year condition were 0.05-0.16, 0.96, 30-85, and 0.157, respectively. Meanwhile, the default values of other parameters, including SURLAG, GW_DELAY, and ALPHA_BF, were used for model calibration and validation. The summary of optimum parameter values for the wet year condition is displayed in Table 6.5.

Table 6.5 Optimum parameter values of SWAT model for hydrologic component estimation under wet year condition.

Parameter	Unit	Range	Final Calibrated
SOL_AWC [a]		0-1	0.05-0.16
SURLAG	day	0-10	4
GW_DELAY	day	0-100	31
ESCO		0-1	0.96
CN2 [b]		30-100	30-85
GW_REVAP		0-1	0.157
ALPHA_BF	day^{-1}	0-1	0.048

Note: [a] Varies with soil type, [b] Varies with land use, soil and slope.

As a result, it can be noted that the optimum value of available soil water capacity (SOL_AWC) varies according to soil type. At the same time, the curve number at moisture condition II (CN2) depends on land use, soil and slope. The average annual water balance components in the Khlong Bang Yai watershed during the calibration and the validation periods under wet year condition were reported in Table 6.6.

Table 6.6 Average annual water balance components in calibration and validation periods of Khlong Bang Yai watershed under wet year condition.

Water Balance Component	Calibration	Validation
Rainfall	2,698.80	3,394.00
Evapotranspiration	1,214.50	1,291.30
Surface runoff	552.86	1,147.55
Lateral flow	122.68	95.82
Groundwater (shallow aquifer)	267.05	143.44
Groundwater (deep aquifer)	32.02	24.48
Total water yield	**974.61**	**1,411.29**

As a result, water yield was 974.61 mm under the calibration period, while surface runoff, lateral flow, and groundwater (shallow and deep aquifers) were about 552.86 mm, 122.68 mm, and 299.07 mm, respectively. In the meantime, under the validation period, water yield was 1,411.29 mm, while surface runoff, lateral flow, and groundwater (shallow and deep aquifers) were about 1,147.55 mm, 95.82 mm, and 167.92 mm, respectively.

In the meantime, the result of model performance under calibration and validation periods based on the estimated and observed hydrologic data at X.191 station under wet year condition are summarized in Table 6.7 and Figures 6.10 and 6.11. The RSR, NSE, and PBIAS values for model calibration were 0.58, 0.66, and 14.90, respectively. They indicate good performance of SWAT model for estimated hydrologic data under wet year condition. Meanwhile, the RSR, NSE, and PBIAS values for model validation were 0.59, 0.65, and -13.84, respectively. They are indicating the good performance of the SWAT model, according to Moriasi et al. (2007).

The R^2 value of model calibration and validation under wet year condition (Figures 6.12 and 6.13) were approximately 0.70 and 0.89, respectively.

Table 6.7 Model performance of the SWAT model for water flow estimation under wet year condition.

Parameter	Calibration (year)		Validation (year)	
	In 1999-2000	Performance rating	In 2016-2017	Performance rating
RSR	0.58	Good	0.59	Good
NSE	0.66	Good	0.65	Good
PBIAS	14.90	Good	-13.84	Good

Note: Model performance rating scale by Moriasi et al. (2007).

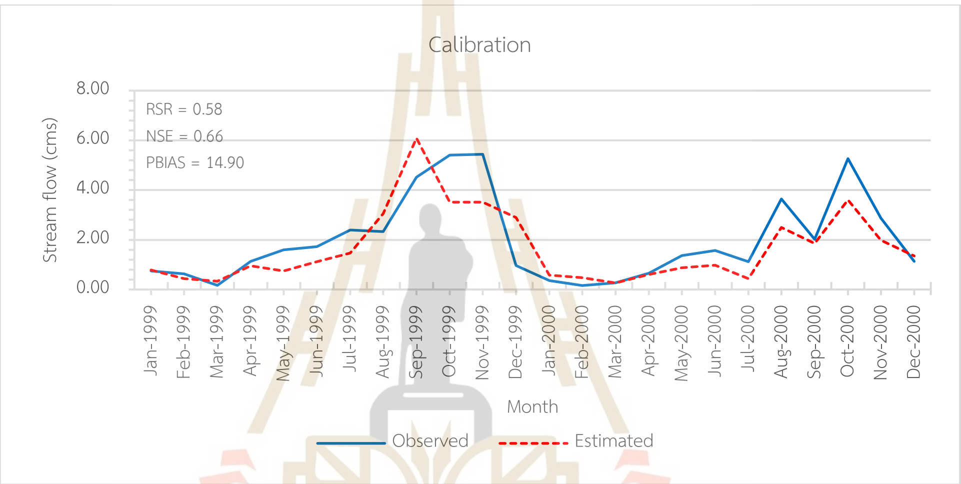

Figure 6.10 Monthly streamflow during calibration period of Khlong Bang Yai watershed under wet year condition.

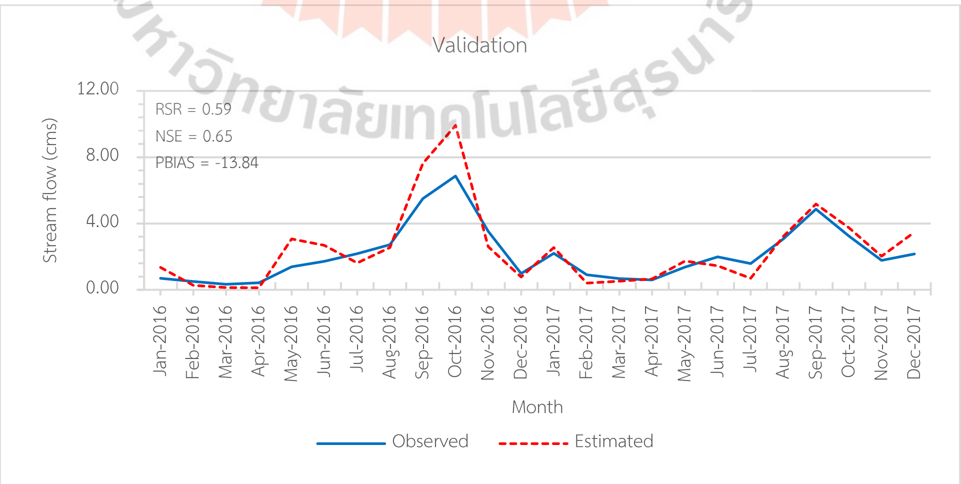

Figure 6.11 Monthly streamflow during validation period of Khlong Bang Yai watershed under wet year condition.

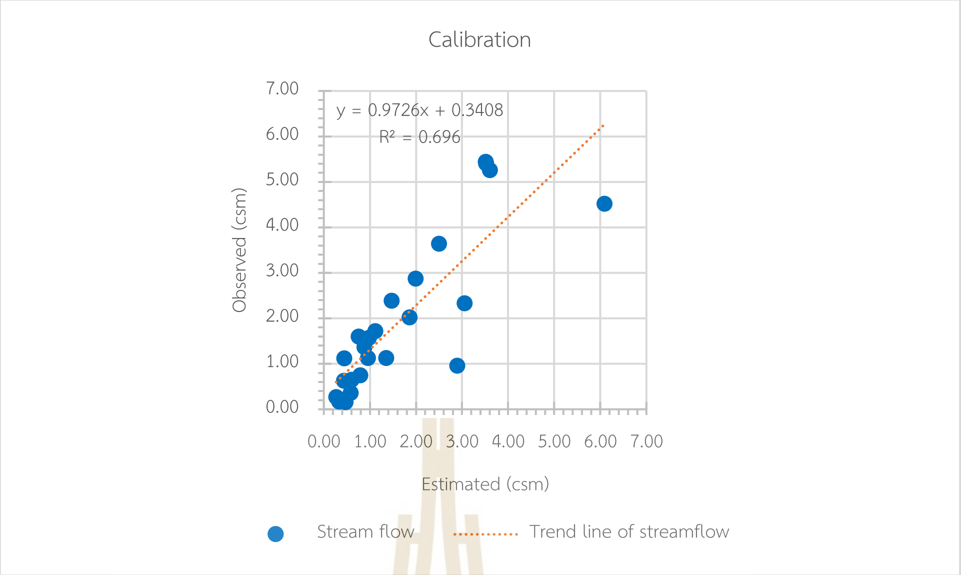

Figure 6.12 Scatter plot between observed and estimated streamflow of Khlong Bang Yai watershed during calibration period under wet year condition.

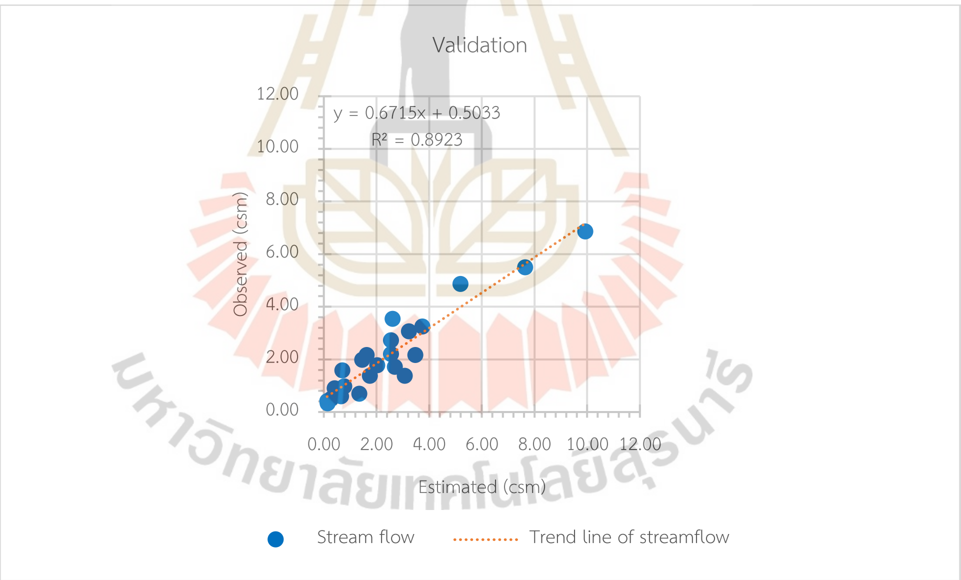

Figure 6.13 Scatter plot between observed and estimated streamflow of Khlong Bang Yai watershed during validation period under wet year condition.

In summary, four sensitive parameters from selected seven parameters, including SOL_AWC, ESCO, CN2, and GW_REVAP, show different values when applied to calibrate and validate under dry and wet year conditions. A brief explanation of four sensitive parameters under dry and wet years is summarized below.

In this study, the SOL_AWC (soil water availability) value is adjusted higher in the dry year than the wet year. The SOL_AWC value varies from 0.19 and 0.30 under the dry year condition, and it varies from 0.05 to 0.16 under the wet year condition. Gao, Chen, Biggs, and Yao (2018) stated that the soil vadose zone is generally thicker in a dry year than wet years due to the lower water table in dry years, leading to higher water retention capacity.

Meanwhile, the ESCO (soil evaporation compensation factor), a coefficient in the SWAT model, denotes the depth of water evaporated from the soil. The ESCO value under dry year condition is 0.80, while it is 0.96 under wet year condition. These values indicate that more water is extracted from the deep soil layer to satisfy the evaporative demand in dry conditions. In contrast, wet year condition account for smaller water evaporation from the deep soil layer (Nasab et al., 2018).

The CN2 (curve number at moisture condition II) directly impacts surface runoff estimation and a function of soil type, land use and land cover, soil moisture, and other conditions. In this study, the CN2 value was adjusted lower in dry year condition than wet year condition. The CN2 values for the dry and wet years vary from 30 to 68 and from 30 to 85, respectively. These values indicate that the surface runoff in the wet year condition should be higher than the dry year condition because surface runoff in both conditions depends on rainfall.

GW_REVAP (groundwater “revap” coefficient) controls the water flow from the shallow aquifer to the unsaturated zone (Arnold, Kiniry, et al., 2012). The GW_REVAP value under the dry year condition is 0.050, while it is 0.157 under the wet year condition. This setting infers that water available for the base flow in wet year condition is higher than in dry year condition.

6.4 Baseline information of water yield estimation in 2019

Under this session, the optimum local parameters of dry conditions were used to estimate the base year Phuket Island’s water yield in 2019. In practice, Phuket’s water yield in 2019 was estimated based on interpreted LULC data in 2019, soil, and slope data in each watershed. Meanwhile, the multiple HRU definition was created using a combination of 20 percent land use, 10 percent soil, and 20 percent slope threshold. The weather data from six weather stations from 2017 to 2019 were used for model estimation.

As a result, the estimated Phuket Island's annual water yield in 2019 was 966.14 mm or 504.37 million m^3. Meanwhile, monthly Phuket Island's water yield in 2019 is displayed in Figure 6.14. The water yield from the estimated summer season (December to March) varied from the lowest value of 3.72 mm or 1.94 million m^3 in March to the highest value of 63.15 or 32.97 million m^3 in December. On the contrary, the water yield from the estimated rainy season (April to November) varied from the lowest value of 28.83 mm or 15.05 million m^3 in May to the highest value of 195.67 mm or 102.15 million m^3 in October.

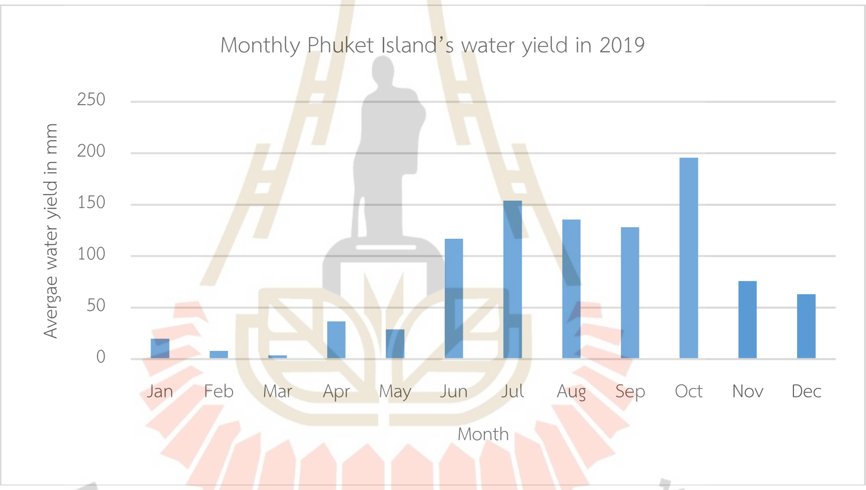

Figure 6.14 Monthly Phuket Island's water yield in 2019.

6.5 Water yield estimation between 2020 and 2029

Under this session, the optimum local parameters of dry and wet year conditions were used to estimate the time-series water yield in Phuket Island between 2020 and 2029. In practice, 25 watersheds in Phuket Island were delineated based on streams network and elevation (DEM) to estimate water yield in Phuket Island (522.05 km^2) in two different scenarios: dry and wet, as shown in Figure 6.15. The results of the water yield estimation of two different scenarios are separately described and discussed in the following sections.

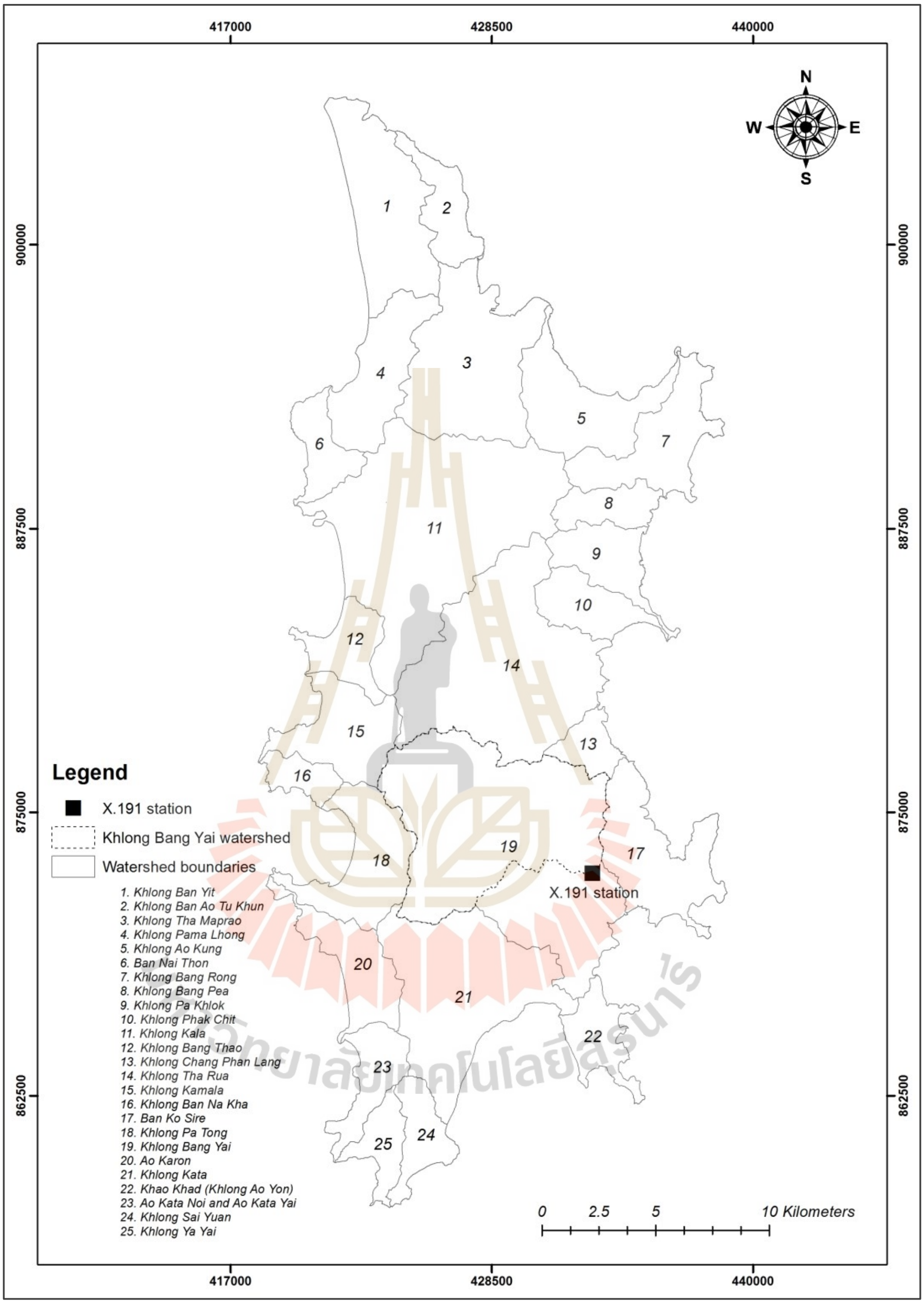
417000
428500
440000
900000
887500
875000
862500
N
W
E
S
1
2
3
4
5
6
7
8
9
10
11
12
13
14
15
16
17
18
19
20
21
22
23
24
25
X.191 station
Legend
X.191 station
Khlong Bang Yai watershed
Watershed boundaries
1. Khlong Ban Yit
2. Khlong Ban Ao Tu Khun
3. Khlong Tha Maprao
4. Khlong Pama Lhong
5. Khlong Ao Kung
6. Ban Nai Thon
7. Khlong Bang Rong
8. Khlong Bang Pea
9. Khlong Pa Khlok
10. Khlong Phak Chit
11. Khlong Kala
12. Khlong Bang Thao
13. Khlong Chang Phan Lang
14. Khlong Tha Rua
15. Khlong Kamala
16. Khlong Ban Na Kha
17. Ban Ko Sire
18. Khlong Pa Tong
19. Khlong Bang Yai
20. Ao Karon
21. Khlong Kata
22. Khao Khad (Khlong Ao Yon)
23. Ao Kata Noi and Ao Kata Yai
24. Khlong Sai Yuan
25. Khlong Ya Yai
0
2.5
5
10 Kilometers

Figure 6.15 Twenty-five watershed for water yield estimation in Phuket Island.

6.5.1 Water yield estimation of dry year scenario

Annual water balance components of the dry year scenario between 2020 and 2029 were estimated based on long-term historical rainfall data between 1999 and 2019. Herewith, rainfall data in 2019 with a value of 2,376.50 mm (dry year) was chosen as significant input data for water yield estimation using the SWAT model under the dry year scenario. The annual water balance of the dry year scenario between 2020 and 2029 is displayed in Table 6.8.

Table 6.8 Annual water balance of Phuket Island between 2020 and 2029 under dry year scenario (mm).

Year	Surface Runoff	Lateral flow	Groundwater		Evapotranspiration	Water Yield
			Shallow aquifer	Deep aquifer		
2020	575.23	110.68	264.10	17.35	1,298.60	967.36
2021	578.95	109.98	262.55	17.25	1,297.90	968.73
2022	582.68	109.41	260.65	17.14	1,297.50	969.89
2023	587.34	110.49	257.20	16.92	1,296.90	971.96
2024	590.45	107.93	258.30	16.95	1,295.70	973.63
2025	601.77	106.19	252.51	16.58	1,294.20	977.05
2026	646.69	100.71	229.32	15.20	1,286.70	991.92
2027	652.05	99.15	228.90	15.11	1,284.10	995.21
2028	656.34	98.73	226.44	14.97	1,283.60	996.48
2029	664.12	96.80	223.77	14.79	1,281.50	999.49
Average	**613.56**	**105.01**	**246.37**	**16.23**	**1,291.67**	**981.17**

As a result (Table 6.8), it can be seen that the estimated annual water yield of the dry year scenario between 2020 and 2029 varied from 967.36 mm or 505.01 million m^3 in 2020 to 999.49 mm or 521.79 million m^3 in 2029, with an average annual water yield of 981.17 mm or 512.22 million m^3. The annual water yield of Phuket Island under the dry year scenario is relatively stable from 2020 to 2025, but it continuously increases from 2026 to 2029 (Figure 6.16). Likewise, the proportional hydrologic components of water yield include surface runoff, lateral flow, groundwater (shallow aquifer), groundwater (deep aquifer), is relatively stable from 2020 to 2025. Still, surface runoff continuously increases from 2026 to 2029, while shallow groundwater continuously decreases in the same period, as shown in Figure 6.17.

On the contrary, the estimated annual evapotranspiration of dry year condition between 2020 and 2029 varied from 1,281.50 mm in 2029 to 1,298.60 mm in 2020, with an average annual evapotranspiration value of 1,291.67 mm. Unlike annual water yield, the annual evapotranspiration of Phuket Island under the dry year scenario is relatively stable from 2020 to 2025, but it continuously decreases from 2026 to 2029 (Figure 6.18).

These findings indicate an effect of LULC change on water yield with its hydrologic component and evapotranspiration because rainfall data as significant input data for water yield estimation is fixed. Meanwhile, time-series LULC data between 2020 and 2029 were simulated using the CLUE-S model.

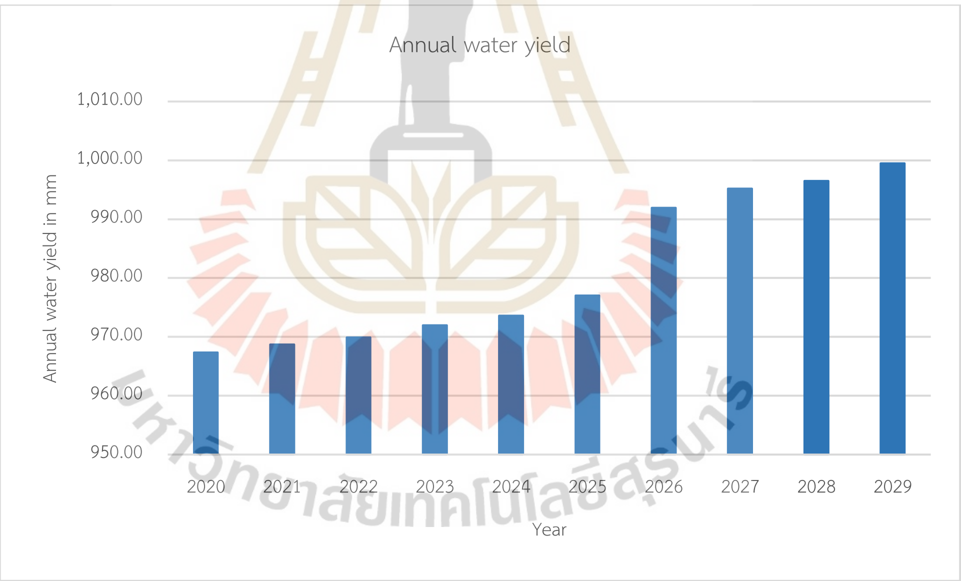

Figure 6.16 Temporal estimated water yield of Phuket Island between 2020 and 2029 under dry year scenario.

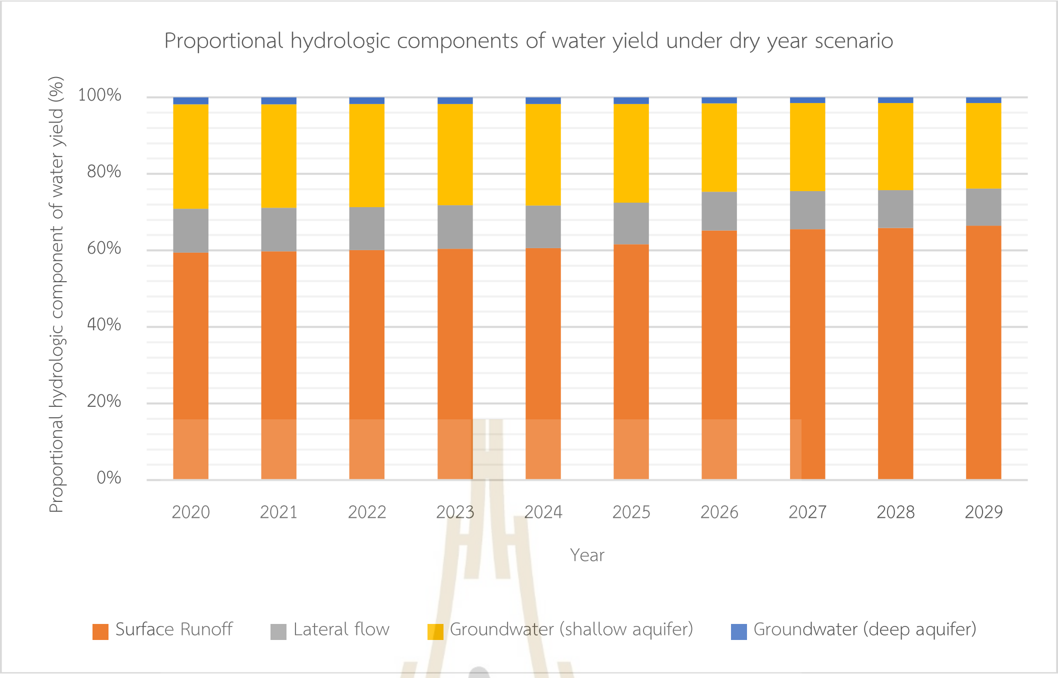

Figure 6.17 Proportional hydrologic components of Phuket Island between 2020 and 2029 under dry year scenario.

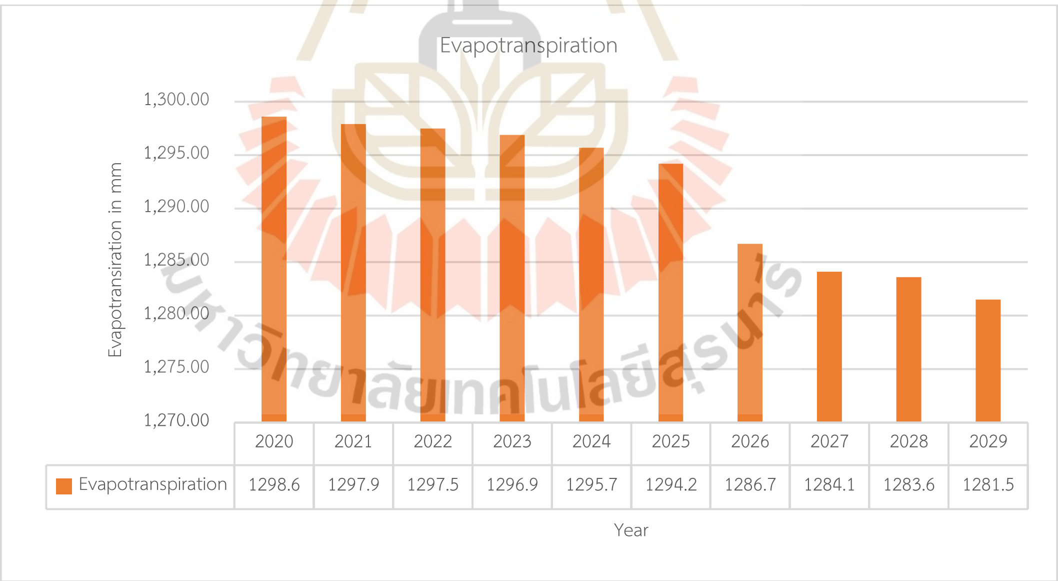

Figure 6.18 Temporal estimated evapotranspiration of Phuket Island between 2020 and 2029 under dry year scenarios.

In the meantime, statistical data of annual water yield in 25 watersheds in Phuket Island between 2020 and 2029 under the dry year scenario is summarized in Tables 6.9 and 6.10. Figure 6.19 displays the average water yield of each watershed and the average water yield of twenty-five watersheds between 2020 and 2029 under the dry year scenario.

As a result, the annual water yield in 25 watersheds is quite different under the dry year scenario. The highest average water yield is found in the Khlong Bang Yai watershed, with 1,428.35 mm or 110.90 million m^3, while the lowest average water yield occurs in the Ban Nai Thon watershed with a value of 379.90 mm or 3.08 million m^3. Additionally, only six watersheds, including Khlong Tha Maprao, Khlong Kala, Khlong Tha Rua, Khlong Pa Tong, Khlong Bang Yai, and Khlong Kata, can provide an average water yield higher than the average value of all watersheds in Phuket Island, with a value of 894.93 mm or 20.48 million m^3. These results indicate topographic features' effect, particularly the distribution of LULC types, soil types, and slope classes in each watershed and its area and rainfall pattern.

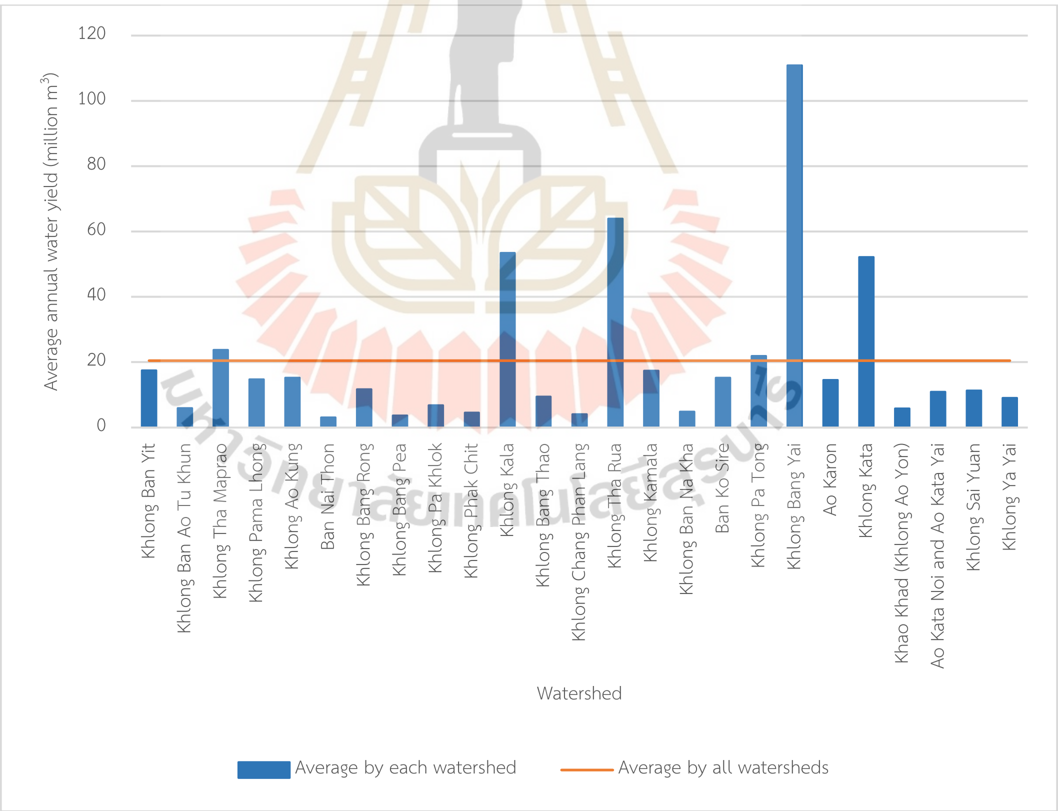

Figure 6.19 Average water yield between 2020 and 2029 in 25 watersheds under dry year scenario.

Table 6.9 Annual water yield and average in each watershed between 2020 and 2029 under dry year scenario (mm).

No	Watershed	Area (km^2)	Water yield between 2020 and 2029 (mm)										
			2020	2021	2022	2023	2024	2025	2026	2027	2028	2029	Average
1	Khlong Ban Yit	26.31	663.78	663.78	663.78	663.78	663.78	663.78	663.83	664.26	664.60	664.99	664.04
2	Khlong Ban Ao Tu Khun	9.20	643.49	643.49	643.49	643.49	646.14	646.14	646.13	643.48	643.46	643.45	644.28
3	Khlong Tha Maprao	34.07	696.62	696.62	696.62	696.62	703.16	702.77	695.27	694.11	692.87	697.88	697.25
4	Khlong Pama Lhong	16.94	868.03	868.03	868.03	867.97	868.04	868.01	868.08	868.06	868.17	868.12	868.05
5	Khlong Ao Kung	19.45	790.63	790.63	790.63	790.63	780.18	780.18	780.13	779.54	779.11	778.69	784.03
6	Ban Nai Thon	8.13	383.62	383.55	383.33	382.87	381.63	380.59	379.21	377.12	374.99	372.04	379.90
7	Khlong Bang Rong	17.66	666.04	666.04	666.04	666.04	666.04	666.04	666.04	666.04	666.04	666.04	666.04
8	Khlong Bang Pea	7.35	506.07	506.07	506.07	506.07	506.07	506.07	506.07	506.07	506.07	506.07	506.07
9	Khlong Pa Khlok	10.66	642.71	642.71	642.71	642.71	642.71	642.71	642.71	642.71	642.71	642.71	642.71
10	Khlong Phak Chit	9.89	432.65	432.65	432.65	432.65	432.65	432.65	432.65	524.40	524.63	524.63	460.22
11	Khlong Kala	69.10	729.41	729.41	729.41	729.41	729.32	728.78	835.71	838.58	841.33	845.02	773.63
12	Khlong Bang Thao	9.13	1,033.61	1,033.62	1,033.56	1,033.36	1,033.20	1,033.18	1,032.90	1,032.66	1,032.67	1,032.54	1,033.13
13	Khlong Chang Phan Lang	5.58	726.55	726.55	724.37	729.96	736.35	737.52	738.62	745.40	746.22	746.68	735.82
14	Khlong Tha Rua	53.58	1,187.06	1,187.09	1,187.79	1,190.54	1,193.04	1,196.07	1,199.88	1,194.50	1,198.19	1,202.82	1,193.70
15	Khlong Kamala	16.27	1,058.99	1,059.38	1,060.87	1,064.74	1,067.72	1,070.37	1,073.84	1,076.92	1,080.15	1,083.01	1,069.60
16	Khlong Ban Na Kha	4.97	966.99	966.99	966.99	966.99	966.97	966.97	966.97	966.97	966.98	966.98	966.98
17	Ban Ko Sire	21.30	713.87	713.10	712.87	716.52	716.56	716.75	716.80	716.76	716.74	716.82	715.68
18	Khlong Pa Tong	18.50	1,149.18	1,159.68	1,168.39	1,174.38	1,180.99	1,186.44	1,193.47	1,195.94	1,198.97	1,201.81	1,180.92
19	Khlong Bang Yai	77.66	1,428.47	1,428.41	1,428.40	1,428.35	1,428.33	1,428.35	1,428.33	1,428.30	1,428.28	1,428.27	1,428.35
20	Ao Karon	13.19	1,065.41	1,077.84	1,086.23	1,094.15	1,101.38	1,106.82	1,111.49	1,118.16	1,124.91	1,129.99	1,101.64
21	Khlong Kata	40.12	1,279.99	1,285.21	1,290.64	1,297.65	1,302.99	1,306.47	1,308.55	1,309.76	1,310.66	1,310.94	1,300.29
22	Khao Khad (Khlong Ao Yon)	8.80	592.87	602.86	598.67	612.45	620.09	710.75	710.95	711.02	710.94	710.87	658.15
23	Ao Kata Noi and Ao Kata Yai	9.27	1,122.78	1,128.66	1,135.55	1,144.66	1,151.24	1,154.53	1,159.37	1,233.81	1,238.39	1,242.24	1,171.12
24	Khlong Sai Yuan	8.14	1,359.17	1,359.22	1,359.72	1,361.01	1,363.57	1,417.86	1,417.90	1,418.06	1,418.11	1,418.17	1,389.28
25	Khlong Ya Yai	6.80	1,305.74	1,308.58	1,315.12	1,323.31	1,330.70	1,338.30	1,343.38	1,346.57	1,354.27	1,458.08	1,342.40
		Minimum water yield	**383.62**	**383.55**	**383.33**	**382.87**	**381.63**	**380.59**	**379.21**	**377.12**	**374.99**	**372.04**	**379.90**
		Maximum water yield	**1,428.47**	**1,428.41**	**1,428.40**	**1,428.35**	**1,428.33**	**1,428.35**	**1,428.33**	**1,428.30**	**1,428.28**	**1,458.08**	**1,428.35**
		Average water yield	**880.55**	**882.41**	**883.68**	**886.41**	**888.51**	**895.52**	**900.73**	**907.97**	**909.18**	**914.35**	**894.93**

Table 6.10 Annual water yield and average in each watershed between 2020 and 2029 under dry year scenario (million m^3).

No	Watershed	Area (km^2)	Water yield between 2020 and 2029 (million m^3)										
			2020	2021	2022	2023	2024	2025	2026	2027	2028	2029	Average
1	Khlong Ban Yit	26.31	17.46	17.46	17.46	17.46	17.46	17.46	17.46	17.47	17.48	17.49	**17.47**
2	Khlong Ban Ao Tu Khun	9.20	5.92	5.92	5.92	5.92	5.94	5.94	5.94	5.92	5.92	5.92	**5.93**
3	Khlong Tha Maprao	34.07	23.73	23.73	23.73	23.73	23.95	23.94	23.68	23.64	23.60	23.77	**23.75**
4	Khlong Pama Lhong	16.94	14.73	14.73	14.73	14.73	14.73	14.73	14.73	14.73	14.73	14.73	**14.73**
5	Khlong Ao Kung	19.45	15.38	15.38	15.38	15.38	15.18	15.18	15.18	15.17	15.16	15.15	**15.26**
6	Ban Nai Thon	8.13	3.11	3.11	3.10	3.10	3.09	3.08	3.07	3.05	3.04	3.01	**3.08**
7	Khlong Bang Rong	17.66	11.75	11.75	11.75	11.75	11.75	11.75	11.75	11.75	11.75	11.75	**11.75**
8	Khlong Bang Pea	7.35	3.71	3.71	3.71	3.71	3.71	3.71	3.71	3.71	3.71	3.71	**3.71**
9	Khlong Pa Khlok	10.66	6.84	6.84	6.84	6.84	6.84	6.84	6.84	6.84	6.84	6.84	**6.84**
10	Khlong Phak Chit	9.89	4.29	4.29	4.29	4.29	4.29	4.29	4.29	5.20	5.20	5.20	**4.57**
11	Khlong Kala	69.10	50.43	50.43	50.43	50.43	50.43	50.39	57.78	57.98	58.17	58.43	**53.49**
12	Khlong Bang Thao	9.13	9.44	9.44	9.44	9.43	9.43	9.43	9.43	9.43	9.43	9.43	**9.43**
13	Khlong Chang Phan Lang	5.58	4.05	4.05	4.04	4.07	4.11	4.11	4.12	4.16	4.16	4.16	**4.10**
14	Khlong Tha Rua	53.58	63.58	63.58	63.62	63.77	63.90	64.06	64.27	63.98	64.17	64.42	**63.93**
15	Khlong Kamala	16.27	17.22	17.23	17.25	17.31	17.36	17.40	17.46	17.51	17.56	17.61	**17.39**
16	Khlong Ban Na Kha	4.97	4.81	4.81	4.81	4.81	4.81	4.81	4.81	4.81	4.81	4.81	**4.81**
17	Ban Ko Sire	21.30	15.18	15.17	15.16	15.24	15.24	15.24	15.24	15.24	15.24	15.25	**15.22**
18	Khlong Pa Tong	18.50	21.29	21.48	21.64	21.75	21.88	21.98	22.11	22.15	22.21	22.26	**21.87**
19	Khlong Bang Yai	77.66	110.91	110.90	110.90	110.90	110.90	110.90	110.90	110.89	110.89	110.89	**110.90**
20	Ao Karon	13.19	14.04	14.20	14.31	14.41	14.51	14.58	14.64	14.73	14.82	14.89	**14.51**
21	Khlong Kata	40.12	51.38	51.59	51.81	52.09	52.31	52.45	52.53	52.58	52.61	52.62	**52.20**
22	Khao Khad (Khlong Ao Yon)	8.80	5.22	5.31	5.28	5.40	5.46	6.26	6.26	6.27	6.26	6.26	**5.80**
23	Ao Kata Noi and Ao Kata Yai	9.27	10.44	10.49	10.56	10.64	10.70	10.73	10.78	11.47	11.51	11.55	**10.89**
24	Khlong Sai Yuan	8.14	11.05	11.05	11.05	11.07	11.09	11.53	11.53	11.53	11.53	11.53	**11.29**
25	Khlong Ya Yai	6.80	8.86	8.87	8.92	8.97	9.02	9.08	9.11	9.13	9.18	9.89	**9.10**
		Minimum water yield	**3.11**	**3.11**	**3.10**	**3.10**	**3.09**	**3.08**	**3.07**	**3.05**	**3.04**	**3.01**	**3.08**
		Maximum water yield	**110.91**	**110.90**	**110.90**	**110.90**	**110.90**	**110.90**	**110.90**	**110.89**	**110.89**	**110.89**	**110.90**
		Average water yield	**20.19**	**20.22**	**20.25**	**20.29**	**20.32**	**20.40**	**20.71**	**20.77**	**20.80**	**20.86**	**20.48**

In addition, the monthly water yield estimation results between 2020 and 2029 under the dry year scenario are presented in Tables 6.11 and 6.12. As a result, the average water yield from the estimated period in the summer season (December to March) varied from the lowest value of 3.53 mm or 1.84 million m^3 in March to the highest value of 61.03 or 31.86 million m^3 in December. Meanwhile, the average water yield from the estimated period in the rainy season (April to November) varied from the lowest value of 30.84 mm or 16.10 million m^3 in May to the highest value of 195.89 mm or 102.26 million m^3 in October (see Figure 6.20).

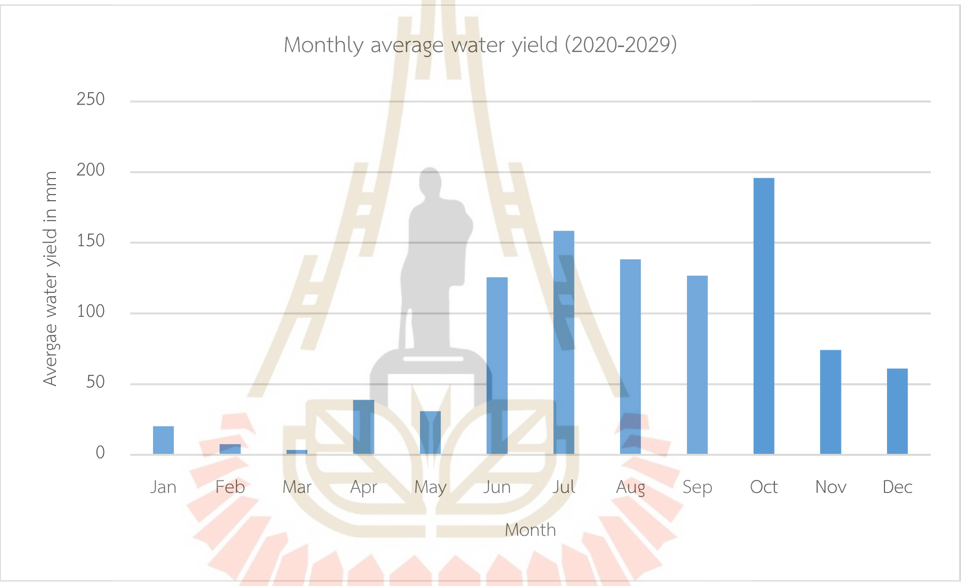

Figure 6.20 Monthly average water yield in Phuket Island between 2020 and 2029 under dry year scenario.

Table 6.11 Average monthly water yield of Phuket Island between 2020 and 2029 under dry year scenario (mm).

Month	Water yield between 2020 and 2029 (mm)										
	2020	**2021**	**2022**	**2023**	**2024**	**2025**	**2026**	**2027**	**2028**	**2029**	**Average**
Jan	19.93	19.89	19.85	19.80	19.66	19.50	21.13	21.14	21.15	21.21	20.33
Feb	7.92	7.89	7.86	7.81	7.91	7.83	7.02	6.98	6.91	6.87	7.50
Mar	3.70	3.67	3.65	3.61	3.61	3.56	3.40	3.38	3.35	3.32	3.53
Apr	36.86	37.15	37.47	38.00	38.38	39.11	39.43	40.08	40.31	40.83	38.76
May	28.94	29.10	29.26	29.61	29.63	30.03	32.41	32.89	33.10	33.44	30.84
Jun	117.44	118.12	118.72	119.71	119.30	121.09	133.96	134.86	135.79	136.94	125.59
Jul	154.30	154.75	155.18	155.93	156.51	157.90	161.49	162.08	162.50	163.38	158.40
Aug	135.85	136.03	136.20	136.52	137.09	137.66	140.26	140.94	141.11	141.80	138.35
Sep	128.00	127.93	127.83	127.70	128.19	127.97	124.93	125.09	124.89	124.77	126.73
Oct	195.86	196.06	196.25	196.60	197.29	197.99	194.62	194.58	194.64	194.96	195.89
Nov	75.58	75.34	75.02	74.43	73.89	72.96	73.92	74.04	73.80	73.34	74.23
Dec	62.98	62.80	62.61	62.23	62.17	61.44	59.35	59.16	58.94	58.64	61.03
Average	**80.61**	**80.73**	**80.83**	**81.00**	**81.14**	**81.42**	**82.66**	**82.94**	**83.04**	**83.29**	**81.76**

Table 6.12 Average monthly water yield of Phuket Island between 2020 and 2029 under dry year scenario (million m^3).

Month	Water yield between 2020 and 2029 (million m^3)										
	2020	**2021**	**2022**	**2023**	**2024**	**2025**	**2026**	**2027**	**2028**	**2029**	**Average**
Jan	10.40	10.38	10.36	10.34	10.26	10.18	11.03	11.04	11.04	11.07	10.61
Feb	4.13	4.12	4.10	4.08	4.13	4.09	3.66	3.64	3.61	3.59	3.92
Mar	1.93	1.92	1.91	1.88	1.88	1.86	1.77	1.76	1.75	1.73	1.84
Apr	19.24	19.39	19.56	19.84	20.04	20.42	20.58	20.92	21.04	21.32	20.24
May	15.11	15.19	15.28	15.46	15.47	15.68	16.92	17.17	17.28	17.46	16.10
Jun	61.31	61.66	61.98	62.49	62.28	63.22	69.93	70.40	70.89	71.49	65.57
Jul	80.55	80.79	81.01	81.40	81.71	82.43	84.31	84.61	84.83	85.29	82.69
Aug	70.92	71.01	71.10	71.27	71.57	71.87	73.22	73.58	73.67	74.03	72.22
Sep	66.82	66.79	66.73	66.67	66.92	66.81	65.22	65.30	65.20	65.14	66.16
Oct	102.25	102.35	102.45	102.64	103.00	103.36	101.60	101.58	101.61	101.78	102.26
Nov	39.46	39.33	39.16	38.86	38.57	38.09	38.59	38.65	38.53	38.29	38.75
Dec	32.88	32.78	32.69	32.49	32.46	32.07	30.98	30.88	30.77	30.61	31.86
Average	**42.08**	**42.14**	**42.19**	**42.29**	**42.36**	**42.51**	**43.15**	**43.29**	**43.35**	**43.48**	**42.68**

6.5.2 Water yield estimation of wet year scenario

Annual water balance components of the wet year scenario between 2020 and 2029 were estimated based on long-term historical rainfall data between 1999 and 2019. Herein, rainfall data in 2016 with a value of 3,686.00 mm (wet year) was chosen as significant input data for water yield estimation using the SWAT model under the wet year scenario. The annual water balance of the wet year scenario between 2020 and 2029 is displayed in Table 6.13.

Table 6.13 Annual water balance in Phuket Island between 2020 and 2029 under wet year scenario (mm).

Year	Surface Runoff	Lateral flow	Groundwater		Evapotranspiration	Water Yield
			Shallow aquifer	Deep aquifer		
2020	1,264.17	147.02	882.84	53.39	935.00	2,347.42
2021	1,269.98	146.04	880.12	53.22	934.80	2,349.36
2022	1,275.22	145.45	877.16	53.06	934.50	2,350.89
2023	1,287.41	147.66	865.83	52.43	936.10	2,353.33
2024	1,294.66	143.86	863.70	52.31	935.50	2,354.53
2025	1,313.41	141.63	852.02	51.67	935.60	2,358.73
2026	1,397.25	134.91	791.27	48.60	936.00	2,372.03
2027	1,417.47	132.88	777.66	47.84	935.40	2,375.84
2028	1,424.99	132.35	772.17	47.56	935.50	2,377.06
2029	1,439.43	129.48	763.20	47.12	934.30	2,379.23
Average	**1,338.40**	**140.13**	**832.60**	**50.72**	**935.27**	**2,361.84**

As a result (Table 6.13), it can be observed that the estimated annual water yield of the wet year scenario between 2020 and 2029 varied from 2,347.42 mm or 1,225.48 million m^3 in 2020 to 2,379.23 mm or 1,242.08 million m^3 in 2029, with an average annual water yield of 2,361.84 mm or 1,233.00 million m^3. The annual water yield of Phuket Island under the wet year scenario is relatively stable from 2020 to 2025, but it continuously increases from 2026 to 2029 (Figure 6.21). Likewise, the proportional hydrologic components of water yield include surface runoff, lateral flow, groundwater (shallow aquifer), groundwater (deep aquifer), is relatively stable from 2020 to 2025. Still, surface runoff continuously increases from 2026 to 2029, while shallow groundwater continuously decreases in the same period, as shown in Figure 6.22.

In the meantime, the estimated annual evapotranspiration of wet year condition between 2020 and 2029 varies from 934.30 mm to 936.10 mm, with an average annual evapotranspiration value of 935.27 mm. However, the annual evapotranspiration of Phuket Island under the wet year scenario is relatively stable during estimated years (Figure 6.23).

Like the dry year scenarios, these findings indicate an effect of LULC change on water yield with its hydrologic component and evapotranspiration because rainfall data as significant input data for water yield estimation is fixed.

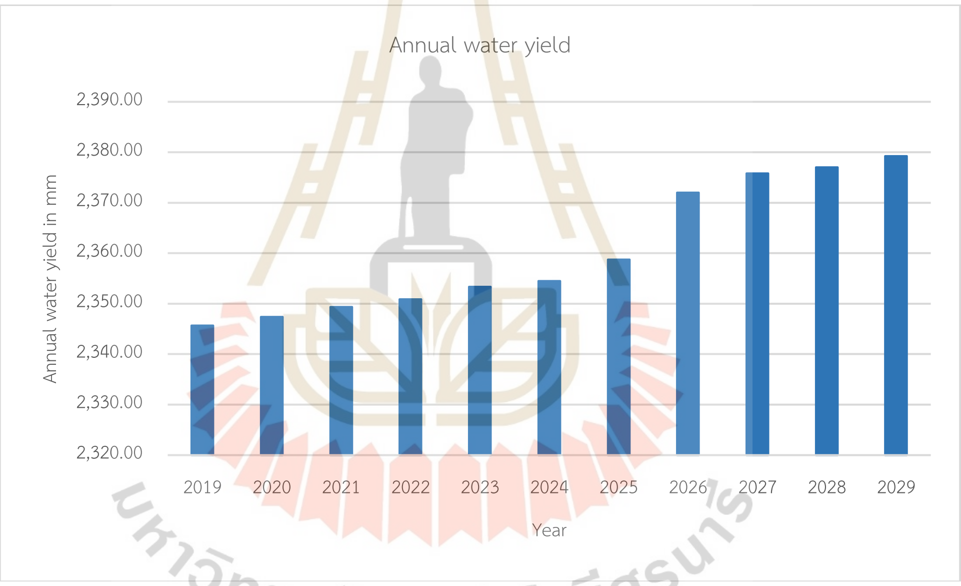

Figure 6.21 Temporal estimated water yield of Phuket Island between 2020 and 2029 under wet year scenario.

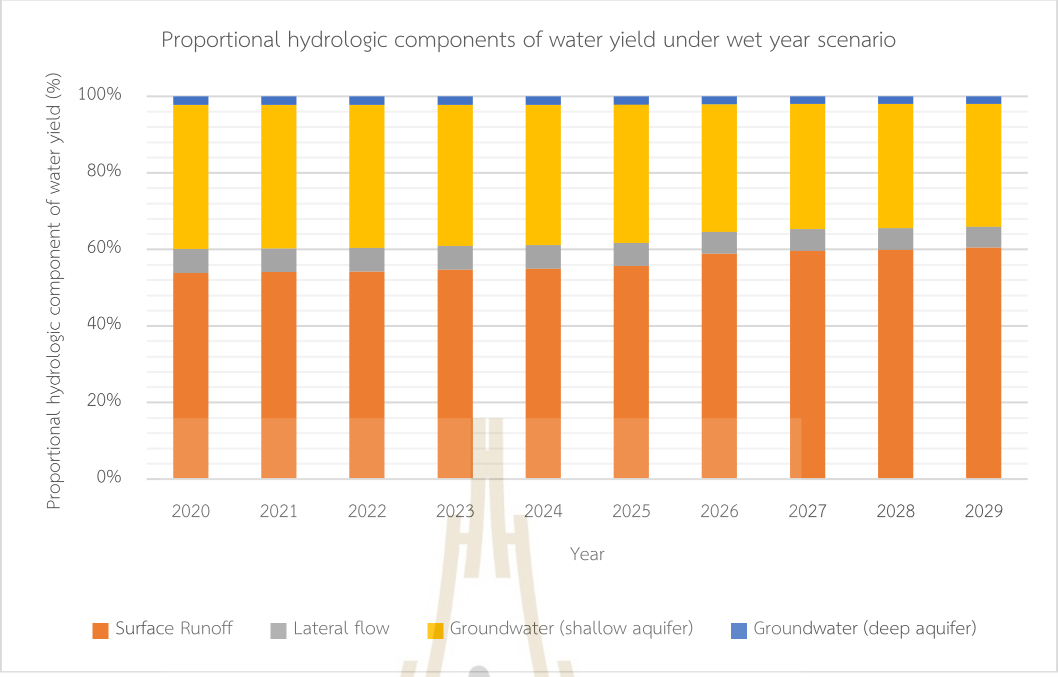

Figure 6.22 Proportional hydrologic components of Phuket Island between 2020 and 2029 under wet year scenario.

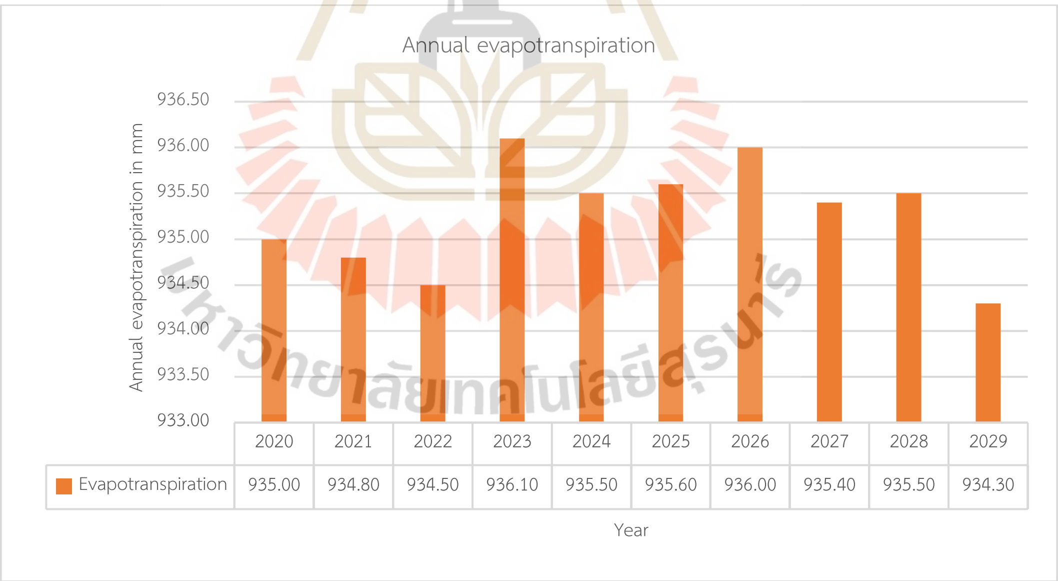

	2020	2021	2022	2023	2024	2025	2026	2027	2028	2029
Evapotranspiration	935.00	934.80	934.50	936.10	935.50	935.60	936.00	935.40	935.50	934.30

Figure 6.23 Temporal estimated evapotranspiration of Phuket Island between 2020 and 2029 under wet year scenario.

Statistical data of annual water yield in 25 watersheds in Phuket Island between 2020 and 2029 under the wet year scenario is summarized in Tables 6.14 and 6.15. Figure 6.24 displays the average water yield of each watershed and the average water yield of twenty-five watersheds between 2020 and 2029 under the wet year scenario.

As a result, the annual water yield in 25 watersheds is quite different under the wet year scenario. The highest average water yield is found in the Khlong Bang Yai watershed, with 2,849.24 mm or 221.21 million m^3, while the lowest average water yield occurs in the Khlong Chang Phan Lang watershed with a value of 1,767.22 mm or 9.85 million m^3. Additionally, only six watersheds, including Khlong Ban Yit, Khlong Tha Maprao, Khlong Kala, Khlong Tha Rua, Khlong Bang Yai, Khlong Kata, can provide an average water yield higher than the average value of all watersheds in Phuket Island, with a value of 2,212.33 mm or 49.31 million m^3. Like the dry year scenario, these results indicate the effect of topographic features, particularly the distribution of LULC, soil types, and slope classes in each watershed and its area and rainfall pattern.

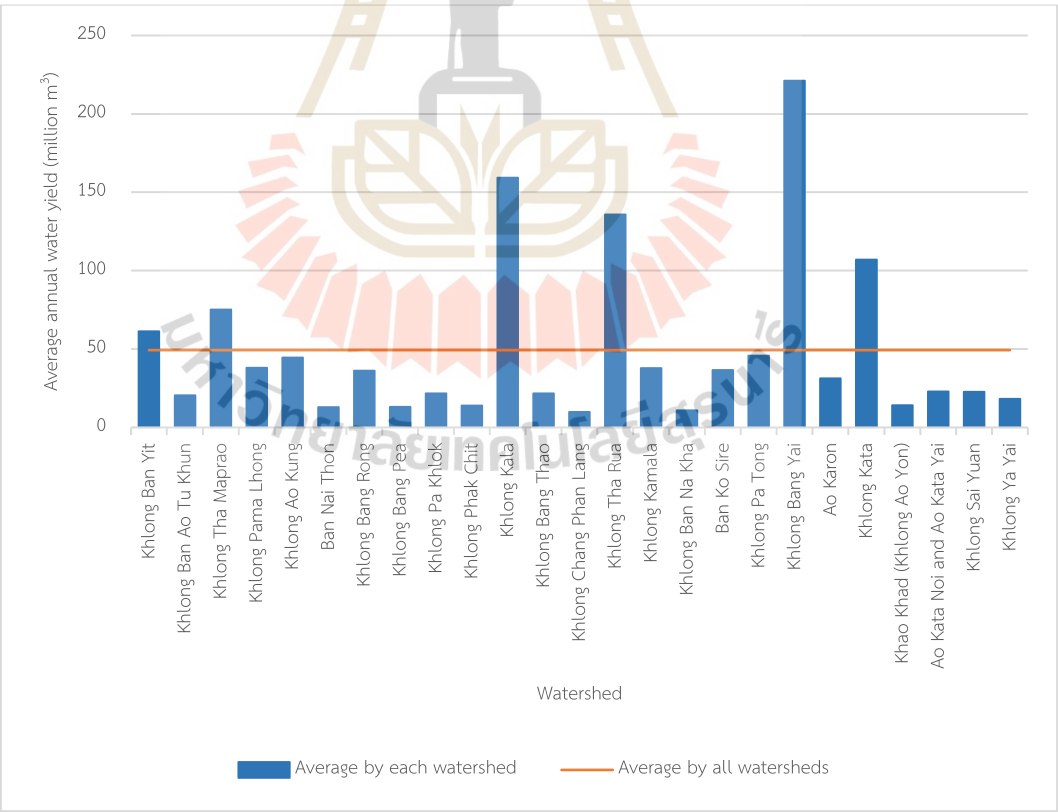

Figure 6.24 Average water yield between 2020 and 2029 in 25 watersheds under wet year scenario.

Table 6.14 Annual water yield and average in each watershed between 2020 and 2029 under wet year scenario (mm).

No	Watershed	Area (km^2)	Water yield between 2020 and 2029 (mm)										
			2020	2021	2022	2023	2024	2025	2026	2027	2028	2029	Average
1	Khlong Ban Yit	26.31	2,327.73	2,327.73	2,327.73	2,327.73	2,327.73	2,327.73	2,327.74	2,327.98	2,327.86	2,327.85	2,327.78
2	Khlong Ban Ao Tu Khun	9.20	2,229.29	2,229.29	2,229.29	2,229.29	2,229.85	2,229.80	2,229.36	2,228.06	2,227.51	2,226.81	2,228.86
3	Khlong Tha Maprao	34.07	2,212.70	2,212.70	2,212.70	2,212.70	2,202.31	2,201.66	2,210.50	2,208.65	2,207.09	2,194.28	2,207.53
4	Khlong Pama Lhong	16.94	2,237.00	2,237.00	2,237.00	2,236.98	2,237.02	2,237.00	2,237.03	2,237.07	2,237.06	2,236.96	2,237.01
5	Khlong Ao Kung	19.45	2,296.18	2,296.18	2,296.18	2,296.18	2,294.41	2,294.36	2,294.15	2,292.97	2,291.98	2,291.10	2,294.37
6	Ban Nai Thon	8.13	1,602.47	1,602.47	1,602.72	1,602.81	1,601.67	1,601.27	1,600.54	1,598.78	1,596.29	1,592.53	1,600.15
7	Khlong Bang Rong	17.66	2,054.22	2,054.22	2,054.22	2,054.22	2,054.22	2,054.22	2,054.22	2,054.22	2,054.22	2,054.22	2,054.22
8	Khlong Bang Pea	7.35	1,777.00	1,777.00	1,777.00	1,777.00	1,777.00	1,777.00	1,777.00	1,777.00	1,777.00	1,777.00	1,777.00
9	Khlong Pa Khlok	10.66	2,039.06	2,039.06	2,039.06	2,039.06	2,039.06	2,039.06	2,039.06	2,039.06	2,039.06	2,039.06	2,039.06
10	Khlong Phak Chit	9.89	1,366.21	1,366.21	1,366.21	1,366.21	1,366.21	1,366.21	1,366.21	1,484.21	1,484.50	1,484.50	1,401.67
11	Khlong Kala	69.10	2,270.23	2,270.23	2,270.23	2,270.23	2,270.04	2,268.97	2,351.83	2,353.01	2,354.07	2,355.37	2,303.42
12	Khlong Bang Thao	9.13	2,382.21	2,382.14	2,382.05	2,381.72	2,381.26	2,380.70	2,380.28	2,380.12	2,379.94	2,379.65	2,381.01
13	Khlong Chang Phan Lang	5.58	1,770.55	1,770.55	1,760.41	1,760.62	1,766.23	1,766.51	1,766.66	1,770.16	1,770.22	1,770.32	1,767.22
14	Khlong Tha Rua	53.58	2,527.03	2,527.07	2,527.94	2,531.85	2,535.22	2,539.39	2,544.01	2,533.75	2,537.87	2,543.33	2,534.75
15	Khlong Kamala	16.27	2,307.47	2,308.00	2,310.14	2,315.80	2,320.17	2,324.08	2,329.26	2,333.75	2,338.48	2,342.70	2,322.99
16	Khlong Ban Na Kha	4.97	2,172.57	2,172.57	2,172.57	2,172.57	2,172.58	2,172.58	2,172.58	2,172.58	2,172.58	2,172.58	2,172.57
17	Ban Ko Sire	21.30	1,722.01	1,719.43	1,717.95	1,720.51	1,720.24	1,720.40	1,720.41	1,720.54	1,720.81	1,721.06	1,720.34
18	Khlong Pa Tong	18.50	2,428.12	2,442.83	2,455.29	2,464.00	2,473.60	2,481.72	2,496.92	2,500.57	2,505.01	2,509.12	2,475.72
19	Khlong Bang Yai	77.66	2,849.31	2,849.27	2,849.27	2,849.23	2,849.21	2,849.25	2,849.24	2,849.22	2,849.19	2,849.18	2,849.24
20	Ao Karon	13.19	2,317.10	2,335.52	2,348.01	2,359.87	2,370.64	2,378.74	2,385.76	2,395.63	2,405.62	2,413.15	2,371.00
21	Khlong Kata	40.12	2,644.30	2,650.68	2,656.37	2,662.96	2,667.99	2,672.18	2,674.71	2,676.22	2,677.36	2,677.92	2,666.07
22	Khao Khad (Khlong Ao Yon)	8.80	1,490.36	1,511.97	1,516.81	1,536.47	1,549.39	1,691.21	1,692.52	1,693.30	1,693.78	1,694.20	1,607.00
23	Ao Kata Noi and Ao Kata Yai	9.27	2,402.14	2,411.06	2,421.35	2,435.29	2,445.49	2,450.42	2,457.71	2,567.01	2,575.89	2,581.68	2,474.80
24	Khlong Sai Yuan	8.14	2,781.89	2,781.91	2,782.10	2,782.43	2,783.14	2,813.19	2,813.20	2,813.23	2,813.24	2,813.25	2,797.76
25	Khlong Ya Yai	6.80	2,662.44	2,665.34	2,671.37	2,677.14	2,680.88	2,688.36	2,693.31	2,696.46	2,698.99	2,834.11	2,696.84
		Minimum water yield	**1,366.21**	**1,366.21**	**1,366.21**	**1,366.21**	**1,366.21**	**1,366.21**	**1,366.21**	**1,484.21**	**1,484.50**	**1,484.50**	**1,401.67**
		Maximum water yield	**2,849.31**	**2,849.27**	**2,849.27**	**2,849.23**	**2,849.21**	**2,849.25**	**2,849.24**	**2,849.22**	**2,849.19**	**2,849.18**	**2,849.24**
		Average water yield	**2,194.78**	**2,197.62**	**2,199.36**	**2,202.51**	**2,204.62**	**2,213.04**	**2,218.57**	**2,228.14**	**2,229.42**	**2,235.28**	**2,212.33**

Table 6.15 Annual water yield and average in each watershed between 2020 and 2029 under wet year scenario (million m^3).

No	Watershed	Area (km^2)	Water yield between 2020 and 2029 (million m^3)										
			2020	2021	2022	2023	2024	2025	2026	2027	2028	2029	Average
1	Khlong Ban Yit	26.31	61.23	61.23	61.23	61.23	61.23	61.23	61.23	61.23	61.23	61.23	61.23
2	Khlong Ban Ao Tu Khun	9.20	20.51	20.51	20.51	20.51	20.51	20.51	20.51	20.49	20.49	20.48	20.50
3	Khlong Tha Maprao	34.07	75.37	75.37	75.37	75.37	75.02	75.00	75.30	75.24	75.18	74.75	75.20
4	Khlong Pama Lhong	16.94	37.96	37.96	37.96	37.96	37.96	37.96	37.96	37.96	37.96	37.96	37.96
5	Khlong Ao Kung	19.45	44.68	44.68	44.68	44.68	44.65	44.65	44.64	44.62	44.60	44.58	44.65
6	Ban Nai Thon	8.13	12.97	12.97	12.98	12.98	12.97	12.96	12.96	12.94	12.92	12.89	12.95
7	Khlong Bang Rong	17.66	36.23	36.23	36.23	36.23	36.23	36.23	36.23	36.23	36.23	36.23	36.23
8	Khlong Bang Pea	7.35	13.04	13.04	13.04	13.04	13.04	13.04	13.04	13.04	13.04	13.04	13.04
9	Khlong Pa Khlok	10.66	21.72	21.72	21.72	21.72	21.72	21.72	21.72	21.72	21.72	21.72	21.72
10	Khlong Phak Chit	9.89	13.55	13.55	13.55	13.55	13.55	13.55	13.55	14.72	14.73	14.73	13.91
11	Khlong Kala	69.10	156.97	156.97	156.97	156.97	156.96	156.89	162.62	162.70	162.77	162.86	159.27
12	Khlong Bang Thao	9.13	21.75	21.75	21.75	21.74	21.74	21.73	21.73	21.73	21.73	21.72	21.74
13	Khlong Chang Phan Lang	5.58	9.87	9.87	9.82	9.82	9.85	9.85	9.85	9.87	9.87	9.87	9.85
14	Khlong Tha Rua	53.58	135.35	135.35	135.40	135.61	135.79	136.01	136.26	135.71	135.93	136.22	135.76
15	Khlong Kamala	16.27	37.52	37.53	37.56	37.65	37.73	37.79	37.87	37.95	38.02	38.09	37.77
16	Khlong Ban Na Kha	4.97	10.81	10.81	10.81	10.81	10.81	10.81	10.81	10.81	10.81	10.81	10.81
17	Ban Ko Sire	21.30	36.62	36.57	36.54	36.59	36.59	36.59	36.59	36.59	36.60	36.60	36.59
18	Khlong Pa Tong	18.50	44.98	45.25	45.48	45.64	45.82	45.97	46.25	46.32	46.40	46.48	45.86
19	Khlong Bang Yai	77.66	221.22	221.22	221.22	221.21	221.21	221.22	221.22	221.21	221.21	221.21	221.21
20	Ao Karon	13.19	30.53	30.77	30.93	31.09	31.23	31.34	31.43	31.56	31.69	31.79	31.24
21	Khlong Kata	40.12	106.15	106.41	106.63	106.90	107.10	107.27	107.37	107.43	107.48	107.50	107.02
22	Khao Khad (Khlong Ao Yon)	8.80	13.13	13.32	13.37	13.54	13.65	14.90	14.91	14.92	14.93	14.93	14.16
23	Ao Kata Noi and Ao Kata Yai	9.27	22.33	22.41	22.51	22.64	22.73	22.78	22.85	23.86	23.94	24.00	23.00
24	Khlong Sai Yuan	8.14	22.62	22.62	22.62	22.62	22.63	22.87	22.87	22.87	22.87	22.87	22.75
25	Khlong Ya Yai	6.80	18.06	18.08	18.12	18.16	18.18	18.23	18.26	18.29	18.30	19.22	18.29
		Minimum water yield	**9.87**	**9.87**	**9.82**	**9.82**	**9.85**	**9.85**	**9.85**	**9.87**	**9.87**	**9.87**	**9.85**
		Maximum water yield	**221.22**	**221.22**	**221.22**	**221.21**	**221.21**	**221.22**	**221.22**	**221.21**	**221.21**	**221.21**	**221.21**
		Average water yield	**49.01**	**49.05**	**49.08**	**49.13**	**49.16**	**49.24**	**49.52**	**49.60**	**49.63**	**49.67**	**49.31**

In the meantime, the monthly water yield estimation results between 2020 and 2029 under the wet year scenario are presented in Tables 6.16 and 6.17. As a result, the average water yield from the estimated period in the summer season (December to March) varied from the lowest value of 9.48 mm or 4.95 million m^3 in March to the highest value of 112.86 mm or 58.92 million m^3 in December. Meanwhile, the average water yield from the estimated rainy season (April to November) varied from the lowest value of 5.36 mm or 2.80 million m^3 in April to the highest value of 548.73 mm or 286.47 million m^3 in October (Figure 6.25).

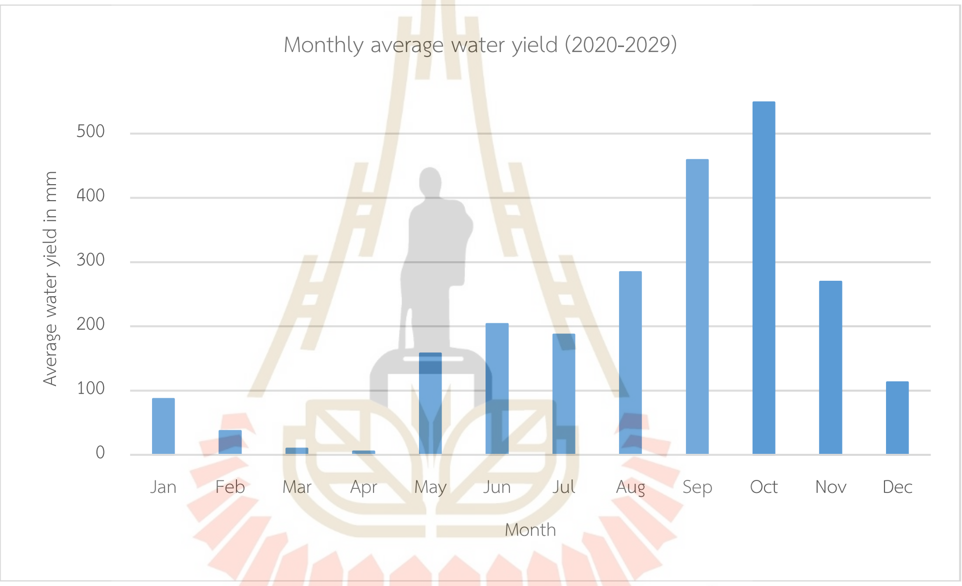

Figure 6.25 Monthly average water yield in Phuket Island between 2020 and 2029 under wet year scenario.

Table 6.16 Average monthly water yield of Phuket Island between 2020 and 2029 under wet year scenario (mm).

Month	Water yield between 2020 and 2029 (mm)										
	2020	**2021**	**2022**	**2023**	**2024**	**2025**	**2026**	**2027**	**2028**	**2029**	**Average**
Jan	85.01	85.25	85.55	85.98	86.30	86.85	87.86	88.03	88.28	88.73	86.78
Feb	38.34	38.23	38.09	37.71	37.54	37.13	36.81	36.52	36.36	36.06	37.28
Mar	10.23	10.14	10.04	9.84	9.75	9.47	9.02	8.87	8.77	8.62	9.48
Apr	5.60	5.57	5.54	5.49	5.48	5.43	5.19	5.13	5.09	5.06	5.36
May	144.60	145.70	146.72	148.36	148.36	151.40	169.52	172.50	173.84	175.82	157.68
Jun	194.93	195.83	196.58	197.81	198.94	201.17	209.63	211.84	212.70	214.61	203.40
Jul	188.50	188.69	188.72	189.09	189.27	189.43	185.20	185.18	184.98	184.64	187.37
Aug	282.78	282.92	282.94	284.10	284.14	284.63	285.18	286.20	286.27	286.25	284.54
Sep	457.22	457.30	457.41	458.44	458.76	459.38	459.56	460.47	460.63	460.90	459.01
Oct	547.57	547.62	547.74	548.45	548.68	549.30	549.11	549.45	549.60	549.79	548.73
Nov	274.26	274.05	273.81	272.23	271.79	270.54	265.89	264.30	263.80	262.85	269.35
Dec	118.39	118.07	117.74	115.81	115.51	114.01	109.07	107.35	106.73	105.90	112.86
Average	**195.62**	**195.78**	**195.91**	**196.11**	**196.21**	**196.56**	**197.67**	**197.99**	**198.09**	**198.27**	**196.82**

Table 6.17 Average monthly water yield of Phuket Island between 2020 and 2029 under wet year scenario (million m^3).

Month	Water yield between 2020 and 2029 (million m^3)										
	2020	2021	2022	2023	2024	2025	2026	2027	2028	2029	Average
Jan	44.38	44.50	44.66	44.89	45.05	45.34	45.87	45.96	46.09	46.32	45.31
Feb	20.02	19.96	19.88	19.69	19.60	19.38	19.22	19.07	18.98	18.83	19.46
Mar	5.34	5.29	5.24	5.14	5.09	4.94	4.71	4.63	4.58	4.50	4.95
Apr	2.92	2.91	2.89	2.87	2.86	2.83	2.71	2.68	2.66	2.64	2.80
May	75.49	76.06	76.60	77.45	77.45	79.04	88.50	90.05	90.75	91.79	82.32
Jun	101.76	102.23	102.62	103.27	103.86	105.02	109.44	110.59	111.04	112.04	106.19
Jul	98.41	98.51	98.52	98.71	98.81	98.89	96.68	96.67	96.57	96.39	97.82
Aug	147.63	147.70	147.71	148.31	148.34	148.59	148.88	149.41	149.45	149.44	148.55
Sep	238.69	238.73	238.79	239.33	239.50	239.82	239.91	240.39	240.47	240.61	239.62
Oct	285.86	285.89	285.95	286.32	286.44	286.76	286.66	286.84	286.92	287.02	286.47
Nov	143.18	143.07	142.94	142.12	141.89	141.24	138.81	137.98	137.72	137.22	140.62
Dec	61.81	61.64	61.47	60.46	60.30	59.52	56.94	56.04	55.72	55.29	58.92
Average	**102.12**	**102.21**	**102.27**	**102.38**	**102.43**	**102.61**	**103.19**	**103.36**	**103.41**	**103.51**	**102.75**

6.6 Effect of LULC change on water yield

Under this session, the effect of LULC change on water yield in Phuket Island under dry and wet year scenarios between 2020 and 2029 was first examined and discussed. This study applied simple linear regression analysis to identify the relationship between water yield (dependent variable) and the dominant LULC type (independent variable) using the MS Excel software. The annual water yield under the dry and wet year scenarios between 2020 and 2029, separately applied in regression analysis, is summarized in Table 6.18. Meanwhile, the area of four dominant LULC types, perennial tree and orchards, urban and built-up area, evergreen forest, and idle land, is displayed in Table 6.19.

Table 6.18 Annual water balance in Phuket Island between 2020 and 2029 under dry and wet year scenarios (million m^3).

Year	Water Yield (million m^3).	
	Dry year scenario	Wet year scenario
2020	505.01	1,225.48
2021	505.73	1,226.49
2022	506.34	1,227.28
2023	507.41	1,228.55
2024	508.28	1,229.18
2025	510.06	1,231.38
2026	517.83	1,238.32
2027	519.55	1,240.31
2028	520.22	1,240.94
2029	521.79	1,242.08

Table 6.19 Area of primary LULC type in Phuket Island between 2020 and 2029 (km^2).

Year	LULC type (km^2)			
	Urban and built-up area	Perennial tree and orchard	Idle land	Evergreen forest
2020	145.03	182.16	40.03	72.96
2021	148.29	180.01	40.29	71.79
2022	151.54	177.87	40.54	70.62
2023	154.81	175.74	40.82	69.47
2024	158.07	173.55	41.01	68.27
2025	161.32	171.46	41.32	67.15
2026	164.55	169.35	41.59	65.98
2027	167.83	167.20	41.85	64.83
2028	170.92	165.21	42.09	63.71
2029	174.34	162.90	42.35	62.49
Avg. area	**159.67**	**172.55**	**41.19**	**67.73**
Avg. percentage	**30.59**	**33.05**	**7.89**	**12.97**

The simple linear regression analysis results between water yield and dominant LULC type from dry and wet scenarios are presented in Figures 6.26 to 6.27. As a result, annual water yield in dry and wet year scenarios showed a positively high correlation with urban and built-up areas with the R^2 of 0.91 and 0.92, respectively (see Figure 6.26(a) and Figure 6.27(a)). This finding indicates that when urban and built-up areas increases, water yield increases. This phenomenon shows an expected result because surface runoff, as a significant hydrologic component of water yield, will increase when urban and built-up areas with the impervious surface increase. Likewise, annual water yield in both scenarios positively correlated with idle land (abandoned and fallowed fields) with the R^2 of 0.91 and 0.93, respectively (see Figure 6.26(b) and Figure 6.27(b)). This finding shows that when idle land increases, water yield increases.

On the contrary, annual water yield in dry and wet year scenarios disclosed a high negative correlation with perennial trees and orchards with the R^2 of 0.91 and 0.92, respectively (see Figure 6.26(c) and Figure 6.27(c)). This finding indicates that when perennial trees and orchards increase, water yield decreases. This phenomenon shows an expected result because surface runoff will decrease when areas are covered by vegetation. Likewise, annual water yield in both scenarios showed a negatively high correlation with evergreen forest with the R^2 of 0.91 and 0.92, respectively (see Figure 6.26(d) and Figure 6.27(d)). This finding confirms the influence of LULC covers on the surface runoff in the watershed.

According to the derived results as mentioned earlier, it can be concluded that the increase of urban and built-up areas with impervious surface and idle land with less covered vegetation leads to high annual water yield since these LULC types decrease the infiltration and cause more surface runoff and less groundwater replenishment. On the contrary, the increase of perennial trees and orchards and evergreen forest areas leads to low annual water yield because they induce a higher water infiltration rate. However, perennial tree and orchards and evergreen forest conversion to other LULC types will increase the surface runoff and decrease groundwater replenishment.

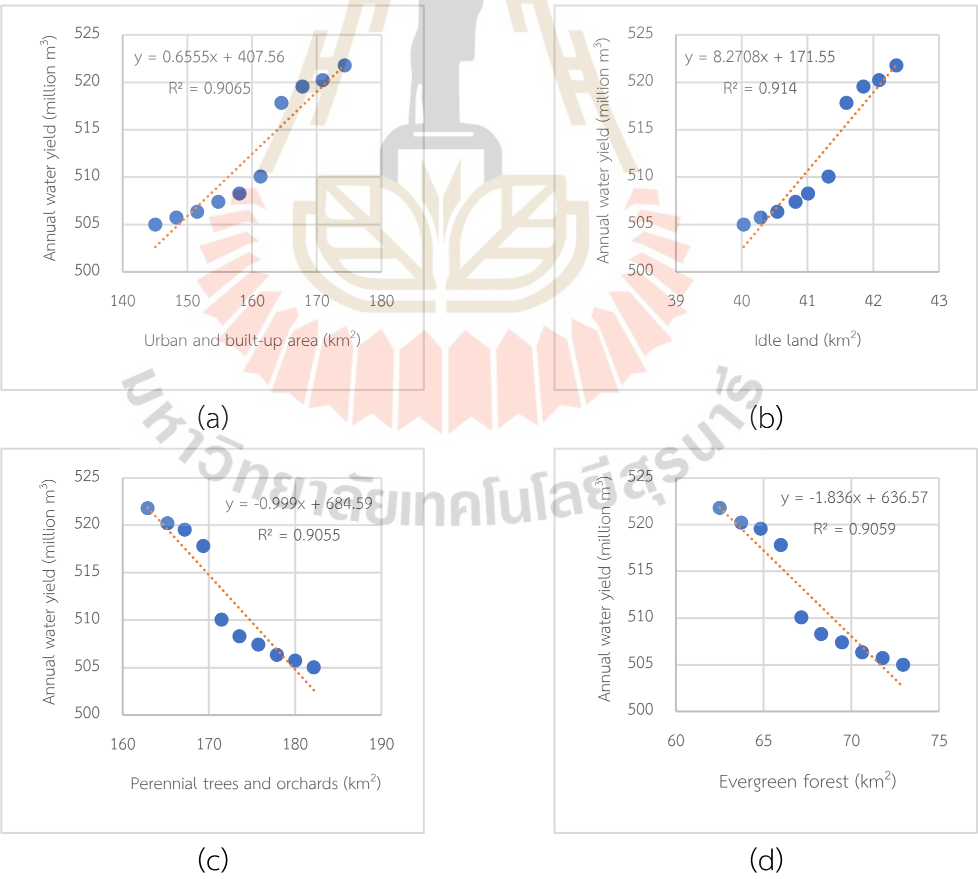

(a) (b)

(c) (d)

Figure 6.26 Simple linear regression analysis between LULC type and water yield under dry year scenario.

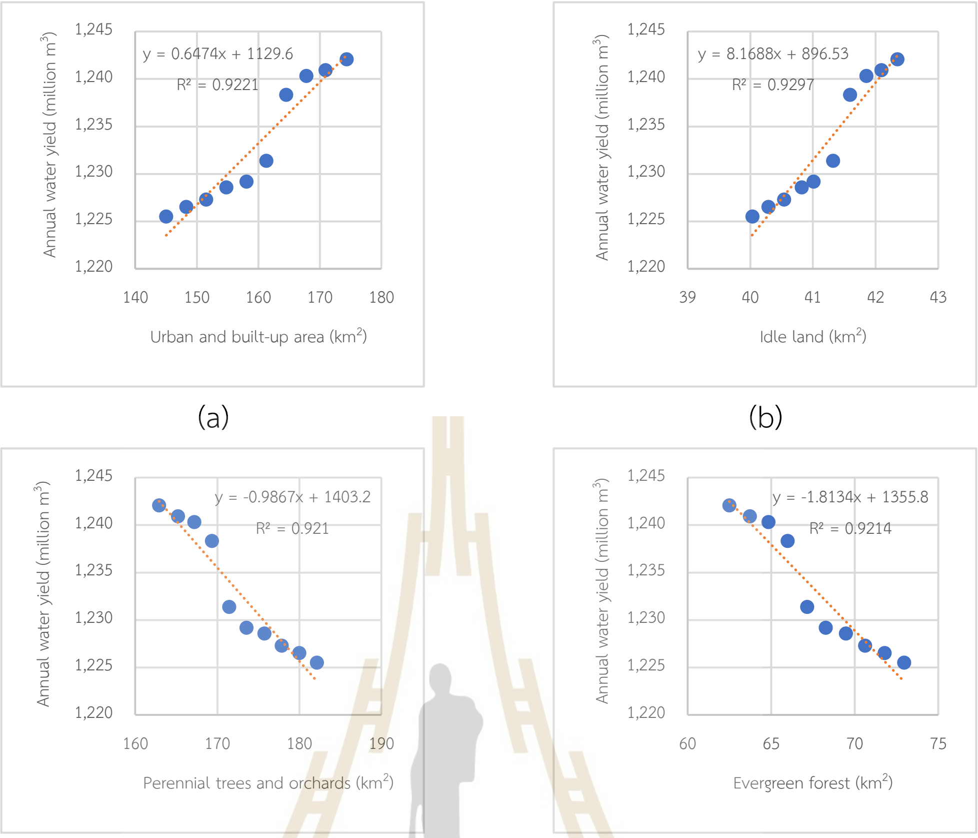

(a) (b)

(c) (d)

Figure 6.27 Simple linear regression analysis between LULC type and water yield under wet year scenario.

Besides, four LULC types, including urban and built-up area, perennial trees and orchards, idle land and evergreen forest, were extracted in six selected watersheds, which represent the top three largest areas (Khlong Bang Yai, Khlong Kala, and Khlong Tha Rua) and top three smallest areas (Khlong Ban Na Kha, Khlong Chang Phan Lang, Khlong Ya Yai) for simple linear regression analysis with their water yield data in cubic meter under dry and wet year scenarios, a summary in Tables 6.20 to 6.27.

Table 6.20 Data of urban and built-up area and water yield between 2020 and 2029 for six selected watersheds under dry year scenario.

LULC type and water yield	Year									
	2020	2021	2022	2023	2024	2025	2026	2027	2028	2029
KHLONG BANG YAI (77.66 km^2)										
Urban and built-up area (km^2)	35.79	36.27	36.82	37.11	37.44	37.88	38.16	38.43	38.64	38.92
Water yield (million m^3)	110.91	110.90	110.90	110.90	110.90	110.90	110.90	110.89	110.89	110.89
KHLONG KALA (69.10 km^2)										
Urban and built-up area (km^2)	13.34	13.34	13.35	13.36	13.45	13.71	14.11	14.61	15.13	15.72
Water yield (million m^3)	50.43	50.43	50.43	50.43	50.43	50.39	57.78	57.98	58.17	58.43
KHLONG THA RUA (53.58 km^2)										
Urban and built-up area (km^2)	12.24	12.25	12.32	12.54	12.78	13.10	13.53	14.05	14.48	14.99
Water yield (million m^3)	63.58	63.58	63.62	63.77	63.90	64.06	64.27	63.98	64.17	64.42
KHLONG BAN NA KHA (4.97 km^2)										
Urban and built-up area (km^2)	0.76	0.76	0.78	0.79	0.82	0.85	0.87	0.90	0.92	0.94
Water yield (million m^3)	4.81	4.81	4.81	4.81	4.81	4.81	4.81	4.81	4.81	4.81
KHLONG CHANG PHAN LANG (5.58 km^2)										
Urban and built-up area (km^2)	2.09	2.11	2.19	2.36	2.48	2.55	2.61	2.68	2.74	2.78
Water yield (million m^3)	4.05	4.05	4.04	4.07	4.11	4.11	4.12	4.16	4.16	4.16
KHLONG YA YAI (6.80 km^2)										
Urban and built-up area (km^2)	1.88	1.93	2.04	2.20	2.35	2.50	2.59	2.67	2.72	2.79
Water yield (million m^3)	8.86	8.87	8.92	8.97	9.02	9.08	9.11	9.13	9.18	9.89

Table 6.21 Data of urban and built-up area and water yield between 2020 and 2029 for six selected watersheds under wet year scenario.

LULC type and water yield	Year									
	2020	**2021**	**2022**	**2023**	**2024**	**2025**	**2026**	**2027**	**2028**	**2029**
KHLONG BANG YAI (77.66 km^2)										
Urban and built-up area (km^2)	35.79	36.27	36.82	37.11	37.44	37.88	38.16	38.43	38.64	38.92
Water yield (million m^3)	221.22	221.22	221.22	221.21	221.21	221.22	221.22	221.21	221.21	221.21
KHLONG KALA (69.10 km^2)										
Urban and built-up area (km^2)	13.34	13.34	13.35	13.36	13.45	13.71	14.11	14.61	15.13	15.72
Water yield (million m^3)	156.97	156.97	156.97	156.97	156.96	156.89	162.62	162.70	162.77	162.86
KHLONG THA RUA (53.58 km^2)										
Urban and built-up area (km^2)	12.24	12.25	12.32	12.54	12.78	13.10	13.53	14.05	14.48	14.99
Water yield (million m^3)	135.35	135.35	135.40	135.61	135.79	136.01	136.26	135.71	135.93	136.22
KHLONG BAN NA KHA (4.97 km^2)										
Urban and built-up area (km^2)	0.76	0.76	0.78	0.79	0.82	0.85	0.87	0.90	0.92	0.94
Water yield (million m^3)	10.81	10.81	10.81	10.81	10.81	10.81	10.81	10.81	10.81	10.81
KHLONG CHANG PHAN LANG (5.58 km^2)										
Urban and built-up area (km^2)	2.09	2.11	2.19	2.36	2.48	2.55	2.61	2.68	2.74	2.78
Water yield (million m^3)	9.87	9.87	9.82	9.82	9.85	9.85	9.85	9.87	9.87	9.87
KHLONG YA YAI (6.80 km^2)										
Urban and built-up area (km^2)	1.88	1.93	2.04	2.20	2.35	2.50	2.59	2.67	2.72	2.79
Water yield (million m^3)	18.06	18.08	18.12	18.16	18.18	18.23	18.26	18.29	18.30	19.22

Table 6.22 Data of idle land and water yield between 2020 and 2029 for six selected watersheds under dry year scenario.

LULC type and water yield	Year									
	2020	**2021**	**2022**	**2023**	**2024**	**2025**	**2026**	**2027**	**2028**	**2029**
	KHLONG BANG YAI (77.66 km^2)									
Idle land (km^2)	5.46	5.59	5.62	5.67	5.65	5.62	5.62	5.61	5.58	5.57
Water yield (million m^3)	110.91	110.90	110.90	110.90	110.90	110.90	110.90	110.89	110.89	110.89
	KHLONG KALA (69.10 km^2)									
Idle land (km^2)	9.85	9.86	9.90	9.96	10.04	10.15	10.23	10.35	10.44	10.55
Water yield (million m^3)	50.43	50.43	50.43	50.43	50.43	50.39	57.78	57.98	58.17	58.43
	KHLONG THA RUA (53.58 km^2)									
Idle land (km^2)	5.85	5.85	5.85	5.86	5.86	5.87	5.87	5.89	5.91	5.94
Water yield (million m^3)	63.58	63.58	63.62	63.77	63.90	64.06	64.27	63.98	64.17	64.42
	KHLONG BAN NA KHA (4.97 km^2)									
Idle land (km^2)	0.39	0.39	0.39	0.38	0.38	0.38	0.38	0.37	0.37	0.37
Water yield (million m^3)	4.81	4.81	4.81	4.81	4.81	4.81	4.81	4.81	4.81	4.81
	KHLONG CHANG PHAN LANG (5.58 km^2)									
Idle land (km^2)	0.90	0.90	0.90	0.92	0.92	0.94	0.97	0.99	1.02	1.07
Water yield (million m^3)	4.05	4.05	4.04	4.07	4.11	4.11	4.12	4.16	4.16	4.16
	KHLONG YA YAI (6.80 km^2)									
Idle land (km^2)	0.68	0.68	0.68	0.68	0.68	0.68	0.67	0.67	0.66	0.66
Water yield (million m^3)	8.86	8.87	8.92	8.97	9.02	9.08	9.11	9.13	9.18	9.89

Table 6.23 Data of idle land and water yield between 2020 and 2029 for six selected watersheds under wet year scenario.

LULC type and water yield	Year									
	2020	2021	2022	2023	2024	2025	2026	2027	2028	2029
KHLONG BANG YAI (77.66 km^2)										
Idle land (km^2)	5.46	5.59	5.62	5.67	5.65	5.62	5.62	5.61	5.58	5.57
Water yield (million m^3)	221.22	221.22	221.22	221.21	221.21	221.22	221.22	221.21	221.21	221.21
KHLONG KALA (69.10 km^2)										
Idle land (km^2)	9.85	9.86	9.90	9.96	10.04	10.15	10.23	10.35	10.44	10.55
Water yield (million m^3)	156.97	156.97	156.97	156.97	156.96	156.89	162.62	162.70	162.77	162.86
KHLONG THA RUA (53.58 km^2)										
Idle land (km^2)	5.85	5.85	5.85	5.86	5.86	5.87	5.87	5.89	5.91	5.94
Water yield (million m^3)	135.35	135.35	135.40	135.61	135.79	136.01	136.26	135.71	135.93	136.22
KHLONG BAN NA KHA (4.97 km^2)										
Idle land (km^2)	0.39	0.39	0.39	0.38	0.38	0.38	0.38	0.37	0.37	0.37
Water yield (million m^3)	10.81	10.81	10.81	10.81	10.81	10.81	10.81	10.81	10.81	10.81
KHLONG CHANG PHAN LANG (5.58 km^2)										
Idle land (km^2)	0.90	0.90	0.90	0.92	0.92	0.94	0.97	0.99	1.02	1.07
Water yield (million m^3)	9.87	9.87	9.82	9.82	9.85	9.85	9.85	9.87	9.87	9.87
KHLONG YA YAI (6.80 km^2)										
Idle land (km^2)	0.68	0.68	0.68	0.68	0.68	0.68	0.67	0.67	0.66	0.66
Water yield (million m^3)	18.06	18.08	18.12	18.16	18.18	18.23	18.26	18.29	18.30	19.22

Table 6.24 Data of perennial trees and orchards and water yield between 2020 and 2029 for six selected watersheds under dry year scenario.

LULC type and water yield	Year									
	2020	2021	2022	2023	2024	2025	2026	2027	2028	2029
	KHLONG BANG YAI (77.66 km^2)									
Perennial trees and Orchards (km^2)	13.16	12.69	12.17	11.98	11.67	11.39	11.20	11.13	11.08	11.03
Water yield (million m^3)	110.91	110.90	110.90	110.90	110.90	110.90	110.90	110.89	110.89	110.89
	KHLONG KALA (69.10 km^2)									
Perennial trees and Orchards (km^2)	28.99	28.99	28.99	28.99	28.94	28.69	28.31	27.82	27.32	26.72
Water yield (million m^3)	50.43	50.43	50.43	50.43	50.43	50.39	57.78	57.98	58.17	58.43
	KHLONG THA RUA (53.58 km^2)									
Perennial trees and Orchards (km^2)	22.25	22.25	22.17	21.98	21.75	21.44	21.03	20.54	20.13	19.69
Water yield (million m^3)	63.58	63.58	63.62	63.77	63.90	64.06	64.27	63.98	64.17	64.42
	KHLONG BAN NA KHA (4.97 km^2)									
Perennial trees and Orchards (km^2)	2.58	2.58	2.58	2.58	2.57	2.57	2.57	2.57	2.56	2.56
Water yield (million m^3)	4.81	4.81	4.81	4.81	4.81	4.81	4.81	4.81	4.81	4.81
	KHLONG CHANG PHAN LANG (5.58 km^2)									
Perennial trees and Orchards (km^2)	0.41	0.40	0.38	0.33	0.29	0.26	0.25	0.23	0.21	0.19
Water yield (million m^3)	4.05	4.05	4.04	4.07	4.11	4.11	4.12	4.16	4.16	4.16
	KHLONG YA YAI (6.80 km^2)									
Perennial trees and Orchards (km^2)	1.97	1.95	1.88	1.78	1.67	1.56	1.50	1.44	1.41	1.36
Water yield (million m^3)	8.86	8.87	8.92	8.97	9.02	9.08	9.11	9.13	9.18	9.89

Table 6.25 Data of perennial trees and orchards and water yield between 2020 and 2029 for six selected watersheds under wet year scenario.

LULC type and water yield	Year									
	2020	2021	2022	2023	2024	2025	2026	2027	2028	2029
KHLONG BANG YAI (77.66 km^2)										
Perennial trees and orchards (km^2)	13.16	12.69	12.17	11.98	11.67	11.39	11.20	11.13	11.08	11.03
Water yield (million m^3)	221.22	221.22	221.22	221.21	221.21	221.22	221.22	221.21	221.21	221.21
KHLONG KALA (69.10 km^2)										
Perennial trees and orchards (km^2)	28.99	28.99	28.99	28.99	28.94	28.69	28.31	27.82	27.32	26.72
Water yield (million m^3)	156.97	156.97	156.97	156.97	156.96	156.89	162.62	162.70	162.77	162.86
KHLONG THA RUA (53.58 km^2)										
Perennial trees and orchards (km^2)	22.25	22.25	22.17	21.98	21.75	21.44	21.03	20.54	20.13	19.69
Water yield (million m^3)	135.35	135.35	135.40	135.61	135.79	136.01	136.26	135.71	135.93	136.22
KHLONG BAN NA KHA (4.97 km^2)										
Perennial trees and orchards (km^2)	2.58	2.58	2.58	2.58	2.57	2.57	2.57	2.57	2.56	2.56
Water yield (million m^3)	10.81	10.81	10.81	10.81	10.81	10.81	10.81	10.81	10.81	10.81
KHLONG CHANG PHAN LANG (5.58 km^2)										
Perennial trees and orchards (km^2)	0.41	0.40	0.38	0.33	0.29	0.26	0.25	0.23	0.21	0.19
Water yield (million m^3)	9.87	9.87	9.82	9.82	9.85	9.85	9.85	9.87	9.87	9.87
KHLONG YA YAI (6.80 km^2)										
Perennial trees and orchards (km^2)	1.97	1.95	1.88	1.78	1.67	1.56	1.50	1.44	1.41	1.36
Water yield (million m^3)	18.06	18.08	18.12	18.16	18.18	18.23	18.26	18.29	18.30	19.22

Table 6.26 Data of evergreen forest and water yield between 2020 and 2029 for six selected watersheds under dry year scenario.

LULC type and water yield	Year									
	2020	2021	2022	2023	2024	2025	2026	2027	2028	2029
KHLONG BANG YAI (77.66 km^2)										
Evergreen forest (km^2)	12.35	12.18	12.03	11.91	11.80	11.72	11.63	11.48	11.31	11.17
Water yield (million m^3)	110.91	110.90	110.90	110.90	110.90	110.90	110.90	110.89	110.89	110.89
KHLONG KALA (69.10 km^2)										
Evergreen forest (km^2)	9.78	9.77	9.73	9.66	9.56	9.44	9.32	9.13	9.02	8.79
Water yield (million m^3)	50.43	50.43	50.43	50.43	50.43	50.39	57.78	57.98	58.17	58.43
KHLONG THA RUA (53.58 km^2)										
Evergreen forest (km^2)	4.40	4.40	4.40	4.38	4.37	4.35	4.32	4.30	4.26	4.21
Water yield (million m^3)	63.58	63.58	63.62	63.77	63.90	64.06	64.27	63.98	64.17	64.42
KHLONG BAN NA KHA (4.97 km^2)										
Evergreen forest (km^2)	1.00	1.00	0.99	0.98	0.98	0.96	0.95	0.94	0.93	0.92
Water yield (million m^3)	4.81	4.81	4.81	4.81	4.81	4.81	4.81	4.81	4.81	4.81
KHLONG CHANG PHAN LANG (5.58 km^2)										
Evergreen forest (km^2)	0.89	0.87	0.82	0.72	0.66	0.60	0.52	0.45	0.38	0.31
Water yield (million m^3)	4.05	4.05	4.04	4.07	4.11	4.11	4.12	4.16	4.16	4.16
KHLONG YA YAI (6.80 km^2)										
Evergreen forest (km^2)	1.17	1.15	1.14	1.13	1.11	1.10	1.08	1.07	1.05	1.03
Water yield (million m^3)	8.86	8.87	8.92	8.97	9.02	9.08	9.11	9.13	9.18	9.89

Table 6.27 Data of evergreen forest and water yield between 2020 and 2029 for six selected watersheds under wet year scenario.

LULC type and water yield	Year									
	2020	2021	2022	2023	2024	2025	2026	2027	2028	2029
KHLONG BANG YAI (77.66 km^2)										
Evergreen forest (km^2)	12.35	12.18	12.03	11.91	11.80	11.72	11.63	11.48	11.31	11.17
Water yield (million m^3)	221.22	221.22	221.22	221.21	221.21	221.22	221.22	221.21	221.21	221.21
KHLONG KALA (69.10 km^2)										
Evergreen forest (km^2)	9.78	9.77	9.73	9.66	9.56	9.44	9.32	9.13	9.02	8.79
Water yield (million m^3)	156.97	156.97	156.97	156.97	156.96	156.89	162.62	162.70	162.77	162.86
KHLONG THA RUA (53.58 km^2)										
Evergreen forest (km^2)	4.40	4.40	4.40	4.38	4.37	4.35	4.32	4.30	4.26	4.21
Water yield (million m^3)	135.35	135.35	135.40	135.61	135.79	136.01	136.26	135.71	135.93	136.22
KHLONG BAN NA KHA (4.97 km^2)										
Evergreen forest (km^2)	1.00	1.00	0.99	0.98	0.98	0.96	0.95	0.94	0.93	0.92
Water yield (million m^3)	10.81	10.81	10.81	10.81	10.81	10.81	10.81	10.81	10.81	10.81
KHLONG CHANG PHAN LANG (5.58 km^2)										
Evergreen forest (km^2)	0.89	0.87	0.82	0.72	0.66	0.60	0.52	0.45	0.38	0.31
Water yield (million m^3)	9.87	9.87	9.82	9.82	9.85	9.85	9.85	9.87	9.87	9.87
KHLONG YA YAI (6.80 km^2)										
Evergreen forest (km^2)	1.17	1.15	1.14	1.13	1.11	1.10	1.08	1.07	1.05	1.03
Water yield (million m^3)	18.06	18.08	18.12	18.16	18.18	18.23	18.26	18.29	18.30	19.22

Results of simple linear regression analysis between areas of four selected LULC types and their water yield data from six watersheds under dry and wet year scenarios are presented in Figures 6.28 to 6.35. The summary of the linear relationship between LULC type and water yield from six watersheds with R^2 value under dry and wet year scenarios is separately summarized in Tables 6.28 and 6.29.

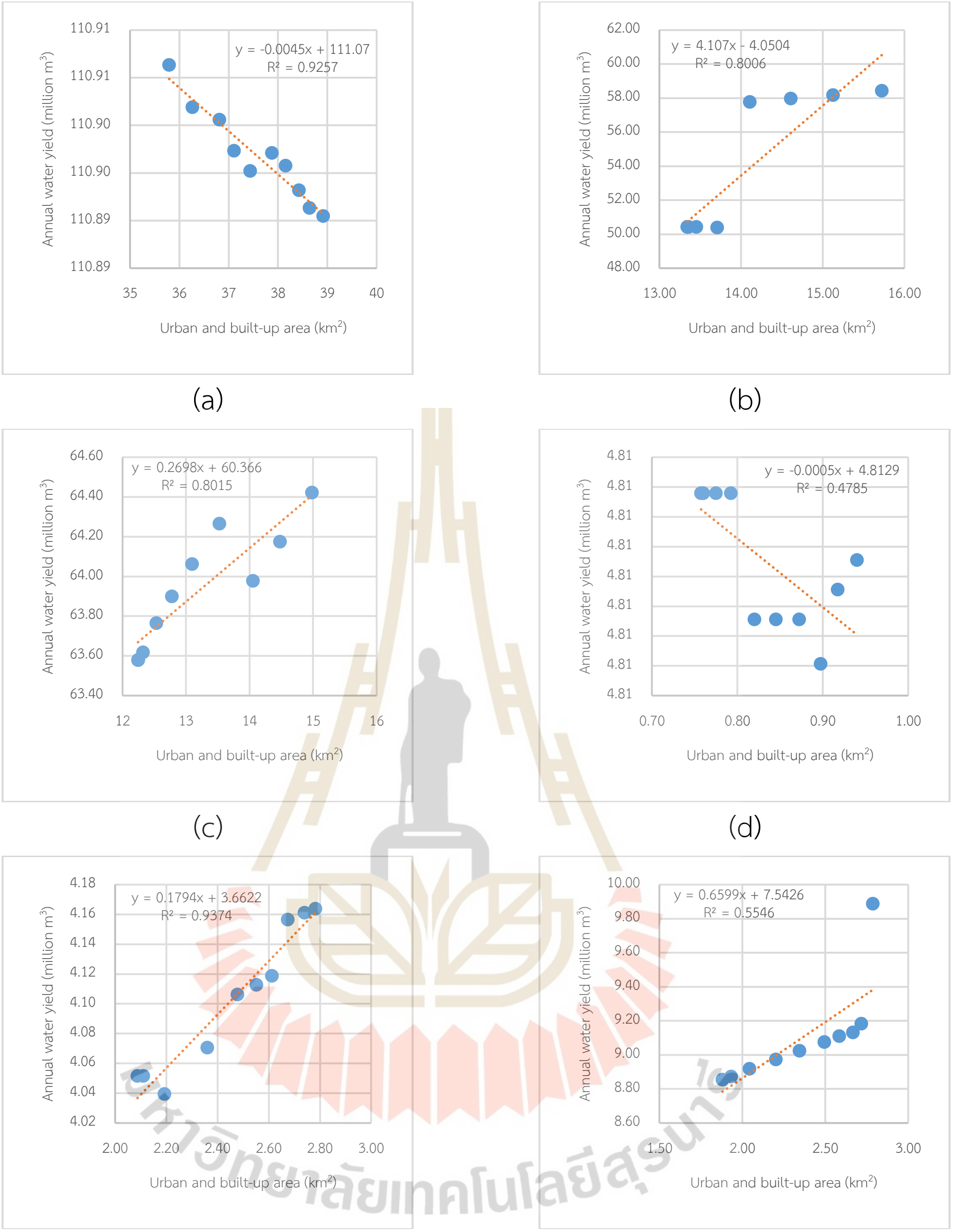

(a) (b)

(c) (d)

(e) (f)

Figure 6.28 Simple linear regression analysis between areas of urban and built-up area and water yield data from six watersheds under dry year scenario: (a) Khlong Bang Yai, (b) Khlong Kala, (c) Khlong Tha Rua, (d) Khlong Ban Na Kha, (e) Khlong Chang Phan Lang, and Khlong Ya Yai.

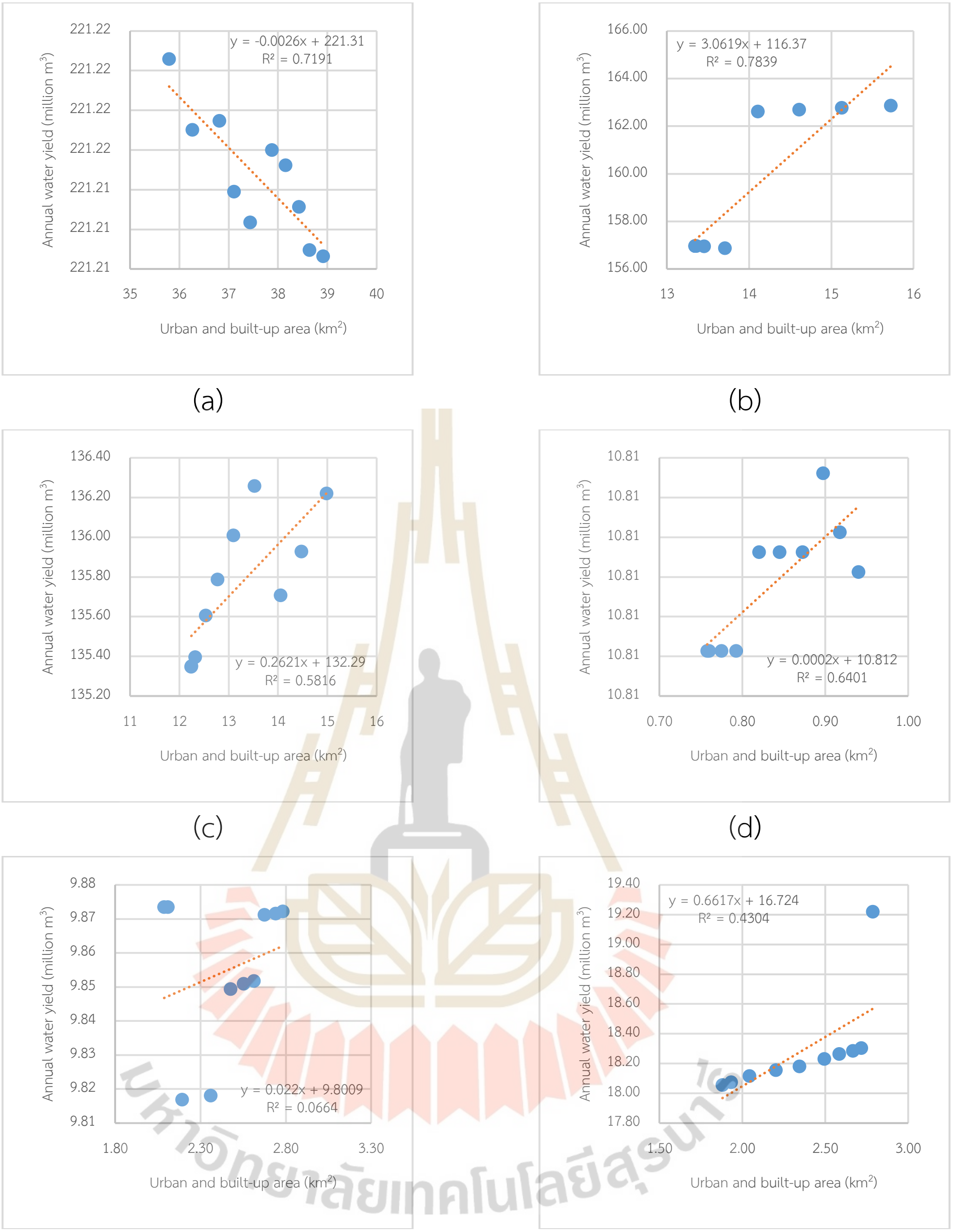

(a) (b)

(c) (d)

(e) (f)

Figure 6.29 Simple linear regression analysis between areas of urban and built-up area and water yield data from six watersheds under wet year scenario: (a) Khlong Bang Yai, (b) Khlong Kala, (c) Khlong Tha Rua, (d) Khlong Ban Na Kha, (e) Khlong Chang Phan Lang, and Khlong Ya Yai.

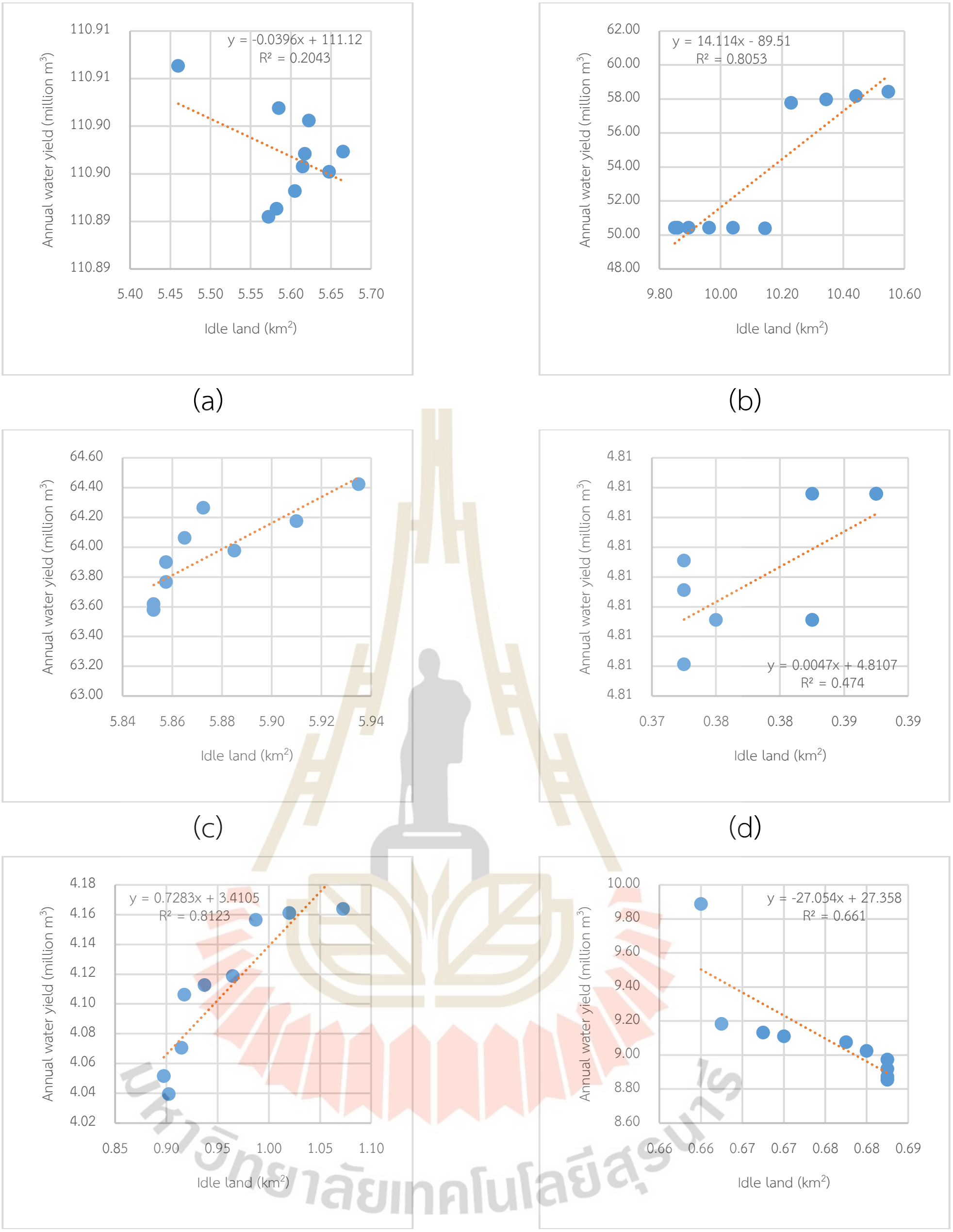

(a) (b)

(c) (d)

(e) (f)

Figure 6.30 Simple linear regression analysis between areas of idle land and water yield data from six watersheds under dry year scenario: (a) Khlong Bang Yai, (b) Khlong Kala, (c) Khlong Tha Rua, (d) Khlong Ban Na Kha, (e) Khlong Chang Phan Lang, and Khlong Ya Yai.

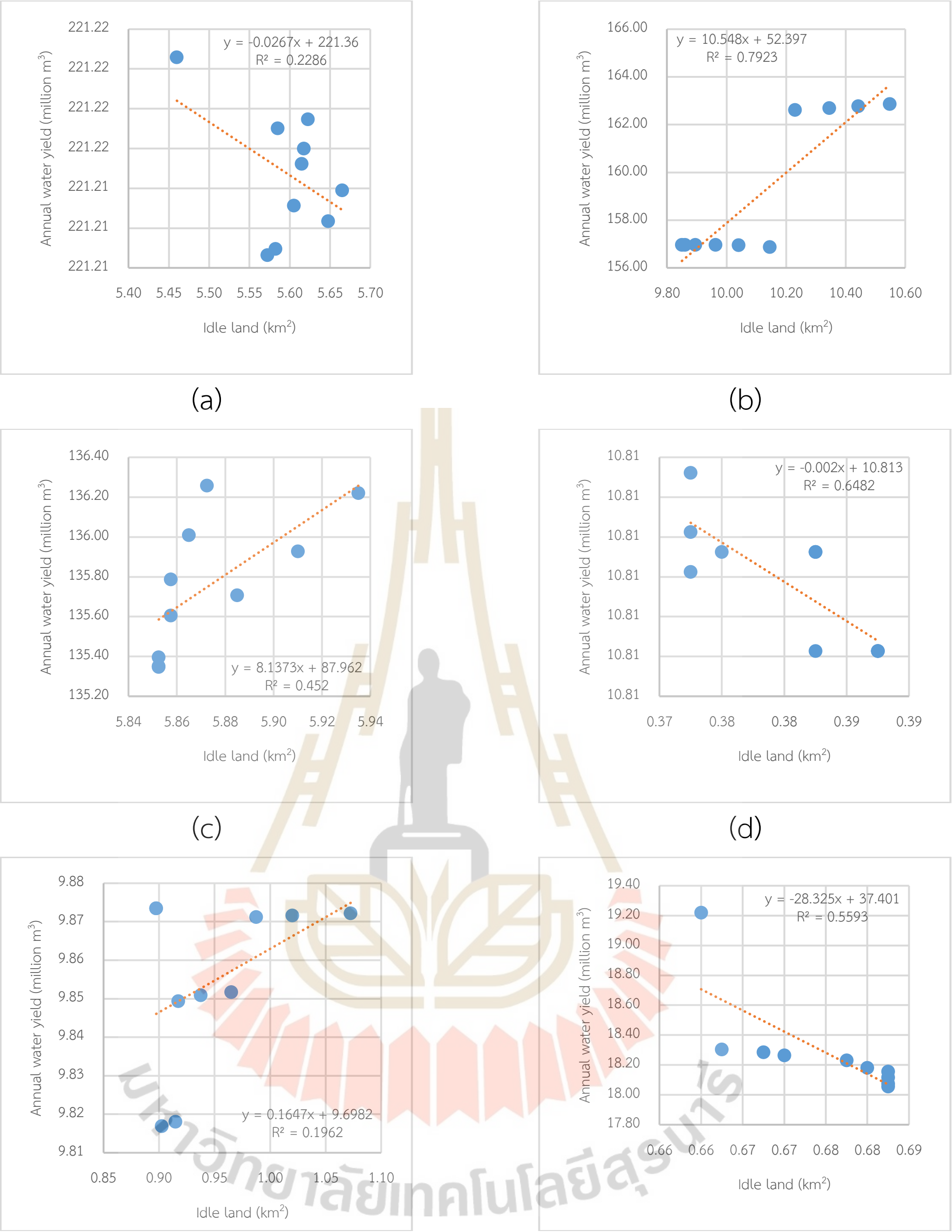

(a) (b)

(c) (d)

(e) (f)

Figure 6.31 Simple linear regression analysis between areas of idle land and water yield data from six watersheds under wet year scenario: (a) Khlong Bang Yai, (b) Khlong Kala, (c) Khlong Tha Rua, (d) Khlong Ban Na Kha, (e) Khlong Chang Phan Lang, and Khlong Ya Yai.

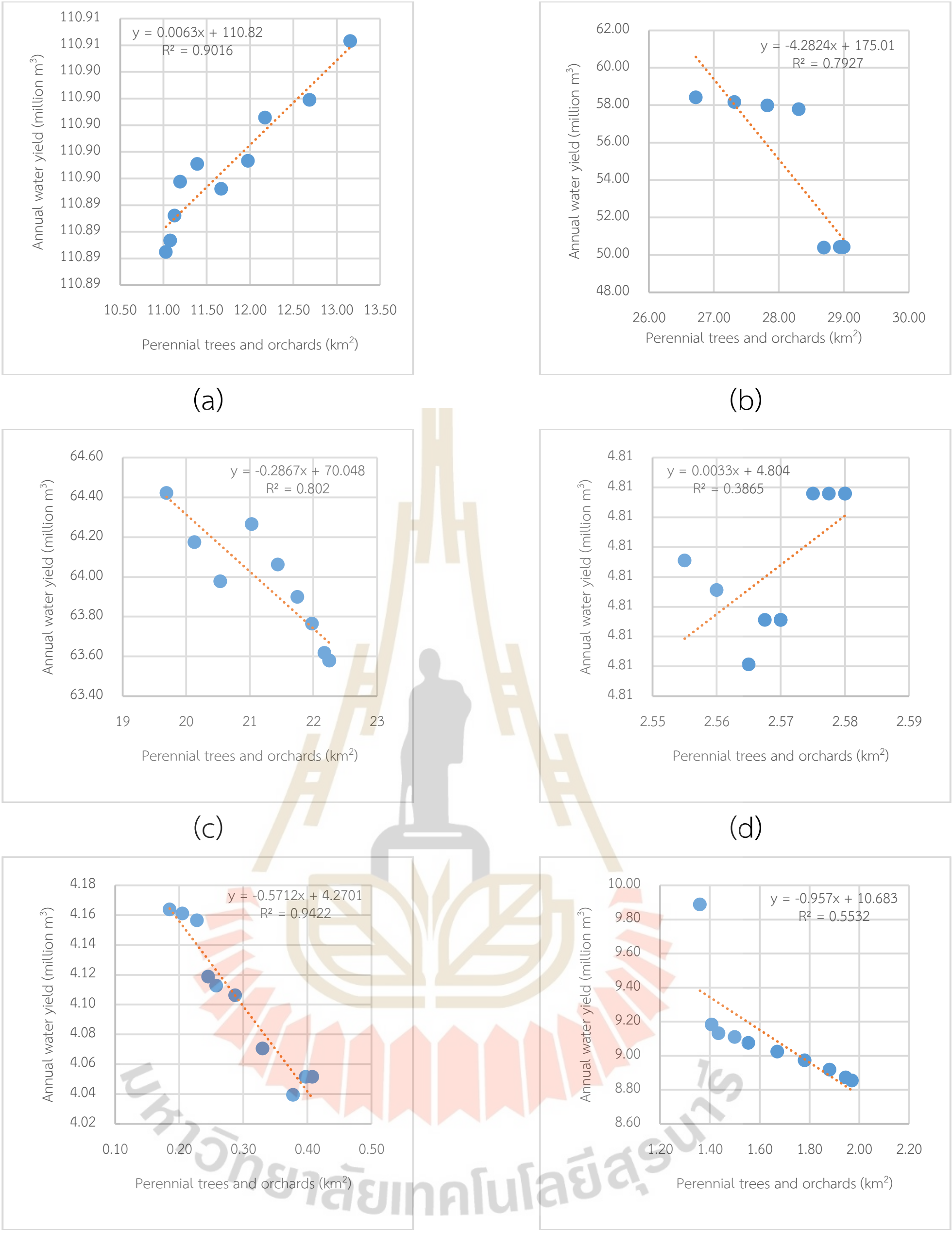

(a) (b)

(c) (d)

(e) (f)

Figure 6.32 Simple linear regression analysis between areas of perennial trees and orchards and water yield data from six watersheds under dry year scenario: (a) Khlong Bang Yai, (b) Khlong Kala, (c) Khlong Tha Rua, (d) Khlong Ban Na Kha, (e) Khlong Chang Phan Lang, and Khlong Ya Yai.

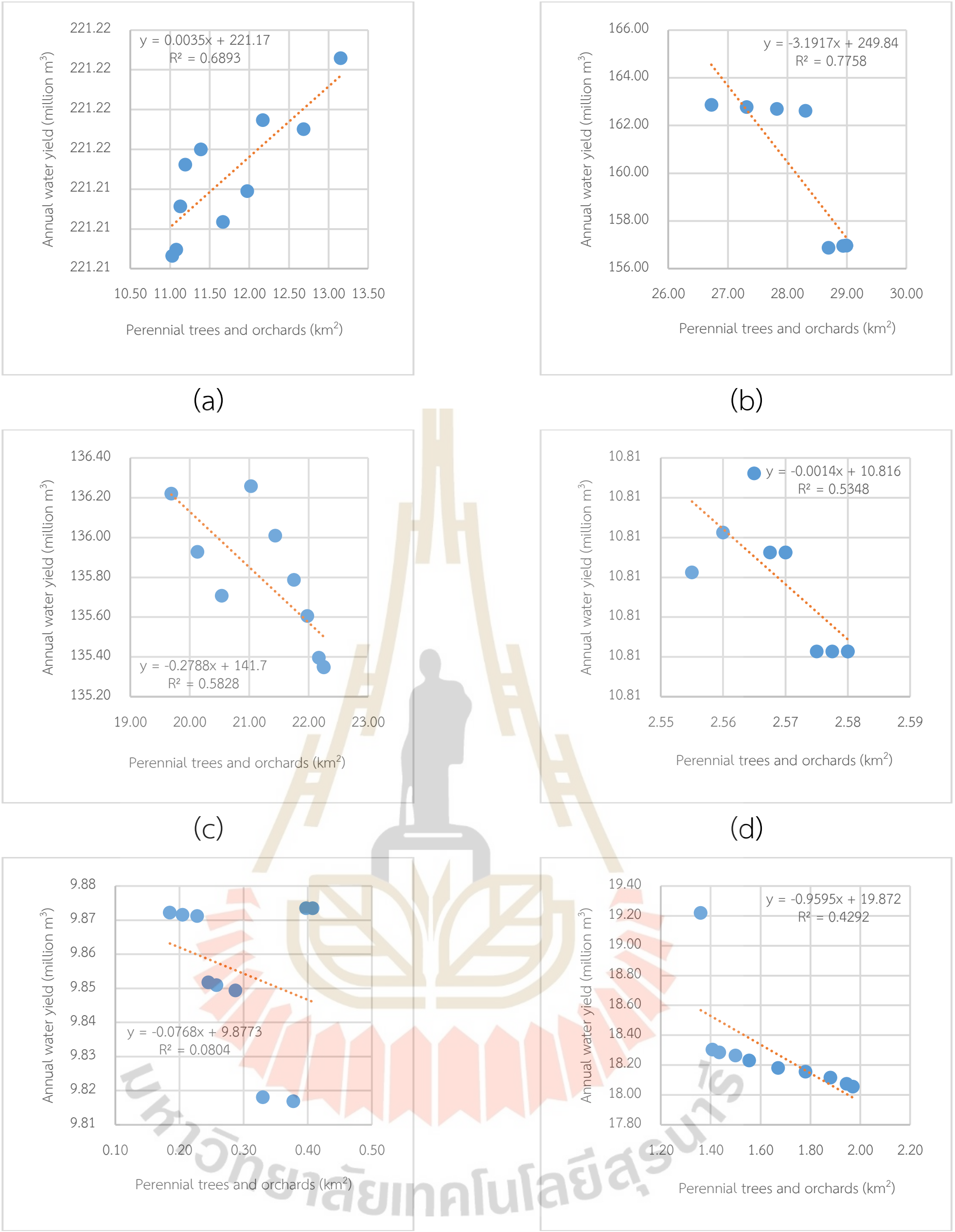

Figure 6.33 Simple linear regression analysis between areas of perennial trees and orchards and water yield data from six watersheds under wet year scenario: (a) Khlong Bang Yai, (b) Khlong Kala, (c) Khlong Tha Rua, (d) Khlong Ban Na Kha, (e) Khlong Chang Phan Lang, and Khlong Ya Yai.

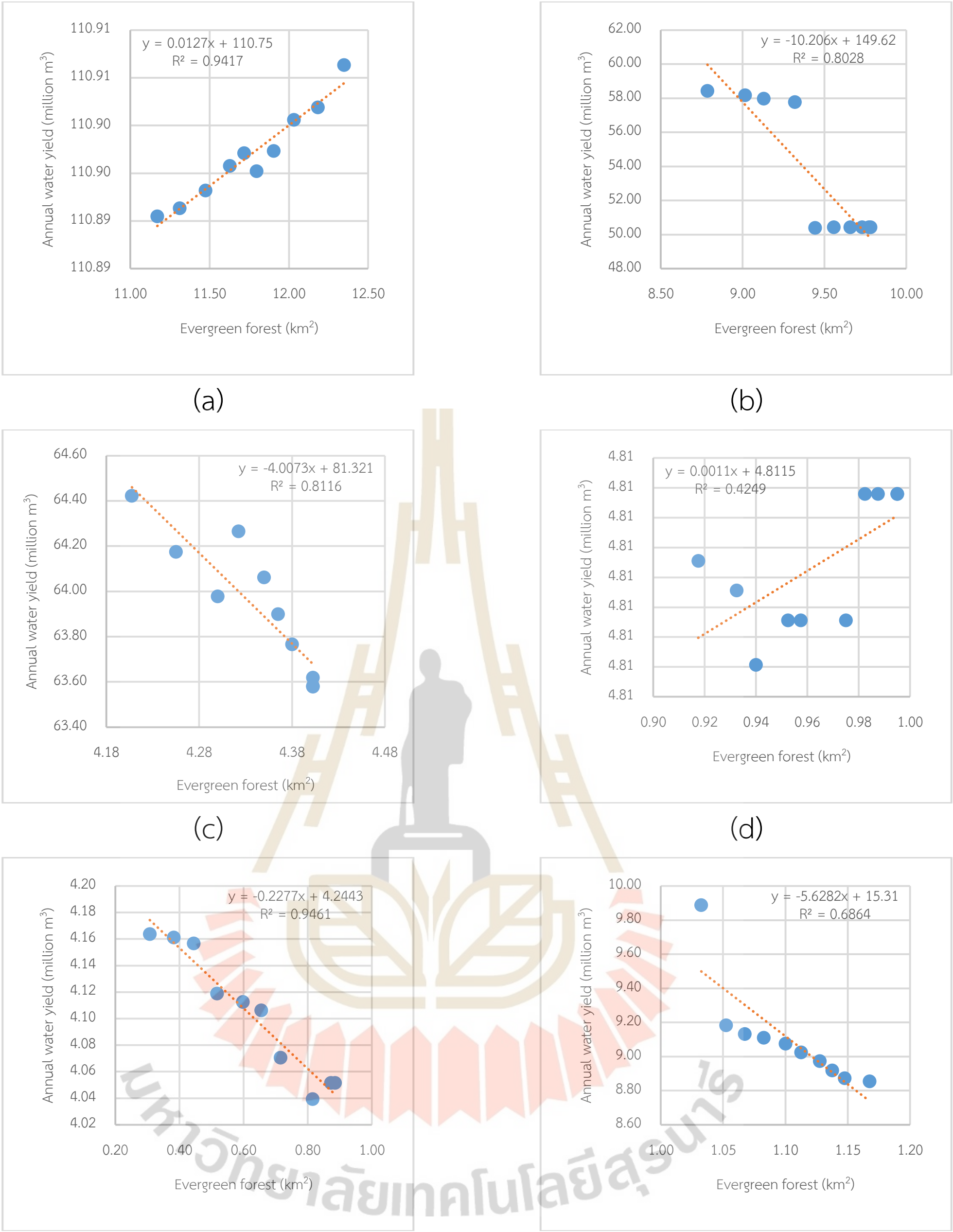

(a) (b)

(c) (d)

(e) (f)

Figure 6.34 Simple linear regression analysis between areas of evergreen forest and water yield data from six watersheds under dry year scenario: (a) Khlong Bang Yai, (b) Khlong Kala, (c) Khlong Tha Rua, (d) Khlong Ban Na Kha, (e) Khlong Chang Phan Lang, and Khlong Ya Yai.

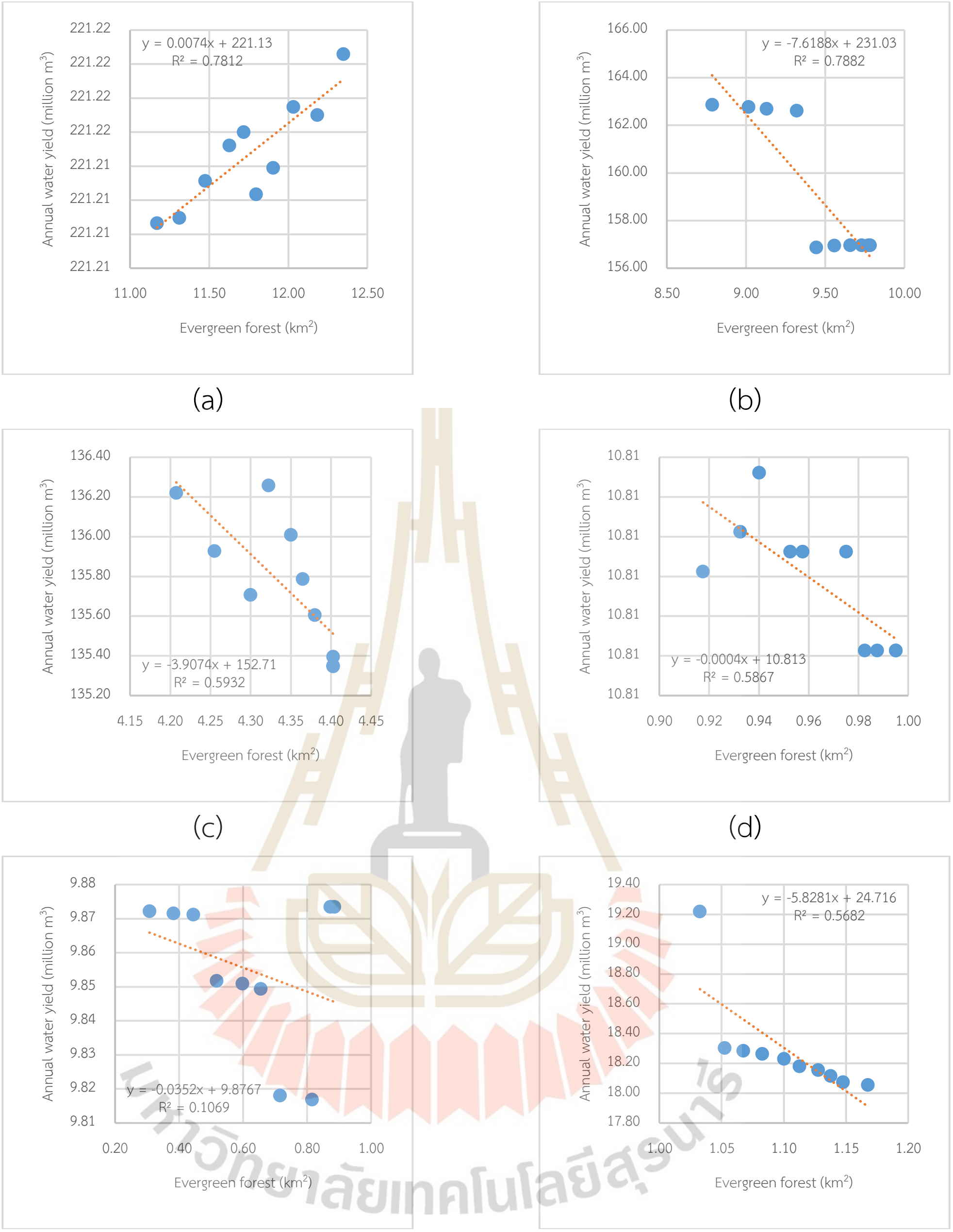

(a) (b)

(c) (d)

(e) (f)

Figure 6.35 Simple linear regression analysis between areas of evergreen forest and water yield data from six watersheds under wet year scenario: (a) Khlong Bang Yai, (b) Khlong Kala, (c) Khlong Tha Rua, (d) Khlong Ban Na Kha, (e) Khlong Chang Phan Lang, and Khlong Ya Yai.

Table 6.28 Summary basic information about the relationship between four LULC types and water yield in six watersheds under dry year scenario.

LULC type	Watershed	Relationship type	R^2
Urban and built-up area	Khlong Bang Yai	Negative	0.9257
	Khlong Kala	Positive	0.8006
	Khlong Tha Rua	Positive	0.8015
	Khlong Ban Na Kha	Negative	0.4785
	Khlong Chang Phan Lang	Positive	0.9374
	Khlong Ya Yai	Positive	0.5546
Idle land	Khlong Bang Yai	Negative	0.2043
	Khlong Kala	Positive	0.8053
	Khlong Tha Rua	Positive	0.6825
	Khlong Ban Na Kha	Positive	0.4740
	Khlong Chang Phan Lang	Positive	0.8123
	Khlong Ya Yai	Negative	0.6610
Perennial trees and orchards	Khlong Bang Yai	Positive	0.9016
	Khlong Kala	Negative	0.7927
	Khlong Tha Rua	Negative	0.8020
	Khlong Ban Na Kha	Positive	0.3865
	Khlong Chang Phan Lang	Negative	0.9422
	Khlong Ya Yai	Negative	0.5532
Evergreen forest	Khlong Bang Yai	Positive	0.9417
	Khlong Kala	Negative	0.8028
	Khlong Tha Rua	Negative	0.8116
	Khlong Ban Na Kha	Positive	0.4249
	Khlong Chang Phan Lang	Negative	0.9461
	Khlong Ya Yai	Negative	0.6864

Table 6.29 Summary basic information about the relationship between four LULC types and water yield in six watersheds under wet year scenario.

LULC type	Watershed	Relationship type	R^2
Urban and built-up area	Khlong Bang Yai	Negative	0.7191
	Khlong Kala	Positive	0.7839
	Khlong Tha Rua	Positive	0.5816
	Khlong Ban Na Kha	Positive	0.6401
	Khlong Chang Phan Lang	Positive	0.0664
	Khlong Ya Yai	Positive	0.4304
Idle land	Khlong Bang Yai	Negative	0.2286
	Khlong Kala	Positive	0.7923
	Khlong Tha Rua	Positive	0.4520
	Khlong Ban Na Kha	Negative	0.6482
	Khlong Chang Phan Lang	Positive	0.1962
	Khlong Ya Yai	Negative	0.5593
Perennial trees and orchards	Khlong Bang Yai	Positive	0.6893
	Khlong Kala	Negative	0.7758
	Khlong Tha Rua	Negative	0.5828
	Khlong Ban Na Kha	Negative	0.5348
	Khlong Chang Phan Lang	Negative	0.0804
	Khlong Ya Yai	Negative	0.4292
Evergreen forest	Khlong Bang Yai	Positive	0.7812
	Khlong Kala	Negative	0.7882
	Khlong Tha Rua	Negative	0.5932
	Khlong Ban Na Kha	Negative	0.5867
	Khlong Chang Phan Lang	Negative	0.1069
	Khlong Ya Yai	Negative	0.5682

As a result in Table 6.28, the linear relationship between urban and built-up area and water yield under dry year scenario at the watershed level is primarily consistent with Phuket Island, except Khlong Bang Yai and Khlong Ban Na Kha. Similarly, the linear relationship between idle land and water yield under the dry year scenario at the watershed level is consistent with Phuket Island, except Khlong Bang Yai and Khlong Ya Yai. At the same time, the linear relationship between perennial trees and orchards and water yield under dry year scenario at the watershed level is mostly the same with Phuket Island, except Khlong Bang Yai and Khlong Ban Na Kha. Likewise, the linear relationship between evergreen forest and water yield under the dry year scenario at the watershed level is primarily consistent with Phuket Island, except Khlong Bang Yai and Khlong Ban Na Kha.

At the same time, the result of a simple linear regression between LULC type and water yield under wet scenario is similar to dry year scenario. As a result in Table 6.29, the linear relationship between urban and built-up area and water yield under the wet year scenario at the watershed level is primarily consistent with Phuket Island, except Khlong Bang Yai. However, the linear relationship between idle land and water yield under the wet year scenario at the watershed level differs from Phuket Island, except Khlong Bang Yai, Khlong Ban Na Kha, and Khlong Ya Yai. Meanwhile, the linear relationship between perennial trees and orchards and water yield under the wet year scenario at the watershed level is mostly consistent with Phuket Island, except Khlong Bang Yai. Likewise, the linear relationship between evergreen forest and water yield under the wet year scenario at the watershed level is primarily consistent with Phuket Island, except Khlong Bang Yai.

These findings reveal that the linear relationship between four LULC types and water yield at a watershed level under dry and wet scenarios is consistent with Phuket Island in three watersheds with large and small areas, including Khlong Kala, Khlong Tha Rua, and Khlong Chang Phan Lang. However, the linear relationship between four LULC types and water yield in the Khlong Bang Yai watershed is inconsistent with Phuket Island. The relationship between urban and built-up area or idle land with water yield is a highly negative correlation with water yield. On the contrary, the relationship between urban and built-up area or idle land with water yield positively correlates with water yield. The possible reason to explain this finding is the effect of a proportional LULC area in the watershed on surface runoff and water yield. Figure 6.36 compares the proportional LULC type area in Phuket Island and Khlong Bang Yai watershed between 2020 and 2029. It can be observed that the average urban and built-up area of the Khlong Bang Yai watershed, about 48.35%, is higher than Phuket Island, about 30.59%. The urban and built-up area of the Khlong Bang Yai watershed leads to a relatively stable water yield since the influence of other LULC changes cannot significantly change water yield in the watershed area.

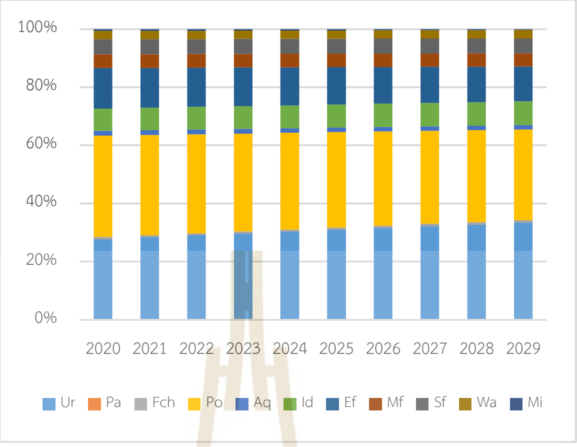

(a)

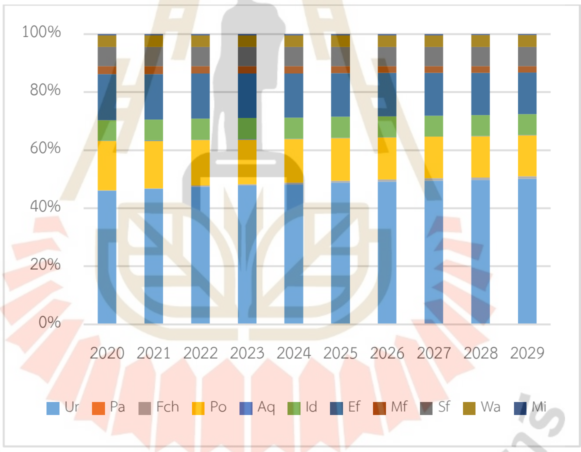

(b)

Figure 6.36 Proportional LULC type area between 2020 and 2029: (a) Phuket Island and (b) Khlong Bang Yai watershed.

The finding from this study is comparable with other studies. Ongsomwang and Kunto (2013) applied the SWAT model to estimate surface runoff and the CA Markov model to predict land use changes for studying the impact of land use change on surface runoff at Huay Tung Lung Watershed of Mun Basin. They found that land use changes that occurred in the watershed area directly affected surface runoff. Ayivi and Jha (2018) applied the SWAT model to estimate water balance and water yield in the Reedy Fork-Buffalo Creek Watershed in North Carolina, USA. They found that the surface runoff and water yield at the watershed outlet were significantly increased by converting forest and grassland to impervious surfaces. Likewise, Hu, Fan, and Zhang (2020) integrated GIS and remote sensing methods with the SCS-CN model to assess the impact of land use change on surface runoff, Beijing, China. They found that the changes in surface runoff were positively correlated with impervious land changes while negatively correlated with woodland, grassland, farmland, and water changes.

Similarly, Puno, Puno, and Talisay (2019) applied the SWAT model to determine the hydrologic responses to land cover and climate change of Muleta watershed, Bukidnon, Philippines. The result showed that urbanization had influenced the increase in surface runoff, evapotranspiration, and baseflow. The increase of forest vegetation resulted in a minimal decrease in baseflow and surface runoff.

In summary, water yield is one of the critical parameters for sustainable water resource management. In this study, the results show that LULC change significantly influences water yield between 2020 and 2029. In particular, the change in the urban and built-up areas, idle land, perennial trees and orchards, and evergreen forest significantly contributed to the change in the water yield in Phuket Island. However, the proportional LULC type area characteristics contribute to the amount of water yield in each watershed. The linear relationship between LULC type and water yield in each watershed should be considered on the water yield of each LULC type; it may behave the better result. Besides, the SWAT model can provide a reasonably estimated water yield (water supply) in two different scenarios of Phuket Island. The results are helpful information relating to the localities and policymakers for sustainable water resources management in the future, mainly to prevent water scarcity.

CHAPTER VII

WATER DEMAND ESTIMATION

This chapter presents the results of the third objective focusing on the water demand estimation based on water footprint. The main results, which consist of (1) baseline information of water demand estimation in 2019, (2) residential water demand between 2020 and 2029, (3) tourist water demand between 2020 and 2029, and (4) water demand for agriculture and forest uses between 2020 and 2029, are described and discussed in the details.

7.1 Baseline information of water demand estimation in 2019

Under this session, baseline information of water demand in 2019 was estimated based on basic data in 2019, including the number of residential population, tourists, and agriculture and forest area under the water consumption rate types and the evapotranspiration coefficient and reference evapotranspiration, respectively.

As a result, the total the number of residential population in 2019 was 572,261 persons. Meanwhile, the number of tourists was 14,576,466 persons. The total agriculture and forest areas were 187.97 km^2 and 125.88 km^2, respectively.

Therefore, the total estimated Phuket Island water demand in 2019 was 474.61 million m^3, including residential water demand (29.84 million m^3), tourist water demand (16.62 million m^3), and water demand for agriculture use (267.19 million m^3) and forest use (160.97 million m^3).

7.2 Residential water demand between 2020 and 2029

Under normal and new normal conditions, residential water demand between 2020 and 2029 was estimated using the water consumption rate in different community characteristics of the Royal Irrigation Department (2011b) (see details in Chapter III).

In practice, the number of registered populations in 2020 was extracted from the DOPA database, Ministry of Interior, while the number of non-registered populations was calculated by subtraction between censused and registered populations. The censused data in the same period were estimated based on historical data between 1980 and 2010 using Trend Analysis under MS Excel software.

The number of people (registered and non-registered populations) between 2021 and 2029 was estimated based on historical data using Trend Analysis with simple linear regression under MS Excel software. The registered population was estimated based on historical data between 2012 and 2020, while censused data were estimated based on historical data between 1980 and 2010.

The registered and non-registered population of Phuket Island between 2020 and 2029 are presented in Tables 7.1 and 7.2. As a result, the total number of registered populations will be increased from 414,471 persons in 2020 to 481,761 persons in 2029 (see Table 7.1). Meanwhile, the number of non-registered populations will be increased from 212,262 persons in 2020 to 249,802 persons in 2029 (see Table 7.2). In this study, the increase of registered populations of Phuket Island between 2020 and 2029 is estimated using a constant growth rate with the coefficient of determination of 0.99, as shown in Figure 7.1. Meanwhile, non-registered populations will be increased by the increase of registered populations in the corresponding year.

The registered and non-registered populations by sub-district and municipality were further combined, as a summary in Table 7.3, to calculate residential water demand in Phuket Island between 2020 and 2029.

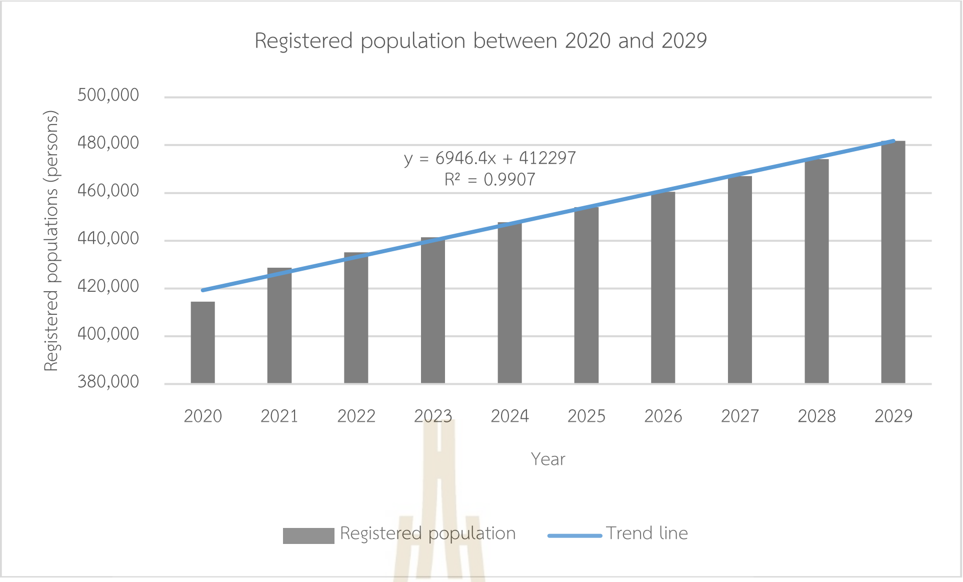

Figure 7.1 The total number of registered populations of Phuket Island between 2020 and 2029.

Table 7.1 Register population by different community characteristics in Phuket Island between 2020 and 2029.

	Number of registered populations by different community characteristics																	
Year	Maikhaow Sub-district	Thepkrasattri Sub-district Municipality	Thepkrasattri Sub-district	Paklok Sub-district Municipality	Sakhu Sub-district	Cherngtalay Sub-district Municipality	Cherngtalay Sub-district	Srisunthon Sub-district Municipality	Kamala Sub-district	Kathu Town Municipality	Patong Town Municipality	Vichit Sub-district Municipality	Phuket City Municipality	Kohkeaw Sub-district	Rasada Sub-district Municipality	Chalong Sub-district Municipality	Rawai Sub-district Municipality	Karon Sub-district Municipality	Total
2020	13,498	9,256	15,899	17,894	6,864	6,870	11,739	26,032	7,037	30,263	20,122	52,283	77,778	16,628	48,696	27,119	18,760	7,733	414,471
2021	13,664	9,589	16,015	18,408	7,098	7,159	11,934	27,748	7,212	32,245	21,210	54,016	79,980	17,299	49,796	28,009	19,375	7,995	428,751
2022	13,801	9,858	16,425	18,881	7,263	7,204	12,012	28,512	7,274	33,038	21,256	55,089	80,005	17,993	50,322	28,621	19,690	7,937	435,180
2023	13,938	10,127	16,851	19,375	7,436	7,233	12,084	29,264	7,330	33,772	21,276	56,150	80,006	18,676	50,813	29,232	20,011	7,872	441,445
2024	14,060	10,412	17,256	19,861	7,592	7,279	12,177	29,978	7,382	34,471	21,315	57,205	80,025	19,358	51,311	29,889	20,335	7,820	447,724
2025	14,186	10,688	17,645	20,351	7,735	7,328	12,272	30,761	7,438	35,144	21,344	58,194	80,100	20,014	51,915	30,532	20,645	7,766	454,056
2026	14,307	10,970	18,023	20,826	7,902	7,385	12,357	31,590	7,496	35,856	21,352	59,195	80,228	20,653	52,477	31,162	20,929	7,713	460,421
2027	14,431	11,245	18,383	21,293	8,056	7,455	12,448	32,458	7,553	36,661	21,385	60,209	80,420	21,273	53,024	31,782	21,268	7,676	467,021
2028	14,568	11,512	18,735	21,765	8,225	7,531	12,538	33,372	7,625	37,538	21,524	61,323	80,766	21,908	53,597	32,401	21,616	7,647	474,191
2029	14,704	11,804	19,118	22,268	8,399	7,604	12,641	34,230	7,699	38,445	21,731	62,490	81,074	22,620	54,220	33,097	21,977	7,641	481,761

Table 7.2 Non-register population by different community characteristics in Phuket Island between 2020 and 2029.

	Number of the non-register population by different community characteristics																	
Year	Maikhaow Sub-district	Thepkrasattri Sub-district Municipality	Thepkrasattri Sub-district	Paklok Sub-district Municipality	Sakhu Sub-district	Cherngtalay Sub-district Municipality	Cherngtalay Sub-district	Srisunthon Sub-district Municipality	Kamala Sub-district	Kathu Town Municipality	Patong Town Municipality	Vichit Sub-district Municipality	Phuket City Municipality	Kohkeaw Sub-district	Rasada Sub-district Municipality	Chalong Sub-district Municipality	Rawai Sub-district Municipality	Karon Sub-district Municipality	Total
2020	6,913	4,740	8,142	9,164	3,515	3,518	6,012	13,332	3,604	15,498	10,305	26,776	39,832	8,516	24,939	13,888	9,607	3,960	212,262
2021	5,870	4,119	6,880	7,908	3,050	3,076	5,127	11,921	3,098	13,853	9,112	23,205	34,360	7,432	21,392	12,033	8,323	3,435	184,193
2022	6,643	4,745	7,906	9,089	3,496	3,468	5,782	13,725	3,501	15,903	10,232	26,518	38,512	8,661	24,224	13,777	9,478	3,821	209,482
2023	6,460	4,694	7,810	8,980	3,446	3,353	5,600	13,563	3,397	15,653	9,861	26,024	37,081	8,656	23,550	13,548	9,275	3,648	204,598
2024	6,906	5,114	8,476	9,756	3,729	3,575	5,982	14,725	3,626	16,932	10,470	28,099	39,308	9,509	25,204	14,681	9,988	3,841	219,923
2025	6,927	5,219	8,616	9,937	3,777	3,578	5,992	15,020	3,632	17,161	10,422	28,416	39,112	9,773	25,350	14,909	10,081	3,792	221,713
2026	7,223	5,538	9,100	10,515	3,990	3,729	6,239	15,949	3,785	18,103	10,780	29,887	40,506	10,428	26,495	15,733	10,567	3,894	232,460
2027	7,323	5,706	9,328	10,805	4,088	3,783	6,316	16,470	3,833	18,603	10,852	30,551	40,807	10,794	26,906	16,127	10,792	3,895	236,978
2028	7,524	5,946	9,677	11,242	4,248	3,890	6,476	17,237	3,938	19,389	11,117	31,673	41,716	11,316	27,683	16,735	11,165	3,950	244,921
2029	7,624	6,121	9,913	11,546	4,355	3,943	6,555	17,749	3,992	19,935	11,268	32,402	42,038	11,729	28,114	17,161	11,395	3,962	249,802

Table 7.3 Residential population by different community characteristics in Phuket Island between 2020 and 2029.

Year	Number of residential populations by different community characteristics																	
	Maikhaow Sub-district	Thepkrasattri Sub-district Municipality	Thepkrasattri Sub-district	Paklok Sub-district Municipality	Sakhu Sub-district	Cherngtalay Sub-district Municipality	Cherngtalay Sub-district	Srisunthon Sub-district Municipality	Kamala Sub-district	Kathu Town Municipality	Patong Town Municipality	Vichit Sub-district Municipality	Phuket City Municipality	Kohkeaw Sub-district	Rasada Sub-district Municipality	Chalong Sub-district Municipality	Rawai Sub-district Municipality	Karon Sub-district Municipality	Total
2020	20,411	13,996	24,041	27,058	10,379	10,388	17,751	39,364	10,641	45,761	30,427	79,059	117,610	25,144	73,635	41,007	28,367	11,693	626,733
2021	19,534	13,708	22,895	26,316	10,148	10,234	17,061	39,669	10,311	46,097	30,322	77,221	114,340	24,730	71,188	40,041	27,698	11,430	612,944
2022	20,445	14,603	24,331	27,969	10,760	10,672	17,794	42,236	10,775	48,941	31,488	81,607	118,517	26,655	74,546	42,399	29,168	11,758	644,662
2023	20,397	14,821	24,661	28,355	10,882	10,586	17,684	42,827	10,727	49,425	31,137	82,173	117,086	27,332	74,363	42,781	29,286	11,520	646,042
2024	20,966	15,526	25,732	29,617	11,321	10,854	18,159	44,703	11,008	51,404	31,785	85,304	119,333	28,867	76,515	44,570	30,323	11,661	667,648
2025	21,113	15,906	26,262	30,288	11,512	10,906	18,264	45,781	11,070	52,304	31,766	86,609	119,212	29,787	77,265	45,441	30,726	11,558	675,770
2026	21,530	16,508	27,123	31,341	11,892	11,114	18,596	47,539	11,281	53,959	32,132	89,081	120,735	31,081	78,973	46,895	31,495	11,608	692,881
2027	21,754	16,951	27,711	32,098	12,144	11,238	18,764	48,928	11,386	55,264	32,237	90,760	121,226	32,067	79,930	47,910	32,060	11,570	703,999
2028	22,092	17,459	28,412	33,007	12,474	11,420	19,014	50,608	11,563	56,927	32,641	92,996	122,482	33,224	81,280	49,137	32,781	11,596	719,113
2029	22,328	17,925	29,031	33,814	12,755	11,547	19,196	51,979	11,691	58,380	32,999	94,892	123,112	34,348	82,334	50,258	33,372	11,602	731,563
2029 in Percent	**3.05**	**2.45**	**3.97**	**4.62**	**1.74**	**1.58**	**2.62**	**7.11**	**1.60**	**7.98**	**4.51**	**12.97**	**16.83**	**4.70**	**11.25**	**6.87**	**4.56**	**1.59**	**100.00**

According to the number of residential populations (registered and non-registered populations) in Table 7.3, the top three highest numbers of populations are Phuket City Municipality, Vichit Sub-district Municipality, and Rasada Sub-district Municipality. They have the number of people of 123,112 persons (16.83%), 94,892 persons (12.97%), and 82,334 persons (11.25%), respectively. Conversely, the top three least number of populations are Cherngtalay Sub-district Municipality, Karon Sub-district Municipality, and Kamala Sub-district. They have the number of people of 11,547 persons (1.58%), 11,603 persons (1.59%), and 11,691 persons (1.60%), respectively.

Phuket Island's annual residential water demand for the registered population between 2020 and 2029 varies from 21.54 million m^3 in 2020 to 24.53 million m^3 in 2029 (Table 7.4). In the meantime, Phuket Island's annual residential water demand for the non-register population between 2020 and 2029 varies from 9.56 million m^3 in 2021 to 12.72 million m^3 in 2029 (Table 7.5). Consequently, Phuket Island's total annual residential water demand between 2020 and 2029 varies from 32.58 million m^3 in 2020 to 37.25 million m^3 in 2029 (Table 7.6). In addition, the spatial distribution of the average annual residential water demand in Phuket Island between 2020 and 2029 is displayed in Figure 7.2.

Table 7.4 Residential water demand for the registered population by different community characteristics between 2020 and 2029.

Year	Residential water demand for the registered population by different community characteristics (million m³)																	
	Maikhaow Sub-district	Thepkrasattri Sub-district Municipality	Thepkrasattri Sub-district	Paklok Sub-district Municipality	Sakhu Sub-district	Cherngtalay Sub-district Municipality	Cherngtalay Sub-district	Srisunthon Sub-district Municipality	Kamala Sub-district	Kathu Town Municipality	Patong Town Municipality	Vichit Sub-district Municipality	Phuket City Municipality	Kohkeaw Sub-district	Rasada Sub-district Municipality	Chalong Sub-district Municipality	Rawai Sub-district Municipality	Karon Sub-district Municipality	Total
2020	0.25	0.41	0.29	0.79	0.13	0.30	0.21	1.14	0.13	2.22	1.47	2.30	7.12	0.30	2.14	1.19	0.82	0.34	21.54
2021	0.25	0.42	0.29	0.81	0.13	0.31	0.22	1.22	0.13	2.35	1.55	2.37	7.30	0.32	2.18	1.23	0.85	0.35	22.26
2022	0.25	0.43	0.30	0.83	0.13	0.32	0.22	1.25	0.13	2.41	1.55	2.41	7.30	0.33	2.20	1.25	0.86	0.35	22.53
2023	0.25	0.44	0.31	0.85	0.14	0.32	0.22	1.28	0.13	2.47	1.55	2.46	7.30	0.34	2.23	1.28	0.88	0.34	22.79
2024	0.26	0.46	0.32	0.87	0.14	0.32	0.22	1.32	0.14	2.52	1.56	2.51	7.32	0.35	2.25	1.31	0.89	0.34	23.11
2025	0.26	0.47	0.32	0.89	0.14	0.32	0.22	1.35	0.14	2.57	1.56	2.55	7.31	0.37	2.27	1.34	0.90	0.34	23.31
2026	0.26	0.48	0.33	0.91	0.14	0.32	0.23	1.38	0.14	2.62	1.56	2.59	7.32	0.38	2.30	1.36	0.92	0.34	23.58
2027	0.26	0.49	0.34	0.93	0.15	0.33	0.23	1.42	0.14	2.68	1.56	2.64	7.34	0.39	2.32	1.39	0.93	0.34	23.87
2028	0.27	0.51	0.34	0.96	0.15	0.33	0.23	1.47	0.14	2.75	1.58	2.69	7.39	0.40	2.35	1.42	0.95	0.34	24.26
2029	0.27	0.52	0.35	0.98	0.15	0.33	0.23	1.50	0.14	2.81	1.59	2.74	7.40	0.41	2.37	1.45	0.96	0.33	24.53
Avg.	**0.26**	**0.46**	**0.32**	**0.88**	**0.14**	**0.32**	**0.22**	**1.33**	**0.14**	**2.54**	**1.55**	**2.53**	**7.31**	**0.36**	**2.26**	**1.32**	**0.90**	**0.34**	**23.18**

Table 7.5 Residential water demand for the non-registered population by different community characteristics between 2020 and 2029.

Year	Residential water demand for the non-registered population by different community characteristics (million m^3)																	
	Maikhaow Sub-district	Thepkrasattri Sub-district Municipality	Thepkrasattri Sub-district	Paklok Sub-district Municipality	Sakhu Sub-district	Cherngtalay Sub-district Municipality	Cherngtalay Sub-district	Srisunthon Sub-district Municipality	Kamala Sub-district	Kathu Town Municipality	Patong Town Municipality	Vichit Sub-district Municipality	Phuket City Municipality	Kohkeaw Sub-district	Rasada Sub-district Municipality	Chalong Sub-district Municipality	Rawai Sub-district Municipality	Karon Sub-district Municipality	Total
2020	0.13	0.21	0.15	0.40	0.06	0.15	0.11	0.59	0.07	1.13	0.75	1.18	3.64	0.16	1.10	0.61	0.42	0.17	11.03
2021	0.11	0.18	0.13	0.35	0.06	0.13	0.09	0.52	0.06	1.01	0.67	1.02	3.14	0.14	0.94	0.53	0.36	0.15	9.56
2022	0.12	0.21	0.14	0.40	0.06	0.15	0.11	0.60	0.06	1.16	0.75	1.16	3.51	0.16	1.06	0.60	0.42	0.17	10.85
2023	0.12	0.21	0.14	0.39	0.06	0.15	0.10	0.59	0.06	1.14	0.72	1.14	3.38	0.16	1.03	0.59	0.41	0.16	10.56
2024	0.13	0.22	0.16	0.43	0.07	0.16	0.11	0.65	0.07	1.24	0.77	1.23	3.60	0.17	1.11	0.64	0.44	0.17	11.35
2025	0.13	0.23	0.16	0.44	0.07	0.16	0.11	0.66	0.07	1.25	0.76	1.24	3.57	0.18	1.11	0.65	0.44	0.17	11.38
2026	0.13	0.24	0.17	0.46	0.07	0.16	0.11	0.70	0.07	1.32	0.79	1.31	3.70	0.19	1.16	0.69	0.46	0.17	11.91
2027	0.13	0.25	0.17	0.47	0.07	0.17	0.12	0.72	0.07	1.36	0.79	1.34	3.72	0.20	1.18	0.71	0.47	0.17	12.11
2028	0.14	0.26	0.18	0.49	0.08	0.17	0.12	0.76	0.07	1.42	0.81	1.39	3.82	0.21	1.22	0.74	0.49	0.17	12.53
2029	0.14	0.27	0.18	0.51	0.08	0.17	0.12	0.78	0.07	1.46	0.82	1.42	3.84	0.21	1.23	0.75	0.50	0.17	12.72
Avg.	**0.13**	**0.23**	**0.16**	**0.43**	**0.07**	**0.16**	**0.11**	**0.66**	**0.07**	**1.25**	**0.76**	**1.24**	**3.59**	**0.18**	**1.11**	**0.65**	**0.44**	**0.17**	**11.40**

Table 7.6 Total residential water demand by different community characteristics between 2020 and 2029.

	Residential water demand by different community characteristics (million m^3)																		
Year	Maikhaow Sub-district	Thepkrasattri Sub-district Municipality	Thepkrasattri Sub-district	Paklok Sub-district Municipality	Sakhu Sub-district	Cherngtalay Sub-district Municipality	Cherngtalay Sub-district	Srisunthon Sub-district Municipality	Kamala Sub-district	Kathu Town Municipality	Patong Town Municipality	Vichit Sub-district Municipality	Phuket City Municipality	Kohkeaw Sub-district	Rasada Sub-district Municipality	Chalong Sub-district Municipality	Rawai Sub-district Municipality	Karon Sub-district Municipality	Total
2020	0.37	0.61	0.44	1.19	0.19	0.46	0.32	1.73	0.19	3.35	2.23	3.47	10.76	0.46	3.23	1.80	1.25	0.51	32.58
2021	0.36	0.60	0.42	1.15	0.19	0.45	0.31	1.74	0.19	3.37	2.21	3.38	10.43	0.45	3.12	1.75	1.21	0.50	31.83
2022	0.37	0.64	0.44	1.23	0.20	0.47	0.32	1.85	0.20	3.57	2.30	3.57	10.81	0.49	3.27	1.86	1.28	0.51	33.38
2023	0.37	0.65	0.45	1.24	0.20	0.46	0.32	1.88	0.20	3.61	2.27	3.60	10.68	0.50	3.26	1.87	1.28	0.50	33.35
2024	0.38	0.68	0.47	1.30	0.21	0.48	0.33	1.96	0.20	3.76	2.33	3.75	10.92	0.53	3.36	1.96	1.33	0.51	34.46
2025	0.39	0.70	0.48	1.33	0.21	0.48	0.33	2.01	0.20	3.82	2.32	3.79	10.88	0.54	3.38	1.99	1.35	0.51	34.70
2026	0.39	0.72	0.49	1.37	0.22	0.49	0.34	2.08	0.21	3.94	2.35	3.90	11.02	0.57	3.46	2.05	1.38	0.51	35.49
2027	0.40	0.74	0.51	1.41	0.22	0.49	0.34	2.14	0.21	4.03	2.35	3.98	11.06	0.59	3.50	2.10	1.40	0.51	35.98
2028	0.40	0.77	0.52	1.45	0.23	0.50	0.35	2.22	0.21	4.17	2.39	4.08	11.21	0.61	3.57	2.16	1.44	0.51	36.79
2029	0.41	0.79	0.53	1.48	0.23	0.51	0.35	2.28	0.21	4.26	2.41	4.16	11.23	0.63	3.61	2.20	1.46	0.51	37.25
Avg.	**0.38**	**0.69**	**0.48**	**1.31**	**0.21**	**0.48**	**0.33**	**1.99**	**0.20**	**3.79**	**2.32**	**3.77**	**10.90**	**0.54**	**3.38**	**1.97**	**1.34**	**0.51**	**34.58**

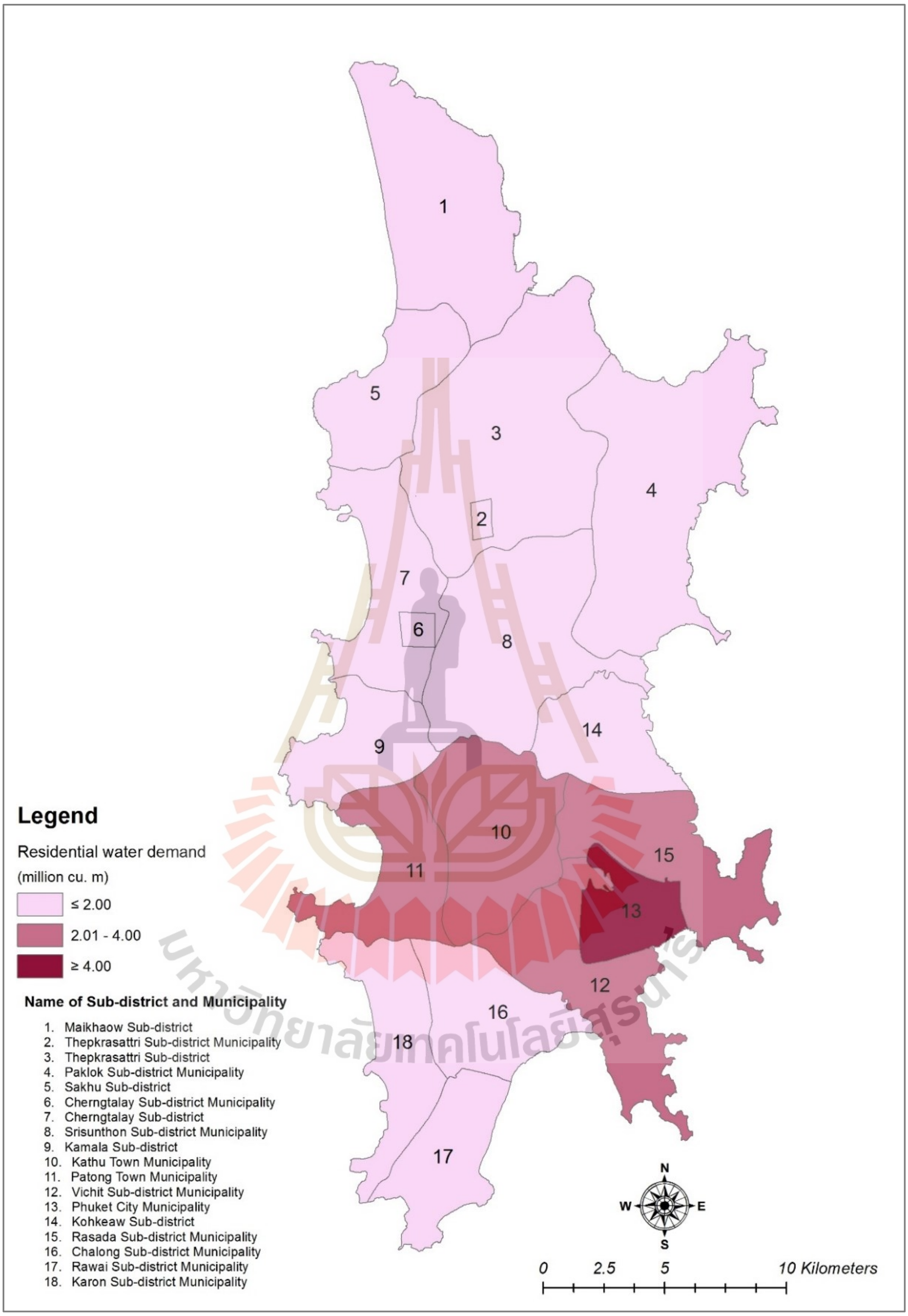
1
5
3
2
4
7
6
8
14
9
10
15
11
13
12
16
18
17
Legend
Residential water demand
(million cu. m)
≤ 2.00
2.01 - 4.00
≥ 4.00
Name of Sub-district and Municipality
1. Maikhaow Sub-district
2. Thepkrasattri Sub-district Municipality
3. Thepkrasattri Sub-district
4. Paklok Sub-district Municipality
5. Sakhu Sub-district
6. Cherngtalay Sub-district Municipality
7. Cherngtalay Sub-district
8. Srisunthon Sub-district Municipality
9. Kamala Sub-district
10. Kathu Town Municipality
11. Patong Town Municipality
12. Vichit Sub-district Municipality
13. Phuket City Municipality
14. Kohkeaw Sub-district
15. Rasada Sub-district Municipality
16. Chalong Sub-district Municipality
17. Rawai Sub-district Municipality
18. Karon Sub-district Municipality
N
W
E
S
0
2.5
5
10 Kilometers

Figure 7.2 The spatial distribution of Phuket Island’s average annual residential water demand between 2020 and 2029.

Meanwhile, the top three most dominant areas by average total residential water demands between 2020 and 2029 (Figure 7.3) are Phuket City Municipality, with average residential water demand of 10.90 million m^3, flowing by Kathu Town Municipality and Vichit Sub-district Municipality of 3.79 million m^3 and 3.77 million m^3, respectively. The top three least dominant areas by average total residential water demands between 2020 and 2029 (Figure 7.3) are Kamala Sub-district, with an average residential water demand of 0.20 million m^3, flowing by Sakhu Sub-district and Cherngtalay Sub-district of 0.21 million m^3 and 0.33 million m^3, respectively.

As a result, Phuket Island's average annual residential water demand between 2020 and 2029 is continuously increasing. Notably, residential water demand in urban areas is higher than in rural areas of Phuket Island. This finding indicates the different growth rates of the population and consumption patterns in urban and rural areas of Phuket Island, as suggested by Boretti and Rosa (2019). They found that increasing water demand follows population growth, economic development, and changing consumption patterns.

Furthermore, the finding from this study is comparable with other studies. For instance, Wijitkosum and Sriburi (2008) studied the urban expansion of Nakhon Ratchasima City, the regional center of Northeastern Thailand, in water demand and water usage in the Lam Ta Kong Watershed. The results found that urbanization affects the water usage pattern and the high living standard of the people continuously increases the water consumption rate. Likewise, Liu, Zhao, Cai, Wang, and Lu (2019) integrated weight methods to evaluate urban and rural water poverty in Northwest China. The results showed that urban areas characterized by rapid economic growth display accelerated improvement in water poverty.

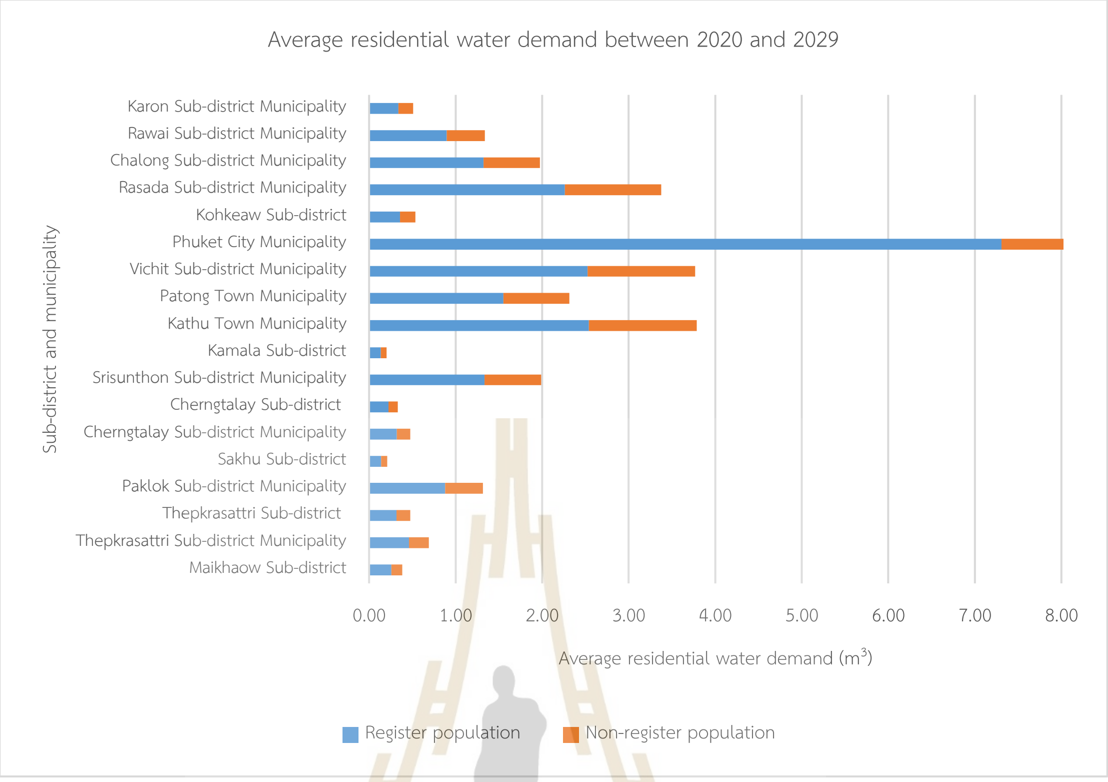

Figure 7.3 Average annual residential water demand between 2020 and 2029 in different community characteristics.

Therefore, understanding the current status and future trend of residential water demand and consumption patterns base on driving factors (population growth, economic development, high living standards, and climate change). However, the consumption rate in different community characteristics is a limitation in this study. Only the City municipality consumption rate was confirmed with information of Phuket City municipality during November and December in 2019. Future research should study the consumption rate in different community characteristics, and the result will give high authenticity and efficiency.

7.3 Tourist water demand between 2020 and 2029

Under this session, the tourist water demand between 2020 and 2029 was estimated based on the modified water consumption rate of Pansawad (1997) and the Department of Public Works and Town and Country Planning (1993), as cited in Royal Irrigation Department (2011b); Srichai et al. (2016) (see details in Chapter III).

At the same time, the number of tourists under normal conditions between 2010 and 2019 were extracted from the TAT Intelligence Center database, Tourism Authority of Thailand and the Economics Tourism and Sports Division, Ministry of Tourism and Sports. Likewise, the number of tourists between 2020 and 2029 was estimated using Trend Analysis based on historical data between 2010 and 2019 using MS Excel software. In contrast, the number of tourists under new normal conditions (COVID-19 pandemic) was adopted from the projected tourists in the future by the Economics Tourism and Sports Division, Ministry of Tourism and Sports (2020), according to historical data and projected data, in 2019 and 2020, respectively. In this condition, three future tourist scenarios were presented with 45%, 65%, and 85% of tourists in 2019 for 2021, 2022, and 2023 respectively. In the meantime, the number of tourists between 2024 and 2029 was used the same data as normal conditions.

Finally, tourist water demand between 2020 and 2029 under normal and new normal conditions were estimated based on the modified water consumption rate with an average length of stay (day) by four days (The average between 2015 and 2019) (TAT Intelligence Center, Tourism Authority of Thailand, 2019).

As a result, the number of tourists under normal conditions between 2020 and 2029 varies from 16,534,377 persons in 2020 to 21,671,107 persons in 2029, with an average tourist of 18,828,364 persons per year (Figure 7.4 and Table 7.7). At the same time, tourist water demand under normal conditions continuously increases from 18,861,284 m^3 in 2020 to 24,757,427 m^3 in 2029, with an average tourist water demand of 21,493,892 m^3 (Figure 7.5 and Table 7.7).

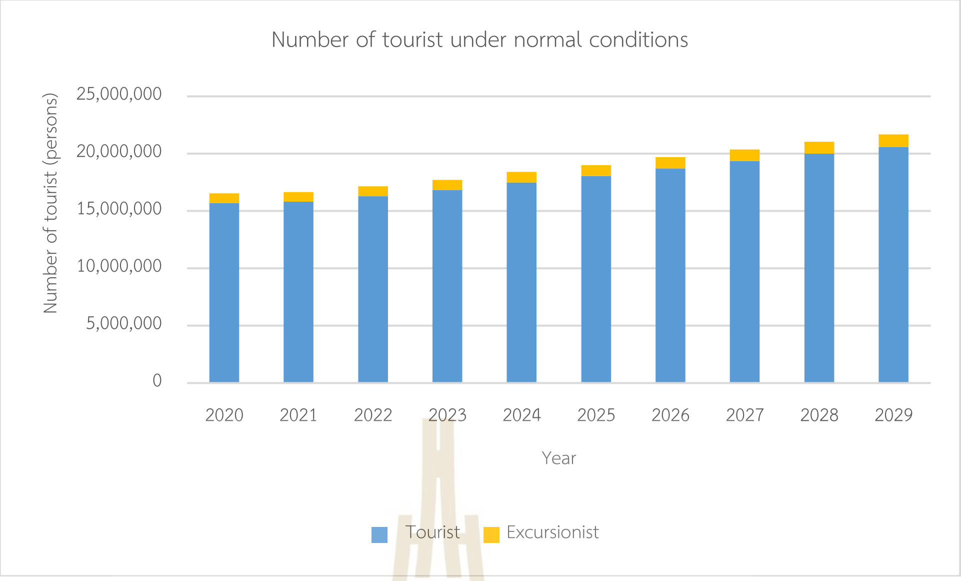

Figure 7.4 Number of tourists between 2020 and 2029 under normal conditions.

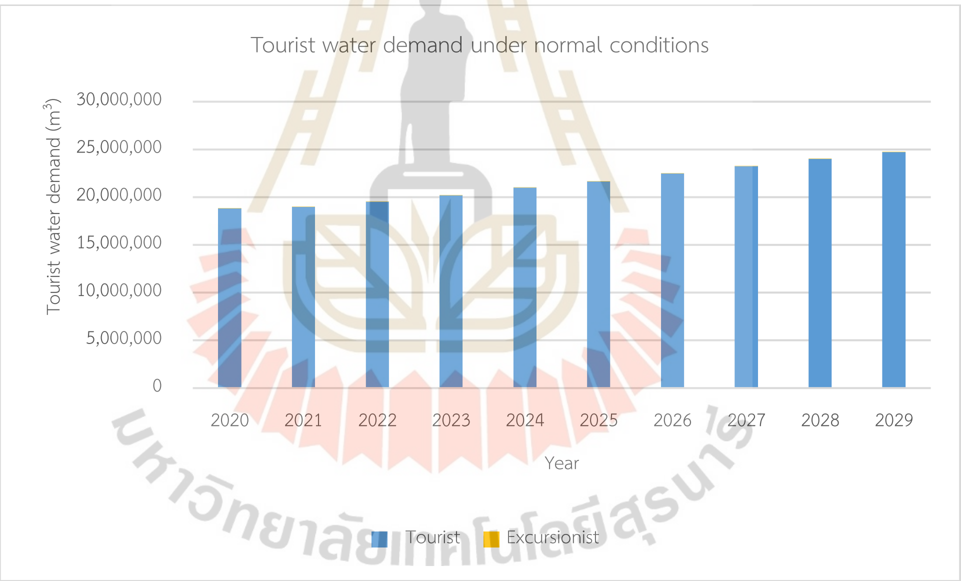

Figure 7.5 Tourist water demand between 2020 and 2029 under normal conditions.

Table 7.7 Tourist water demand between 2020 and 2029 under normal conditions.

Year	Number of tourists (persons)			Tourist water demand (m^3)		
	Tourist	Excursionist	Total	Tourist	Excursionist	Total
2020	15,696,798	837,580	16,534,377	18,836,157	25,127	18,861,284
2021	15,817,031	839,472	16,656,503	18,980,437	25,184	19,005,621
2022	16,285,696	869,848	17,155,544	19,542,835	26,095	19,568,931
2023	16,832,320	895,237	17,727,557	20,198,784	26,857	20,225,641
2024	17,493,473	922,615	18,416,087	20,992,167	27,678	21,019,845
2025	18,045,498	949,648	18,995,145	21,654,597	28,489	21,683,087
2026	18,728,566	978,676	19,707,243	22,474,279	29,360	22,503,640
2027	19,366,852	1,006,502	20,373,354	23,240,222	30,195	23,270,418
2028	20,009,937	1,036,790	21,046,726	24,011,924	31,104	24,043,028
2029	20,604,525	1,066,583	21,671,107	24,725,430	31,997	24,757,427
Average	**17,888,069**	**940,295**	**18,828,364**	**21,465,683**	**28,209**	**21,493,892**

Note: Tourist water demand was calculated based on an average length of stay (day) by four days (the average between 2015 and 2019) from the TAT Intelligence Center, Tourism Authority of Thailand (2019).

On the contrary, the number of tourists under new normal conditions between 2020 and 2029 varies from 4,003,290 persons in 2020 to 21,671,107 persons in 2029, with an average tourist of 15,263,706 persons per year (Figure 7.6 and Table 7.8.). Under new normal conditions in the same period, the tourist water demand varies from 4,524,179 m^3 to 24,757,427 m^3, with an average tourist water demand of 17,417,294 m^3 (Figure 7.7 and Table 7.8). Under new normal conditions, the tourist water demand is dropped in 2020 and 2023 due to the COVID-19 pandemic, but it will increase from 2024 to 2029 when the COVID-19 pandemic can be controlled back to normal conditions.

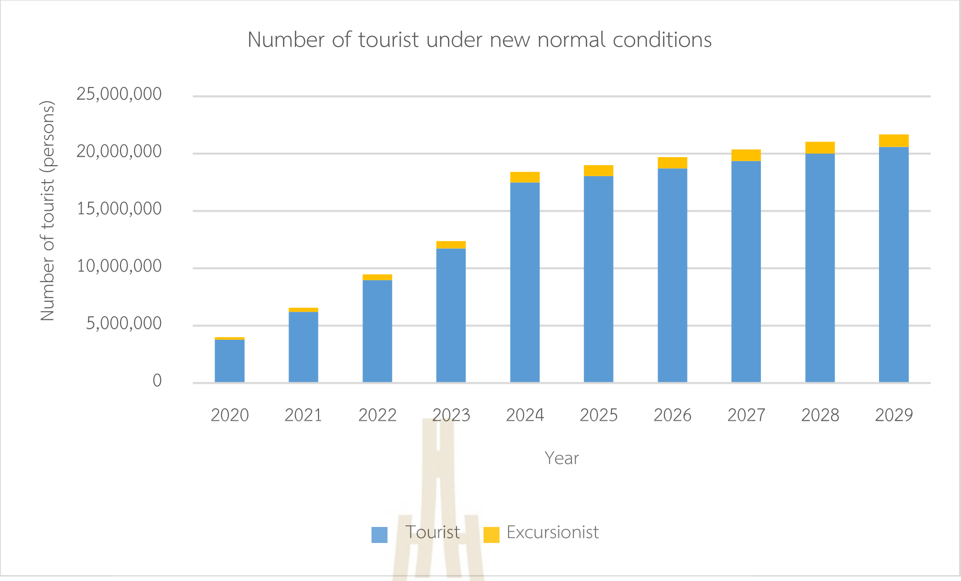

Figure 7.6 Number of tourists between 2020 and 2029 under new normal conditions.

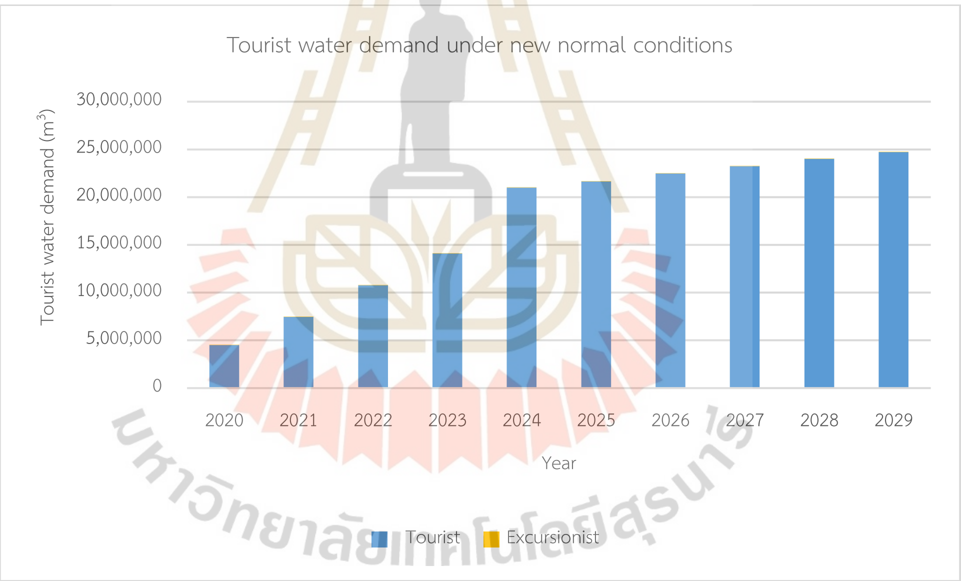

Figure 7.7 Tourist water demand between 2020 and 2029 under new normal conditions.

Table 7.8 Tourist water demand between 2020 and 2029 under new normal conditions.

Year	Number of tourists (persons)			Tourist water demand (m^3)		
	Tourist	Excursionist	Total	Tourist	Excursionist	Total
2020	3,764,171	239,119	4,003,290	4,517,005	7,174	4,524,179
2021	6,216,685	342,725	6,559,410	7,460,022	10,282	7,470,303
2022	8,979,656	495,047	9,474,703	10,775,587	14,851	10,790,438
2023	11,742,627	647,370	12,389,996	14,091,152	19,421	14,110,573
2024	17,493,473	922,615	18,416,087	20,992,167	27,678	21,019,845
2025	18,045,498	949,648	18,995,145	21,654,597	28,489	21,683,087
2026	18,728,566	978,676	19,707,243	22,474,279	29,360	22,503,640
2027	19,366,852	1,006,502	20,373,354	23,240,222	30,195	23,270,418
2028	20,009,937	1,036,790	21,046,726	24,011,924	31,104	24,043,028
2029	20,604,525	1,066,583	21,671,107	24,725,430	31,997	24,757,427
Average	**14,495,199**	**768,507**	**15,263,706**	**17,394,239**	**23,055**	**17,417,294**

Note: Tourist water demand was calculated based on an average length of stay (day) by four days (the average between 2015 and 2019) from the TAT Intelligence Center, Tourism Authority of Thailand (2019).

In addition, even though the number of tourists contributes significantly to their economic growth, tourist increase has been among the leading causes of environmental degradation, particularly the facilities construction to support tourism (Reyes Perez, 2017). The relationship between tourism growth and urban expansion in Phuket Island is interesting to discuss in this session. Thus, simple linear regression analysis was applied to examine the relationship between tourism growth and urban expansion in Phuket Island under normal and new normal conditions based on the derived data between 2020 and 2029 from the current study (displayed in Figures 7.8 and 7.9).

As a result, tourism growth under normal conditions shows a positive correlation to urban expansion in Phuket Island (Figure 7.8), with a strong coefficient of determination of 0.99. In the meantime, tourism growth under new normal conditions also positively correlates to urban expansion in Phuket Island (Figure 7.9), with a strong coefficient of determination of 0.89. These findings are in line with

Rempis, Alexandrakis, and Kampanis (2018) stated that urbanization has driven either anthropogenic, such as population growth, or from the economic geography factors contributing to expanding the extensive and intensive settlement.

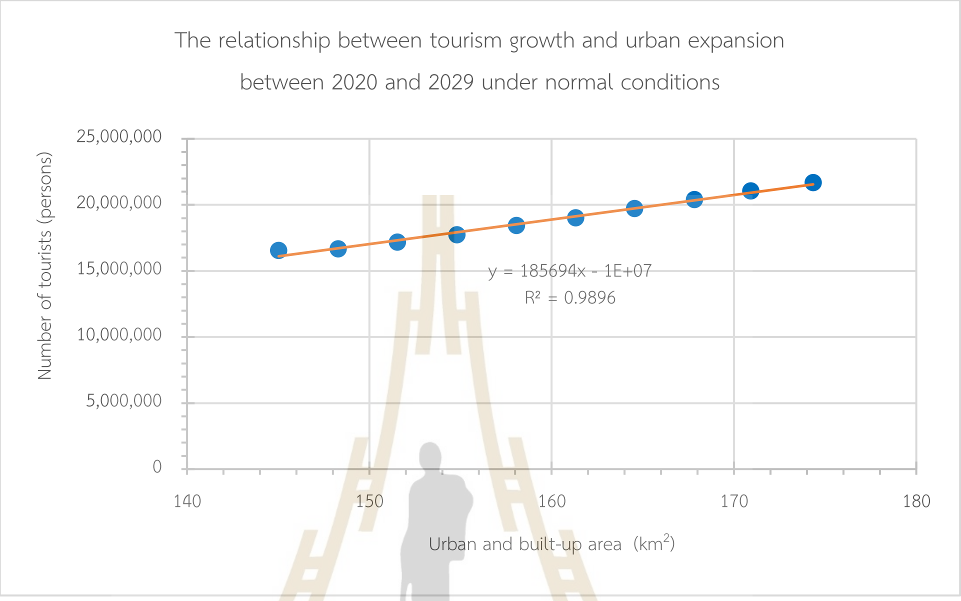

Figure 7.8 The relationship between tourism growth and urban expansion in Phuket Island between 2020 and 2029 under normal conditions.

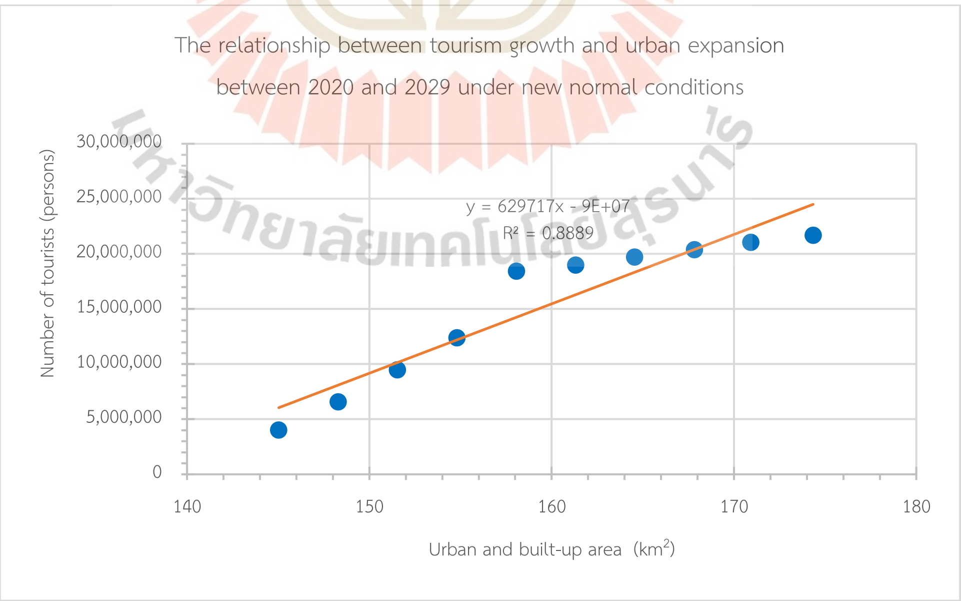

Figure 7.9 The relationship between tourism growth and urban expansion in Phuket Island between 2020 and 2029 under new normal conditions.

Moreover, the increase in tourists led to the high resource demand of Phuket Island. Notably, water resource is a primary factor in the daily life of many activities. A small island like Phuket Island has limited water supply storage during summer seasons, while water demand is high due to the high season for tourism in Phuket Island. These findings agree with the studies of Tokarchuk, Gabriele, and Maurer (2017). They found that the increasing tourists' flows affect local economies and the lives of residents, the development of tourist facilities such as the construction of large hotels, huge recreational and commercial areas. The construction led to the degradation of natural resources. For example, the littering of waste resulted from the tourist traffic and water resources decreased by over demand, etc. (Troanca, 2012).

Recently, Phuket Island has been developed to support many initiated projects such as Phuket Island to world-class tourism destination, Smart city, and MICE city, infrastructures (Phuket airport expansion, light rail transit, and underpass), international schools, medical hub, international exhibition and conference center, and shopping malls, etc. (Information Technology and Communication Division, Phuket Provincial Office, 2016). As a result, the incoming development led to expected LULC change and tourism growth shortly.

Consequently, sustainable tourism in Phuket Island is a daunting challenge in the future. This study provides essential information to support decision-makers, policymakers, and planners for the sustainable use of natural resources to balance local people's use and tourism activity in Phuket Island.

7.4 Water demand for agriculture and forest uses between 2020 and 2029

Under this session, the water demand for agriculture and forest uses was estimated based on the evapotranspiration coefficient and reference evapotranspiration (Allen et al., 1998). In practice, the water demand for agriculture and forest from 2020 to 2029 was calculated based on the area of each agriculture and forest type, evapotranspiration coefficient, and reference evapotranspiration under the Penman-Monteith method from the Royal Irrigation Department (2011a) (see details in Chapter III).

The area of each agriculture and forest type between 2020 and 2029 was summarized in Table 7.9. The total agriculture area was decreased from 185.76 km^2 in 2020 to 167.57 km^2 in 2029, with an average area of 176.67 km^2, while the total forest area was decreased from 124.49 km^2 in 2020 to 113.00 km^2 in 2029, with an average area of 118.78 km^2.

Table 7.9 Area of each agriculture and forest type between 2020 and 2029.

Year	Area of agriculture type (km^2)				Area of forest type (km^2)			
	Field crop	Paddy field	Para rubber trees	Agriculture total	Evergreen forest	Mangrove forest	Scrub forest	Forest total
2020	3.47	0.13	182.16	185.76	72.96	24.68	26.85	124.49
2021	3.52	0.13	180.01	183.66	71.79	24.66	26.84	123.29
2022	3.82	0.10	177.87	181.79	70.62	24.44	26.81	121.87
2023	3.76	0.09	175.74	179.59	69.47	24.44	26.79	120.70
2024	3.99	0.07	173.55	177.61	68.27	24.44	26.74	119.45
2025	4.19	0.06	171.46	175.71	67.15	24.19	26.76	118.10
2026	4.30	0.05	169.35	173.70	65.98	24.10	26.75	116.83
2027	4.44	0.03	167.20	171.67	64.83	24.01	26.74	115.58
2028	4.39	0.02	165.21	169.62	63.71	24.01	26.77	114.49
2029	4.67	0.00	162.90	167.57	62.49	23.82	26.69	113.00
Average	**4.06**	**0.07**	**172.55**	**176.67**	**67.73**	**24.28**	**26.77**	**118.78**

The water demand for agriculture and forest uses from 2020 to 2029 is reported in Tables 7.10 and 7.11. As a result, the water demand for agriculture use in this period will decrease from 264.84 million m^3 in 2020 to 237.35 million m^3 in 2029. The average water demand for agriculture use is 250.93 million m^3 (Table 7.10). Meanwhile, the water demand for forest use in the same period will decrease from 159.58 million m^3 in 2020 to 142.74 million m^3 in 2029. The average water demand for forest use is 151.10 million m^3 (Table 7.11).

Moreover, the monthly water demand for agriculture use between 2020 and 2029 is presented in Table 7.10. As a result, the average water demand for agriculture use from the calculated period in the summer season (December to March) varies from the lowest value of 20.35 million m^3 in December to the highest value of 24.77 million m^3 in March. Meanwhile, the average water demand for agriculture use from the calculated period in the rainy season (April to November) varies from the lowest value of 18.23 million m^3 in October to the highest value of 22.84 million m^3 in April (Figure 7.10).

Meanwhile, the monthly water demand for forest use between 2020 and 2029 is presented in Table 7.11. As a result, the average water demand for forest use from the calculated period in the summer season (December to March) varies from the lowest value of 12.25 million m^3 in December to the highest value of 14.92 million m^3 in March. Meanwhile, the average water demand for forest use from the calculated period in the rainy season (April to November) varies from the lowest value of 10.98 million m^3 in October to the highest value of 13.75 million m^3 in April (Figure 7.11).

Table 7.10 Water demand for agriculture use between 2020 and 2029.

Year	Water demand for agriculture use between 2020 and 2029 (million m^3)												
	Jan	Feb	Mar	Apr	May	Jun	Jul	Aug	Sep	Oct	Nov	Dec	Total
2020	23.80	24.03	26.08	24.05	22.20	21.40	22.00	22.17	19.22	19.20	19.27	21.43	264.84
2021	23.52	22.93	25.78	23.78	21.94	21.15	21.75	21.92	18.99	18.98	19.05	21.18	260.98
2022	23.27	22.68	25.50	23.52	21.71	20.92	21.51	21.68	18.79	18.77	18.84	20.95	258.14
2023	22.99	22.41	25.20	23.24	21.44	20.67	21.25	21.42	18.56	18.55	18.62	20.70	255.03
2024	22.72	22.94	24.90	22.97	21.19	20.43	21.00	21.17	18.35	18.33	18.40	20.46	252.87
2025	22.47	21.90	24.63	22.71	20.96	20.20	20.77	20.93	18.14	18.12	18.19	20.23	249.25
2026	22.20	21.64	24.33	22.44	20.71	19.96	20.52	20.68	17.93	17.91	17.98	19.99	246.31
2027	21.93	21.38	24.04	22.17	20.46	19.72	20.28	20.43	17.71	17.69	17.76	19.75	243.33
2028	21.67	21.88	23.75	21.91	20.22	19.49	20.03	20.19	17.50	17.48	17.55	19.51	241.19
2029	21.39	20.86	23.45	21.62	19.96	19.24	19.78	19.93	17.27	17.26	17.32	19.26	237.35
Average	**22.60**	**22.27**	**24.77**	**22.84**	**21.08**	**20.32**	**20.89**	**21.05**	**18.25**	**18.23**	**18.30**	**20.35**	**250.93**

Table 7.11 Water demand for forest use between 2020 and 2029.

Year	Water demand for forest use between 2020 and 2029 (million m^3)												
	Jan	Feb	Mar	Apr	May	Jun	Jul	Aug	Sep	Oct	Nov	Dec	Total
2020	14.34	14.48	15.72	14.49	13.38	12.89	13.26	13.36	11.58	11.57	11.61	12.91	159.58
2021	14.19	13.83	15.55	14.34	13.23	12.76	13.11	13.22	11.45	11.44	11.49	12.77	157.37
2022	14.00	13.65	15.35	14.15	13.06	12.59	12.95	13.05	11.31	11.30	11.34	12.61	155.36
2023	13.85	13.51	15.19	14.00	12.92	12.46	12.81	12.91	11.19	11.18	11.22	12.47	153.70
2024	13.70	13.83	15.01	13.84	12.78	12.32	12.66	12.76	11.06	11.05	11.09	12.33	152.42
2025	13.52	13.18	14.82	13.67	12.61	12.16	12.50	12.60	10.92	10.91	10.95	12.17	150.00
2026	13.36	13.02	14.64	13.50	12.46	12.01	12.35	12.44	10.79	10.78	10.82	12.03	148.19
2027	13.20	12.86	14.46	13.34	12.31	11.87	12.20	12.29	10.66	10.65	10.69	11.88	146.40
2028	13.05	13.18	14.31	13.19	12.18	11.74	12.07	12.16	10.54	10.53	10.57	11.75	145.27
2029	12.87	12.54	14.10	13.00	12.00	11.57	11.89	11.99	10.39	10.38	10.42	11.58	142.74
Average	**13.61**	**13.41**	**14.91**	**13.75**	**12.69**	**12.24**	**12.58**	**12.68**	**10.99**	**10.98**	**11.02**	**12.25**	**151.10**

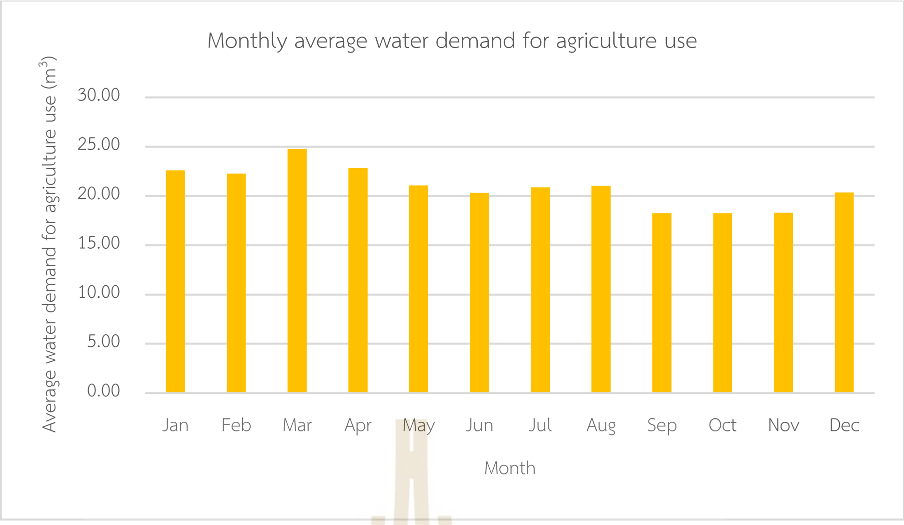

Figure 7.10 Monthly average water demand for agriculture use in Phuket Island between 2020 and 2029.

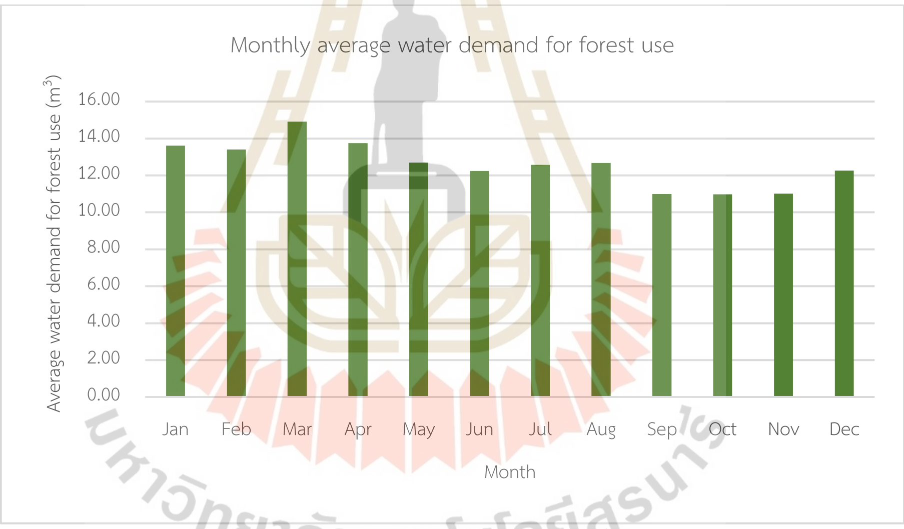

Figure 7.11 Monthly average water demand for forest use in Phuket Island between 2020 and 2029.

In summary, the annual water demand, including residential, tourism, agriculture, and forest use, under normal condition in Phuket Island between 2020 and 2029 varies from 442.09 million m^3 in 2029 to 475.86 million m^3 in 2020, with an average annual water demand of 458.10 million m^3. Meanwhile, the new normal condition in the same period varies from 442.09 million m^3 in 2029 to 461.53 million m^3 in 2020, with an average annual water demand of 454.03 million m^3. The water demand is mainly attributed to agriculture use. Under normal conditions, a percentage of average water demand in agriculture is approximately 54.78%, followed by forest use, residential, and tourism, approximately 32.98%, 7.55%, and 4.69%, respectively. On the contrary, under new normal conditions, a percentage of average water demand in agriculture is approximately 55.27%, followed by forest use, residential, and tourism, which are approximately 33.28%, 7.62%, and 3.84%, respectively. The residential and tourism water demand was continuously increased, while water demand for agriculture and forest uses was continuously decreased in the same period. Detail of total water demand in different conditions between 2020 and 2029 is summarized in Table 7.12.

The increase in annual residential water demand of Phuket Island between 2020 and 2029 was continuously increased from 32.58 million m^3 in 2020 to 37.25 million m^3 in 2029. Notably, residential water demand was higher in the urban areas than in the rural areas of Phuket Island. It causes the growth of the population in the same period, and the consumption patterns are different.

The tourist water demand under normal conditions in the same period was continuously increased from 18.86 million m^3 in 2020 to 24.76 million m^3 in 2029. Meanwhile, the tourist water demand under new normal conditions between 2020 and 2029 varies from 4.52 million m^3 to 24.76 million m^3. The tourist water demand was dropped between 2020 and 2023 since the COVID-19 pandemic. Still, it continuously increases from 2024 to 2029.

Table 7.12 Total water demand in different conditions between 2020 and 2029.

Years	Water demand (million m^3)									
	Residential		Tourist		Agriculture use		Forest use		Total	
	Normal	New normal	Normal	New normal	Normal	New normal	Normal	New normal	Normal	New normal
2020	32.58	32.58	18.86	4.52	264.84	264.84	159.58	159.58	475.86	461.53
2021	31.83	31.83	19.01	7.47	260.98	260.98	157.37	157.37	469.19	457.65
2022	33.38	33.38	19.57	10.79	258.14	258.14	155.36	155.36	466.45	457.67
2023	33.35	33.35	20.23	14.11	255.03	255.03	153.70	153.70	462.31	456.19
2024	34.46	34.46	21.02	21.02	252.87	252.87	152.42	152.42	460.77	460.77
2025	34.70	34.70	21.68	21.68	249.25	249.25	150.00	150.00	455.62	455.62
2026	35.49	35.49	22.50	22.50	246.31	246.31	148.19	148.19	452.48	452.48
2027	35.98	35.98	23.27	23.27	243.33	243.33	146.40	146.40	448.98	448.98
2028	36.79	36.79	24.04	24.04	241.19	241.19	145.27	145.27	447.29	447.29
2029	37.25	37.25	24.76	24.76	237.35	237.35	142.74	142.74	442.09	442.09
Average	**34.58**	**34.58**	**21.49**	**17.42**	**250.93**	**250.93**	**151.10**	**151.10**	**458.10**	**454.03**

In addition, the relationship between tourism growth and urban expansion in Phuket Island between 2020 and 2029 was presented a strong relation, particularly under normal conditions. Thus, the increase in tourists led to the high resource demand of Phuket Island even though water supply is a limitation in water supply storage and a little rainfall in summer seasons (high seasons).

The water demand for agriculture use was continuously decreased from 264.84 million m^3 in 2020 to 237.35 million m^3 in 2029. Meanwhile, the water demand for forest use in the same period will decrease from 159.58 million m^3 in 2020 to 142.74 million m^3 in 2029. Due to the characteristic of LULC change in Phuket Island was major decreased of para rubber trees area (perennial trees and orchards) converted to urban and built-up areas led to a supported tourism facility for tourists, and the primarily decreased forest area covert to the para rubber trees area (perennial trees and orchards) and led to a supported the new agriculture area.

However, this study's results will help understand the current status and future trend of residential water and support decision-making and water resources planning for each water demand component, especially during the dry season.

CHAPTER VIII

WATER BALANCE EVALUATION

This chapter presents the results of the fourth objective focusing on the water balance evaluation in terms of water surplus and deficit for water resource management. The main results are composed of (1) baseline information of water balance in 2019, (2) annual and monthly water balance of dry and wet year scenario under normal and new normal conditions (COVID-19 pandemic) without ecological water requirement consideration, and (3) annual and monthly water balance of dry and wet year scenario under normal and new normal conditions (COVID-19 pandemic) with ecological water requirement consideration. The structure of water balance description with and without ecological water requirement consideration is displayed in Figure 8.1 for understanding. Additionally, some recommendations are addressed for water resource management.

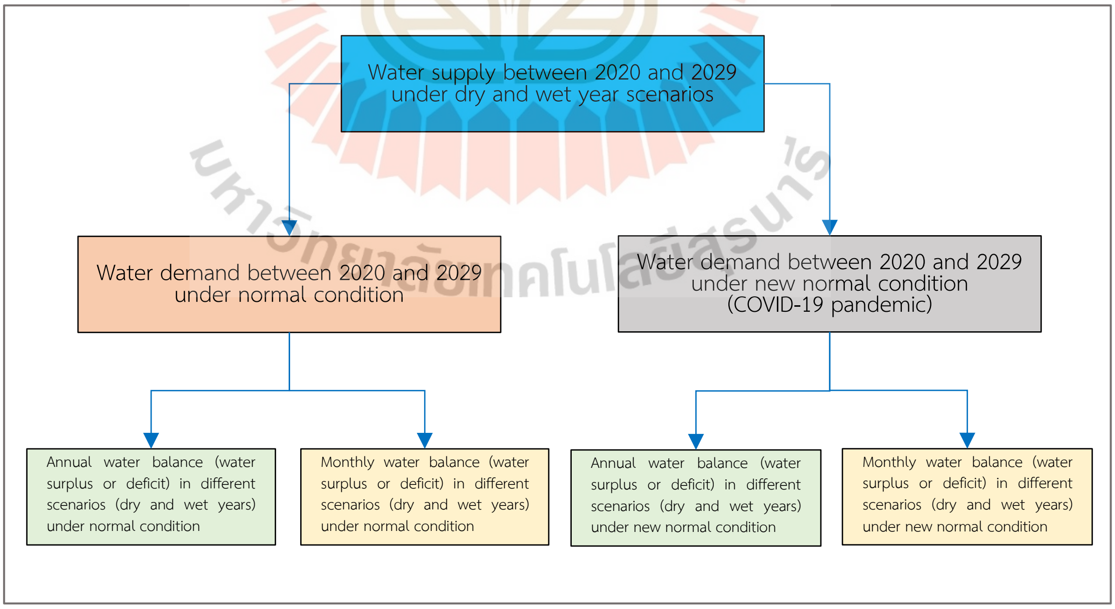
Water supply between 2020 and 2029 under dry and wet year scenarios
Water demand between 2020 and 2029 under normal condition
Water demand between 2020 and 2029 under new normal condition (COVID-19 pandemic)
Annual water balance (water surplus or deficit) in different scenarios (dry and wet years) under normal condition
Monthly water balance (water surplus or deficit) in different scenarios (dry and wet years) under normal condition
Annual water balance (water surplus or deficit) in different scenarios (dry and wet years) under new normal condition
Monthly water balance (water surplus or deficit) in different scenarios (dry and wet years) under new normal condition

Figure 8.1 Structure of water balance description with and without ecological water requirement consideration.

8.1 Baseline information of water balance in 2019

The water supply of Phuket Island in 2019, which was estimated using the SWAT model, was 504.37 million m^3. Meanwhile, the monthly water supply varied from 1.94 million m^3 in March to 102.15 million m^3 in October.

Meanwhile, the water demand of Phuket Island in 2019, which was estimated into four categories: residential, tourists, agriculture use, and forest use, was 474.61 million m^3. It consists of 29.84 million m^3 for residential, 16.62 million m^3 for tourists, 267.19 million m^3 for agriculture use, and 160.97 million m^3 for forest use.

Therefore, the water balance in 2019 is water surplus, with a water surplus of 29.76 million m^3. Meanwhile, the monthly water balance is water deficit from December to May.

8.2 Annual and monthly water balance without ecological water requirement consideration

Under this section, annual and monthly water balance based on the derived water supply without ecological water requirement consideration and water demand between 2020 and 2029 in two different scenarios (dry and wet years) under normal and new normal conditions were evaluated in terms of surplus and deficit for water resource management. The annual and monthly water balance evaluation is separately discussed and described according to different scenarios and conditions in the following sections.

8.2.1 Annual water balance without ecological water requirement consideration

Annual water supply by SWAT model without ecological water requirement consideration and water demand estimation based on water footprint was used as the primary input to evaluate water balance between 2020 and 2029 in terms of water surplus or deficit under two different scenarios (dry and wet years) and conditions (normal and new normal) (see more details in Chapters VI and VII).

The result of the annual water balance evaluation without ecological water requirement consideration in two different scenarios and conditions in terms of water surplus or deficit between 2020 and 2029 is reported in Table 8.1.

The annual water supply (water yield) without ecological water requirement consideration under the dry year scenario between 2020 and 2029 varies from 505.01 million m^3 in 2020 to 521.79 million m^3 in 2029, with an average annual water supply of 512.22 million m^3. In the meantime, the annual water supply without ecological water requirement consideration under the wet year scenario in the same period varies from 1,225.48 million m^3 in 2020 to 1,242.08 million m^3 in 2029, with an average annual water supply of 1,233.00 million m^3.

On the contrary, the annual water demand of the normal conditions in the same period varies from 442.09 million m^3 in 2029 to 475.86 million m^3 in 2020, with an average annual water demand of 458.11 million m^3. Meanwhile, the annual water demand of the new normal condition in the same period varies from 442.09 million m^3 in 2029 to 461.53 million m^3 in 2020, with an average annual water demand of 454.03 million m^3.

The annual water balance without ecological water requirement consideration under the dry year scenario with the normal condition between 2020 and 2029 is water surplus in all years. The water surplus varies from 29.15 million m^3 in 2020 to 79.70 million m^3 in 2029, with an average water surplus of 54.12 million m^3. On the contrary, the annual water balance without ecological water requirement consideration under the dry year scenario with the new normal condition in the same period is also water surplus in all years. The water surplus varies from 43.38 million m^3 in 2020 to 79.70 million m^3 in 2029, with an average water surplus of 58.19 million m^3.

Meanwhile, the annual water balance without ecological water requirement consideration under the wet year scenario with the normal condition between 2020 and 2029 is water surplus in all years. The water surplus varies from 749.61 million m^3 in 2020 to 799.98 million m^3 in 2029, with an average water surplus of 774.89 million m^3. On the contrary, the annual water balance without ecological water requirement consideration under the wet year scenario with the new normal condition between 2020 and 2029 is also surplus in all years. The water surplus varies from 763.95 million m^3 in 2020 to 799.98 million m^3 in 2029, with an average water surplus of 778.97 million m^3.

Table 8.1 The annual water supply and demand balance evaluation without considering ecological water requirements between 2020 and 2029.

Year	Water supply in different scenarios (million m^3)		Type of water demand (million m^3)							Water balance evaluation (surplus or deficit) (million m^3)			
	Dry year	Wet year	Residential	Tourist		Agriculture use	Forest use	Total water demand		Dry year		Wet year	
				Normal	New normal			Normal	New normal	Normal	New normal	Normal	New normal
2020	505.01	1,225.48	32.58	18.86	4.52	264.84	159.58	475.86	461.53	29.15	43.48	749.61	763.95
2021	505.73	1,226.49	31.83	19.01	7.47	260.98	157.37	469.19	457.65	36.54	48.08	757.30	768.84
2022	506.34	1,227.28	33.38	19.57	10.79	258.14	155.36	466.45	457.67	39.88	48.66	760.82	769.60
2023	507.41	1,228.55	33.35	20.23	14.11	255.03	153.70	462.31	456.19	45.10	51.21	766.24	772.35
2024	508.28	1,229.18	34.46	21.02	21.02	252.87	152.42	460.77	460.77	47.51	47.51	768.40	768.40
2025	510.06	1,231.38	34.70	21.68	21.68	249.25	150.00	455.62	455.62	54.44	54.44	775.76	775.76
2026	517.83	1,238.32	35.49	22.50	22.50	246.31	148.19	452.48	452.48	65.35	65.35	785.84	785.84
2027	519.55	1,240.31	35.98	23.27	23.27	243.33	146.40	448.98	448.98	70.57	70.57	791.32	791.32
2028	520.22	1,240.94	36.79	24.04	24.04	241.19	145.27	447.29	447.29	72.93	72.93	793.65	793.65
2029	521.79	1,242.08	37.25	24.76	24.76	237.35	142.74	442.09	442.09	79.70	79.70	799.98	799.98
Avg.	**512.22**	**1,233.00**	**34.58**	**21.49**	**17.42**	**250.93**	**151.10**	**458.11**	**454.03**	**54.12**	**58.19**	**774.89**	**778.97**

Figure 8.2 displays the annual water supply with ecological water requirement consideration and water demand between 2020 and 2029 under the dry year scenario with normal and new normal conditions. As shown in the figure, it indicates that the water balance of Phuket Island between 2020 and 2029 is water surplus under the dry year scenario with normal and new normal conditions.

Likewise, Figure 8.3 displays the annual water supply with ecological water requirement consideration and water demand under wet year scenario with normal and new normal conditions between 2020 and 2029. As a result, it obviously indicates that the water balance of Phuket Island between 2020 and 2029 is water surplus under wet year scenario with normal and new normal conditions.

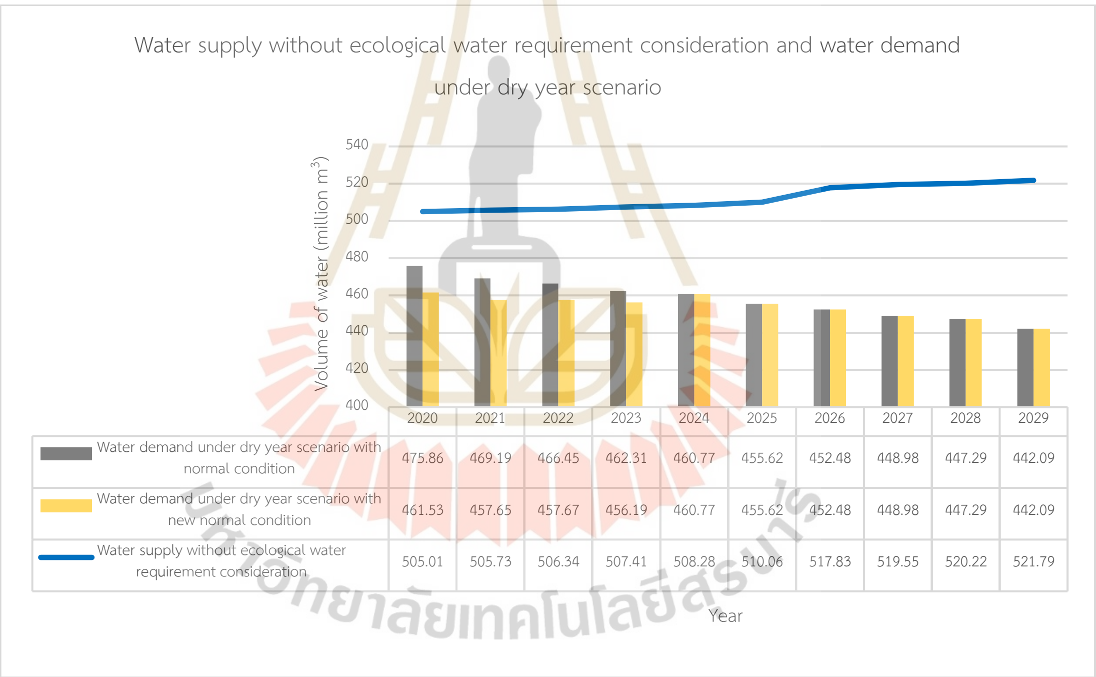

	2020	2021	2022	2023	2024	2025	2026	2027	2028	2029
Water demand under dry year scenario with normal condition	475.86	469.19	466.45	462.31	460.77	455.62	452.48	448.98	447.29	442.09
Water demand under dry year scenario with new normal condition	461.53	457.65	457.67	456.19	460.77	455.62	452.48	448.98	447.29	442.09
Water supply without ecological water requirement consideration	505.01	505.73	506.34	507.41	508.28	510.06	517.83	519.55	520.22	521.79

Figure 8.2 Annual water supply without consideration for ecological water requirement and water demand between 2020 and 2029 under dry year scenario with normal and new conditions.

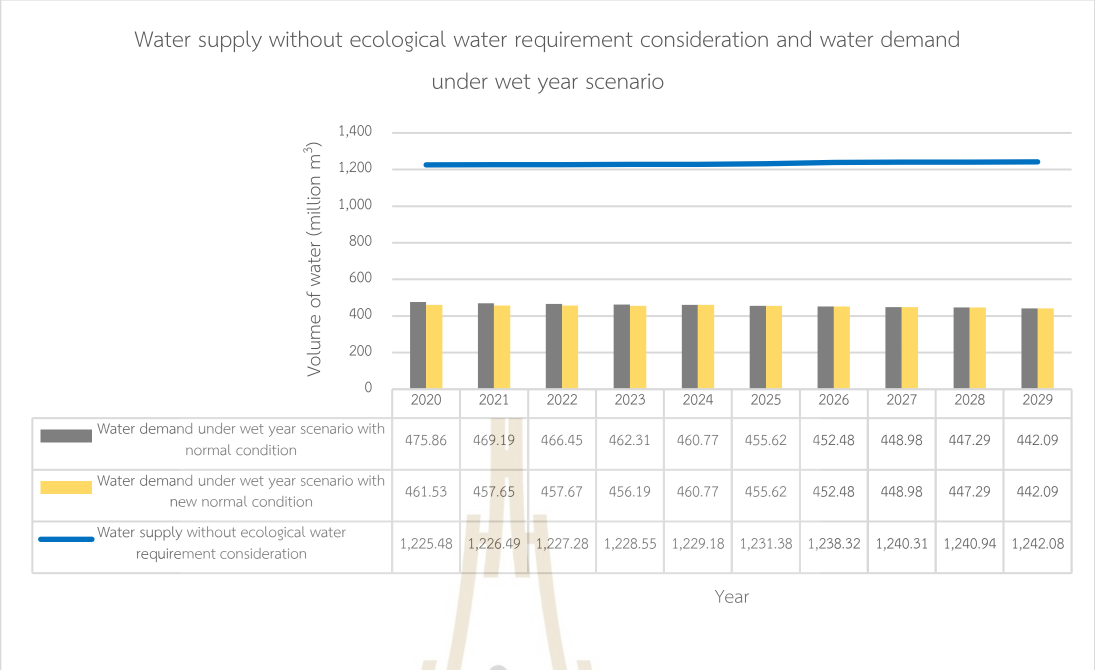

	2020	2021	2022	2023	2024	2025	2026	2027	2028	2029
Water demand under wet year scenario with normal condition	475.86	469.19	466.45	462.31	460.77	455.62	452.48	448.98	447.29	442.09
Water demand under wet year scenario with new normal condition	461.53	457.65	457.67	456.19	460.77	455.62	452.48	448.98	447.29	442.09
Water supply without ecological water requirement consideration	1,225.48	1,226.49	1,227.28	1,228.55	1,229.18	1,231.38	1,238.32	1,240.31	1,240.94	1,242.08

Figure 8.3 Annual water supply without consideration for ecological water requirement and water demand between 2020 and 2029 under wet year scenario with normal and new normal conditions.

8.2.2 Monthly water balance without ecological water requirement consideration

For the whole year, under dry year scenario with normal and new normal conditions, the average monthly water supply without ecological water requirement consideration, which was derived from the SWAT model with rainfall data in 2019, varies from 1.84 million m^3 in March to 102.26 million m^3 in October, with an average water supply of 42.68 million m^3.

In the meantime, the average water supply in the summer season (December to March) varies from the lowest value of 1.84 million m^3 in March to the highest value of 31.86 million m^3 in December. Meanwhile, the average water supply in the rainy season (April to November) varies from the lowest value of 16.10 million m^3 in May to the highest value of 102.26 million m^3 in October (see more details in Tables 6.12 in Chapter VI).

Likewise, for the whole year under wet year scenarios of both conditions, the average monthly water supply without ecological water requirement consideration derived from the SWAT model with rainfall data in 2016 varies from 2.80 million m^3 in April to 286.47 million m^3 in October, with an average water supply of 102.75 million m^3. In the meantime, the average water supply in the summer season (December to March) varies from the lowest value of 4.95 million m^3 in March to the highest value of 58.92 million m^3 in December. Meanwhile, the average water supply in the rainy season (April to November) varies from the lowest value of 2.80 million m^3 in April to the highest value of 286.47 million m^3 in October (see more details in Tables 6.17 in Chapter VI).

Meanwhile, the monthly water demand of four different types (residential, tourist, agriculture, and forest uses) was estimated based on the derived annual water demand with the specific assumptions below.

(1) Monthly residential water demand estimation. The summation of average monthly water demand from each administrative boundary with a value of 34.58 million m^3 per year was applied to estimate monthly water demand between 2020 and 2029 because the registered and non-registered populations in the study area are stable. Consequently, monthly residential water demand between 2020 and 2029 was 2.88 million m^3 per month (see detail in Table. 7.6 in Chapter VII).

(2) Monthly tourist water demand estimation under two different conditions. The average monthly tourist (tourists and excursionists) water demand under two different conditions (normal and new normal) was estimated based on tourist arrival between 2015 and 2019 as a summary in Table 8.2 and the average annual tourists between 2020 and 2029 (see details in Tables 7.7 and 7.8 in Chapter VII).

In practice, the monthly tourist arrival is first applied to calculate monthly tourists' proportional rate (see Table 8.2 and Figure 8.4). The monthly tourists (tourist and excursionist) between 2020 and 2029 under normal and new normal conditions were then estimated by multiplication between the proportional rate of monthly tourists and annual tourists for each condition, resulting in Tables 8.3 and 8.4, respectively.

Table 8.2 Monthly tourist arrival and proportional rate.

Year	Monthly tourist arrival (million persons)												
	Jan	Feb	Mar	Apr	May	Jun	Jul	Aug	Sep	Oct	Nov	Dec	Total
2015	1.30	1.25	1.25	0.99	0.76	0.98	0.70	0.69	0.70	1.05	0.96	1.29	11.93
2016	1.33	1.24	1.28	1.03	0.79	1.01	0.72	0.73	0.73	0.97	0.92	1.26	12.02
2017	1.39	1.26	1.35	1.08	0.79	1.05	0.76	0.76	0.77	1.01	0.95	1.32	12.50
2018	1.46	1.33	1.44	1.17	0.85	1.10	0.72	0.73	0.72	0.97	0.98	1.37	12.83
2019	1.53	1.37	1.48	1.15	0.84	1.06	0.75	0.72	0.77	1.01	0.96	1.41	13.05
Total	7.02	6.45	6.81	5.43	4.02	5.21	3.65	3.63	3.69	5.02	4.78	6.64	62.33
Avg.	1.40	1.29	1.36	1.09	0.80	1.04	0.73	0.73	0.74	1.00	0.96	1.33	12.47
Proportional rate	0.11	0.10	0.11	0.09	0.06	0.08	0.06	0.06	0.06	0.08	0.08	0.11	1.00

Source: Economics Tourism and Sports Division, Ministry of Tourism and Sports (2019).

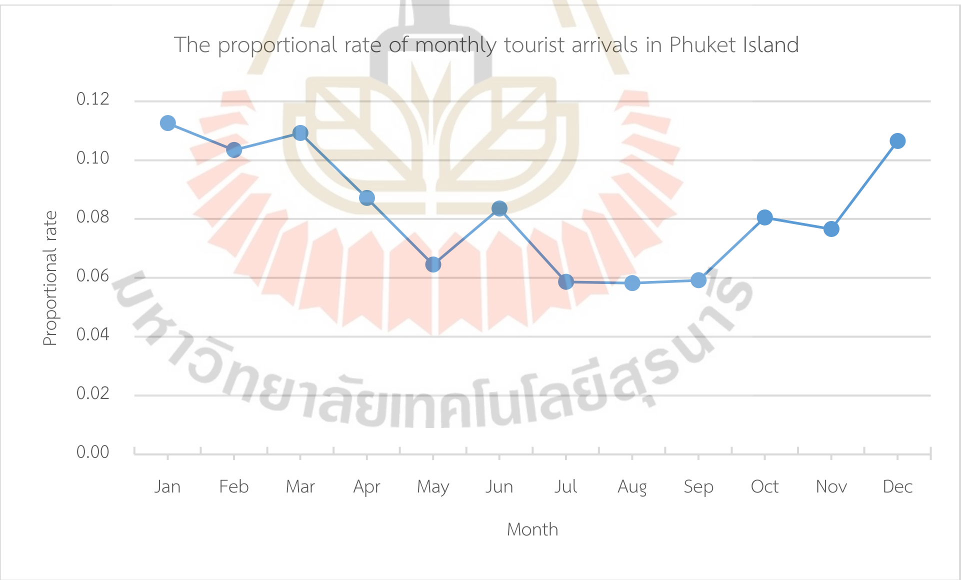

Figure 8.4 The proportional rate of monthly tourist arrival in Phuket Island.

Table 8.3 The average monthly tourists and excursionists between 2020 and 2029 under normal condition.

Tourist type	Monthly tourist and excursionist (million persons)												
	Jan	Feb	Mar	Apr	May	Jun	Jul	Aug	Sep	Oct	Nov	Dec	Total
Tourist	2.01	1.85	1.95	1.56	1.15	1.49	1.05	1.04	1.06	1.44	1.37	1.91	17.89
Excursionist	0.11	0.10	0.10	0.08	0.06	0.08	0.06	0.05	0.06	0.08	0.07	0.10	0.94
Total	**2.12**	**1.95**	**2.06**	**1.64**	**1.21**	**1.57**	**1.10**	**1.10**	**1.11**	**1.51**	**1.44**	**2.01**	**18.83**

Table 8.4 The average monthly tourists and excursionists between 2020 and 2029 under new normal condition.

Tourist type	Monthly tourist and excursionist (million persons)												
	Jan	Feb	Mar	Apr	May	Jun	Jul	Aug	Sep	Oct	Nov	Dec	Total
Tourist	1.63	1.50	1.58	1.26	0.93	1.21	0.85	0.84	0.86	1.17	1.11	1.54	14.50
Excursionist	0.09	0.08	0.08	0.07	0.05	0.06	0.05	0.04	0.05	0.06	0.06	0.08	0.77
Total	**1.72**	**1.58**	**1.67**	**1.33**	**0.98**	**1.28**	**0.89**	**0.89**	**0.90**	**1.23**	**1.17**	**1.63**	**15.26**

According to Table 8.3, the average number of monthly tourists and excursionists in Phuket Island under the normal condition varies from 1.10 million persons in July and August to 2.12 million persons in January. The top three most dominant months for tourists and excursionists are January, March, and December, while the top three least dominant months for both groups are July, August, and September.

Meanwhile, average monthly tourists and excursionists in Phuket Island under the new normal condition varies from 0.89 million persons in July and August to 1.72 million persons in January. The top three dominant months for the highest tourists and excursionists are January, March, and December. The top three least dominant months for the lowest tourists and excursionists are July, August, and September (see Table 8.4).

The average monthly tourist (tourists and excursionists) water demand between 2020 and 2029 is reported in Table 8.5.

Table 8.5 The average monthly tourist water demand between 2020 and 2029 under normal and new normal conditions.

Condition	Monthly water demand (million m^3)												
	Jan	Feb	Mar	Apr	May	Jun	Jul	Aug	Sep	Oct	Nov	Dec	Total
Normal	2.42	2.22	2.35	1.87	1.39	1.80	1.26	1.25	1.27	1.73	1.65	2.29	21.49
New normal	1.96	1.80	1.90	1.52	1.12	1.46	1.02	1.01	1.03	1.40	1.33	1.86	17.42

As a result, in Table 8.5, tourist water demand under normal condition varies from 1.25 million m^3 in August to 2.42 million m^3 in January. Meanwhile, the top three dominant months of highest average monthly tourist water demand are January, March, and December. The top three dominant months of lowest average monthly tourist water demand are August, July, and September.

In contrast, tourist water demand under new normal condition varies from 1.01 million m^3 in August to 1.96 million m^3 in January. Likewise, the top three dominant months of highest average monthly tourist water demand are January, March, and December. The top three dominant months of lowest average monthly tourist water demand are August, July, and September.

(3) Monthly water demand estimation for agriculture use. The average monthly water demand for agriculture use between 2020 and 2029 was estimated based on evapotranspiration coefficient, reference evapotranspiration, and area, as a result in Table 8.6. As a result, the average monthly water demand estimation for agriculture use varies from 18.23 million m^3 in October to 24.77 million m^3 in March. The top three dominant months for the highest water demand in agriculture use are March, April, and January. October, September, and November are the top three dominant months for the lowest water demand in agriculture use.

(4) Monthly water demand estimation for forest use. The average monthly water demand for forest use between 2020 and 2029 was estimated based on evapotranspiration coefficient, reference evapotranspiration, and area, as a result in Table 8.6. The average monthly water demand estimation for forest use varies from 10.98 million m^3 in October to 14.91 million m^3 in March. The top three dominant months for the highest water demand in forest use are March, April, and January. The top three dominant months for the lowest water demand in forest use are October, September, and November.

Table 8.6 The average monthly water demand estimation for agriculture and forest uses between 2020 and 2029.

Month	Water demand estimation for agriculture and forest uses (million m^3)	
	Agriculture use	Forest use
Jan	22.60	13.61
Feb	22.27	13.41
Mar	24.77	14.91
Apr	22.84	13.75
May	21.08	12.69
Jun	20.32	12.24
Jul	20.89	12.58
Aug	21.05	12.68
Sep	18.25	10.99
Oct	18.23	10.98
Nov	18.30	11.02
Dec	20.35	12.25
Total	**250.93**	**151.10**

The comparison of monthly water demand estimation of each category between 2020 and 2029 under normal and new normal conditions is reported in Table 8.7. As a result, total water demand by month of four categories between 2020 and 2029 under normal condition varies from 33.39 million m^3 in September to 44.91 million m^3 in March. Meanwhile, total water demand by month of four categories in the summer season (December to March) under this condition varies from the lowest value of 37.77 million m^3 in December to the highest value of 44.91 million m^3 in March. On the contrary, total water demand by month of four categories in the rainy season (April to November) under this condition varies from the lowest value of 33.39 million m^3 in September to the highest value of 41.35 million m^3 in April.

On the contrary, under new normal condition, total water demand by month of four categories between 2020 and 2029 varies from 33.15 million m^3 in September to 44.47 million m^3 in March. Meanwhile, total water demand by month of four categories in the summer season (December to March) under this condition varies from the lowest value of 37.33 million m^3 in December to the highest value of 44.47 million m^3 in March. In the meantime, total water demand by month of four categories in the rainy season (April to November) under this condition varies from the lowest value of 33.15 million m^3 in September to the highest value of 40.99 million m^3 in April.

Consequently, monthly water balance without ecological water requirement consideration in terms of surplus and deficit under normal and new normal conditions between 2020 and 2029 was estimated as shown in Table 8.8.

Table 8.7 Average monthly water demand estimation of each category between 2020 and 2029 under normal and new normal conditions.

Month	Type of water demand (million m^3)						
	Residential	Tourist		Agriculture use	Forest use	Total water demand	
		Normal	New normal			Normal	New normal
Jan	2.88	2.42	1.96	22.60	13.61	41.51	41.05
Feb	2.88	2.22	1.80	22.27	13.41	40.78	40.36
Mar	2.88	2.35	1.90	24.77	14.91	44.91	44.47
Apr	2.88	1.87	1.52	22.84	13.75	41.35	40.99
May	2.88	1.39	1.12	21.08	12.69	38.04	37.78
Jun	2.88	1.80	1.46	20.32	12.24	37.23	36.89
Jul	2.88	1.26	1.02	20.89	12.58	37.61	37.37
Aug	2.88	1.25	1.01	21.05	12.68	37.86	37.62
Sep	2.88	1.27	1.03	18.25	10.99	33.39	33.15
Oct	2.88	1.73	1.40	18.23	10.98	33.82	33.49
Nov	2.88	1.65	1.33	18.30	11.02	33.85	33.53
Dec	2.88	2.29	1.86	20.35	12.25	37.77	37.33
Total	**34.58**	**21.49**	**17.42**	**250.93**	**151.10**	**458.11**	**454.03**

Table 8.8 Monthly water supply and demand balance evaluation without ecological water requirement consideration between 2020 and 2029.

Month	Water supply (million m^3)		Water demand (million m^3)		Water balance (surplus or deficit) (million m^3)			
					Dry year		Wet year	
	Dry year	Wet year	Normal	New normal	Normal	New normal	Normal	New normal
Jan	10.61	45.31	41.51	41.05	-30.89	-30.44	3.80	4.26
Feb	3.92	19.46	40.78	40.36	-36.86	-36.44	-21.32	-20.89
Mar	1.84	4.95	44.91	44.47	-43.07	-42.63	-39.97	-39.52
Apr	20.24	2.80	41.35	40.99	-21.11	-20.76	-38.55	-38.20
May	16.10	82.32	38.04	37.78	-21.94	-21.68	44.28	44.54
Jun	65.57	106.19	37.23	36.89	28.33	28.67	68.95	69.29
Jul	82.69	97.82	37.61	37.37	45.09	45.32	60.21	60.45
Aug	72.22	148.54	37.86	37.62	34.36	34.60	110.68	110.92
Sep	66.16	239.62	33.39	33.15	32.77	33.01	206.24	206.48
Oct	102.26	286.47	33.82	33.49	68.44	68.77	252.65	252.97
Nov	38.75	140.62	33.85	33.53	4.91	5.22	106.77	107.08
Dec	31.86	58.92	37.77	37.33	-5.91	-5.47	21.15	21.58
Total	**512.22**	**1,233.00**	**458.11**	**454.03**	**54.12**	**58.19**	**774.89**	**778.97**

As a result in Table 8.8, under dry year scenarios with the normal condition, the monthly water balance between 2020 and 2029 is a water deficit from December to May. It varies from -43.07 million m^3 in March to -5.91 million m^3 in December. In the meantime, the monthly water balance in the same period is water surplus from June to November, and it varies from 4.91 million m^3 in November to 68.44 million m^3 in October.

On the contrary, under dry year scenarios with the new normal condition, the monthly water balance between 2020 and 2029 is water deficit from December to May, and it varies from -42.63 million m^3 in March to -5.47 million m^3 in December. In the meantime, the monthly water balance in the same period is water surplus from June to November, and it varies from 5.22 million m^3 in November to 68.77 million m^3 in October.

Figure 8.5 compares the monthly deficit and surplus water balance between 2020 and 2029 under a dry year scenario with normal and new normal.

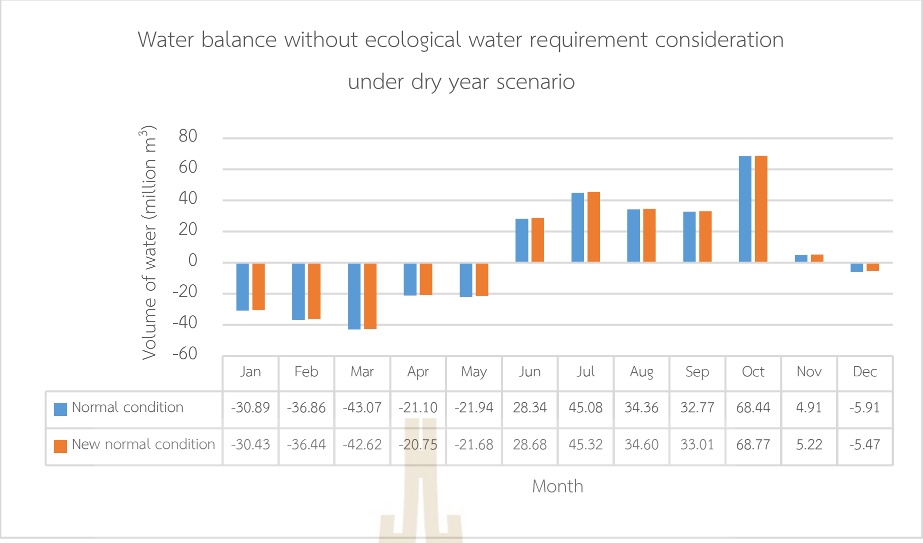

Figure 8.5 Monthly water balance without ecological water requirement consideration between 2020 and 2029 under dry year scenario with normal and new normal condition.

In the meantime, under wet year scenarios with the normal condition as a result in Table 8.8, the monthly water balance without ecological water requirement consideration between 2020 and 2029 is water deficit from February to April. It varies from -39.97 million m^3 in March to -21.32 million m^3 in February. Meanwhile, the monthly water balance in the same period is water surplus from May to January. It varies from 3.80 million m^3 in January to 252.65 million m^3 in October.

On the contrary, the monthly water balance between 2020 and 2029 is a water deficit from February to April under the wet year scenario with the new normal condition. It varies from -39.52 million m^3 in March to -20.89 million m^3 in February. In the meantime, the monthly water balance in the same period is water surplus from May to January, and it varies from 4.26 million m^3 in January to 252.97 million m^3 in October.

Figure 8.6 compares the monthly deficit and surplus water balance between 2020 and 2029 under the wet year scenario with normal and new normal.

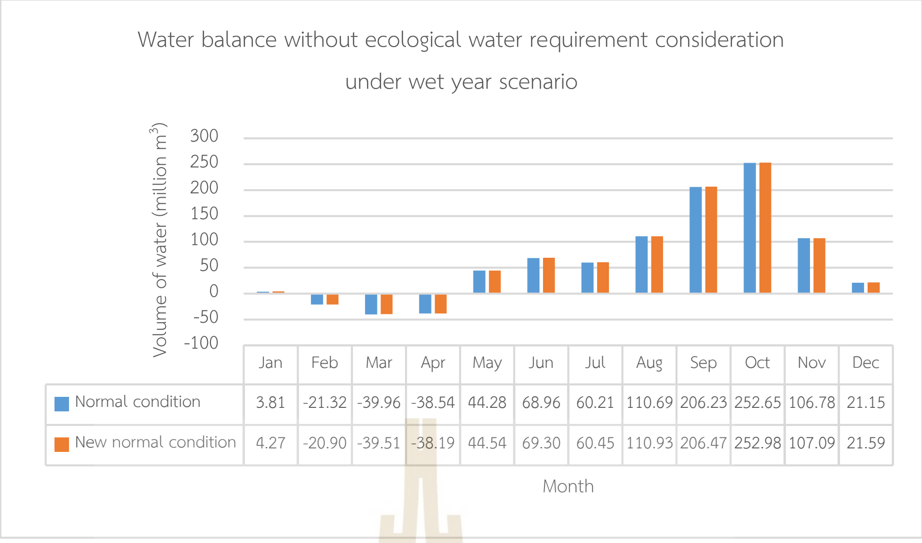

Figure 8.6 Monthly water balance without ecological water requirement consideration between 2020 and 2029 under wet year scenario with normal and new normal condition.

In summary, the water balance evaluation without ecological water requirement consideration between 2020 and 2029 was divided into two main results: annual and monthly water balance under two different scenarios with two different conditions.

In the study period, the annual water balance in Phuket Island discovered water surplus all years under dry and wet year scenarios with normal and new normal conditions. On the contrary, the monthly water balance in Phuket Island in the same period exposed water deficit and surplus under dry and wet year scenarios with normal and new normal conditions. The monthly water deficit occurred in six months (December to May) under dry year scenarios with normal and new normal conditions, while the monthly water deficit occurred in three months (February to April) under wet year scenarios with normal and new normal conditions.

8.3 Annual and monthly water balance with ecological water requirement consideration

Under this section, annual and monthly water balance based on the derived water supply and demand between 2020 and 2029 in two different scenarios (dry and wet years) under normal and new normal conditions were evaluated with ecological water requirement consideration in terms of surplus and deficit for water resource management.

Due to water demands and restoring ecological features are more significant concerns about integrating spatial and temporal scales of multi-dimensional management issues (Navarrete, Ioris, and Granados, 2012). The sustainable use and conservation of water require should be fair and balance. Gleick (1998) stressed that guaranteed access to a basic amount of water is necessary to maintain human health and sustain ecosystems for sustainable water planning. Thus, the ecological water requirement of Phuket Island was calculated based on the water supply, which was derived from the SWAT model under normal criteria of minimum water from the flow duration curve suggest by Southern Region Irrigation Hydrology Center, Royal Irrigation Department (2021) (see details in Chapter III). As a result, the annual ecological water requirement of Phuket Island was 147.64 million m^3 per year. Thus, the monthly ecological water requirement was 12.30 million m^3 per month. The annual and monthly ecological water requirement is further applied to reduce available water supply data between 2020 and 2029, estimated using the SWAT model. The annual and monthly water balance evaluation is separately discussed and described according to different scenarios and conditions in the following sections.

8.3.1 Annual water balance with ecological water requirement consideration

The evaluation of the annual water balance in terms of water surplus or deficit between 2020 and 2029 with ecological water requirement consideration in two different scenarios and conditions is reported in Table 8.9.

As a result, the annual water supply (water yield) with ecological water requirement consideration under the dry year scenario between 2020 and 2029 varies from 357.37 million m^3 in 2020 to 374.15 million m^3 in 2029, an average annual water supply of 364.58 million m^3. In the meantime, the annual water supply under the wet year scenario in the same period varies from 1,077.84 million m^3 in 2020 to 1,094.44 million m^3 in 2029, with an average annual water supply of 1,085.36 million m^3.

On the contrary, an annual water demand with ecological water requirement consideration under the normal condition in the same period varies from 442.09 million m^3 in 2029 to 475.86 million m^3 in 2020, with an average annual water demand of 458.11 million m^3. Meanwhile, an annual water demand with ecological water requirement consideration under the new normal condition in the same period varies from 442.09 million m^3 in 2029 to 461.53 million m^3 in 2020, with an average annual water demand of 454.03 million m^3.

The annual water balance with ecological water requirement consideration under the dry year scenario with the normal condition between 2020 and 2029 is a water deficit in all years. The water deficit varies from 67.94 million m^3 in 2029 to 118.49 million m^3 in 2020, with an average water deficit of 93.52 million m^3. On the contrary, the annual water balance with ecological water requirement consideration under the dry year scenario with the new normal condition in the same period is also a water deficit in all years. The water deficit varies from 67.94 million m^3 in 2029 to 104.16 million m^3 in 2020, with an average water deficit of 89.45 million m^3.

Meanwhile, the annual water balance with ecological water requirement consideration under the wet year scenario with the normal condition in the same period is water surplus in all years. The water surplus varies from 601.97 million m^3 in 2020 to 652.35 million m^3 in 2029, with an average water surplus of 627.26 million m^3. On the contrary, the annual water balance with ecological water requirement consideration under the wet year scenario with the new normal condition in the same period is also water surplus in all years. The water surplus varies from 616.31 million m^3 in 2020 to 652.35 million m^3 in 2029, with an average water surplus of 631.33 million m^3.

Table 8.9 The annual water supply and demand balance evaluation with ecological water requirement consideration between 2020 and 2029.

Year	Water supply in different scenarios (million m^3)		Type of water demand (million m^3)							Water balance evaluation (surplus or deficit) (million m^3)			
	Dry year	Wet year	Residential	Tourist		Agriculture use	Forest use	Total water demand		Dry year		Wet year	
				Normal	New normal			Normal	New normal	Normal	New normal	Normal	New normal
2020	357.37	1,077.84	32.58	18.86	4.52	264.84	159.58	475.86	461.53	-118.49	-104.16	601.97	616.31
2021	358.09	1,078.85	31.83	19.01	7.47	260.98	157.37	469.19	457.65	-111.10	-99.56	609.66	621.20
2022	358.70	1,079.64	33.38	19.57	10.79	258.14	155.36	466.45	457.67	-107.75	-98.98	613.19	621.96
2023	359.77	1,080.91	33.35	20.23	14.11	255.03	153.70	462.31	456.19	-102.54	-96.43	618.60	624.71
2024	360.65	1,081.54	34.46	21.02	21.02	252.87	152.42	460.77	460.77	-100.13	-100.13	620.77	620.77
2025	362.43	1,083.74	34.70	21.68	21.68	249.25	150.00	455.62	455.62	-93.20	-93.20	628.12	628.12
2026	370.19	1,090.69	35.49	22.50	22.50	246.31	148.19	452.48	452.48	-82.29	-82.29	638.20	638.20
2027	371.92	1,092.67	35.98	23.27	23.27	243.33	146.40	448.98	448.98	-77.07	-77.07	643.68	643.68
2028	372.58	1,093.30	36.79	24.04	24.04	241.19	145.27	447.29	447.29	-74.71	-74.71	646.01	646.01
2029	374.15	1,094.44	37.25	24.76	24.76	237.35	142.74	442.09	442.09	-67.94	-67.94	652.35	652.35
Avg.	**364.58**	**1,085.36**	**34.58**	**21.49**	**17.42**	**250.93**	**151.10**	**458.11**	**454.03**	**-93.52**	**-89.45**	**627.26**	**631.33**

Figure 8.7 displays the annual water supply with ecological water requirement consideration and water demand between 2020 and 2029 under the dry year scenario with normal and new normal conditions. As a result, it obviously indicates a water deficit between 2020 and 2029 under the dry year scenario with normal and new normal conditions.

Meanwhile, Figure 8.8 displays the annual water supply with ecological water requirement consideration and water demand between 2020 and 2029 under the wet year scenario with normal and new normal conditions. As a result, it obviously indicates a water surplus between 2020 and 2029 under the wet year scenario with normal and new normal conditions.

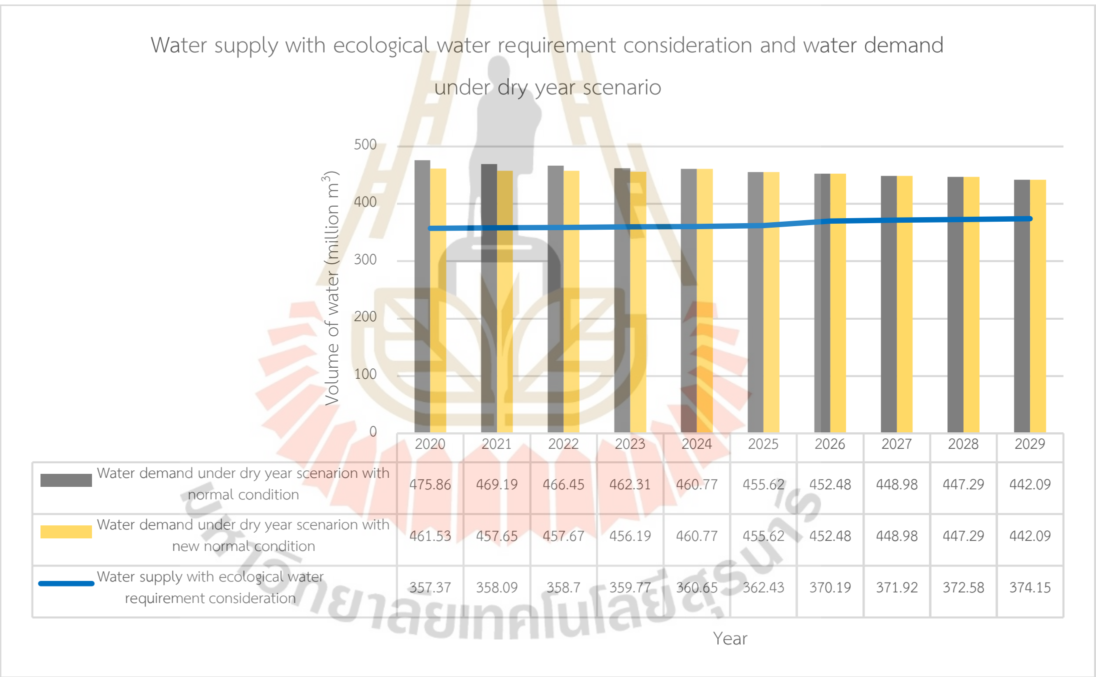

	2020	2021	2022	2023	2024	2025	2026	2027	2028	2029
▬ Water demand under dry year scenarion with normal condition	475.86	469.19	466.45	462.31	460.77	455.62	452.48	448.98	447.29	442.09
▬ Water demand under dry year scenarion with new normal condition	461.53	457.65	457.67	456.19	460.77	455.62	452.48	448.98	447.29	442.09
— Water supply with ecological water requirement consideration	357.37	358.09	358.7	359.77	360.65	362.43	370.19	371.92	372.58	374.15

Figure 8.7 Annual water supply with ecological water requirement consideration and water demand between 2020 and 2029 under dry year scenario with normal and new normal conditions.

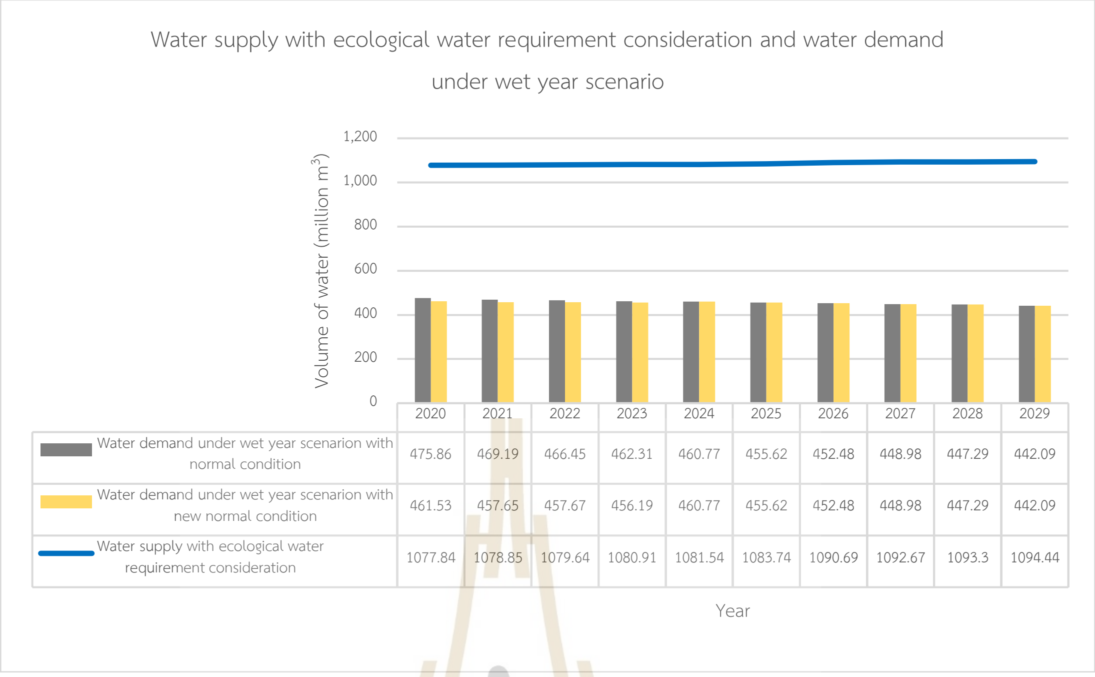

	2020	2021	2022	2023	2024	2025	2026	2027	2028	2029
▬ Water demand under wet year scenarion with normal condition	475.86	469.19	466.45	462.31	460.77	455.62	452.48	448.98	447.29	442.09
▬ Water demand under wet year scenarion with new normal condition	461.53	457.65	457.67	456.19	460.77	455.62	452.48	448.98	447.29	442.09
― Water supply with ecological water requirement consideration	1077.84	1078.85	1079.64	1080.91	1081.54	1083.74	1090.69	1092.67	1093.3	1094.44

Figure 8.8 Annual water supply with ecological water requirement consideration and water demand between 2020 and 2029 under wet year scenario with normal and new normal conditions.

8.3.2 Monthly water balance with ecological water requirement consideration

In general, under the dry year scenario with normal and new normal conditions, the average monthly water supply was derived from the SWAT model with rainfall data in 2019 (see more details in Tables 6.12 in Chapter VI). Meanwhile, under the wet year scenario with normal and new normal conditions, the average monthly water supply was derived from the SWAT model with rainfall data in 2016 (see more details in Tables 6.17 in Chapter VI).

In this study, the monthly water supply with ecological water requirement consideration was calculated based on the water supply, which was derived from the SWAT model under normal criteria of minimum water from the flow duration curve suggest by Southern Region Irrigation Hydrology Center, Royal Irrigation Department (2021) (see details in Chapter III). As a result, the monthly ecological water requirement was 12.30 million m^3 per month. Monthly water supply with ecological water requirement consideration under dry and wet year scenarios between 2020 and 2029 is summarized and compared water supply without and with ecological water requirement consideration in Table 8.10.

Table 8.10 Monthly water supply without and with ecological water requirement consideration under dry and wet year scenarios between 2020 and 2029.

Month	Water supply without ecological water requirement consideration (million m^3)		Water supply with ecological water requirement consideration (million m^3)	
	Dry year	Wet year	Dry year	Wet year
Jan	10.61	45.31	-1.69	33.01
Feb	3.92	19.46	-8.38	7.16
Mar	1.84	4.95	-10.46	-7.35
Apr	20.24	2.80	7.94	-9.50
May	16.10	82.32	3.80	70.02
Jun	65.57	106.19	53.27	93.89
Jul	82.69	97.82	70.39	85.52
Aug	72.22	148.54	59.92	136.24
Sep	66.16	239.62	53.86	227.32
Oct	102.26	286.47	89.96	274.17
Nov	38.75	140.62	26.45	128.32
Dec	31.86	58.92	19.56	46.62
Total	**512.22**	**1,233.00**	**364.62**	**1,085.40**
Average	**42.69**	**102.75**	**30.39**	**90.45**

As a result, the monthly water supply with ecological water requirement consideration under the dry year scenario varies from -10.46 million m^3 in March to 89.96 million m^3 in October, with an average water supply of 30.39 million m^3 per month. In the meantime, the average water supply in the summer season (December to March) varies from the lowest value of -10.46 million m^3 in March to the highest value of 19.56 million m^3 in December. Meanwhile, the average water supply in the rainy season (April to November) varies from the lowest value of 3.80 million m^3 in May to the highest value of 89.96 million m^3 in October.

Meanwhile, under the wet year scenario, the monthly water supply with ecological water requirement consideration varies from -9.50 million m^3 in April to 274.17 million m^3 in October, with an average water supply of 90.45 million m^3 per month. In the meantime, the average water supply in the summer season (December to March) varies from the lowest value of -7.35 million m^3 in March to the highest value of 46.62 million m^3 in December. Meanwhile, the average water supply in the rainy season (April to November) varies from the lowest value of -9.50 million m^3 in April to the highest value of 274.17 million m^3 in October.

Besides, monthly water demand data of four different categories (residential, tourism, agriculture, and forest uses) for monthly water balance with ecological water requirement consideration, which were estimated based on the derived annual water demand with specific assumptions, had been mentioned in the previous section (see Table. 8.7).

Consequently, monthly water balance with ecological water requirement consideration in terms of surplus and deficit under normal and new normal conditions between 2020 and 2029 was estimated as reported in Table 8.11.

Table 8.11 Monthly water supply and demand balance evaluation with ecological water requirement consideration between 2020 and 2029.

Month	Water supply (million m^3)		Water demand (million m^3)		Water balance (surplus or deficit) (million m^3)			
					Dry year		Wet year	
	Dry year	Wet year	Normal	New normal	Normal	New normal	Normal	New normal
Jan	-1.69	33.01	41.51	41.05	-43.19	-42.74	-8.50	-8.04
Feb	-8.38	7.16	40.78	40.36	-49.16	-48.74	-33.62	-33.19
Mar	-10.46	-7.35	44.91	44.47	-55.37	-54.93	-52.27	-51.82
Apr	7.94	-9.50	41.35	40.99	-33.41	-33.06	-50.85	-50.50
May	3.80	70.02	38.04	37.78	-34.24	-33.98	31.98	32.24
Jun	53.27	93.89	37.23	36.89	16.03	16.37	56.65	56.99
Jul	70.39	85.52	37.61	37.37	32.79	33.02	47.91	48.15
Aug	59.92	136.24	37.86	37.62	22.06	22.30	98.38	98.62
Sep	53.86	227.32	33.39	33.15	20.47	20.71	193.94	194.18
Oct	89.96	274.17	33.82	33.49	56.14	56.47	240.35	240.67
Nov	26.45	128.32	33.85	33.53	-7.39	-7.08	94.47	94.78
Dec	19.56	46.62	37.77	37.33	-18.21	-17.77	8.85	9.28
Total	**364.62**	**1,085.40**	**458.11**	**454.03**	**-93.48**	**-89.41**	**627.29**	**631.37**

As a result in Table 8.11, under dry year scenarios with the normal condition, the monthly water balance with ecological water requirement consideration between 2020 and 2029 is water deficit from November to May, and it varies from -55.37 million m^3 in March to -7.39 million m^3 in November. In the meantime, the monthly water balance in the same period is water surplus from June to October, and it varies from 16.03 million m^3 in June to 56.14 million m^3 in October.

On the contrary, under dry year scenarios with the new normal condition, the monthly water balance between 2020 and 2029 is water deficit from November to May, and it varies from -54.93 million m^3 in March to -7.08 million m^3 in November. In the meantime, the monthly water balance in the same period is water surplus from June to October, and it varies from 16.37 million m^3 in June to 56.47 million m^3 in October.

Figure 8.9 compares monthly deficit and surplus water balance with ecological water requirement consideration between 2020 and 2029 under dry year scenario with normal and new normal.

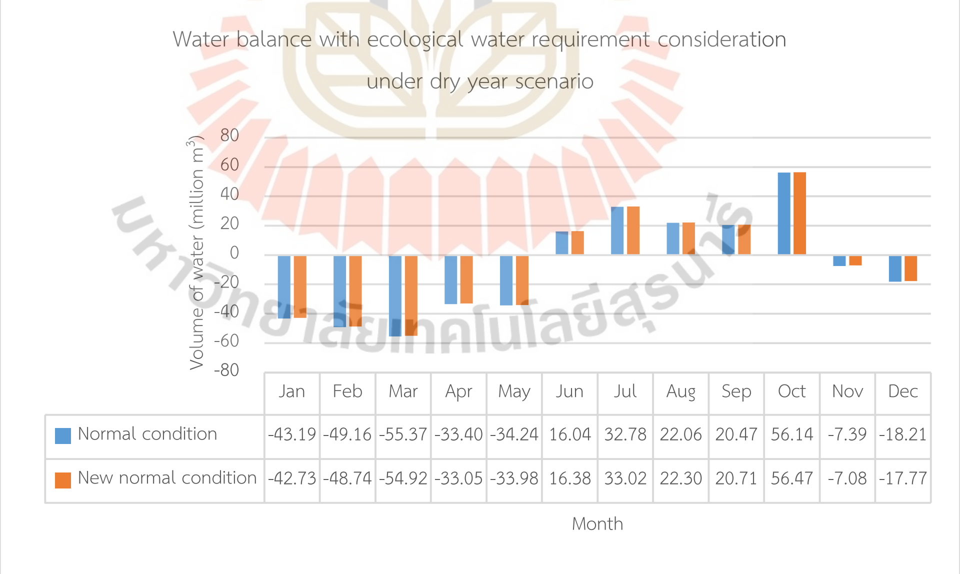

	Jan	Feb	Mar	Apr	May	Jun	Jul	Aug	Sep	Oct	Nov	Dec
🟦 Normal condition	-43.19	-49.16	-55.37	-33.40	-34.24	16.04	32.78	22.06	20.47	56.14	-7.39	-18.21
🟧 New normal condition	-42.73	-48.74	-54.92	-33.05	-33.98	16.38	33.02	22.30	20.71	56.47	-7.08	-17.77

Figure 8.9 Monthly water balance with ecological water requirement consideration between 2020 and 2029 under dry year scenario with normal and new normal condition.

In the meantime, under wet year scenarios with the normal condition as a result in Table 8.11, the monthly water balance with ecological water requirement consideration between 2020 and 2029 is water deficit from January to April. It varies from -52.27 million m^3 in March to -8.50 million m^3 in January. Meanwhile, the monthly water balance in the same period is water surplus from May to December, and it varies from 8.85 million m^3 in December to 240.35 million m^3 in October.

On the contrary, the monthly water balance between 2020 and 2029 is a water deficit from January to April under wet year scenario with the new normal condition. It varies from -51.82 million m^3 in March to -8.04 million m^3 in January. In the meantime, the monthly water balance in the same period is water surplus from May to December, and it varies from 9.28 million m^3 in December to 240.67 million m^3 in October.

Figure 8.10 compares monthly deficit and surplus water balance with ecological water requirement consideration between 2020 and 2029 under wet year scenario with normal and new normal.

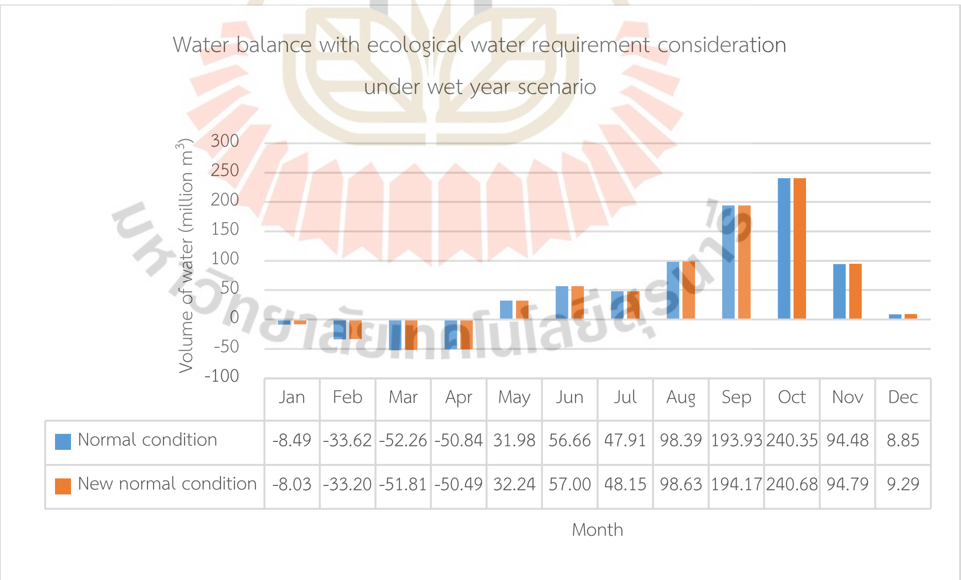

	Jan	Feb	Mar	Apr	May	Jun	Jul	Aug	Sep	Oct	Nov	Dec
🟦 Normal condition	-8.49	-33.62	-52.26	-50.84	31.98	56.66	47.91	98.39	193.93	240.35	94.48	8.85
🟧 New normal condition	-8.03	-33.20	-51.81	-50.49	32.24	57.00	48.15	98.63	194.17	240.68	94.79	9.29

Figure 8.10 Monthly water balance with ecological water requirement consideration between 2020 and 2029 under wet year scenario with normal and new normal condition.

In summary, the water balance evaluation with ecological water requirement consideration between 2020 and 2029 was divided into two main results: annual and monthly water balance under two different scenarios with two different conditions.

In the study period, the annual water balance with ecological water requirement consideration in Phuket Island discovered water deficit all years under dry year scenarios, while water surplus all years under wet year scenarios with normal and new normal conditions.

On the contrary, the monthly water balance with ecological water requirement consideration in Phuket Island in the same period exposed water deficit and surplus under dry and wet year scenarios with normal and new normal conditions. It was found that the monthly water deficit occurred in seven months (November to May) under dry year scenario with normal and new normal conditions, while monthly water deficit occurred in four months (January to April) under wet year scenario with normal and new normal conditions.

In addition, the water balance of agricultural and forest uses in 25 watersheds, excluding residential and tourist water demand, without and with ecological water requirement consideration is summarized in Tables 8.12 and 8.13, respectively.

As a result in Table 8.12, the water balance of agricultural and forest uses in 25 watersheds without ecological water requirement consideration under dry year scenario was found water deficit in 12 watersheds and water surplus in 13 watersheds in 2019, while the water deficit in 10 watersheds and water surplus in 15 watersheds in 2029. The highest water deficit occurred in the Khlong Tha Maprao watershed, with a value of -10.36 and -8.39 million m^3 in 2019 and 2029, while the highest water surplus occurred in the Khlong Bang Yai watershed, with a value of 66.21 and 72.39 million m^3 in 2019 and 2029. On the contrary, the water balance in 25 watersheds without ecological water requirement consideration was found water surplus in 25 watersheds under the wet year scenario. The highest water surplus occurred in the Khlong Bang Yai watershed, with a value of 176.52 and 182.71 million m^3 in 2019 and 2029. Mean

Furthermore, as a result, in Table 8.13, the water balance evaluation of agricultural and forest uses in 25 watersheds with ecological water requirement consideration under dry year scenario was found water deficit in 22 watersheds and water surplus in 3 watersheds in 2019, while water deficit in 20 watersheds and water surplus in 5 watersheds in 2029. The highest water deficit occurred in the Khlong Tha Maprao watershed, with a value of -17.80 and -15.83 million m^3 in 2019 and 2029, while the highest water surplus occurred in the Khlong Bang Yai watershed, with a value of 58.77, 64.94 million m^3 in 2019 and 2029. On the contrary, the water balance in 25 watersheds without ecological water requirement consideration under wet year scenario was found water deficit in 5 watersheds and water surplus in 20 watersheds in 2019, while water deficit in 4 watersheds and water surplus in 21 watersheds in 2029. The highest water deficit occurred in the Ban Nai Thon watershed, with a value of -4.79 and -4.40 million m^3 in 2019 and 2029, while the highest water surplus occurred in the Khlong Bang Yai watershed, with a value of 169.07 and 175.26 million m^3 in 2019 and 2029.

Moreover, the significant change of the water balance in 25 watersheds with and without ecological water requirement consideration from 2019 to 2029 was found in the Khlong Kala watershed under both dry and wet year scenarios.

Table 8.12 The annual water supply and demand balance evaluation in 25 watersheds without ecological water requirement consideration.

No	Watershed	Water supply in different scenarios (million m^3)						Water demand for agriculture and forest uses (million m^3)			Water balance evaluation (surplus or deficit) (million m^3)					
		Dry year			Wet year						Dry year			Wet year		
		2019	2029	Δ	2019	2029	Δ	2019	2029	Δ	2019	2029	Δ	2019	2029	Δ
1	Khlong Ban Yit	17.46	17.49	0.03	61.23	61.23	0.00	25.18	24.40	-0.78	-7.72	-6.91	0.81	36.05	36.83	0.78
2	Khlong Ban Ao Tu Khun	5.92	5.92	0.00	20.51	20.48	-0.02	10.99	10.60	-0.40	-5.08	-4.68	0.40	9.51	9.88	0.37
3	Khlong Tha Maprao	23.73	23.77	0.04	75.37	74.75	-0.62	34.09	32.16	-1.93	-10.36	-8.39	1.97	41.28	42.59	1.30
4	Khlong Pama Lhong	14.73	14.73	0.00	37.96	37.96	0.00	12.91	12.23	-0.68	1.82	2.50	0.68	25.05	25.73	0.68
5	Khlong Ao Kung	15.38	15.15	-0.23	44.68	44.58	-0.10	21.03	20.46	-0.57	-5.65	-5.31	0.34	23.65	24.12	0.48
6	Ban Nai Thon	3.11	3.01	-0.09	12.97	12.89	-0.08	10.33	9.85	-0.48	-7.22	-6.84	0.38	2.65	3.04	0.40
7	Khlong Bang Rong	11.75	11.75	0.00	36.23	36.23	0.00	19.52	19.23	-0.29	-7.78	-7.48	0.29	16.71	17.00	0.29
8	Khlong Bang Pea	3.71	3.71	0.00	13.04	13.04	0.00	8.36	8.36	0.00	-4.64	-4.64	0.00	4.68	4.68	0.00
9	Khlong Pa Khlok	6.84	6.84	0.00	21.72	21.72	0.00	10.65	10.59	-0.06	-3.81	-3.75	0.06	11.06	11.12	0.06
10	Khlong Phak Chit	4.29	5.20	0.91	13.55	14.73	1.17	8.79	8.72	-0.08	-4.50	-3.51	0.99	4.76	6.01	1.25
11	Khlong Kala	50.43	58.43	7.99	156.97	162.86	5.88	58.92	54.43	-4.49	-8.49	3.99	12.48	98.05	108.43	10.38
12	Khlong Bang Thao	9.44	9.43	-0.01	21.75	21.72	-0.02	4.91	4.42	-0.49	4.52	5.00	0.48	16.84	17.30	0.46
13	Khlong Chang Phan Lang	4.05	4.16	0.11	9.87	9.87	0.00	2.38	1.28	-1.10	1.67	2.88	1.21	7.49	8.59	1.10
14	Khlong Tha Rua	63.58	64.42	0.84	135.35	136.22	0.87	42.74	38.78	-3.96	20.84	25.64	4.80	92.61	97.44	4.83
15	Khlong Kamala	17.22	17.61	0.39	37.52	38.09	0.57	16.79	15.22	-1.57	0.43	2.39	1.96	20.73	22.87	2.14
16	Khlong Ban Na Kha	4.81	4.81	0.00	10.81	10.81	0.00	5.28	5.09	-0.19	-0.46	-0.28	0.19	5.54	5.72	0.19
17	Ban Ko Sire	15.20	15.25	0.04	36.71	36.60	-0.10	14.95	8.44	-6.51	0.25	6.80	6.55	21.75	28.16	6.41
18	Khlong Pa Tong	20.97	22.26	1.29	44.61	46.48	1.87	15.44	12.55	-2.89	5.53	9.72	4.18	29.17	33.93	4.76
19	Khlong Bang Yai	111.05	110.89	-0.16	221.36	221.21	-0.15	44.84	38.50	-6.34	66.21	72.39	6.18	176.52	182.71	6.19
20	Ao Karon	13.90	14.89	0.99	30.32	31.79	1.47	13.77	11.21	-2.56	0.13	3.68	3.55	16.55	20.58	4.03
21	Khlong Kata	51.27	52.62	1.35	106.02	107.50	1.48	22.00	17.02	-4.98	29.28	35.61	6.33	84.02	90.48	6.46
22	Khao Khad (Khlong Ao Yon)	5.04	6.26	1.23	12.78	14.93	2.14	7.16	2.87	-4.29	-2.12	3.40	5.52	5.63	12.06	6.43
23	Ao Kata Noi and Ao Kata Yai	10.39	11.55	1.15	22.27	24.00	1.73	7.91	6.68	-1.23	2.49	4.87	2.38	14.36	17.32	2.96
24	Khlong Sai Yuan	11.05	11.53	0.48	22.62	22.87	0.25	3.81	3.02	-0.79	7.24	8.51	1.27	18.81	19.85	1.04
25	Khlong Ya Yai	8.85	9.89	1.04	18.05	19.22	1.17	5.06	3.96	-1.10	3.79	5.93	2.14	12.99	15.26	2.27
	Max	**111.05**	**110.89**	**7.99**	**221.36**	**221.21**	**5.88**	**58.92**	**54.43**	**0.00**	**66.21**	**72.39**	**12.48**	**176.52**	**182.71**	**10.38**
	Min	**3.11**	**3.01**	**-0.23**	**9.87**	**9.87**	**-0.62**	**2.38**	**1.28**	**-6.51**	**-10.36**	**-8.39**	**0.00**	**2.65**	**3.04**	**0.00**

Table 8.13 The annual water supply and demand balance evaluation in 25 watersheds with ecological water requirement consideration.

No	Watershed	Water supply in different scenarios (million m^3)						Water demand for agriculture and forest uses (million m^3)			Water balance evaluation (surplus or deficit) (million m^3)					
		Dry year			Wet year						Dry year			Wet year		
		2019	2029	Δ	2019	2029	Δ	2019	2029	Δ	2019	2029	Δ	2019	2029	Δ
1	Khlong Ban Yit	10.02	10.05	0.03	53.78	53.79	0.00	25.18	24.40	-0.78	-15.16	-14.35	0.81	28.60	29.39	0.78
2	Khlong Ban Ao Tu Khun	-1.52	-1.52	0.00	13.06	13.04	-0.02	10.99	10.60	-0.40	-12.52	-12.12	0.40	2.07	2.44	0.37
3	Khlong Tha Maprao	16.29	16.33	0.04	67.93	67.30	-0.62	34.09	32.16	-1.93	-17.80	-15.83	1.97	33.84	35.14	1.30
4	Khlong Pama Lhong	7.29	7.29	0.00	30.52	30.52	0.00	12.91	12.23	-0.68	-5.62	-4.94	0.68	17.61	18.29	0.68
5	Khlong Ao Kung	7.94	7.71	-0.23	37.24	37.14	-0.10	21.03	20.46	-0.57	-13.09	-12.75	0.34	16.21	16.68	0.48
6	Ban Nai Thon	-4.34	-4.43	-0.09	5.53	5.45	-0.08	10.33	9.85	-0.48	-14.66	-14.28	0.38	-4.79	-4.40	0.40
7	Khlong Bang Rong	4.30	4.31	0.00	28.79	28.79	0.00	19.52	19.23	-0.29	-15.22	-14.93	0.29	9.27	9.56	0.29
8	Khlong Bang Pea	-3.73	-3.73	0.00	5.60	5.60	0.00	8.36	8.36	0.00	-12.08	-12.08	0.00	-2.76	-2.76	0.00
9	Khlong Pa Khlok	-0.60	-0.60	0.00	14.27	14.27	0.00	10.65	10.59	-0.06	-11.25	-11.19	0.06	3.62	3.68	0.06
10	Khlong Phak Chit	-3.15	-2.24	0.91	6.11	7.29	1.17	8.79	8.72	-0.08	-11.94	-10.95	0.99	-2.68	-1.43	1.25
11	Khlong Kala	42.99	50.99	7.99	149.53	155.42	5.88	58.92	54.43	-4.49	-15.93	-3.45	12.48	90.61	100.98	10.38
12	Khlong Bang Thao	1.99	1.98	-0.01	14.31	14.28	-0.02	4.91	4.42	-0.49	-2.92	-2.44	0.48	9.40	9.86	0.46
13	Khlong Chang Phan Lang	-3.39	-3.28	0.11	2.43	2.43	0.00	2.38	1.28	-1.10	-5.77	-4.56	1.21	0.05	1.15	1.10
14	Khlong Tha Rua	56.14	56.98	0.84	127.91	128.78	0.87	42.74	38.78	-3.96	13.40	18.20	4.80	85.16	89.99	4.83
15	Khlong Kamala	9.78	10.17	0.39	30.08	30.65	0.57	16.79	15.22	-1.57	-7.01	-5.05	1.96	13.29	15.43	2.14
16	Khlong Ban Na Kha	-2.63	-2.63	0.00	3.37	3.37	0.00	5.28	5.09	-0.19	-7.91	-7.72	0.19	-1.91	-1.72	0.19
17	Ban Ko Sire	7.76	7.80	0.04	29.26	29.16	-0.10	14.95	8.44	-6.51	-7.19	-0.64	6.55	14.31	20.72	6.41
18	Khlong Pa Tong	13.53	14.82	1.29	37.17	39.04	1.87	15.44	12.55	-2.89	-1.91	2.27	4.18	21.73	26.49	4.76
19	Khlong Bang Yai	103.61	103.45	-0.16	213.92	213.77	-0.15	44.84	38.50	-6.34	58.77	64.94	6.18	169.07	175.26	6.19
20	Ao Karon	6.46	7.45	0.99	22.88	24.35	1.47	13.77	11.21	-2.56	-7.31	-3.76	3.55	9.11	13.14	4.03
21	Khlong Kata	43.83	45.18	1.35	98.58	100.06	1.48	22.00	17.02	-4.98	21.84	28.17	6.33	76.58	83.04	6.46
22	Khao Khad (Khlong Ao Yon)	-2.40	-1.18	1.23	5.34	7.49	2.14	7.16	2.87	-4.29	-9.56	-4.04	5.52	-1.81	4.62	6.43
23	Ao Kata Noi and Ao Kata Yai	2.95	4.11	1.15	14.82	16.56	1.73	7.91	6.68	-1.23	-4.95	-2.57	2.38	6.92	9.88	2.96
24	Khlong Sai Yuan	3.61	4.09	0.48	15.18	15.43	0.25	3.81	3.02	-0.79	-0.20	1.07	1.27	11.37	12.41	1.04
25	Khlong Ya Yai	1.41	2.45	1.04	10.61	11.78	1.17	5.06	3.96	-1.10	-3.65	-1.51	2.14	5.55	7.82	2.27
	Max	**103.61**	**103.45**	**7.99**	**213.92**	**213.77**	**5.88**	**58.92**	**54.43**	**0.00**	**58.77**	**64.94**	**12.48**	**169.07**	**175.26**	**10.38**
	Min	**-4.34**	**-4.43**	**-0.23**	**2.43**	**2.43**	**-0.62**	**2.38**	**1.28**	**-6.51**	**-17.80**	**-15.83**	**0.00**	**-4.79**	**-4.40**	**0.00**

Recommendation for water resource management in Phuket Island

Referring to previous studies and provincial reports on surface water in Phuket Island, Information Technology and Communication Division, Phuket Provincial Office (2010) states that surface water supply accounts for about 38 million m^3 per year. Likewise, Sma-air (2012) found that the 99 surface water sites have a total volume of 36.54 million m^3 per year. In recent years, Prince of Songkla University, Phuket Campus (2017) reported that the 111 surface water sites for water consumption in Phuket Island have a total volume of 38.42 million m^3 per year.

According to these studies, it can be concluded that Phuket Island's surface water supply is approximately 38 million m^3 per year. Additionally, Information Technology and Communication Division, Phuket Provincial Office (2010) reported that the productivity of groundwater sources was about 4 million m^3 per year and seawater was about 4 million m^3 per year. Thus, the water supply in Phuket Island from three sources (surface water, groundwater, and seawater) is 46 million m^3 per year. Meanwhile, according to the current study, water demand (residential and tourist) between 2020 and 2029 was about 56 million m^3 under the normal condition and about 52.00 million m^3 under the new normal condition.

Consequently, water scarcity might be happening in the future. Mitigation of water scarcity is a big challenge to manage water resources in Phuket Island. Some recommendations for water resources management from highest to lowest priority are discussed and addressed as the following.

1. The existing surface water supply sites (e.g., reservoir or old mine pit) should be improved to increase their capacities by reconstruction. The construction of a new reservoir for increasing water storage capacity in Phuket Island is limited since most suitable areas are located in protected forest areas (national park and national reserved forests), primarily situated in mountainous areas covered with tropical evergreen forest. Additionally, some areas such as mine pits had been developed to support tourism facilities, leading to exceptionally high land prices.

2. Groundwater is another alternative source for increasing water supply to Phuket Island. In this alternative, the local authorities should manage groundwater

pumping by themselves instead of providing the individual license. However, the local authorities should study more about groundwater potential and the suitable sites in more detail. Ideally, groundwater utilization should install deep wells and create adequate distribution networks for local communities.

3. Seawater desalination plant is another alternative source that might be suitable for Phuket Island. Nevertheless, the cost of water and environmental threats, particularly negative physicochemical and ecological impacts on marine environments, from hypersaline discharges (brine) causing plumes with elevated salinities, should be seriously considered.

4. Importing water supply from the mainland, like Phang Nga Province, proposed by the Government might be another source for increasing water supply capacity. This project should be exercised by the Environmental Impact Assessment (EIA) to minimize adverse effects on local people. Particularly, sharing of water supply in the project should meet local people first, then share it to Phuket Island.

These recommendations are not guaranteed to solve water scarcity problems sustainably since water scarcity depends on future water demand in Phuket Island. To confirm the previously studied, the local authorities must study more about the current surface water storage and the accessibility of possible groundwater and seawater. Together, the number of registered and non-registered populations tourists and excursionists should be carefully estimated based on historical and current records. This study estimated a non-registered population based on the historical trend of the censused data between 1980 and 2010. Additionally, the consumption rate in a different community type should be updated from the field survey by responding agencies, such as Phuket Provincial Waterworks Authority.

Nevertheless, these recommendations with the required information are essential to prevent future water scarcity in Phuket Island.

CHAPTER IX

CONCLUSION AND RECOMMENDATIONS

In this chapter, five main results, which were reported according to research objectives of the study in the previous chapters, including (1) land use and land cover assessment and change detection, (2) land use and land cover simulation, (3) water yield estimation, (4) water demand estimation, and (5) water balance evaluation, are concluded, and recommendations for future research and development are suggested.

9.1 Conclusion

Brief information of research methodology and high light from each research objective was separately concluded in the following.

9.1.1 Land use and land cover assessment and change detection

The historical record of LULC data in 2014 was collected from the previous study of Boonchoo (2015). Meanwhile, the recent LULC data in 2019 were successfully extracted eleven LULC types, including (1) urban and built-up areas (city and commercial, institutional land, industrial land, poultry farms, houses, airport, and seaport), (2) paddy fields, (3) field crops and horticulture, (4) perennial trees and orchards (para rubber and mixed orchards), (5) aquaculture areas, (6) idle land, (7) evergreen forests, (8) mangrove forests, (9) scrub forests, (10) water bodies (natural and artificial), and (11) miscellaneous land (beaches, soil pits, laterite pits, and landfill) from Pleiades and SPOT imageries using visual interpretation.

As a result, the top three most dominant LULC types in 2019 were perennial trees and orchards (35.32%), urban and built-up area (27.13%), and evergreen forest (14.20%). The overall accuracy and Kappa hat coefficient of the interpreted LULC map in 2019 were 96.06% and 95.15%. According to change detection between LULC in 2014 and 2019, the significantly increasing LULC types in this period were urban and built-up areas and idle land. The significant decreasing LULC types are perennial trees and orchards, and evergreen forests. The increasing of urban and built-up areas in 2019 were mostly converted from perennial trees and orchards and idle land in 2014 for supporting tourist facilities such as hotels, resorts, recreational and commercial areas.

9.1.2 Land use and land cover simulation

The LULC data from 2020 to 2029 were simulated using the CLUE-S model based on the historical LULC change between 2014 and 2019. In practice, the conversion matrix and elasticity of LULC change and land demand were first estimated and then combined simultaneously with driving factors on LULC change to simulate LULC data between 2020 and 2029. The driving factors on LULC change for specific land use type allocation were analyzed using multicollinearity test and binomial logistics regression analysis included elevation, slope, soil fertility, distance to road, distance to settlement, distance to water bodies, population density at the sub-district level, and the average income per capita at the sub-district level.

As a result, the most significant driving factor for allocating LULC type was the distance to water bodies. The derived multiple linear equations delivered the AUC values from 0.65 to 0.94, and the deviation values between the estimated (land demand) and the simulated areas varied from -0.01 to 0.00 km^2. The simulated LULC data showed an increase in urban and built-up areas, field crop and horticulture, idle land, scrub forest, water bodies, decreasing paddy fields, perennial trees, and orchards aquaculture, evergreen forest, mangrove forest, and miscellaneous land.

9.1.3 Water yield estimation

The SWAT model was effectively estimated the time-series water yield between 2020 and 2029 in Phuket Island under two different scenarios: dry and wet years. In practice, Klong Bang Yai watershed was selected to calibrate and validate the optimal local model parameters, including curve number at moisture condition II, available soil water capacity, soil evaporation compensation factor, surface runoff lag coefficient, baseflow alpha factor, groundwater “revap” coefficient, and groundwater delay, for dry and wet years. After that, the optimum model parameters were applied to estimate the water yield of the baseline year (2019) and time series years (2020-2029).

As a result, the most sensitive parameter in the Khlong Bang Yai watershed was available soil water capacity. The optimum local parameter of the

SWAT model provided at least good model performance under dry and wet conditions under calibration and validation periods. The annual water yield between 2020 and 2029 varied from 505.01 million m^3 to 521.79 million m^3, with an average value of 512.22 million m^3 under the dry year scenario. The average monthly water yield in the summer season (December to March) varied from 1.84 million m^3 in March to 31.86 million m^3 in December. The average monthly water yield in the rainy season (April to November) varied from 16.10 million m^3 in May to 102.26 million m^3 in October. On the contrary, under the wet year scenario, the annual water yield in the same period varied from 1,225.48 million m^3 to 1,242.08 million m^3, with an average value of 1,233.00 million m^3. In the summer season, the average monthly water yield varied from 4.95 million m^3 in March to 58.92 million m^3 in December. The average monthly water yield in the rainy season varied from 2.80 million m^3 in April to 286.47 million m^3 in October.

In addition, the simple linear regression analysis between water yield in Phuket Island under dry and wet year scenarios and dominant LULC types (urban and built-up areas, idle land, perennial trees and orchards, evergreen forest) were conducted in this study. As a result, annual water yield in dry and wet year scenarios showed a positively high correlation with urban and built-up areas and idle land with the R^2 of 0.91 and 0.92, and 0.91 and 0.93, respectively. On the contrary, annual water yield in both scenarios disclosed a high negative correlation with perennial trees and orchards and evergreen forest with the R^2 of 0.91 and 0.92, and 0.91 and 0.92, respectively. Likewise, the linear relationship between water yield and four LULC types at six selected watershed levels under dry and wet scenarios was consistent with Phuket Island in three watersheds with large and small areas, including Khlong Kala and Khlong Tha Rua, and Khlong Chang Phan Lang. However, the linear relationship between water yield and four LULC types at the Khlong Bang Yai watershed was inconsistent with Phuket Island. The possible reason for this finding is the effect of a proportional LULC area in the watershed on surface runoff and water yield.

9.1.4 Water demand estimation

The water consumption rate for residential and tourists and water requirements for agriculture and forest were successfully applied to estimate water demand for each component under normal and new normal (COVID-19 pandemic) conditions.

As a result, the water demand of Phuket Island between 2020 and 2029 under the normal condition varied from 442.09 million m^3 to 475.86 million m^3, with an average value of 458.10 million m^3. Meanwhile, the water demand of Phuket Island in the same period under the new normal condition varied from 442.09 million m^3 to 461.53 million m^3, with an average value of 454.03 million m^3. Water demand under two scenarios mainly was contributed to agriculture and forest uses. The contribution of water demand of agriculture use, forest use, and residential and tourists under normal conditions were about 54.78%, 32.98%, 7.55%, and 4.69%, respectively. On the contrary, the contribution of water demand of those components under the new normal condition was approximately 55.27%, 33.28%, 7.62%, and 3.84%, respectively.

In addition, in both scenarios, Phuket Island's average annual residential water demand between 2020 and 2029 was continuously increased from 32.58 million m^3 in 2020 to 37.25 million m^3 in 2029. Notably, residential water demand was higher in the urban areas than in the rural areas of Phuket Island. It causes the growth of the population in the same period, and the consumption patterns are different. In the meantime, the tourist water demand under the normal condition in the same period was continuously increased from 18.86 million m^3 in 2020 to 24.76 million m^3 in 2029. On the contrary, under the new normal condition, the tourist water demand varied from 4.52 million m^3 to 24.76 million m^3. The tourist water demand was dropped between 2020 and 2023 since the COVID-19 pandemic. Still, it continuously increases from 2024 to 2029. Meanwhile, water demand for agriculture and forest uses under both scenarios continuously decreased between 2020 and 2029 because the predicted perennial trees and orchards and evergreen forests decreased in the same period.

9.1.5 Water balance evaluation

Annual and monthly water balance between 2020 and 2029 based on the derived water supply (with and without ecological water requirement considerations) and water demand under dry and wet year scenarios (with normal and new normal conditions) were successfully evaluated in terms of surplus and deficit for water resource management.

As a result, the annual water balance evaluation without ecological water requirement consideration in Phuket Island between 2020 and 2029 disclosed water surplus every year under dry and wet year scenarios with normal and new normal conditions. In the meantime, the monthly water balance exposed water deficit and surplus under dry and wet year scenarios with normal and new normal conditions. The monthly water deficit occurred in six months (December to May) under dry year scenarios with normal and new normal conditions, while the monthly water deficit occurred in three months (February to April) under wet year scenarios with normal and new normal conditions.

On the contrary, the annual water balance with ecological water requirement consideration in Phuket Island between 2020 and 2029 revealed water deficit in every year under dry year scenario with normal and new normal conditions. Still, it exposed water surplus every year under wet year scenarios with identical conditions. Meanwhile, the monthly water balance exposed water deficit and surplus under both scenarios with both conditions. The monthly water deficit occurred in seven months (November to May) under the dry year scenario with normal and new normal conditions. The monthly water deficit occurred in four months (January to April) under the wet year scenario with normal and new normal conditions.

Consequently, it can be concluded that integrating remote sensing data (very high spatial resolution) with advanced geospatial models (CLUE-S model, SWAT model, and water footprint assessment) can deliver essential information to mitigate water scarcity in Phuket Island in the future.

9.2 Recommendations

Four research objectives were successfully implemented for land use and land cover assessment and change detection, land use and land cover simulation, water yield estimation, water demand estimation, and water balance evaluation in Phuket Island, Thailand. The possible expected recommendations and implications could be made for further studies as follows.

(1) Dry and wet year conditions should be identified using a standardized precipitation index (SPI), as suggested by many researchers (e.g., Shahvari, Khalilian,

Mosavi, and Mortazavi, 2019; Kimaru, Gathenya, and Cheruiyot, 2019; Nasta, Allocca, Deidda, and Romano, 2020). It might be easier to identify both conditions using the long-term rainfall data. This study categorized annual runoff data into two conditions: dry and wet years, with mean annual runoff (between 1999 and 2019) at the X.191 station.

(2) The consumption rate in different community types should be updated from the field survey by responding agencies. Consequently, the estimation of residential water demand will be more precise.

(3) The conceptual framework and research workflows of this study (Figure 9.1) can be used as a guideline for government agencies, particularly the Department of Disaster Prevention and Mitigation, to examine another area where water deficit exists in many provinces in the Northeast Region, Thailand.

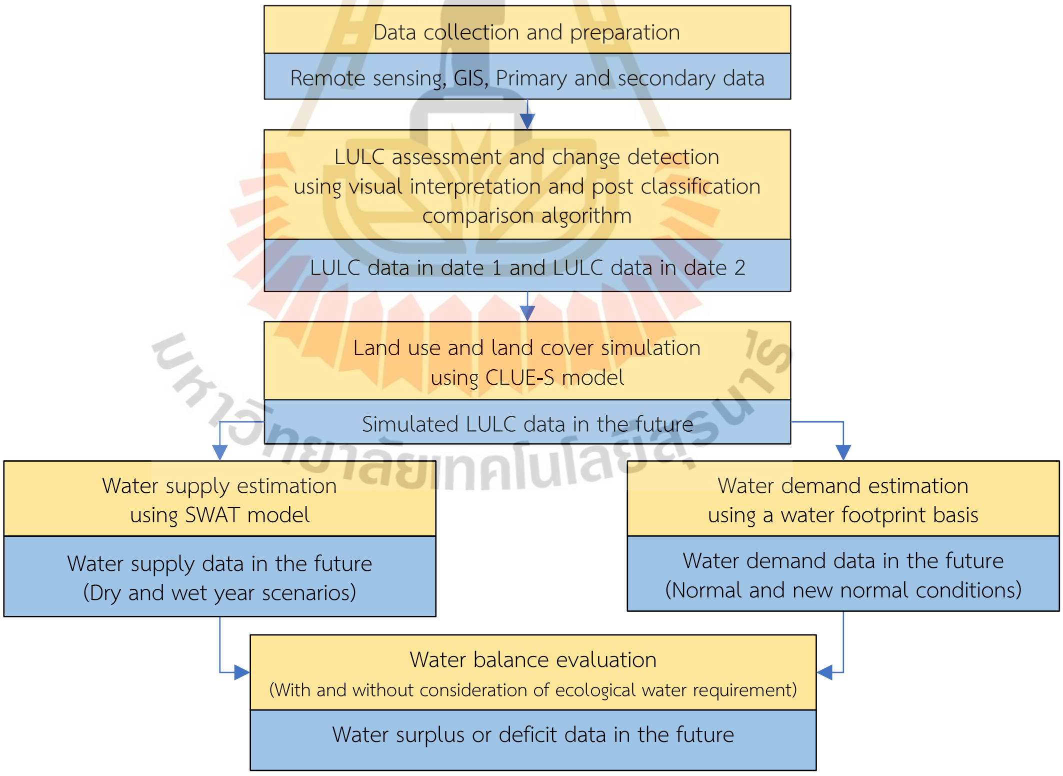
Data collection and preparation
Remote sensing, GIS, Primary and secondary data
LULC assessment and change detection using visual interpretation and post classification comparison algorithm
LULC data in date 1 and LULC data in date 2
Land use and land cover simulation using CLUE-S model
Simulated LULC data in the future
Water supply estimation using SWAT model
Water supply data in the future (Dry and wet year scenarios)
Water demand estimation using a water footprint basis
Water demand data in the future (Normal and new normal conditions)
Water balance evaluation
(With and without consideration of ecological water requirement)
Water surplus or deficit data in the future

Figure 9.1 The conceptual framework and research workflows.

REFERENCES

REFERENCES

Abou Rafee, S., Uvo, C., Martins, J., Domingues, L., Rudke, A., Fujita, T., & Freitas, E. (2019). Large-Scale Hydrological Modelling of the Upper Paraná River Basin. *Water, 11,* 882.

Adeniyi, G. A., Bolaji, F. S., Adebayo, W. S., & Michael, O. D. (2014). Validation of SWAT Model for Prediction of Water Yield and Water Balance: Case Study of Upstream Catchment of Jebba Dam in Nigeria. *International Scholarly and Scientific Research & Innovation, 8*(2), 264-270.

Alam, K. (2015). Farmers' adaptation to water scarcity in drought-prone environments: A case study of Rajshahi District, Bangladesh. *Agricultural Water Management, 148,* 196-206.

Allen, R. G., Pereira, L. S., Raes, D., & Smith, M. (1998). *Crop evapotranspiration - Guidelines for computing crop water requirements - FAO Irrigation and drainage paper 56.* Rome: Food and Agriculture Organization.

Anderson, J. R., Hardy, E. E., Roach, J. T., & Witmer, R. E. (1976). *A land use and land cover classification system for use with remote sensor data.* Washington: Geological Survey of United States.

Arnold, J. G., & Fohrer, N. (2005). SWAT2000: current capabilities and research opportunities in applied watershed modelling. *Hydrol. Process, 19*(3), 563-572.

Arnold, J. G., Moriasi, D. N., Gassman, P. W., Abbaspour, K. C., White, M. J., Srinivasan, R., Santhi, C., Harmel, R. D., Van Griensven, A., Van Liew, M. W., Kannan, N., & Jha, M. K. (2012). SWAT: MODEL USE, CALIBRATION, AND VALIDATION. *Transactions of the ASABE, 55*(4), 1491-1508.

Arnold, J. G., Srinivasan, R., Muttiah, R. S., & Williams, J. R. (1998). Large Area Hydrologic Modeling and Assessment Part I: Model Development. *Journal of the American Water Resources Association, 34*(1), 73-89.

Arnold, J. G., Kiniry, J. R., Srinivasan, R., Williams, J. R., Haney, E. B., & Neitsch, S. L. (2012). *SWAT 2012 Input/Output Documentation.* Retrieved from https://swat.tamu.edu/media/69296/swat-io-documentation-2012.pdf.

Ayivi, F., & Jha, M. K. (2018). Estimation of water balance and water yield in the Reedy Fork-Buffalo Creek Watershed in North Carolina using SWAT. *International Soil and Water Conservation Research, 6*(3), 203-213.

Baker, T. J., & Miller, S. N. (2013). Using the Soil and Water Assessment Tool (SWAT) to assess land use impact on water resources in an East African watershed. *Journal of Hydrology, 486,* 100-111.

Boonchoo, K. (2015). *Geospatial models for land use and land cover prediction and deforestation vulnerability analysis in Phuket Island, Thailand* (Doctoral dissertation). Suranaree University of Technology, Nakhon Ratchasima.

Boretti, A., & Rosa, L. (2019). Reassessing the projections of the World Water Development Report. *Nature Partner Journals Clean Water, 2*(1), 15.

Cabral, P., & Zamyatin, A. (2009). Markov processes in modeling land use and land cover changes in Sintra-Cascais, Portugal. *Dyna, 76*(158), 191-198.

Campbell, J. B., & Wynne, R. H. (2011). *Introduction to Remote Sensing.* (5th ed). New York: The Guilford Press.

Charupongsopon, W. (1990). *Potential of Water Resources in Changwat Phuket* (Master's thesis). Chiang Mai University, Chiang Mai.

Congalton, R. G., & Green, K. (2009). *Assessing the Accuracy of Remotely Sensed Data: Principles and Practices.* (2nd ed.). Boca Raton: CRC Press.

Coppin, P., Jonckheere, I., Nackaerts, K., Muys, B., & Lambin, E. (2004). Digital change detection methods in ecosystem monitoring: a review. *International Journal of Remote Sensing, 25*(9), 1565-1596.

Department of Provincial Administration, Ministry of Interior. (2020). *Population of Phuket Province during 1993-2020.* Retrieved from http://stat.bora.dopa.go.th/new_stat/webPage/statByYear.php.

Dhopte, A. M. (2017). *Agrotechnology for Dryland Farming*. (2nd ed.). India: Scientific Publisher.

Douglas-Mankin, K., Srinivasan, R., & Arnold, J. (2010). Soil and Water Assessment Tool (SWAT) Model: Current Developments and Applications. *Transactions of the ASABE, 53*(5), 1423-1431.

Economics Tourism and Sports Division, Ministry of Tourism and Sports. (2019). *Domestic Tourism Statistics Q1-Q4 (Classify by region and province).* Retrieved from https://www.mots.go.th/more_news_new.php?cid=411.

Economics Tourism and Sports Division, Ministry of Tourism and Sports. (2020). *Domestic Tourism Statistics (Classify by region and province 2020).* Retrieved from https://www.mots.go.th/more_news_new.php?cid=594.

Fitzpatrick-Lins, K. (1981). Comparison of sampling procedures and data analysis for a land-use and land cover map. *Photogrammetric Engineering and Remote Sensing, 47*(3), 343 – 351.

Gao, X., Chen, X., Biggs, T., & Yao, H. (2018). Separating Wet and Dry Years to Improve Calibration of SWAT in Barrett Watershed, Southern California. *Water, 10*, 274.

Gassman, P. W., Reyes, M. R., Green, C. H., & Arnold, J. G. (2007). The Soil and Water Assessment Tool: Historical Development, Applications, and Future Research Directions. *Transactions of the ASABE, 50*(4), 1211-1250.

Giri, S., Arbab, N. N., & Lathrop, R. G. (2018). Water security assessment of current and future scenarios through an integrated modeling framework in the Neshanic River Watershed. *Journal of Hydrology, 563*, 1025-1041.

Gleick, P. H. (1998). Water in crisis: paths to sustainable water use. *Ecological Applications, 8*(3), 571–579.

Gupta, H. V., Sorooshian, S., & Yapo, P. O. (1999). Status of Automatic Calibration for Hydrologic Models: Comparison with Multilevel Expert Calibration. *Journal of Hydrologic Engineering, 4*(2), 135-143.

Han, H., Yang, C., & Song, J. (2015). Scenario Simulation and the Prediction of Land Use and Land Cover Change in Beijing, China. *Sustainability, 7*, 4260-4279.

Hanuphab, T. (2013). *Water budget assessment in Phuket province* (Master's thesis). Prince of Songkla University, Songkhla.

Herold, M., Liu, X., & Clarke, K. (2003). Spatial Metrics and Image Texture for Mapping Urban Land Use. *Photogrammetric Engineering and Remote Sensing, 69,* 991-1001.

Hoekstra, A. Y., Chapagain, A. K., Aldaya, M. M., & Mekonnen, M. M. (2011). *The Water Footprint Assessment Manual: Setting the Global Standard.* London: Earthscan.

Hosmer, D., Lemeshow, S., & Sturdivant, R. (2013). *Applied Logistic Regression.* (3rd ed). United States of America: John Wiley & Sons.

Hu, S., Fan, Y., & Zhang, T. (2020). Assessing the Effect of Land Use Change on Surface Runoff in a Rapidly Urbanized City: A Case Study of the Central Area of Beijing. *Land, 9*(1).

Hu, Y., Zheng, Y., & Zheng, X. (2013). Simulation of land-use scenarios for Beijing using CLUE-S and Markov composite models. *Chinese Geographical Science, 23,* 92-100.

Imran, H. M., Hossain, A., Islam, A. K. M. S., Rahman, A., Bhuiyan, M. A. E., Paul, S., & Alam. A. (2021). Impact of Land Cover Changes on Land Surface Temperature and Human Thermal Comfort in Dhaka City of Bangladesh. *Earth Systems and Environment, 5,* 667-693.

Information Technology and Communication Division, Phuket Provincial Office. (2010). *Phuket province briefing 2010.* Retrieved from http://123.242.171.10/descr/introduce/dataPK53/chapter4.pdf.

Information Technology and Communication Division, Phuket Provincial Office. (2012). *Phuket province briefing 2012.* Retrieved from http://123.242.171.10/descr/introduce/dataPK55.pdf.

Information Technology and Communication Division, Phuket Provincial Office. (2016). *Phuket province briefing 2016.* Retrieved from https://www.phuket.go.th/webpk/file_data/intropk/dataPK59.pdf.

Jensen, J. R. (2015). *Introductory Digital Image Processing: A Remote Sensing Perspective.* (4 th ed). Illinois: Pearson Education.

Jermar, M. K. (1987). *Water Resources and Water Management.* Netherlands: Elsevier.

Kifle, A. B., Mengistu, T. G., Stoffberg, G. H., & Tadesse, T. (2017). Climate change and population growth impacts on surface water supply and demand of Addis Ababa, Ethiopia. *Climate Risk Management, 18,* 21-33.

Kimaru, A. N., Gathenya, J. M., & Cheruiyot, C. K. (2019). The Temporal Variability of Rainfall and Streamflow into Lake Nakuru, Kenya, Assessed Using SWAT and Hydrometeorological Indices. *Hydrology, 6*(4).

Kundu, S., Khare, D., & Mondal, A. (2017). Past, present, and future land use changes and their impact on water balance. *Journal of Environmental Management, 197*, 582-596.

Kunto, S., & Ongsomwang, S. (2013). Optimum parameters for water runoff estimating in Huay Tung Lung watershed of Mun basin, Ubon Ratchathani province. In *The 1st Geoinformatics Conference for Graduate Students and Young Researchers 2013 (1st GI-GRAD 2013)* (pp. 1-16). Nakhon Ratchasima: Suranaree University of Technology.

Land Development Department. (2000). *Soil erosion in Thailand (In Thailand). Ministry of Agriculture and Cooperatives.* Bangkok: Land Development Department.

Leelawattanagoon, P. (2003). *Streamflow Characteristics of Phuket Island* (Master's thesis). Kasetsart University, Bangkok.

Legates, D., & McCabe, G. (1999). Evaluating the Use of “Goodness-of-Fit” Measures in Hydrologic and Hydroclimatic Model Validation. *Water Resources Research, 35*(1), 233-241.

Leta, O. T., El-Kadi, A. I., Dulai, H., & Ghazal, K. A. (2016). Assessment of climate change impacts on water balance components of Heeia watershed in Hawaii. *Journal of Hydrology: Regional Studies, 8,* 182-197.

Li, T., Yang, S., & Tan, M. (2019). Simulation and optimization of water supply and demand balance in Shenzhen: A system dynamics approach. *Journal of Cleaner Production, 207,* 882-893.

Liersch, S., Fournet, S., Koch, H., Djibo, A. G., Reinhardt, J., Kortlandt, J., Van Weert, F., Seidou, O., Klop, E., Baker, C., & Hattermann, F. F. (2019). Water resources planning in the Upper Niger River basin: Are their gaps between water demand

and supply. *Journal of Hydrology: Regional Studies, 21,* 176-194.

Lillesand, T. M., Kiefer, R. W., & Chipman, J. W. (2004). *Remote Sensing and Image Interpretation.* (5th ed). New York: John Wiley.

Lillesand, T. M., Kiefer, R. W., & Chipman, J. W. (2015). *Remote Sensing and Image Interpretation.* (7th ed). New York: John Wiley.

Liu, G., Jin, Q., Li, J., Li, L., He, C., Huang, Y., & Yao, Y. (2017). Policy factors impact analysis based on remote sensing data and the CLUE-S model in the Lijiang River Basin, China. *CATENA, 158,* 286-297.

Liu, M., Wang, Y., Li, D., & Xia, B. (2013). Dyna-CLUE Model Improvement Based on Exponential Smoothing Method and Land Use Dynamic Simulation. In: Bian, F., Xie, Y., Cui, X., & Zeng, Y. (Eds.). *Geo-Informatics in Resource Management and Sustainable Ecosystem* (pp. 266–277). Heidelberg: Springer.

Liu, W., Zhao, M., Cai, Y., Wang, R., & Lu, W. (2019). Synergetic Relationship between Urban and Rural Water Poverty: Evidence from Northwest China. *International journal of environmental research and public health, 16*(9), 1647.

Luan, X., Wu, P., Sun, S., Wang, Y., & Gao, X. (2018). Quantitative study of the crop production water footprint using the SWAT model. *Ecological Indicators, 89,* 1-10.

Miguel Ayala, L., van Eupen, M., Zhang, G., Pérez-Soba, M., Martorano, L. G., Lisboa, L. S., & Beltrao, N. E. (2016). Impact of agricultural expansion on water footprint in the Amazon under climate change scenarios. *Science of The Total Environment, 569-570,* 1159-1173.

Moriasi, D. N., Arnold, J. G., Van Liew, M. W., Bingner, R. L., Harmel, R. D., & Veith, T. L. (2007). Model Evaluation Guidelines for Systematic Quantification of Accuracy in Watershed Simulations. *Transactions of the ASABE, 50*(3), 885-900.

Mosase, E., Ahiablame, L., & Srinivasan, R. (2019). Spatial and temporal distribution of blue water in the Limpopo River Basin, Southern Africa: A case study. *Ecohydrology & Hydrobiology, 19*(2), 252-265.

Muratoglu, A. (2019). Water footprint assessment within a catchment: A case study for Upper Tigris River Basin. *Ecological Indicators, 106,* 105467.

Myint, S., & Wang, L. (2006). Multi-criteria Decision Approach for Land Use Land Cover Change Using Markov Chain Analysis and Cellular Automata Approach. *Canadian Journal of Remote Sensing, 32*(6), 390-404.

Naikoo, M. W., Rihan, M., Ishtiaque, M., & Shahfahad. (2020). Analyses of land use land cover (LULC) change and built-up expansion in the suburb of a metropolitan city: Spatio-temporal analysis of Delhi NCR using landsat datasets. *Journal of Urban Management, 9*(3), 347-359.

Nasab, M. T., Grimm, K., Bazrkar, M. H., Zeng, L., Shabani, A., Zhang, X., & Chu, X. (2018). SWAT Modeling of Non-Point Source Pollution in Depression-Dominated Basins under Varying Hydroclimatic Conditions. *International journal of environmental research and public health, 15*(11), 2492.

Nash, J. E., & Sutcliffe, J. V. (1970). River flow forecasting through conceptual models part I - A discussion of principles. *Journal of Hydrology, 10*(3), 282-290.

Nasta, P., Allocca, C., Deidda, R., & Romano, N. (2020). Assessing the impact of seasonal-rainfall anomalies on catchment-scale water balance components. *Hydrology and Earth System Sciences, 24,* 3211-3227.

Navarrete, J. M., Ioris, A. A. R., & Granados, J. (2012). Water Sustainability and Politics – Examples from Latin America and Implications for Agroecology. In Campbell, W. B. & López Ortíz, S. (Eds.). *Integrating Agriculture, Conservation and Ecotourism: Societal Influences* (pp.227-277). Dordrecht: Springer.

Neitsch, S. L., Arnold, J. G., Kiniry, J. R., & Williams, J. R. (2005). *Soil and Water Assessment Tool Theoretical Documentation Version 2005.* Retrieved from https://swat.tamu.edu/media/1292/SWAT2005theory.pdf.

Neitsch, S. L., Arnold, J. G., Kiniry, J. R., & Williams, J. R. (2009). *Soil and Water Assessment Tool Theoretical Documentation Version 2009.* Retrieved from https://swat.tamu.edu/media/99192/swat2009-theory.pdf.

Nouri, H., Borujeni, S. C., & Hoekstra, A. Y. (2019). The blue water footprint of urban green spaces: An example for Adelaide, Australia. *Landscape and Urban Planning, 190,* 103613.

Oh, Y. G., Yoo, S. H., Lee, S. H., & Choi, J. Y. (2011). Prediction of paddy field change based on climate change scenarios using the CLUE model. *Paddy and Water Environment, 9,* 309-323.

Ongsomwang, S., & Boonchoo, K. (2016). Integration of Geospatial Models for the Allocation of Deforestation Hotspots and Forest Protection Units. *Suranaree Journal of Science and Technology, 23*(3), 283-307.

Ongsomwang, S., & Iamchuen, N. (2015). Integration of geospatial models for optimum land use allocation in three different scenarios. *Suranaree Journal of Science and Technology, 22*(4), 378-396.

Ongsomwang, S., & Kunto, S. (2013). Impact of Land Use Change on Water Runoff A Case Study of Huay Tung Lung Watershed in the Mun Basin. *Journal of Remote Sensing and GIS Association of Thailand, 14*(1), 1-7.

Ongsomwang, S., & Pimjai, M. (2014). Land use and land cover prediction and its impact on surface runoff. *Suranaree Journal of Science and Technology, 22*(2), 205-223.

Ongsomwang, S., Pattanakiat, S., & Srisuwan, A. (2019). Impact of Land Use and Land Cover Change on Ecosystem Service Values: A Case Study of Khon Kaen City, Thailand. *Environment and Natural Resources Journal, 17*(4), 43-58.

Opere, A., & Okello, B. (2011). Hydrologic analysis for river Nyando using SWAT. *Hydrology and Earth System Sciences Discussions, 8*(1), 1765–1797.

Osei, M. A., Amekudzi, L. K., Wemegah, D. D., Preko, K., Gyawu, E. S., & Obiri-Danso, K. (2019). The impact of climate and land-use changes on the hydrological processes of Owabi catchment from SWAT analysis. *Journal of Hydrology: Regional Studies, 25,* 100620.

Prachayasittikul, L. (2006). *Application of soil and water assessment tool (SWAT model) for water balance studies of Songkhla Lake Basin* (Master's thesis). Mahidol University, Bangkok.

Prince of Songkla University, Phuket Campus. (2017). *A summary of the water situation.* Retrieved from http://smartwaterphuket.com/#report.

Puno, R.C.C., Puno, G.R., & Talisay, B.A.M. (2019). Hydrologic responses of watershed assessment to land cover and climate change using soil and water assessment tool model. *Global Journal of Environmental Science and Management, 5*(1), 71-82.

Raksmey, A., & Chantha, O. (2018). Simulating streamflow in an ungauged catchment of Tonlesap Lake Basin in Cambodia using the Soil and Water Assessment Tool (SWAT) model. *Water Science, 32*(1), 89-101.

Rempis, N., Alexandrakis, G., & Kampanis, N. (2018). Urbanization and coastal effects in Agia Pelagia, Crete Island. In *Proceedings of 20th EGU General Assembly, EGU2018* (pp 6313). Vienna: EGU General Assembly.

Reyes Perez, M. F. (2017). *Water supply and demand management in the Galápagos: A case study of Santa Cruz Island* (Doctoral dissertation). Delft University of Technology, Delft.

Royal Irrigation Department. (2011a). *Crop Water Requirement, Reference Crop Evapotranspiration and Crop Coefficient Handbook.* Bangkok: Royal Irrigation Department.

Royal Irrigation Department. (2011b). *Work Manual: Volume 8/16 Assessment of water use in various activities.* Bangkok: Royal Irrigation Department.

Sakunboonpanich, Y. (2011). *History of modern city of Phuket from 1957 to 2007* (Master's thesis). Thammasat University, Bangkok.

Sangkatananon, P., Chotamonsak, C., & Dhanasin, P. (2018). Performance of SWAT Hydrologic Model for Runoff Simulation in Wang River Basin. *The Journal of KMUTNB, 28*(4).

Schilling, K., Jha, M., Zhang, Y.-K., Gassman, P., & Wolter, C. (2008). Impact of Land Use and Land Cover Change on the Water Balance of a Large Agricultural Watershed: Historical Effects and Future Directions. *Water Resources Research, 44*.

Shahvari, N., Khalilian, S., Mosavi, S. H., & Mortazavi, S. (2019). Assessing climate change impacts on water resources and crop yield: a case study of Varamin plain basin, Iran. *Environmental Monitoring and Assessment,* 191.

Sisay, E., Halefom, A., Khare, D., Singh, L., & Meshesha, T. (2017). Hydrological modelling of ungauged urban watershed using SWAT model. *Modeling Earth Systems and Environment, 3*(4).

Sma-air, S. (2012). *Analysis of Surface-Water Resource Amount for Water Management in Phuket Province, Thailand* (Master's thesis). Prince of Songkla University, Songkhla.

Southern Region Irrigation Hydrology Center, Royal Irrigation Department. (2021). *The monitoring low water criteria using flow duration curve.* Bangkok: Bureau of Water Management and Hydrology Royal Irrigation Department.

Srichai, N., Kuayrakan, S., & Suwanprasit, C. (2016). Water Use and Water Demand Modeling for Hotel and Tourism Business, Patong, Phuket Province. *Songklanakarin Journal of Social Sciences and Humanities, 22*(2), 255-292.

Srichaichana, J., Ongsomwang, S., & Trisurat, Y. (2019). Land Use and Land Cover Scenarios for Optimum Water Yield and Sediment Retention Ecosystem Services in Klong U-Tapao Watershed, Songkhla, Thailand. *Sustainability, 11,* 2895.

Suwanprasit, C., Puangkeaw, N., & Srichai, N. (2013). Water balance of Phuket province. *Journal of Remote Sensing and GIS Association of Thailand, 14*(3), 1-8.

Tamm, O., Maasikamäe, S., Padari, A., & Tamm, T. (2018). Modelling the effects of land use and climate change on the water resources in the eastern Baltic Sea region using the SWAT model. *CATENA, 167,* 78-89.

TAT Intelligence Center, Tourism Authority of Thailand. (2019). *Internal Tourism Statistics in 2019 of Phuket.* Retrieved from https://intelligencecenter.tat.or.th/articles/11859.

TAT Intelligence Center, Tourism Authority of Thailand. (2020). *Tourist arrivals to Phuket Island during 1993-2020.* Retrieved from https://intelligencecenter.tat.or.th/articles/11859.

Terra Media And Consulting. (2015). *"Phuket" the highest growing tourist city.* Retrieved from https://www.terrabkk.com/articles/90417/ภูเก็ต-เมืองท่องเที่ยว.

Thai Meteorological Department. (2017). *Agricultural Meteorology to know for Phuket.* Bangkok: Thai Meteorological Department.

Thepnuan, P. (2007). *A System Dynamics Model of Tourism Development Carrying Capacity of water Resource in Changwat Phuket* (Master's thesis). Prince of Songkla University, Songkhla.

Tokarchuk, O., Gabriele, R., & Maurer, O. (2017). Development of city tourism and well-being of urban residents: A case of German Magic Cities. *Tourism Economics, 23*(2), 343-359.

Tolk, J. A. (2003). Plant available soil water. In Stewart, B. A. & Howell, T. A. (Eds.). *Encyclopedia of water science* (pp. 669-672). New York: Marcel Dekker.

Trisurat, Y., Aekakkararungroj, A., Johnston, J. M., Nuon, V., & Phan, N. (2017). *Basin-wide Assessments of Climate Change Impacts on Water and Water-related Resources and Sector in Lower Mekong Basin.* Phnom Penh: Mekong River Commission Planning Division.

Trisurat, Y., Eawpanich, P., & Kalliola, R. (2016). Integrating land use and climate change scenarios and models into assessment of forested watershed services in Southern Thailand. *Environmental Research, 147,* 611-620.

Troanca, D. (2012). The impact of tourism development on urban environment. *Studies in Business and Economics, 7*(3), 160-164.

Van Asselen, S. & Verburg, P. (2013). Land cover change or land-use intensification: Simulating land system change with a global-scale land change model. *Global change biology, 19*(12), 3648-3667.

Veettil, A. V., & Mishra, A. K. (2016). Water security assessment using blue and green water footprint concepts. *Journal of Hydrology, 542,* 589-602.

Veettil, A. V., & Mishra, A. K. (2018). Potential influence of climate and anthropogenic variables on water security using blue and green water scarcity, Falkenmark index, and freshwater provision indicator. *Journal of Environmental Management, 228,* 346-362.

Veldkamp, A., & Fresco, L. O. (1996). CLUE: a conceptual model to study the Conversion of Land Use and its Effects. *Ecological Modelling, 85*(2), 253-270.

Verburg, P. H., & Overmars, K. P. (2007). Dynamic Simulation of Land-Use Change Trajectories with the CLUE-S Model. In Koomen, E., Stillwell, J., Bakema, A., & Scholten, H. J. (Eds.). *Modelling Land-Use Change: Progress and Applications* (pp.321-337). Berlin: Springer.

Verburg, P. H., de Koning, G. H. J., Kok, K., Veldkamp, A., & Bouma, J. (1999). A spatial explicit allocation procedure for modelling the pattern of land-use change based upon actual land use. *Ecological Modelling, 116,* 45-61.

Verburg, P. H., Soepboer, W., Veldkamp, A., Limpiada, R., Espaldon, m. v., & Mastura, S. (2002). Modeling the Spatial Dynamics of Regional Land Use: The CLUE-S Model. *Environmental Management, 30*(3), 391-405.

Vongtanaboon, S., Boochabun, K., Meunpon, R., & Sriyaporn, C. (2010). *Water Quantity Analysis in Phuket Province.* Phuket: Phuket Rajabhat University.

Wangpimool, W., Pongput, K., Sukvibool, C., Sombatpanit, S., & Gassman, P. W. (2013). The effect of reforestation on streamflow in Upper Nan river basin using Soil and Water Assessment Tool (SWAT) model. *International Soil and Water Conservation Research, 1*(2), 53-63.

Wijitkosum, S., & Sriburi, T. (2008). Impact of Urban Expansion on Water Demand: The case study of Nakhon Ratchasima city, Lam Ta Kong Watershed. *Nakhara: Journal of Environmental Design and Planning, 4,* 69-88.

Wongsai, S., Keson, J., & Wongsai, N. (2018). Land use change monitoring and urban expansion of Phuket. *VRU Research and Development Journal Science and Technology, 13*(3), 65-74.

Wuttichaikitcharoen, P., & Santan, C. (2013). Runoff Estimation in Mae Chaem Basin using SWAT. In *The 5th National Convention on Water Resources Engineering* (pp. 1-10). Chiang Rai: Department of Irrigation Engineering, Kasetsart University.

Xu, L., Li, Z., Song, H., & Yin, H. (2013). Land-Use Planning for Urban Sprawl Based on the CLUE-S Model: A Case Study of Guangzhou, China. *Entropy, 15*(9), 3490-3506.

Zang, C., & Liu, J. (2013). Trend analysis for the flows of green and blue water in the Heihe River basin, northwestern China. *Journal of Hydrology, 502,* 27-36.

Zhang, L. P., Zhang, S. W., Zhou, Z. M., Hou, S., Huang, Y. F., & Cao, W. D. (2016). Spatial distribution prediction and benefits assessment of green manure in the Pinggu District, Beijing, based on the CLUE-S model. *Journal of Integrative Agriculture, 15*(2), 465-474.

Zhao, S., Cheng, W., Liu, H.-j., Xia, Y., Chai, H.-x., Song, Y., Zhang, W.-j., & You, T. (2016). Land Use Transformation Rule Analysis in Beijing-Tianjin-Tangshan Region Using Remote Sensing and GIS Technology. *Journal of Sensors, 2016,* 1-10.

Zhou, F., Xu, Y., Chen, Y., Xu, C. Y., Gao, Y., & Du, J. (2013). Hydrological response to urbanization at different spatio-temporal scales simulated by coupling of CLUE-S and the SWAT model in the Yangtze River Delta region. *Journal of Hydrology, 485,* 113-125.

CURRICULUM VITAE

Name Mr. Nattapong Puangkaew

Date of Birth May 22, 1988

Place of Birth Songkhla

Education Background:

2011: Bachelor of Science in Geography, Department of Geography, Faculty of Humanities and Social Sciences, Prince of Songkla University, Pattani Campus, Thailand.

2013: Master of Science in Technology and Environmental Management, Faculty of Technology and Environment, Prince of Songkla University, Phuket Campus, Thailand.

2017: Postgraduate Diploma in Remote Sensing & Geographic Information System, Centre for Space Science and Technology Education in Asia and the Pacific, India.

Work Experiences:

2017-Present: Lecturer, Department of Geography, Faculty of Humanities and Social Sciences, Prince of Songkla University, Pattani Campus, Thailand.

2014-2017: Lecturer, Department of Geoinformatics, Faculty of Science and Technology, Hatyai University, Thailand.

Publications:

Puangkaew, N., & Ongsomwang, S. (2021). Remote Sensing and Geospatial Models to Simulate Land Use and Land Cover and Estimate Water Supply and Demand for Water Balancing in Phuket Island, Thailand. *Applied Sciences, 11*(22).

Puangkaew, N., & Ongsomwang, S. (2020). Prediction of land use and land cover changes using the CLUE-S model, Phuket Island, Thailand. *Journal of Remote Sensing and GIS Association of Thailand*, *21*(3), 16-32.